University of Turin:

Department of Clinical and Biological Sciences

PhD Programme in Experimental Medicine
and Therapy

Cycle: XXXV

A role for SerpinB3 and Oncostatin M in the progression of NASH

Thesis' author: **Francesca Protopapa**

Supervisor: **Prof. Maurizio Parola**

PhD Programme Co-ordinator: **Prof. Pasquale Pagliaro**

Academic years of enrolment: **2019-2023**

Code of scientific discipline: **MED/04**

INDEX

INTRODUCTION

1.1 Remarks on liver fibrosis and fibrogenesis

Liver fibrogenesis is a dynamic and highly integrated molecular, cellular and tissue process that, irrespective of the etiology, results in a progressive accumulation of extracellular matrix (ECM) components and drives the progression of chronic liver disease (CLD) (Novo et al., 2017, Parola and Pinzani 2019). Liver fibrogenesis is sustained by the activation of hepatic myofibroblasts (MFs), a heterogeneous population of proliferative, migratory and profibrogenic cells that also modulate inflammatory/immune response and angiogenesis (Parola and Pinzani, 2019; Lee et al., 2015; Seki and Schwabe, 2015).

Liver fibrosis can develop primarily from three major conditions resulting in chronic liver injury, including chronic infection by hepatotropic viruses (hepatitis B and C viruses), chronic toxic injury from excessive alcohol consumption, and metabolic-related injury, such as non-alcoholic fatty liver disease (NAFLD) and its progressive form, non-alcoholic steatohepatitis (NASH) (Byass, 2014; Marcellin and Kutala, 2018; Thrift et al., 2017; Younoussi et al. 2018, Golabi et al., 2023). NAFLD/NASH is becoming the leading cause of chronic liver disease worldwide (Younoussi et al. 2018, Golabi et al., 2023, Falade-Nwulia et al., 2017; EASL, 2018a; AASLD/IDSA, 2018; Rockey and Friedman, 2021). There are also other less common causes, as reported in important studies (Arndtz and Hirschfield, 2016; Lazaridis and La Russo, 2015; Cannito et al., 2018; Byass, 2014; Marcellin and Kutala, 2018).

Independently of the aetiology, liver fibrosis is believed to provide a major contribution to CLD progression to advanced stages of evident cirrhosis, with portal hypertension and related complications, leading to hepatic failure (Lee et al., 2015; Seki and Schwabe, 2015; Trautwein et al., 2015; Koyama and Brenner, 2017; Parola and Pinzani, 2019; Schwabe et al., 2020; Friedman and Pinzani, 2022). In addition, the progression of the CLD is also related to an increased risk to develop hepatocellular carcinoma (HCC), which is the most common primary liver cancer. More than 90% of HCC patients usually develop liver cancer in the background of a cirrhotic liver, while 25-30% of NASH-associated HCC patients have been reported to develop cancer in the absence of cirrhosis (EASL, 2018b; Marrero et al., 2018a; Llovet et al., 2021; Llovet et al., 2023).

Recent studies have revealed the so-called *pro-fibrotic microenvironment*, that involves molecular mediators and signalling pathways. A major role in driving fibrogenic progression is played by activated hepatic myofibroblasts (MFs) and cells of either innate and adaptative immunity (Trautwein et al., 2015; Higashi et al., 2017; Cannito et al. 2017a; Tacke, 2017;

Parola and Pinzani, 2019; Schwabe et al., 2020; Carter and Friedman, 2022; Peiseler et al., 2022; Wallace et al., 2022).

1.2 NAFLD as the emerging leading cause of CLD

1.2.1 NAFLD: epidemiological data

NAFLD is becoming a global health problem due to its prevalence and incidence that are rapidly increasing worldwide, then representing the emerging leading cause of CLD (Loomba and Sanyal, 2013; Younossi et al., 2016; Younossi et al, 2018; Younossi et al. 2019a; Golabi et al., 2023). NAFLD affects approximately 1 billion of individuals worldwide, with a global prevalence of around 25% in the general population, with geographic variations from 13% in Africa up to 42% in southeast Asia (Younossi et al., 2018; Younossi et al., 2019a; Golabi et al., 2023) whereas in the United States NAFLD may affect as much as 80 million of individuals (Estes et al., 2018). The high global prevalence of NAFLD is believed to parallel the worldwide rising rates of obesity and type 2 diabetes (T2D), with NAFLD commonly interpreted as the hepatic manifestation of the metabolic syndrome and then NAFLD is associated with metabolic risk factors (Marchesini et al., 2001; Neuschwander - Tetri et al., 2010; Chalasani et al., 2018; Samuel and Shulman, 2018). It's important to remember that not all obese patients develop NAFLD and that NAFLD can be also detected in non-obese patients (Kim and Kim, 2017).

1.2.2 NAFLD: definition, diagnosis and natural history

As reported by Chalasani and colleagues in 2018, in patients that consume little or no alcohol and when the involvement of other metabolic, toxic- or drug-induced causes of fatty liver can be excluded, NAFLD can be diagnosed when histopathological analysis of liver biopsies or imaging techniques indicate that more than 5% of hepatocytes presents accumulation of triglycerides (TGs). NAFLD includes a spectrum of conditions ranging from simple steatosis, or fatty liver, to the progressive form of non-alcoholic steatohepatitis or NASH. Simple steatosis, which affect the large majority (75-80%) of NAFLD patients and is sometimes referred to as non-alcoholic fatty liver (NAFL), is benign and considered as a not progressive or slowly progressive condition (Singh et al., 2015; Chalasani et al., 2018). In suspected patients the histopathological diagnosis of NASH requires the evidence of liver steatosis associated with aspects of parenchymal injury like ballooning, apoptosis, focal necrosis, lobular and/or portal inflammatory infiltrate and a variable degree of fibrosis.

Ofrelevance, the patients affected by NASH have a significant risk to undergo fibrogenic progression to a more advanced stage of CLD (Singh et al., 2015; Satapathy and Sanyal, 2015; McPherson et al., 2015; Younossi et al, 2019a; Loomba and Adams, 2019; Powell et al., 2021).

As stated by Powell and colleagues in 2021, the strongest predictor for disease-specific progression and mortality is represented by NASH-associated liver fibrosis. The leading cause of mortality in NAFLD patients is cardiovascular disease, followed by cancer and CLD (Adams et al., 2005). Moreover, cirrhotic NASH patients have a 1,3-2% per year risk of developing HCC (Loomba et al., 2020) and NASH is indicated as the most rapidly growing cause of HCC in liver transplant candidates (Younossi et al., 2019b; Huang et al., 2022). The incidence of NASH-related HCC is significantly increasing worldwide and estimated to represent the prevalent cause of HCC in the next decades (Negro, 2020; Huang et al., 2021; Huang et al., 2022). As previously mentioned, about 25-30% of NASH-associated HCC develop in non-cirrhotic patients, that is a rate much higher than for other aetiologies of CLD (Llovet et al., 2023).

1.2.3 MASLD: the new nomenclature for NAFLD

In June 2023 during the European Association for the Study of Liver (EALS), a multi-society Delphi consensus statement was released in order to make more clarity in the definition of NAFLD, avoiding the terms “non-alcoholic” and “fatty” and, in addition, facilitating a more homogeneous recruitment in clinical trials (Rinella et al., 2023). The term “fatty liver” has been changed with “steatotic liver disease” (SLD). The term commonly used to describe NAFLD, in most cases, has now been replaced with the definition of Metabolic Dysfunction Associated Steatotic Liver Disease (MASLD) when patients exhibit at least one cardiometabolic risk factor alongside hepatic steatosis, excluding significant/high alcohol intake. On the other side, the presence of cardiometabolic risk factors together with higher alcohol consumption is now referred to as Metabolic Alcohol Associated Liver Disease (MetALD). This consensus statement also provides a more precise classification for other forms of steatosis unrelated to metabolic risk factors. The term NAFLD will still be used in this thesis, effectively encompassing what is now defined as MASLD.

1.3 NAFLD: a disease resulting from dysregulated metabolism, lipotoxicity, genetic variants and changes in gut microbiome

1.3.1 Metabolic causes of NAFLD

As previously highlighted, NAFLD is intrinsically linked to obesity and type 2 diabetes. It arises from a complex interplay of metabolic factors that disrupt liver energy metabolism. This disruption occurs when the liver faces an overwhelming influx of lipids and carbohydrates, surpassing its capacity to efficiently process these substrates. Several key factors contribute to this surplus energy accumulation within the liver:

1. Dietary Influence: The consumption of diets rich in lipids, particularly saturated fatty acids, and high levels of carbohydrates, with a particular focus on mono- and di-saccharides, like fructose and sucrose. This dietary pattern is characteristic of the Western diet (Herman and Samuel, 2016; Samuel and Shulman, 2018; Loomba et al., 2021);

2. Muscle-Related Factors: Lipid deposition occurs within skeletal muscles and triggers local insulin resistance (IR). Skeletal muscle IR subsequently inhibits insulin signaling, reducing insulin-stimulated glucose transport and muscle glycogen synthesis. Consequently, dietary glucose is re-routed to the liver (Petersen et al., 2007; Flannery et al., 2012; Samuel and Shulman, 2018);

3. Hepatic Insulin Resistance: Hepatic IR closely correlates with peripheral insulin resistance and intensifies as the disease progresses. This leads to inadequate suppression of hepatic gluconeogenesis and a decrease in glycogen synthesis due to impaired activation of glycogen synthase. Additionally, glucose is redirected towards lipogenic pathways, increasing TGs accumulation within the liver (Tilg et al., 2017; Petersen and Shulman, 2018);

4. Adipose Tissue Implications: IR also extends to expanded and inflamed white adipose tissue (WAT), enhancing lipolysis and increasing the delivery of fatty acids to the liver. This process can promote fatty acid esterification into TGs and the development of NAFLD (Lotta et al., 2017).

1.3.2 Hepatic dysregulation of lipid and carbohydrate metabolism in NAFLD

A critical feature of NAFLD is the significant role played by increased delivery of free fatty

acids to the liver, coupled with the development of IR (Tilg et al., 2017; Petersen and Shulman, 2018; Loomba et al., 2021).
Major events that can additionaly drive the development of NAFLD-related steatosis include the following events:

1. Increased De Novo Lipogenesis (DNL): This process arises from the increased diet delivery of glucose and other carbohydrates, particularly fructose, to the liver. This triggers the up-regulation of key genes responsible for lipogenic enzymes governing DNL. Central to this process are transcription factors, such as sterol regulatory element binding-protein 1c (SREBP1c), carbohydrate response element binding-protein (ChREBP), Liver X receptors (LXRs), and peroxisome proliferator-activated receptor γ (PPARγ);

2. Increased Fatty Acid Esterification into TGs: This event involves the formation of diacylglycerol (DG) and elevated activity of diacylglycerol O-acyltransferase 2 (DGAT2). These changes occur due to the increased influx of fatty acids to the liver, driven by dietary sources and/or sustained lipolysis within white adipose tissue (WAT).

1.3.3 Genetic causes of NAFLD

The progression of NAFLD towards NASH and more advanced stages of CLD is not only attributable to mechanisms causing hepatocyte injury and death, as explained below. It has become evident that this progression is significantly influenced by genetic variants present in patients, with some individuals carrying one or even more of these variants (Anstee et al., 2016; Eslam et al., 2018; Eslam and George, 2020).
This genetic dimension is of crucial importance, as it introduces another layer of complexity to the multifaceted background of NASH progression. These genetic variants further contribute to the substantial inter-patient variability frequently observed in NAFLD/NASH patients (Arrese et al., 2021).
NAFLD can be considered an inheritable disease, supported by different studies highlighting a significant shared genetic component in the development of hepatic steatosis and fibrosis (Schwimmer et al., 2009; Cui et al., 2016, Eslam et al., 2018). Numeorus genetic variants have been characterized for genes related to hepatic lipid metabolism which are strongly associated with the individual susceptibility to develop NAFLD and/or to undergo disease progression. Of the several genes identified in these years, at least five are worthy of

mention, including patatin-like phospholipase domain containing 3 (PNPLA3), transmembrane 6 superfamily member 2 (TM6SF2), membrane-bound O-acyltransferase domain-containing 7 (MBOAT7), glucokinase regulator (GCKR), and hydroxysteroid 17β-dehydrogenase (HSD17B13) (Eslam et al., 2018; Eslam and George, 2020).

- **PNPLA3:** The genetic variant, PNPLA3 I148M (rs738409 C>G) is strongly associated with steatosis, fibrosis, and an increased risk of HCC development (Sookoian et al., 2009; Valenti et al., 2010; Liu et al., 2014a);

- **TM6SF2:** The TM6SF2 rs58542926 C>T polymorphism predicts NASH progression and is linked to a reduced risk of cardiovascular diseases (Liu et al., 2014b; Anstee et al., 2016);

- **MBOAT7:** The rs641738 C>T genetic variant is associated with reduced levels of phosphatidylinositol containing arachidonic acid and is linked to an increased risk of progressive NAFLD/NASH and HCC (Mancina et al., 2016; Luukkonen et al., 2016; Donati et al., 2017);

- **GCKR:** A genetic variant of this gene modulates glucokinase in response to fructose-6-phosphate, increasing substrate availability for fatty acid synthesis and, consequently, the risk of NAFLD (Valenti et al., 2012; Eslam et al., 2018);

- **HSD17B13:** A loss-of-function genetic variant generates a truncated and inactive form of the enzyme, associated with protection from hepatic inflammation, fibrosis, and HCC development in both alcoholic liver disease (ALD) and NAFLD/NASH patients (Abul-Hus n et al., 2018).

Different reviews analyze the relationships between these genetic variants, susceptibility to NAFLD and disease progression (Eslam et al., 2018; Eslam and George, 2020; Trépo and Valenti, 2020).

1.3.4 The role of gut microbiota in NAFLD/NASH development

Regarding the gut microbiome, the connection between NAFLD/NASH development and changes in microbiota composition has become an important concept, supported by different studies (Loomba et al., 2017; Marra and Svegliati Baroni, 2018; Caussy et al., 2019;

Schwimmer et al., 2019; Loomba et al., 2021). As NAFLD progresses, it has been documented that patients' microbiomes become different, with an increased prevalence of Streptococcus and Gram-negative bacteria (Hoyles et al., 2018). Furthermore, steatohepatitis and fibrosis have been associated with the dominance of Bacteroidetes and Ruminococcus (Boursier et al., 2016). These changes in NAFLD patients, particularly those with advanced fibrosis, are often accompanied by a significant decrease in Firmicutes (Loomba et al., 2021). In line with these findings, studies conducted on well-characterized cohorts of NAFLD patients have revealed that a metagenomic signature based on the gut microbiome can be usefull in order to distinguish between patients with mild to moderate fibrosis and those with advanced fibrosis (Loomba et al., 2017). Additionally, it has been suggested that a microbiome signature could even specifically identify NAFLD-related cirrhosis (Caussy et al., 2019).

1.4 Hepatocyte injury and death in NAFLD/NASH

1.4.1 Hepatocyte injury in progressive NAFLD: a role for lipotoxicity, oxidative stress and mitochondrial dysfunction

In the context of NAFLD, the most prevalent feature among patients is the presence of fatty liver. Nonetheless, there is a consensus emerging that steatosis, which was initially considered a risk factor for the progression to NASH and fibros is according to the 2-hit hypothesis (Day and James, 1998), is fundamentally a relatively benign condition. Hepatocyte injury in NAFLD appears to primarily hinge on factors such as lipotoxicity, oxidative stress, mitochondrial dysfunction and other mechanisms, rather than the mere accumulation of TGs (Neuschwander-Tetri, 2010; Marra and Svegliati-Baroni, 2018; Loomba et al., 2021). In the context of lipotoxicity, during the progression of NAFLD/NASH, hepatocytes likely face an excessive influx of lipid substrates and disruptions in lipid-related metabolic pathways, including mitochondrial or peroxisomal β-oxidation, transient storage of excess lipids as inert TGs and secretion of TGs via VLDL. These events are believed to contribute to give rise to lipotoxic lipids, resulting in mitochondrial dysfunction, endoplasmic reticulum (ER) stress, oxidative stress, and, ultimately, hepatocyte injury, genomic instability, persistent inflammation and sustained fibrogenesis (Neuschwander-Tetri, 2010; Marra and Lotersztajn, 2013; Marra and Svegliati-Baroni, 2018; Schuster et al., 2018; Loomba et al., 2021). The key toxic lipids are monounsaturated fatty acids, ceramides, lysophosphatidyl choline, lysophosphatidic acid, and diacylglycerols. Monounsaturated fatty acids like palmitate (C:16) and stearate (C:18) can exhibit direct cytotoxicity, being able of triggering apoptosis via the activation of c-Jun-N-terminal kinases (JNKs) and mitochondrial death pathways.

Additionally, they induce ER stress and promote the activation of inflammasomes (Marra and Svegliati-Baroni, 2018; Schuster et al., 2018). Free cholesterol can exacerbate cell injury mediated by death signals (TNF, TAIL, etc.) and, when accumulated in hepatocytes, as well as other cells like Kupffer cells (KCs) or hepatic stellate cells (HSCs), it can disrupt membrane fluidity, foster oxidative stress, impair mitochondrial function, and deplete ATP, ultimately leading to apoptosis or necrotic -like cell death (Schuster et al., 2018). Moreover, lipotoxicity has been suggested to also contribute to trigger the release of extracellular vesicles (EVs) from fat-laden hepatocytes that can exert various effects on neighboring cells, including pro-angiogenic and pro-inflammatory effects. They induce the up-regulation of the NOD-like receptor protein 3 (NLRP3) inflammasome and direct profibrogenic effects on HSCs (Povero et al., 2013; Povero et al., 2015; Hirsova et al., 2016; Cannito et al., 2017b).

Oxidative stress is another significant contributor to hepatocyte injury during the progression of NAFLD and fibrosis and the degree of oxidative stress and of its markers has been reported to correlate with liver injury in human patients (Parola and Robino, 2001; Novo and Parola, 2008; Parola et al., 2008; Leung and Nieto, 2013; Paik et al., 2014; Cannito et al., 2017a; Bocca et al., 2022). The following major issues can summarize the role of oxidative stress in NAFLD/NASH:

- Oxidative stress itself can contribute to hepatocyte injury, inhibit hepatocytes proliferation and thus perpetuate hepatic injury and the inflammatory response. One should consider that the increased generation of ROS and related intermediates, including reactive nitrogen species (RNS) and aldehydes from lipid peroxidation such as 4-hydroxy-2,3-alkenals, is involved in almost all mechanisms of injury and processes leading to hepatocyte death;

- ROS generation in the injured liver is predominantly linked to the activation of innate immune cells like KCs, recruited macrophages, and neutrophils. Activation often occurs through exposure to damage-associated molecular patterns (DAMPs) and through ligand-receptor related involvement of NADPH-oxidase activation which can occur in several types of liver cells. NADPH-oxidase activation can result from the interaction between growth factors, cytokines, chemokines and other mediators with their respective receptors;

- ROS generation also depends on mitochondrial dysfunction and, specifically in cases of alcoholic hepatitis and NASH, through the up-regulation of different cytochrome P450 isoforms. Under conditions of NASH-related ER stress, ROS are generated at high levels due to dysfunctional mitochondria as a consequence of Calcium leakage from ER: such a release of Calcium, once taken up by mitochondria, can lead to the opening of mitochondrial permeability transition (MPT) pores, to outer mitochondrial membrane permeabilization and to a significant derangement of the mitochondrial electron chain;

- ROS and 4-hydroxy-2,3-alkenals like 4-hydroxy-2,3-nonenal (HNE) can directly induce a pro-fibrogenic response in HSCs and liver MFs. They stimulate the synthesis of extracellular matrix (ECM) components and mediate various chemotactic effects in these cells in response to cytokines, growth factors and chemokines.

Regarding mitochondrial dysfunction, its role is believed to be crucial in the transition from simple steatosis to NASH. The primary drivers of mitochondrial alterations in this context are fatty acid oxidation and lipotoxicity. An increased flow of free fatty acids (FFAs) through the mitochondria can result in a higher production of ROS, which can harm both mitochondrial DNA (mtDNA) and the protein complexes within the respiratory chain. This, in turn, leads to a progressive decline in mitochondrial function, further intensifying oxidative stress, causing ATP depletion, compromising mitochondrial integrity, and ultimately culminating in cell death (Luedde et al., 2014; Machado and Diehl, 2016; Schuster et al., 2018).

1.4.2 Hepatocyte death in NAFLD/NASH: of apoptosis, necroptosis, pyroptosis and autophagy

In the histopathological spectrum of NAFLD, in addition to steatosis, inflammatory infiltrate and fibrosis, NASH is characterized by significant loss of hepatocytes as well as by ballooning degeneration, a peculiar form of cell injury. Ballooned cells, also defined "*undead cells*", are injured but still living hepatocytes with a characteristic morphology and they have been suggested to exacerbate inflammatory and fibrogenic signalling in the surrounding microenvironment (Ibrahim et al., 2018). Concerning true parenchymal cell death, it has been reported that, during NASH, hepatocytes can dye as a consequence of three major variants of regulated cell death (RCD), including apoptosis, necroptosis and pyroptosis (Luedde et al., 2014; Hirsova and Gores, 2015; Schuster et al., 2018; Knorr et al., 2022).
These model processes can use different mechanisms in order to trigger cell death, including or not the hepatocyte release of DAMPs. Moreover, hepatocytes death and

inflammatory response are intimately related and can positively modulate each other.
Apoptosis is considered as critical for progressive NAFLD in human patients and may be triggered by different stimuli, factors or conditions, including lipotoxicity that can induce permeabilization of lysosomes and mitochondria dysfunction (Feldstein et al., 2004; Yamaguchi et al., 2007; Hirsova et al., 2016).
Regarding the role of necroptosis in progressive NAFLD, this form of cell death is a variant of RCD, induced by death signals (TNF-α, FasL, TNF-related apoptosis-inducing ligand-1 or TRAIL-1, etc.), that through a ligand receptor pathway leads to the assembly of the necrosome complex.
Pyroptosis is another variant of RCD which has been more recently involved in the pathogenesis of progressive NAFLD (Knorr et al., 2022). Pyroptosis is an inflammatory-related cell death originally described as a way for phagocytes to clear intracellular pathogens involving cell lysis as well as excess production and release of IL-1β and IL-18to then exacerbate immune response (Zychlinsky et al., 1992; Brennan and Cookson, 2000). Pyroptosis affects several cell types, including hepatocytes, and operates through the proteolytic cleavage of proteins defined as gasdermin D (GSDMD) or gasdermin E (GSDME).
Dysregulation of autophagy is a last mechanism implicated in the pathogenesis of NASH and then in determining hepatocytes injury and death, although it may affect also the behaviour of macrophages and HSCs (Amir and Czaja, 2011; Czaja, 2016).

1.5 Innate and adaptive immunity in progressive NAFLD

1.5.1 Inflammatory and immune responses in NAFLD/NASH

The transition from simple steatosis to steatohepatitis involves a complex interplay of metabolic dysfunctions, lipotoxicity, oxidative stress and damage to hepatocytes, either through apoptosis, necroptosis or pyroptosis. These events sustain a persistent inflammatory response and activate repair mechanisms, engaging both innate and adaptive immunity cells. In the context of hepatocyte injury, hepatocytes can release damage-associated molecular patterns (DAMPs), such as ATP, DNA fragments, histones, and others, activating pattern recognition receptors (PRRs) and innate immunity cells (Gong et al., 2020).
They can also directly release pro-inflammatory cytokines like IL-1β and IL-18 via inflammasome activation (Alegre et al., 2017; Wang et al., 2021), as well as indirectly by releasing extracellular vesicles (EVs) containing CXCL-10, mitochondrial DNA, and other mediators (Ibrahim et al., 2016; Cannito et al., 2017b).

Literature data suggest that innate immune mechanisms and related cells, particularly macrophages, play a pivotal role in sustaining inflammation during NASH progression (Peiseler et al., 2022; Wallace et al., 2022). However, emerging evidence also underscores the crucial contribution of adaptive immunity (Sutti and Albano, 2020).

Metabolic alterations, including increased FFA influx to the liver, lipotoxicity, oxidative stress and gut dysbiosis can trigger inflammation, hepatocytes death and disrupt the immunotolerant hepatic environment (Vallianou et al., 2021; Hughey et al., 2022). These factors also play a significant role in activating HSCs and portal fibroblasts to hepatic MFs (Koyama and Brenner, 2017; Parola and Pinzani, 2019; Schwabe et al., 2020; Carter and Friedman, 2022). Platelets may further contribute to hepatic inflammation, as they infiltrate injured livers in NASH patients (Malehmir et al, 2019; Ramadori et al., 2019).

Platelets, rapidly activate and release various inflammatory and pro-fibrogenic mediators, including TNF-α, IL-6, TGF-β1, PDGF, EGF, IGF-1, VEGF-A, HGF and FGF (Heijnen and van der Sluijs, 2015; Taus et al., 2019), as well as IL1β-loaded microparticles (Brown et al., 2011).

1.5.2 The role of liver macrophages in NAFLD/NASH

Numerous experimental and clinical studies have outlined the heterogeneity of macrophages and of related subpopulations within the context of progressive NAFLD. Kupffer cells (KCs), the resident liver macrophages, as well as monocyte/macrophages recruited from the peripheral blood, commonly referred to as either monocyte-derived macrophages (MoMsss) or bone marrow-derived macrophages (BMDMs), have been reportedto play pivotal roles in NAFLD progression (Peiseler et al., 2022; Wallace et al., 2022). It is known that liver-resident KCs are primarily implicated in the early stages of NAFLD progression, by releasing significant pro-inflammatory mediators, including TNFα, IL-1β, and CCL2. The depletion of KCs during the initial experimental stages of NASH has been shown to mitigate the inflammatory response and the overall severity of liver injury (Huang et al., 2010; Pan et al., 2018). KCs are activated by damage-associated molecular patterns (DAMPs) and, more specifically, by free fatty acids (FFAs) through NLRP3 inflammasome activation (Pan et al., 2018). Additionally, related to gut dysbiosis, they can be activated by lipopolysaccharide (LPS) through the involvement of Toll-like receptor 4 (TLR4) mediated signaling (Csak et al., 2011). In normal murine livers, KCs represent a homogenous lineage expressing markers like F4/80, C-type lectin domain family 4 member F (CLEC4F), and T cell immunoglobulin and mucin domain-containing 4 (Timd4). Conversely, in healthy human livers, monocytes/macrophages form a continuous population, making it challenging to identify a distinct KC population. However, recent scRNAseq studies have identified two

clusters of human liver macrophages: i) a $CD68^{+}MARCO^{+}Timd4^{+}$ subset considered KCs, characterized by the expression of immune-tolerance genes, and ii) a $CD68^{+}MARCO^{-}Timd4^{66}$ subset, likely MoMss, expressing higher levels of pro-inflammatory genes (Mac Parland et al., 2018; Ramachandran et al., 2019; Zhao et al., 2020). Additionally, in NASH- related livers, there is an expansion of hepatic macrophages due to increased recruitment of monocytes from the peripheral blood, resulting in a distinct population of MoMs. In murine NASH livers, this recruitment gives rise to two distinct subsets: $CCR2^{high}Ly6C^{high}$ pro- inflammatory monocytes and $CX3CR1^{+}Ly6C^{low}$ patrolling monocytes (Guilliams et al., 2018). $CCR2^{+}$ macrophages contribute to liver injury, and pharmacological inhibition of their recruitment has been shown to ameliorate IR, hepatic inflammation, and fibrosis (Krenkel et al., 2018). In humans, the recruitment of circulating monocytes leads to the differentiation of three subsets: classical $CD14^{high}CD16^{neg}$ monocytes, intermediate $CD14^{high}CD16^{low}$ monocytes, and non-classical $CD14^{low}CD16^{high}$ cells (Guillot and Tacke, 2019). Interestingly,even in human NASH patients, periportal accumulation of $CCR2^{+}$ inflammatory macrophages has been reported, correlating with NASH severity and fibrosis (Krenkel et al., 2018). Then, during NASH progression, KCs gradually decrease, possibly due to excessivelipid uptake and storage impairing their self-renewal capacity. Experimental studies suggestthat they are replaced by more pro-inflammatory and cytotoxic $Timd4^{neg}$ monocyte-derived KCs, a phenomenon observed in humans as well (Guilliams et al., 2022). Recently, a distinctive macrophage subset has emerged in fibrotic and cirrhotic livers based on the expression of CD9 and triggering receptor expressed on myeloid cells-2 (TREM-2) (Ramachandran et al., 2019). Initially termed "*scar-associated macrophages*" (SAM) due to their localization in fibrotic niches, they were initially considered as pro-fibrogenic cells due to their gene signature and the ability to activate HSCs in culture. Proteogenomic analyses revealed the presence of $CD9^{+}TREM2^{+}$ cells, also known as "*lipid-associated macrophages*"(LAM), in healthy livers in both humans and mice (Guilliams et al., 2022). In physiological conditions, LAMs were found in periportal areas and near bile ducts. In steatotic livers, their numbers increased, accumulating pericentrally. LAMs express high levels of osteopontin (Remmerie et al., 2020), which is up-regulated in murine and human NASH (Glass et al., 2018; Honda et al., 2020). They have been suggested to form "*crown-like structures*", which are $CD11^{+}$ macrophages aggregated around hepatocytes with large lipid droplets (Itoh et al., 2013). Surprisingly, the loss of LAMs prevented the formation of "*crown-like structures*", but was associated with increased fibrosis in a dietary murine model of NASH (Daemen et al., 2021). Additionally, $TREM2^{+}$ deficient mice develop an accelerated form of experimental NASH (Hou et al., 2021). LAMs and SAMs are also detected in the adipose tissue of obese humans and mice and may play a role in regulating energy supply and metabolic homeostasis rather than

promoting disease progression (Jaitin et al., 2019). In addition, hepatic macrophages play a crucial role in detecting metabolic injuries and perpetuating chronic inflammation and liver fibrogenesis. These innate immune cells, as well as monocyte-derived macrophages (MoMss) or bone marrow-derived macrophages (BMDMs), interact with a wide array of cells within the inflammatory and profibrogenic environment of NASH, both within and beyond the liver (Lee and Friedman, 2022; Peiseler et al., 2022; Wallace et al., 2022). The dysregulation of KCs in the context of NASH can lead to an increased production and release of several cytokines, including TNF-α, IL-6, IL-1β, and IL-18, primarily mediated by damage-associated molecular patterns (DAMPs), Toll-like receptor (TLR) activation, and NF-kB signaling, often resulting in the recruitment of substantial numbers of monocytes, with other innate immune cells such as neutrophils (Ramachandran et al., 2012). These cells can also engage with HSCs and/or myofibroblasts (MFs) by releasing pro-fibrogenic growth factors, including transforming growth factor β1 (TGFβ1). Concerning MoMss or BMDMs, in NASH-affected livers, they tend to maintain a pro-inflammatory state marked by high expression of $Ly6C^{high}$, IL-1β, TNFα, CCL2 and they exhibit similarities with macrophages found in adipose tissue and bone marrow (Jaitin et al., 2019; Krenkel et al., 2020), including SAMs and LAMs (Ramachandran et al., 2019). Although these MoMs may interact with various neighboring cell types, it is essential to notethat they predominantly engage with HSCs and MFs. Several critical points deserve to be mentioned:

1. MoMs can stimulate HSCs, inducing their activation and transdifferentiation into MFsprimarily through the release of platelet-derived growth factor (PDGF) and TGFβ1, which

enhances the deposition of extracellular matrix (ECM) components (Parola and Pinzani, 2019; Lee and Friedman, 2022, Peiseler et al., 2022);

2. MoMs can release growth factors (GFs), cytokines, and chemokines, in order to sustain the MF-like phenotype and promote MFs' survival. (Novo et al., 2011; Pellicoro et al., 2014).

Liver macrophages also play a crucial role in resolution of acute injuries or when the underlying etiological factor or condition leading to CLD is removed (Kisseleva and Brenner, 2020; Rockey and Friedman, 2021; Dixon et al., 2004; Hafeez and Ahmed, 2013). It has been proposed that the removal of the underlying etiological factor can lead to the suppression of pro-inflammatory and profibrogenic mediators by halting hepatocyte injury, reducing the release of DAMPs, and through phagocytosis of cell debris.

Resolution macrophages fulfill their role primarily through the secretion of anti-inflammatory cytokines, including IL-10 and IL-1 receptor antagonist (IL1Ra), as well as resolution-inducing growth factors such as VEGF-A and hepatocyte growth factor (HGF). These specialized macrophages also employ potent matrix metalloproteases (MMPs) like MMP-9, MMP-12, and MMP-13 (Tacke, 2017). Furthermore, there is evidence suggesting that the release of MMP-9 and TRAIL contributes to the apoptosis of myofibroblasts (MFs) (Ramachandran etal. 2012).

1.5.3 The role of cells of adaptive immunity

Innate immune cells and their mechanisms are clearly pivotal in maintaining prolonged inflammation in individuals with NASH and in murine models. Nevertheless, there is an increasing evidence suggesting that adaptive immunity and associated cells can make a substantial impact on the advancement toward fibrosis and cirrhosis, as recently reviewed (Sutti and Albano, 2020; Peiseler et al., 2022), as well as on the emergence of HCC in NASH (Cannito et al., 2023).

1.5.4 Liver infiltration of B- and T-lymphocytes in NASH

The presence of adaptive immune cells in NASH patients is substantiated by histopathological findings that reveal the infiltration of B- and T-lymphocytes within lobular and periportal regions (Gadd et al., 2014; Yeh and Brunt, 2014). These B- and T-lymphocytes have been observed to form focal aggregates similar to ectopic lymphoid-like structures seen in other pathological conditions, and this association is positively linked to both lobular inflammation and fibrosis severity (Bruzzì et al., 2018). Similar observations have been described in murine dietary models of NASH, where the infiltration of B cells, $CD4^+$ T-lymphocytes, and $CD8^+$ T-lymphocytes parallels the worsening of parenchymal injury and lobular inflammation (Sutti et al., 2014; Wolf et al., 2014; Grohmann et al., 2018). Specifically, the B-lymphocytes involved lack CD43 but express CD23, while the infiltrating T-lymphocytes consist of proinflammatory $CD4^+$ T-helper 1 (Th-1) cells, IL-17 producing T-helper 17 (Th-17) cells, and cytotoxic $CD8^+$ T-cells (Sutti and Albano, 2020; Ramadori et al., 2022).

1.5.5. The role of $CD4^+$ T-helper cells and T_H17 cells in NAFLD/NASH

$CD4^+$ T helper cells have been consistently identified in the liver of both murine NASH models and human patients, including pediatric cases. These findings are supported by various studies (Inzaugarat et al., 2011; Sutti et al., 2014; Wolf et al., 2014; Weston et al., 2015; Grohmann et al., 2018; Ferreyra Solari et al., 2012). According to the available

literature, during NASH, these $CD4^+$ T helper cells are likely to differentiate into interferon γ (IFNγ)-producing T helper 1 (T_H1) cells, marked by the presence of the Tbet transcription factor (Li et al., 2005; Sutti et al., 2014). Furthermore, it's noteworthy that plasma levels of IFNγ have been shown to correlate with the severity of fibrosis and the extent of lymphocyte aggregates in NASH patients (Bruzzì et al., 2018). Moreover, genetic studies using a murine NASH model have demonstrated that IFNγ deficiency results in a significant reduction of inflammation and fibrosis (Luo et al., 2013). In NASH setting, there's also evidence of the involvement of 17 T helper (T_H17) cells, which can develop from $CD4^+$ T helper cells under inflammatory conditions. Both circulating and liver-resident T_H17 cells, known to produce cytokines such as those from the IL-17 family (IL-17 A-F) and others (IL-21, IL-22, IFNγ, TNFα), have been found to increase in number in both NAFL and NASH patients (Tang et al., 2011; Molina et al., 2019). The rise in hepatic T_H17 cells correlates with the progression of NASH (Rau et al., 2016). Interestingly, experimental models have suggested that the contribution of T_H17 cells to lobular inflammation during NASH progression may be counteracted by $CD4^+$ T_H 22 cells and the expression levels of IL-22. Deficiency in both IL-17 and IL-22 has been shown to have opposing effects on experimental fibrosis (Rolla et al., 2016; Molina et al., 2019).

1.5.6 The role of $CD8^+$ cytotoxic T lymphocytes in NAFLD/NASH

In contrast to what has been described for T_H1 and T_H17 cells, the role of $CD8^+$ cytotoxic T-lymphocytes in NAFLD/NASH remains only partially understood. Several studies have noted an increased presence of these cells in the livers of both human patients and experimental mice with NAFLD/NASH (Sutti et al. 2014; Wolf et al., 2014; Ghazarian et al., 2017; Bhattacharjee et al., 2017; Grohmann et al. 2018). At present, there are limited data demostrating that cytotoxic T-lymphocytes are recruited to injured murine livers in response to IFNα-mediated signals (Ghazarian et al., 2017) and that $CD8^+$ T cells activate HSCs both *in vivo* in murine NASH livers and in *in vitro* experiments (Breuer et al., 2020). In addition, other studies have highlighted that blood levels of $CD8^+$ cytotoxic T cells of NASH patients are elevated (Haas et al., 2019).

1.5.7 The role of B-lymphocytes in NAFLD/NASH

The presence of B-lymphocytes, often found within cell aggregates rich in T-lymphocytes,

has been observed in liver biopsies from NAFLD patients (Bruzzì et al., 2018; Grohmann et al., 2018). In murine models B cells become activated alongside the development of NASH independently of T cells (Tsiantoulas et al., 2015). In murine NASH, most B cells exhibit a

$B220^+IgM^+CD23^+CD43^-$ B2 phenotype, then resembling spleen follicular B cells, with only a minority of cells being $B220^+IgM^+CD23^-CD43^+$ B1 cells (Novobrantseva et al., 2005). B2 cells in murine NASH are associated with increased hepatic expression of B cell-activating factor (BAFF), a cytokine contributing to B cell survival and maturation, which has recently been implicated in fibrosis progression (Kanemitsu-Okada et al., 2023). Elevated circulating BAFF levels in NASH patients, compared to those with simple steatosis, correlate with the severity of steatohepatitis and fibrosis in humans (Miyake et al., 2013). Experimental studies in genetically modified mice have shown that overexpressing a soluble form of the BAFF-APRIL receptor TACI can prevent maturation into plasma cells, leading to reduced inflammation and fibrosis (Bruzzì et al., 2018). Moreover, B lymphocytes contribute to NASH progression by producing pro-inflammatory mediators and through their antigen-presenting abilities (Lund, 2008; Di Lillo et al., 2011). Interestingly, in experimental NASH, B cell activation seems to precede the recruitment of $CD4^+$ and $CD8^+$ T-lymphocytes. Interfering with B2 cells results in reduced T_H1 cell activation and decreased IFNγ release by $CD4^+$ T cells (Bruzzì et al., 2018). It is suggested that B cells, through the release of pro-inflammatory mediators, may stimulate liver macrophages and HSCs. Activated HSCs, in turn, can support B cell survival and maturation into plasma cells through the release of retinoic acid (Thapa et al., 2015).

1.6 Liver myofibroblasts (MFs): general concepts and phenotypic responses

Liver myofibroblasts (MFs) constitute a heterogeneous population of cells easily recognized by the expression of α-smooth muscle actin (α-SMA) and known to play a prominent pro-fibrogenic role in CLDs. These MFs can emerge from various mesenchymal precursor cells via a process termed activation/transdifferentiation, as reviewed by several Authors (Lee et al., 2015; Seki and Schwabe, 2015; Trautwein et al., 2015; Koyama and Brenner, 2017; Parola and Pinzani, 2019; Schwabe et al., 2020; Friedman and Pinzani, 2022). In the scenario of persistently injured livers, activated pro-fibrogenic MFs represent an important cell type able to receive, integrate and responde to several signals and interactions in the fibrogenic microenvironment. These signaling inputs include ROS from damaged hepatocytes or activated innate immune cells, different growth factors, cytokines, chemokines, adipokines, pro-angiogenic factors and various other molecular signals released by hepatic and extrahepatic cells participating to the progression of CLDs (Tsuchida and Friedman, 2017).

Additionally, in the specific context of progressive NAFLD, these cells demonstrate the capability to perceive and react to metabolic signals, along with signals associated with gut dysbiosis and those originating from adipose tissue (Trivedi et al., 2021). According to

literature data, liver MFs in CLDs, including NAFLD/NASH, predominantly originate through the activation/transdifferentiation of HSCs, sometimes referred to as HSC/MFs, as extensively reviewed (Friedman, 2008; Tsuchida and Friedman, 2017; Mederacke et al., 2013). However, it is pertinent to mention that a considerable proportion of MFs can also derive from the activation/transdifferentiation of portal fibroblasts, especially in conditions of chronic injury primarily targeting the biliary epithelium (Dranoff and Wells, 2010; Wells and Schwabe, 2016). Furthermore, a limited fraction of cells has been observed to originate following the recruitment of precursor cells from the bone marrow, specifically mesenchymal stem cells and fibrocytes, as documented in several research studies (Forbes et al., 2004; Russo et al., 2006; di Bonzo et al., 2008). Mesothelial cells may also offer a minor contribution to liver MFs, possibly through a mesothelial-to-mesenchymal transition (Li et al., 2013; Forbes and Parola, 2011; Parola and Pinzani, 2019). Irrespective of their diverse origins, activated liver MFs execute a range of shared phenotypic responses (Friedman, 2008; Tsuchida and Friedman, 2017; Trivedi et al., 2021):

a) Following parenchymal injury, liver MFs display increased proliferation, primarily in response to platelet-derived growth factor (PDGF) but also to other mitogens such as transforming growth factor alpha (TGFα), thrombin, connective tissue growth factor (CTGF), epidermal growth factor (EGF), basic fibroblast growth factor (bFGF) and leptin. A majority of these mitogens, along with TGFβ1, likely sustain the survival and resistance to apoptosis of MFs;

b) Liver MFs are recognized as the principal cell type responsible for increased deposition of extracellular matrix (ECM) components, notably fibrillar collagen type I and type III; moreover, under chronic injury conditions, MFs undergo reprogramming, induced by TGFβ1 but can also occur in response to other growth factors (e.g. CTGF, bFGF), as well as ROS and related intermediates;

c) Liver MFs actively participate in inflammatory responses by expressing receptors for numerous cytokines, chemokines, and other mediators. Following activation, they can also contribute to recruit inflammatory cells by releasing chemoattractants such as CCL-2, CCL-21, and IL-1β;

d) Liver MFs are able to migrate in response to several chemoattractant polypeptides, including PDGF, CCL-2, VEGF, angiotensin I and Angiopoietin I. Most of these polypeptides induce MFs migration by triggering intracellular generation of ROS through ligand-receptor-mediated activation of NADPH-oxidase and activation of ERK and JNK pathways, a

phenomenon observed both under normoxic and hypoxic conditions (Novo et al., 2011; Novo et al., 2012);

e) Liver MFs, being sensitive to hypoxic conditions, can release pro-angiogenic mediators such as VEGF, Angiopoietin-1 or -2, or PDGF, contributing to neoangiogenesis, which parallels fibrogenesis and the formation of fibrotic septa. It is noteworthy that hypoxia and hypoxia-inducible factors are key players in sustaining the progression of fibrogenic CLDs, including NASH (Bocca et al., 2015, Lemoinne et al., 2016; Morello et al., 2018; Foglia et al., 2021);

f) Liver MFs exhibit the ability to contract and relax in response to different vasoactive compounds, like endothelins and nitric oxide (NO).

1.7 Human hepatic stellate cells (HSCs)

Human hepatic stellate cells (HSCs) originate from the septum transversum mesenchyme during embryonic development, and in the adult liver, they reside in the space of Disse, closely interacting with hepatocytes and sinusoidal endothelial cells (SECs) (Asahina et al., 2009; Asahina et al., 2011). In this niche, they play an important role in the production and remodeling of ECM components. Under physiological conditions, HSCs store vitamin A as retinyl esters and serve as liver-specific pericytes (Blomhoff and Wake, 1991; Pinzani et al., 1992). However, when activated, they undergo a process of transdifferentiation in which they loose vitamin A-containing droplets and express the typical characteristics and phenotypic responses of MFs. Activated HSCs play a crucial role in regulating various critical processes, including hepatic growth, inflammation, immune responses, as well as energy and nutrient homeostasis (Trivedi et al., 2021). Given that HSCs are widely acknowledged as the primary source of liver MFs in CLDs, most of the available data pertain to HSCs and their transition into HSC/MFs. Literature data indicate that, in the context of chronic liver injury, quiescent HSCs undergo activation and transdifferentiation, assuming the activated MF-like phenotype that significantly contributes to the fibrogenic progression of CLDs (Tsuchida and Friedman, 2017). When the causative factor of liver injury is removed, HSC/MFs decrease in number, either through apoptosis or by reverting to an "inactive" phenotype characterized by a distinct epigenetic signature. These inactive HSCs have been observed to rapidly re-activate in the event of re-injury (Kisseleva et al., 2012; Troeger et al., 2012; Liu et al., 2020). The activation of HSCs, similar to MFs, is triggered by the diversearray of signals mentioned earlier, leading HSCs to initiate pro-fibrogenic paracrine and autocrine loops.

These loops involve key signaling molecules, including TGFβ-1, PDGF, VEGF, CCL-2 and, possibly, CTGF, all of which play critical roles in the fibrogenic cascade (Higashi et al., 2017).

1.8 Mediators involved in NAFLD/NASH progression: SerpinB3 (SB3) and Oncostatin M (OSM)

At present, the mechanisms underlying disease progression are only partially defined, with literature data suggesting that NAFLD progression is surely dependent on chronic injury and persistent inflammatory response but may be also related to the development of hepatic hypoxia and by the related involvement of hypoxia-inducible factors (HIFs)-dependent release of specific mediators. Accordingly, the present thesis will further investigate the role of two specific mediators like Oncostatin M (OSM), a cytokine belonging to the IL-6 family, and SerpinB3 (SB3), a HIF2α-dependent mediator.

1.8.1 Serpins superfamily and SerpinB3 (SB3)

Serpins represent the largest and functionally diverse family of proteinase inhibitos, role from which they take their name: SERine Protease INhibitors (Potempa et al., 1994). Many members of this family behave as protease-inhibitor performing a lot of important functions, by acting on proteolitic cascades involved in apoptosis, inflammation, digestion, blood cotting and the complement system (Zhen et al., 2009). By contrast, certain SERPINs do not have inhibitory functions but instead serve as hormonal transporters and molecular chaperones (Law et al., 2006). From a phylogenetic perspective, human SERPINs have been classified into nine clades, designated from A to I (Silverman et al., 2001). Serpins possess a metastable structure consisting in a single polypeptidic chain of about 330-500 aminoacids, with a secondary structure highly conserved made of three β-sheets (A, B, C), nine α-helix and one Reactive Centre Loop (RCL) domain. This domain, made of 17 aminoacids placed between A and C β-sheets, is fundamental for the interaction with target proteases and therefore for their correct activity. In the native state, serpins are in a monomeric state with the RCL domain exposed. This domain is then easily recognised by the active catalytic site of the target protease, which will then bind to serpin that, in turn, will act as a suicide substrate inhibiting the enzyme. The proteolytic degradation of the RCL domain made by the target protease induces a series of conformational changes in the new-formed complex Serpin-Protease, promoting a greater conformational stability due to the formation of an irreversible covalent bond between the two molecules. This process, called inhibitory pathway, leads to the inhibition of both serpin and target protease. Sometimes the protease undergoes a deacetylation process that impairs the conformational changes in order to give the right stability to the complex.

In this case the Serpin becomes a real substrate of its target protease; then the still active protease detaches from the now inactive serpin (substrate pathway) (Gettins, 2002; Vidalino et al., 2009).

Among all Serpins, SerpinB3 has been extensively investigated in the past and found, for example, to inhibits apoptosis induced by different types of stress, including UV, radiation, chemotherapy, TNF-α and NK cells. TNF-α-induced cell death is impaired by SerpinB3 by inhibiting the release of mitochondrial cytochrome c and preventing caspase-3 activation (Hashimoto et al., 2005). SerpinB3 is also able to protect from radiation-induced cell death through two signalling pathways: i) reduction of p38 MAPk or MKK3/MKK6 phosphorylation (Murakami et al., 2001); ii) via suppression of c-JUN (Katagiri et al., 2006). Relevant to the present thesis, a study performed by Novo and colleagues in 2017 demonstrated the pro-fibrogenic role of SerpinB3 in experimental conditions of CLD by employing transgenic mice manipulated to overexpress SerpinB3 in hepatocytes. Using two distinct pro-fibrogenic murine protocols of CLD like chronic administration of carbon tetrachloride (CCl_4) or the methionine and choline deficient (MCD) dietary NASH-related protocol, it has been observed that the overexpression of SerpinB3 significantly worsened experimental liver fibrosis. This effect was strictly related to a significant increase in the transcript levels of pro-fibrogenic genes as well as of collagen deposition and the increased number of αSMA-positive MFs, as compared to wild-type mice. Moreover, *in vitro* experiments in the same study demonstrated that human recombinant SerpinB3 strongly and directly upregulated the expression of the same critical pro-fibrogenic genes in either human HSC/MFs or human LX2 cells, including TGFβ1, α-smooth muscle actin (α-SMA), collagen 1A1 (Col1A1), tissue inhibitor of metalloprotease 1 (TIMP-1), platelet-derived growth factor B (PDGF-B) and the related receptor β (PDGFRβ). Furthermore, in the same myofibroblast-like cells human recombinant SerpinB3 also promoted their oriented migration in a reactive oxygen species (ROS) - dependent manner through the activation of Akt and c-Jun-aminoterminal kinases (JNKs).

1.8.2. Oncostatin M (OSM)

Pro-inflammatory cytokines play a crucial role in the complex environment within tumors, influencing inflammatory responses and maintaining immune balance. Among these cytokines, Oncostatin M (OSM), a member of the IL-6 family, stands out as a significant player involved in the progression of CLD and HCC development. OSM is primarily produced by activated immune cells and has been implicated in the development of various cancers, as reviewed by Masjedi et al. in 2021. In humans, OSM possesses a unique capability – it

can bind to two distinct heterodimeric receptors: type I (gp130/LIFRb) and type II (gp130/OSMRb) receptors. Unlike other gp130 cytokines, OSM employs gp130 as its low-affinity α-receptor. OSM receptor b (OSMRβ) functions as its dedicated receptor subunit, forming heterodimers with gp130 to mediate most of OSM's effects (Stephens and Elks, 2017). When OSM binds to the extracellular regions of these receptors, it triggers the activation of Janus-activated kinase -1 (JAK1) or -2 (JAK2). These kinases, in turn, phosphorylate several signaling molecules, including signal transducer and activator of transcription -1 (STAT1), -3 (STAT3), -5 (STAT5), SH2 containing protein tyrosine phosphatase-2 (SHP-2), and the adaptor protein p66 (Shc). Moreover, activated SHP-2 and Shc can activate downstream proteins like mitogen-activated protein kinases (MAPKs), including extracellular-regulated kinase 1/2 (ERK1/2), p38, c-Jun N-terminal kinase (JNK), and the phosphatidylinositol-3-kinase (PI3K)/AKT pathway (Masjedi et al., 2021). Interestingly, OSM was initially identified for its anti-cancer potential, hence the name "oncostatin M," due to its ability to inhibit cell growth in cultured human cancer cells. However, subsequent studies have revealed that OSM, like most gp130-related cytokines, exerts diverse effects on various biological processes. These effects are highly dependent on the specific cell type and tissue context. In several instances, OSM has demonstrated pro-tumorigenic properties, promoting cancer progression by altering the tumor microenvironment. Notably, the binding of OSM to the type II receptor triggers the OSM-JAK2-STAT3 axis, leading to the activation of SMAD3. This, in turn, enhances the expression of MMP2 and VEGF, ultimately promoting angiogenesis and invasive behavior, thereby facilitating tumor progression (Masjedi et al., 2021).

AIM OF THE STUDY

Non-alcoholic fatty liver disease (NAFLD) is the most important chronic liver disease and is becoming a global health problem due to its prevalence and incidence that are rapidly increasing worldwide (Loomba and Sanyal, 2013; Younossi et al., 2016; Younossi et al., 2018; Younossi et al., 2019; Golabi et al., 2023). NAFLD includes a spectrum of conditions ranging from simple steatosis or fatty liver, to the progressive form of non-alcoholic steatohepatitis or NASH, that is at the more severe end of the spectrum (Singh et al., 2015; Chalasani et al., 2018; Ahmed et al., 2015; Machado et al., 2016). In NAFLD, hepatic steatosis is present without evidence of inflammation, while in NASH this feature is associated with lobular inflammation and hepatocyte injury that can lead to fibrosis and cirrhosis (Pouwels et al., 2022; Younossi et al., 2018).

As mentioned before, NAFLD is considered a serious condition and it is often associated with Type 2 Diabetes Mellitus (T2DM) and obesity and it is considered as the hepatic manifestation of metabolic syndrome (Marchesini et al., 2001; Chalasani et al., 2018; Samuel and Shulman, 2018). Patients with NAFLD have characteristics of metabolic syndrome, with the associated cardiovascular disease risk factors (Byrne et al., 2015; Anstee et al., 2013).

NAFLD is a disease resulting from different causes, like dysregulated metabolism (dietary influence, muscle-related factors, hepatic insulin resistance, adipose tissue implications), lipotoxicity (increased DNL, increased fatty acid esterification into TGs), genetic variants (PNPLA3, TM6SF2, MBOAT7, GCKR, HSD17B13) and changes in gut microbiome (increased prevalence of Streptococcus and Gram-negative bacteria). The transition from simple steatosis to steatohepatitis is characterised by several events that sustain a persistent inflammatory response and activated repair mechanisms (Gong et al., 2020). In the background of progressive NAFLD, another important process is liver fibrogenesis, a molecular, cellular and tissue process that results in a progressive accumulation of extracellular matrix (ECM) components and drives the progression of CLD (Novo et al., 2017; Parola and Pinzani, 2019).

An important feature of NAFLD is hepatocyte injury that appears to primarily depend on factors such as lipotoxicity, oxidative stress, mitochondrial dysfunction and other mechanisms, in addition to the accumulation of TGs (Neuschwander-Tetri, 2010; Marra and Svegliati-Baroni, 2018; Loomba et al., 2021). The latter result of hepatocyte injury and death is the release of stressed signals by hepatocytes, also called danger signals, which trigger the activation of the inflammatory pathway that, perpetuating over time, results in chronic

injury and an abnormal wound healing response with fibrosis (Arrese et al., 2016; Arguello et al., 2015; Seki et al., 2015). These events sustain the transition from simple steatosis to steatohepatitis.

The mechanisms involved in the disease progression are not completely undestood, but literature data suggest that NAFLD progression depends on chronic injury, persistent inflammatory response, hypoxia and mediators that are released in a hypoxia-inducible pactors (HIFs)-dependent manner. Along these lines, this study is focused on the analysis of two different mediators involved in NAFLD/NASH progression:

- SerpinB3 (SB3), a HIF2α-dependent mediator;
- Oncostatin M (OSM), pleiotropic cytokine structurally and functionally related to the interleukin-6 (IL-6) cytokine family.

Data from literature show that Serpin B3 (SB3), a protein belonging to the Serine-proteas e inhibitor family and regulated by hypoxia through the hypoxia-inducible factor hypoxia -2α (HIF-2α), is a mediator involved in the progression of CLDs and in the development of HCC (Cannito et al., 2015; Pontisso, 2014). Recent literature data have also shown that SB3 produced by hepatic parenchymal cells plays a major role in the progression of CLDs by modulating the major pro-fibrogenic responses of hepatic myofibroblasts and promoting hepatic fibrogenesis (Novo et al., 2017). Since the inflammatory process plays also a key role in this pro-fibrogenic scenario, the first purpose of the present thesis work was to evaluate the still unexplored pro-inflammatory role of this protein in relation to the progression of NAFLD by using both *in vivo* and *in vitro* models.

To further investigate the role of SerpinB3 in dysregulation of lipid metabolism and NASH progression, a second aim of the study was to investigate the putative protective role of a small compound recently patented and proposed as a specific SerpinB3 inhibitor, 1-Piperidine Propionic Acid (1-PPA) (Toshihiko, 2009; Pontisso et al., 2018).

It is also known that SB3 is not detectable in normal adult hepatocytes; wherease, chronically damaged hepatocytes express SerpinB3 and the highest levels are achieved in the most aggressive forms of HCC (Turato et al., 2014). Literature data suggest also that SB3 increase cell proliferations both through the induction of β-catenin and Myc oncogenea downstream gene of the Wnt pathway (Turato et al., 2012). Based on this knowledge, the third aim of this thesis was to analyse wheter SB3 is involved in the regulation of low-density

lipoprotein receptors (LRPs), fundamental co-receptors for the activation of canonical Wnt signaling.

Concerning OSM, it is already known that this cytokine is involved in the pathogenesis of steatosis and hepatic insulin resistance (Komori et al., 2014) and that OSM reduces cardiac injury by activating Notch signaling and in OSMRβ/KO mice the myocardical injury is exacerbated since Notch signalling is reduced (Zhang et al., 2015). Since recent data suggest the role of Notch in NASH progression (Xu and Wang, 2021), the last aim of this study was to investigate whether Notch was involved in OSM action by using both *in vivo* and *in vitro* models.

MATERIALS AND METHODS

3.1 Materials (unpublished study)

The choline-deficient aminoacid-refined (CDAA) diet, as well as the related control diet, choline-supplemented and aminoacid-refined (CSAA) diet, were provided by Laboratorio Dottori Piccioni srl (Gessate, Milano, Italy). Enhanced chemiluminescence (ECL) reagents, nitrocellulose membranes (Hybond-C extra) were from Amersham Pharmacia Biotech Inc. (Piscataway, NJ, USA). The following reagents were purchased from Merck Life Science (Milan, Italy): sodium chloride (NaCl), bovine serum albumin (BSA), ethanol, phosphate saline buffer (PBS), citric acid, sodium citrate, hydrogen peroxide, TWEEN, Mayer's hematoxylin, sodium azide (NaN3), TRI reagent, diaminobenzidine (DAB), Entellan® Slide Mounting Medium and primers used in Real-Time PCR reactions. The kit for RNA retro-transcription and for real time PCR were purchased from BioRad (Berkeley, CA, USA). Quantitative RT-PCR analyses were carried out using the MiniOpticon™ Real-Time PCR Detection System instrument of the BioRad company (BioRad, Milan, Italy), which also supplied the EvaGreen master mix reagent. Antibody for western blot analysis for anti Notch1 1:1000 (cod. sc- 376403), anti Hes 1 1:1000 (cod. sc- 166410) were raised in mouse and purchased from Santa Cruz Biotechnology (Santa Cruz, CA, USA). Secondary antibody goat anti-mouse (cod. 1706516), were purchased from BioRad (Berkeley, CA, USA). Human recombinant Oncostatin M (OSM) was from Petrotech (Rocky Hill, CT, USA). Trygliceride (TG) colorimetric assay kit (single-reagent, GPO-PAP method) were purchased from Assay Genie (Dublin, Ireland).

3.2 Methods (unpublished study)

For *in vivo* experiments we used wild-type mice and mice with hepatocyte-specific deletion of the OSMRβ, obtained by crossing OSMRβ fl/fl mice and Alb-Cre mice (hepOSMRβ-/- mice) to block the action of murine OSM, that in mice binds the gp-130/OSMRβ heterodimer. These mice, which are all on the C57Bl/6 background, are subjected to establish dietary protocols for the induction of progressive murine NAFLD, in particular choline-deficient L- amino acid-defined (CDAA) diet or fed on the respective control diet (CSAA). The dietary protocol was administered for 26 weeks. Mice were kept under specific pathogen-free conditions and maintained with free access to pellet food and water. Liver samples were obtained and immediately used/processed for morphological or molecular biology analyses or frozen and thereafter maintained at −80 °C for further analysis.

In vitro experiments were carried out on both human hepatic stellate cells-MF like cells (HSC/MFs) and human monocytes of the THP-1 cell line that were differentiated into macrophages by treatment for 48h with phorbol 12-myristate 13-acetate (PMA, 50 nM). HSCs were cultured in Dulbecco's modified Eagle's medium (Sigma Aldrich Spa, Milan, Italy), supplemented with 10% fetal calf serum and 1% antibiotics. HSCs were stimulated with OSM (10 ng/ml) at different time points. THP-1 cells were cultured in RPMI medium containing 10% fetal bovine serum, 100 U/ml of penicillin, 100 mg/ml of streptomycin and 25 mg/ml of Amphotericin-B (Merck Life Science, Milan, Italy). The differentiated THP-1 cells, after 24h of incubation with fresh culture medium, were stimulated with OSM (10 ng/ml).

Hematoxylin-Eosin staining (H&E)

Hematoxylin-Eosin staining was performed on murine liver sections obtained by mice fed with CSAA diet or CDAA diets in order to evaluate liver steatosis. Following the preparation of a paraffin section, all the elements are infiltrated with and surrounded by paraffin wax which is hydrophobic and impervious to aqueous reagents. The majority of cell and tissue components have no natural color and are not visible, so the first step in performing an H&E stain is to dissolve all the wax away with xylene (a hydrocarbon solvent). The slides are passed through several changes of alcohol to remove the xylene, then thoroughly rinsed in water. The sections are now hydrated. The staining is performed by using Hematoxylin, followed by washing in water, then, by using Eosin. Stained sections are dehydrated by washing in alcohols.

Trygliceride (TG) colorimetric assay kit (single-reagent, GPO-PAP method)

After washing a liver tissue sample of approximately 50mg, it was homogenised with Isopropanol at a ratio of 1:10. Then, the homogenate was centrifuged for 10 minutes at 10000 rcf at 4°C, after that the supernatant was removed. Three tubes were prepared for the measurement: blank tube, with 10 µl of double-distilled water, standard tube with 10 µl of standard solution and sample tube with 10 µl of sample. 1 ml of working solution was then added to each tube and left to incubate for 10 minutes. Finally, the absorbance was evaluated by using the spectrophotometer at 510 nm.

Quantitative real-time PCR (q-PCR)

In cell lines and in liver tissue samples total RNA was extracted using RNasy Trizol (Invitrogen, Carlsbad, CA, USA) according to the manufacturer's instructions. After determination of the purity and the integrity, total RNA, complementary DNA synthesis and quantitative real-time PCR reactions (RT-PCR) were carried out using the CFX96 real-time instrument (Bio-Rad Laboratories Inc, Hercules, CA, USA). Relative gene expression was normalized to the housekeeping genes, β-actin and Gliceraldehyde-3-phosp hate dehydrogenase (GAPDH), used as internal reference for murine and human sample respectively, and co-amplified with target samples using identical Q-PCR conditions. Samples were run in triplicate and mRNA expression was generated for each sample. Relative gene expression was calculated using the $2^{-\Delta\Delta CT}$ method. Specificity of the amplified PCR products was determined by melting curve analysis.

GENES	PRIMERS
SREBP-1 (mouse)	(FW) 5' GATCAAAGAGGAGCCAGTGC 3'
	(RV) 5' TAGATGGTGGCTGCTGAGTG 3'
Cpt1 (mouse)	(FW) 5' CCAGGCTACAGTGGGACATT 3'
	(RV) 5' GAACTTGCCCCATGTCCTTGT 3'
CD-36 (mouse)	(FW) 5' TGCTGGAGCTGTTATTGGTG 3'
	(RV) 5' TGGGTTTTGCACATCAAAGA 3'
Notch 1 (mouse)	(FW) 5' AAGTGGGACCTGCCTGAATG 3'
	(RV) 5' GATTGGAGTCCTGGCATCGT 3'
Notch 3 (mouse)	(FW) 5' ATGTGCAAATGGAGGTCGGT 3'
	(RV) 5' CACTGAACTCTGGCAAACGC 3'
Jag 1 (mouse)	(FW) 5' ACGTACTTCAAAGTGTGCCTC 3'
	(RV) 5' CTCCACCAGCAAAGTGTAGGA 3'
Hes 1 (mouse)	(FW) 5' CAACACGACACCGGACAAAC 3'
	(RV) 5' TTGGAATGCCGGGAGCTATC 3'
DLL1 (mouse)	(FW) 5' AGATAACCCTGACGGAGGCT 3'

	(RV) 5’ ACCGGCACAGGTAAGAGTTG 3’
DLL4 (mouse)	(FW) 5’ ATGGGGAGGTCTGTTTTGTGAC 3’
	(RV) 5’ CCTTACAGCTGCCACCATTTCG 3’
β-actin (mouse)	(FW) 5’ AGCCATGTACGTAGGCCATCC 3’
	(RV) 5’ CTCTCAGCTGTGGTGGTGAA 3’
Notch 1 (human)	(FW) 5’ GAATGGCGGGAAGTGTGAAGC 3’
	(RV) 5’ TAGTCTGCCACGCCTCTGC 3’
Notch 3 (human)	(FW) 5’ CCCTTCCTGCGATCAGGACATC 3’
	(RV) 5’ GGTTGCTCAGGCACTCATCCA 3’
Jag 1 (human)	(FW) 5’ CGCGTGACCTGTGATGACTA 3’
	(RV) 5’ TTAAGGACTGCAGCCTTGTCG 3’
Hes 1 (human)	(FW) 5’ GAGAGGCGGCTAAGGTGTTT 3’
	(RV) 5’ CCCCGTTGGGAATGAGGAAA 3’
DLL1 (human)	(FW) 5’ GGAGAAAGTGTGCAACCCTG 3’
	(RV) 5’ CCCACTCTGCACTTGCATTC 3’
DLL4 (human)	(FW) 5’ CCCTGGCAATGTACTTGTGAT 3’
	(RV) 5’ TGGTGGGTGCAGTAGTTGAG 3’
GAPDH (human)	(FW) 5’ TGGTATCGTGGAAGGACTCATGAC 3’
	(RV) 5’ ATGCCAGTGAGCTTCCCGTTCAGC 3’

Western blotting analysis

Briefly, total cell lysates were subjected to sodium dodecyl sulfate-polyacrylamide gel-electrophoresis on 10% acrylamide gels, incubated with desired primary antibodies, then with peroxidaseconjugated anti-mouse or anti-rabbit immunoglobulins in Tris-buffered Saline-Tween containing 2% (w/v) non-fat dry milk and finally developed with the ECL reagents according to manufacturer’s instructions. Sample loading was evaluated by re-blotting the same membrane with β-actin antibody.

Statistical analysis

Statistical significance was determined by non-parametric procedures using the Student's t test or ANOVA for analysis of variance. Normality of distribution for quantitative variables was assessed by Kolmogorov and Smirnov test. The calculations were carried out with Graph Pad InStat Software (San Diego, CA, USA). The null hypothesis was rejected at $P<0.05$. Data in bar graphs represent means $\pm$ SEM and were obtained from at least three independent experiments. Western-blot and morphological images are representative of at least three experiments with similar results.

RESULTS

4.1 PAPER N°1

SerpinB3 as a Pro-Inflammatory Mediator in the Progression of Experimental Non-Alcoholic Fatty Liver Disease

Published on Front Immunol. 2022 Jul 8:13:910526. doi: 10.3389/fimmu.2022.910526. eCollection 2022.

Authors: Erica Novo, Andrea Cappon, Gianmarco Villano, Santina Quarta, Stefania Cannito, Claudia Bocca, Cristian Turato, Maria Guido, Marina Maggiora, **Francesca Protopapa**, Salvatore Sutti, Alessia Provera, Mariagrazia Ruvoletto, Alessandra Biasiolo, Beatrice Foglia, Emanuele Albano, Patrizia Pontisso, Maurizio Parola.

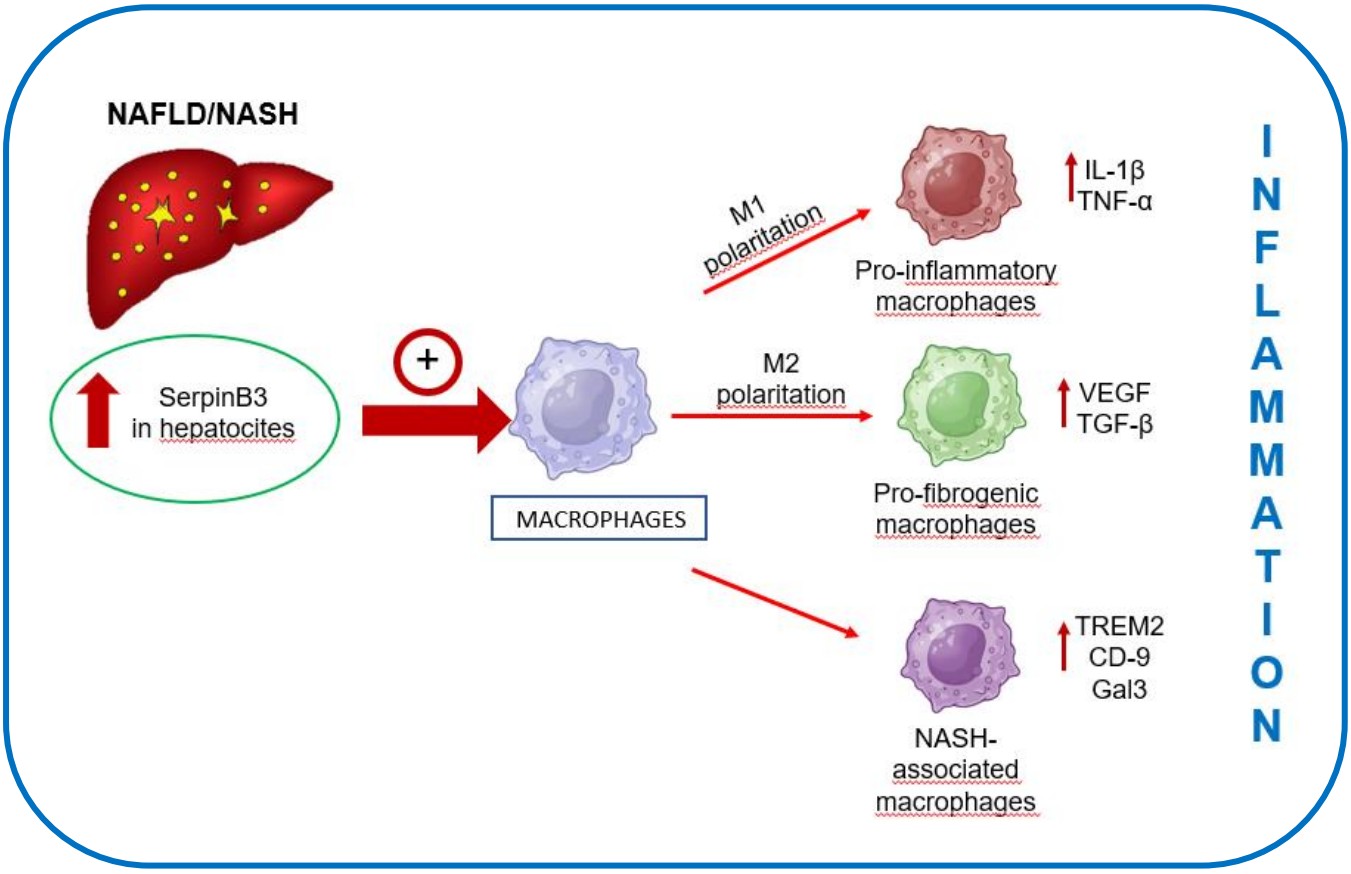

frontiers | Frontiers in Immunology

ORIGINAL RESEARCH
published: 08 July 2022
doi: 10.3389/fimmu.2022.910526

SerpinB3 as a Pro-Inflammatory Mediator in the Progression of Experimental Non-Alcoholic Fatty Liver Disease

Erica Novo[1†], Andrea Cappon[2†], Gianmarco Villano[3], Santina Quarta[2], Stefania Cannito[1], Claudia Bocca[1], Cristian Turato[4], Maria Guido[2], Marina Maggiora[1], Francesca Protopapa[1], Salvatore Sutti[5], Alessia Provera[5], Mariagrazia Ruvoletto[2], Alessandra Biasiolo[2], Beatrice Foglia[1], Emanuele Albano[5], Patrizia Pontisso[2‡] and Maurizio Parola[1*‡]*

[1] Department of Clinical and Biological Sciences, Unit of Experimental Medicine and Clinical Pathology, University of Torino, Torino, Italy, [2] Department of Medicine, University of Padova, Padova, Italy, [3] Department of Surgical, Oncological and Gastroenterological Sciences – DISCOG, University of Padova, Padova, Italy, [4] Department of Molecular Medicine, University of Pavia, Pavia, Italy, [5] Department of Health Sciences, University of Piemonte Orientale, Novara, Italy

OPEN ACCESS

Edited by:
Daniela Bosisio,
University of Brescia, Italy

Reviewed by:
Davide Povero,
Mayo Clinic, United States Janin Henkel-Oberlaender,
University of Bayreuth, Germany

***Correspondence:**
Patrizia Pontisso
patrizia@unipd.it
Maurizio Parola
maurizio.parola@unito.it

[†]These authors have contributed equally to this work and share first authorship

[‡]These authors have contributed equally to this work and share last authorship

Specialty section:
This article was submitted to Inflammation, a section of the journal Frontiers in Immunology

Received: 01 April 2022
Accepted: 20 June 2022
Published: 08 July 2022

Citation: Novo E, Cappon A, Villano G, Quarta S, Cannito S, Bocca C, Turato C, Guido M, Maggiora M, Protopapa F, Sutti S, Provera A, Ruvoletto M, Biasiolo A, Foglia B, Albano E, Pontisso P and Parola M (2022) SerpinB3 as a Pro-Inflammatory Mediator in the Progression of Experimental Non-Alcoholic Fatty Liver Disease. Front. Immunol. 13:910526. doi: 10.3389/fimmu.2022.910526

Non-alcoholic fatty liver disease (NAFLD) is becoming the most common chronic liver disease worldwide. In 20-30% of patients, NAFLD can progress into non-alcoholic steatohepatitis (NASH), eventually leading to fibrosis, cirrhosis and hepatocellular carcinoma development. SerpinB3 (SB3), a hypoxia-inducible factor-2α dependent cysteine protease inhibitor, is up-regulated in hepatocytes during progressive NAFLD and proposed to contribute to disease progression. In this study we investigated the pro-inflammatory role of SB3 by employing phorbol-myristate acetate-differentiated human THP-1 macrophages exposed *in vitro* to human recombinant SB3 (hrSB3) along with mice overexpressing SB3 in hepatocytes (TG/SB3) or knockout for SB3 (KO/SB3) in which NASH was induced by feeding methionine/choline deficient (MCD) or a choline-deficient, L-amino acid defined (CDAA) diets. *In vivo* experiments showed that the induction of NASH in TG/SB3 mice was characterized by an impressive increase of liver infiltrating macrophages that formed crown-like aggregates and by an up-regulation of hepatic transcript levels of pro-inflammatory cytokines. All these parameters and the extent of liver damage were significantly blunted in KO/SB3 mice. *In vitro* experiments confirmed that hrSB3 stimulated macrophage production of M1-cytokines such as TNFα and IL-1β and reactive oxygen species along with that of TGFβ and VEGF through the activation of the NF-kB transcription factor. The opposite changes in liver macrophage activation observed in TG/SB3 or KO/SB3 mice with NASH were associated with a parallel modulation in the expression of triggering receptor expressed on myeloid cells-2 (TREM2), CD9 and galectin-3 markers, recently detected in NASH-associated macrophages. From these results we propose that SB3, produced by activated/injured hepatocytes, may operate as a pro-inflammatory mediator in NASH contributing to the disease progression.

Keywords: NASH, SerpinB3, macrophages, innate immunity, hepatocytes

INTRODUCTION

Non-Alcoholic Fatty Liver Disease (NAFLD) is rapidly becoming the major cause of chronic liver disease (CLD) worldwide, with epidemiological data indicating a 25% prevalence in the general population and an even higher prevalence in obese and Type II diabetes patients (1–5). The term NAFLD encompasses a spectrum of liver diseases ranging from simple hepatic steatosis or NAFL, without significant evidence of hepatocellular damage, to non-alcoholic steatohepatitis (NASH) characterized by cell damage (ballooning), cell death and lobular inflammation, with or without fibrosis. NASH can develop in at least 20-30% of patients and can progress to liver cirrhosis and associated complications (1–5), including the development of hepatocellular carcinoma (HCC) which, in turn, can also develop in non-cirrhotic patients (6–8). At present the mechanisms underlying the progression of NAFLD towards more advanced stages of the disease are only partially defined and validated therapies for this liver disease are not currently available, although several drugs are continuously evaluated in clinical trials and novel therapeutic approaches are being designed (9–14).

A major issue favoring NAFLD progression is represented by the chronic activation of inflammatory response, which involves either macrophages originating from resident hepatic Kupffer cells or $CCR2^{+}$/Ly-$6C^{hi}$ monocyte-derived macrophages (MoMFs) recruited from peripheral blood (15–17). In particular, during NAFLD progression MoMFs acquire peculiar pro-inflammatory, pro-angiogenic and pro-fibrogenic phenotype which plays a major role in sustaining the activation of hepatic stellate cells (HSCs) and other precursor cells into hepatic myofibroblasts (MFs) by the release of several mediators (15–17). More recently, different laboratories have described the emergence, during NAFLD progression and/or in condition of altered lipid metabolism, of a peculiar macrophage phenotype characterized by the expression of Triggering Receptor Expressed on Myeloid cells-2 or TREM2, CD9 and CD68 (18–21), sometimes referred to as NASH-associated macrophages (NAMs) or hepatic lipid-associated macrophages (hepatic LAMs).

The critical persistent activation of hepatic macrophages in NAFLD progression is believed to represent the consequence of complex interactions between growth factors, cytokines, chemokines, reactive oxygen species (ROS) and other less characterized mediators (13–16). Of interest, it has been proposed that NAFLD progression may be closely related to the development of hepatic hypoxia, a tissue event believed to sustain angiogenesis, fibrogenesis as well as inflammatory response through hypoxia-inducible factors (HIFs) - dependent release of specific mediators (16, 22, 23). Along these lines, recent data have outlined the hepatocytes production of histidine-rich glycoprotein (HRG) and SB3 in response to HIF2α-dependent signals (16, 23–26). SerpinB3 is a protein belonging to the family of serine-protease inhibitors (27) which is specifically expressed by hepatocytes and although virtually undetectable in healthy human and murine livers it is greatly up-regulated in liver biopsies from patients with CLD (28–31). Recently, we provided evidence that SB3 can exert a pro-fibrogenic role in the progression of experimental CLD, including experimental NAFLD, by directly acting on activated, myofibroblast-like, hepatic stellate cells (HSC/MFs) in which leads to the up-regulation of major genes involved in fibrogenesis (18). In the present study we take advantage of mice genetically manipulated to carry hepatocyte-specific SB3 overexpression or deletion to provide mechanistic evidence that this protease inhibitor can contribute to NAFLD progression also by acting as a pro-inflammatory mediator.

Abbreviations: NAFLD, non-alcoholic fatty liver disease; NASH, non-alcoholic steatohepatitis; SB3, SerpinB3; hrSB3, human recombinant SB3; HRG, histidine rich glycoprotein; MCD, methionine/choline deficient; CDAA, choline-deficient, L-amino acid defined; TREM2, triggering receptor expressed on myeloid cells-2; HCC, hepatocellular carcinoma; MoMFs, monocyte-derived macrophages; HSCs, hepatic stellate cells; MFs, hepatic myofibroblasts; NAMs, NASH-associated macrophages; LAMs, lipid-associated macrophages; ROS, reactive oxygen species; HRG, histidine-rich glycoprotein; CLD, chronic liver diseases; HSC/MFs, myofibroblast-like, hepatic stellate cells; MCS, methionine choline supplemented diet; CSAA, choline-supplemented and aminoacid-refined diet; ECL, Enhanced chemiluminescence; PBS, phosphate saline buffer; NaCl, sodium chloride; BSA, bovine serum albumin; NaN3, sodium azide; PMA, phorbol 12-myristate 13-acetate; DAB, 3'-3'diaminobenzidine substrate; ALT, alanine aminotransferase; qRT-PCR, quantitative Real Time PCR; DCFH-DA, 2′,7′-Dichlorofluorescin diacetate; SAMs, scar-associated macrophages; FGF21, fibroblast growth factor 21.

MATERIALS AND METHODS

Materials

The methionine and choline-deficient (MCD) diet, the choline-deficient aminoacid-refined (CDAA) diet, as well as the related control diets, methionine choline supplemented (MCS) diet and choline-supplemented and aminoacid-refined (CSAA) diet were provided by Laboratorio Dottori Piccioni srl (Gessate, Milano, Italy). Enhanced chemiluminescence (ECL) reagents, nitrocellulose membranes (Hybond-C extra) were from Amersham Pharmacia Biotech Inc. (Piscataway, NJ, USA). The following reagents were purchased from Merck Life Science (Milan, Italy): sodium chloride (NaCl), bovine serum albumin (BSA), ethanol, phosphate saline buffer (PBS), citric acid, sodium citrate, hydrogen peroxide, TWEEN, Mayer's hematoxylin, sodium azide (NaN3), TRI reagent, diaminobenzidine (DAB), Entellan® Slide Mounting Medium, inhibitor BAY-117082 and primers used in Real-Time PCR reactions. The kit for RNA retro-trascription and for real time PCR were purchased from BioRad (Berkeley, CA, USA). Quantitative RT-PCR analyses were carried out using the MiniOpticon™ Real-Time PCR Detection System instrument of the BioRad company (BioRad, Milan, Italy), which also supplied the EvaGreen master mix reagent. Human recombinant SerpinB3 (hrSB3) was produced in our laboratory, as previously described (28). The antibodies used in immunohistochemistry for F4/80 and for Galectin-3 were purchased from Thermofisher Scientific (Waltham, MA, USA) and R&D system (Minneapolis, MN, USA), respectively. Antibody for western blot analysis for anti NFkB 1:1000 (cod. sc-372), anti IL1β 1:1000 (cod. sc-7884) were raised in rabbit and

purchased from Santa Cruz Biotechnology (Santa Cruz, CA, USA), whereas anti p-IkB 1:1000 (cod. 9246S), anti IkB 1:1000 (cod. 4814S) were raised in mice and purchased from Cell Signaling (Massachusetts, USA). Secondary antibodies, goat anti-rabbit (cod. 1706515) and goat anti-mouse (cod. 1706516), were purchased from BioRad (Berkeley, CA, USA).

Methods

Animal Experimentation

The role of SB3 in NAFLD/NASH progression was evaluated by employing two different types of genetically manipulated mice (n=8 for each experimental group): 1) C57Bl6J mice that overexpress human SB3 (31, 32), thereafter referred to as TG/SB3 mice. Briefly, these mice were generated by Professor G. Cassani (Technogen S.c.p.A, Piana di Monte Verna, CE, Italy) by inserting the sequence of human SerpinB3 (-7/+1238) into the pcDNA3 plasmid vector under the alpha1-antitrypsin promoter. The expression of SerpinB3 mRNA, as assessed in different organs, was shown to be high in brain, lung and liver, while it was low in the genitals and irrelevant in kidney and muscle (33). Moreover, further studies showed that within the liver the protein expression was limited to hepatocytes, whereas in other organs was detectable in cells of monocytic origin (34, 35); 2) BalbC mice deficient of the reactive site loop of Serpinb3a gene (KO/SB3 mice) (36) were a kind gift of Dr. Gary Silverman and Dr. Cliff J. Luke (University of Pittsburg, Children's Hospital, Pittsburg, PA) and were originated in a Balb/C mice background, as detailed in ref. 36. Wild-type (WT) strain-matched C57Bl6J and BalbC mice, 8 weeks old, were used as controls and were purchased by Charles River Laboratories (Charles River UK Ltd., Margate, UK). To induce NASH mice were fed on two distinct dietary regimens: a) methionine and choline deficient (MCD) diet for 8 weeks or a choline-deficient, L-amino acid defined (CDAA) diet for 12 weeks. The respective reference diets were methionine and choline supplemented (MCS) diet or choline-supplemented, L-amino acid defined (CSAA). All animals were kept in specific, pathogen free conditions and kept with free access to food and water at the authorized animal house of the Interdepartmental Center of Experimental Surgery of the University of Padova.

Assessment of Liver Injury

Livers were rapidly removed, rinsed in ice-cold saline and cut in pieces. Aliquots were immediately frozen in liquid nitrogen and kept at −80°C until analysis. Two portions of the left lobe from each liver were fixed in 10% formalin for 24h and embedded in paraffin. Blood was obtained from tail vein and plasma was separated for ALT determination. Liver sections (4-μm thick) were stained with hematoxylin/eosin using a Roche Ventana HE 600 automatic staining system (Roche Diagnostics International AG, Rotkreuz, Switzerland), while collagen deposition was detected by Picro-Sirius Red staining. Liver sections were scored blindly for steatosis and lobular inflammation, as previously described (24).

Cell Lines and Culture Conditions

In vitro experiments described in the present study were performed on the following three different macrophage cell culture models: 1) undifferentiated peripheral blood human monocytes obtained from healthy donors and isolated by centrifugation on Ficoll-Paque solution, seeded on Percoll 46% vol/vol solution (Amersham Biosciences) in RPMI 1640 medium containing 10% FCS and 4mM HEPES buffer. Briefly, monocytes were harvested, re-suspended in medium containing 2% FCS and separated from contaminating lymphocytes by adherence to plastic (1h at 37°C). Adherent monocytes were then washed with medium to remove residual non-adherent cells. The percentages of $CD134^+$ cells were higher than 98%; 2) undifferentiated human monocytes of the THP-1 cell line, acquired from the American Type Culture Collection (ATCC, Manassas, VA 20108 USA); 3) human monocytes of the THP-1 cell line that were differentiated into macrophages by treatment for 48h with phorbol 12-myristate 13-acetate (PMA, 50 nM). THP-1 cells were cultured in RPMI medium containing 10% fetal bovine serum, 100 U/ml of penicillin, 100 μg/ml of streptomycin and 25 μg/ml of Amphotericin-B (Merck Life Science, Milan, Italy). The differentiated THP-1 cells, after 24h of incubation with fresh culture medium, were stimulated with hrSB3 (200 ng/ml); in some experiments the cells were pre-treated with the IKK protein inhibitor BAY-117082 and then treated with hrSB3 (200 ng/ml).

Immunohistochemistry, Sirius Red Staining and Histomorphometric Analysis

Immunohistochemistry analyses were performed on murine liver sections obtained by mice fed on MCD or CDAA diets. Immunostaining procedure was as previously described (24). Briefly, paraffin sections (4 μm thick), mounted on poli-L-lysine coated slides, were incubated with the monoclonal antibody against murine F4/80 (cod. 14-4801-82; Ebioscience, CA, USA; dilution 1:500) or with the polyclonal antibody against murine Galectin-3 (goat anti mouse, cod. AF1197, Biotechne/R&D System, MN, USA; dilution 1:50). After blocking endogenous peroxidase activity with 3% hydrogen peroxide and performing microwave antigen retrieval in sodium citrate buffer pH6, primary antibodies were labeled by using EnVision, HRP-labeled System (cod. K4001, Dako, CA, USA) and visualized by 3'-3'diaminobenzidine substrate (DAB). The nuclei were highlighted by counterstaining with Mayer's hematoxylin. Collagen deposition was evidenced by Picro-Sirius Red staining as previously described (24). In some experiments, hematoxylin/eosin staining was performed on murine liver sections obtained by mice fed with CDAA diets: these sections were scored blind for steatosis and lobular inflammation.

Biochemical Analyses

Plasma alanine aminotransferase (ALT) was determined by spectrometric kits supplied by Gesan Produzione SRL (Campobello di Mazara, Italy).

Quantitative Real Time PCR (qRT-PCR)

RNA extraction, complementary DNA synthesis, quantitative real-time PCR reactions were performed as previously described (31). RNA was extracted from mouse livers and from human cells with TRI reagent and retro-transcribed using the iScript™ cDNA Synthesis Kit (BioRad, Berkeley, CA, USA) according to the manufacturer's instruction. Realtime PCR was performed using either Miniopticon ThermoCycler Instrument (Biorad, Berkeley, CA, USA) or, for some genes (murine CD9, TREM-2 and Gal-3), a Techne TC-312 termacycler (Techne) using TaqMan Gene Expression Master Mix and TaqMan Gene Expression probes (Applied Biosystem Italia). Oligonucleotide sequence of primers used for RT-PCR were listed in **Supplementary Material**.

Western Blotting

Western blotting analysis was performed as previously described (24, 31). Briefly, total cell lysates were subjected to sodium dodecyl sulfate-polyacrylamide gel-electrophoresis on 10% acrylamide gels, incubated with desired primary antibodies, then with peroxidase-conjugated anti-mouse or anti-rabbit immunoglobulins in Tris-buffered Saline-Tween containing 2% (w/v) non-fat dry milk and finally developed with the ECL reagents according to manufacturer's instructions. Sample loading was evaluated by re-blotting the same membrane with the un-phosphorylated form of protein or with β-actin antibody (24, 31).

Detection of Intracellular Generation of ROS

Combination of DCFH-DA (2′,7′-Dichlorofluorescin diacetate) technique and flow cytometric analysis: THP-1 cells differentiated to macrophages were seeded in P35 dishes (5×10^5 cells/dish), cultured for 24 hrs and exposed to hrSB3 200ng/ml for 30 min, 1hr and 3hrs before addition of 5 μM DCFH-DA (15 min of incubation in the dark). Cells were rapidly washed with PBS, collected by trypsinization, briefly centrifuged (1600 rpm for 5 min) and re-suspended in PBS for analysis. Detection of DCF green fluorescence (FL1) was performed on at least 5000 cells per sample with a FACScan equipped with a 488 nm argon laser using the CellQuest software (version 1.0.264.21, Becton-Dickinson, Milano, Italy). The peak of FL1 intensity of DCFH-DA-stained control cells grown without SB3 was set to channel 101 and retained for all measurements (31).

ELISA Quantification

Specific ELISA kits were used to quantify TGFβ1, VEGF, TNFα and IL-1β released in the culture medium by THP-1 cells differentiated to macrophages, exposed or not to hrSB3 for different times, following the instructions of the supplier company (Invitrogen, Thermofisher Scientific Italia, Monza MI, Italy).

Statistical Analysis

Statistical analyses were performed by SPSS statistical software (SPSS Inc. Chicago IL, USA) using one-way ANOVA test with Turkey's correction for multiple comparisons or Kruskal-Wallis test for non-parametric values. Significance was taken at the 5% level. Normality distribution was assessed by the Kolmogorov-Smirnov algorithm. Data from *in vitro* experiments represent means ± SEM obtained from at least three independent experiments. Luminograms and morphological images are representative of at least three experiments with similar results.

RESULTS

Hepatocyte-Specific Manipulation of SB3 Expression Affects Inflammatory Response in Two Distinct Protocols of Murine NASH

Previous studies have evidenced that HIF2α-dependent signals are important in modulating inflammatory responses associated with the progression of NAFLD/NASH (24). Since SB3 is strictly associated with HIF2α regulation (25), here we investigated whether, beside a pro-fibrogenic action, SB3 might have pro-inflammatory role in NAFLD/NASH. In preliminary experiments, we first analyzed liver samples from either WT or TG/SB3 mice fed for 8 weeks on the MCD diet for inflammatory infiltration. Immunohistochemistry analysis for the murine macrophage marker F4/80 revealed that macrophage infiltration was greatly increased in the liver of TG/SB3 mice as compared to WT mice fed on MCD diet (**Figure 1A**). According to previous observations (23, 37), the macrophages accumulating in the livers of MCD-fed mice had a foamy appearance and formed aggregates with a crown-like structures (**Figure 1A**). Histo-morphometric analysis confirmed that the prevalence of these aggregates was significantly increased in TG/SB3 (**Figure 1B**). Accordingly, transcripts for markers of pro-inflammatory macrophage activation such as CD11b, TNFα, and IL-12 were significantly higher in the liver of TG/SB3 mice than in those of WT mice fed on MCD diet (**Figure 1C**).

To further evaluate the effects of SB3 in NASH-associated inflammation, additional experiments were performed by inducing steatohepatitis with choline-deficient aminoacid-refined (CDAA) diet that, differently from the MCD diet, does not cause malnutrition and more closely resembles human NASH (24). We observed that in wild type mice receiving the CDAA diet for 12 weeks the development of steatohepatitis and the increased presence of macrophage crown-like aggregated (**Figures 2A, B**) associated with a three folds up-regulation in the liver transcripts for SB3 (**Figure 2C**). The administration of the same diet to TG/SB3 mice led to a further increase in the prevalence of liver crown-like structures (**Figure 2A**) and a significant up-regulation of liver transcripts for TNFα and IL-1β (**Figures 2D, E**) as compared to CDAA-fed WT mice, while the expression of the monocyte chemokine CCL2 was unchanged (**Figure 2F**). In line with these findings, the release of transaminase was higher in TG/SB3 mice than WT littermates (**Figure 2G**). No significant differences were instead appreciable in the histopathological scores for steatosis (2.1 ± 0.6 vs 2.3 ± 0.6; p=0.55) and lobular inflammation (2.3 ± 0.5 vs 2.7 ± 0.6; p=0.71) (**Figure 2H**). It should be noted that TNFα and IL-1β hepatic transcript levels, but not those of CCL2, were already up-regulated in the liver of TG/SB3 mice vs WT mice fed on control CSAA diet, without signs of hepatic injury (**Figures 2D–F**).

Further support to the involvement of SB3 in promoting macrophage-mediated inflammatory responses was offered by

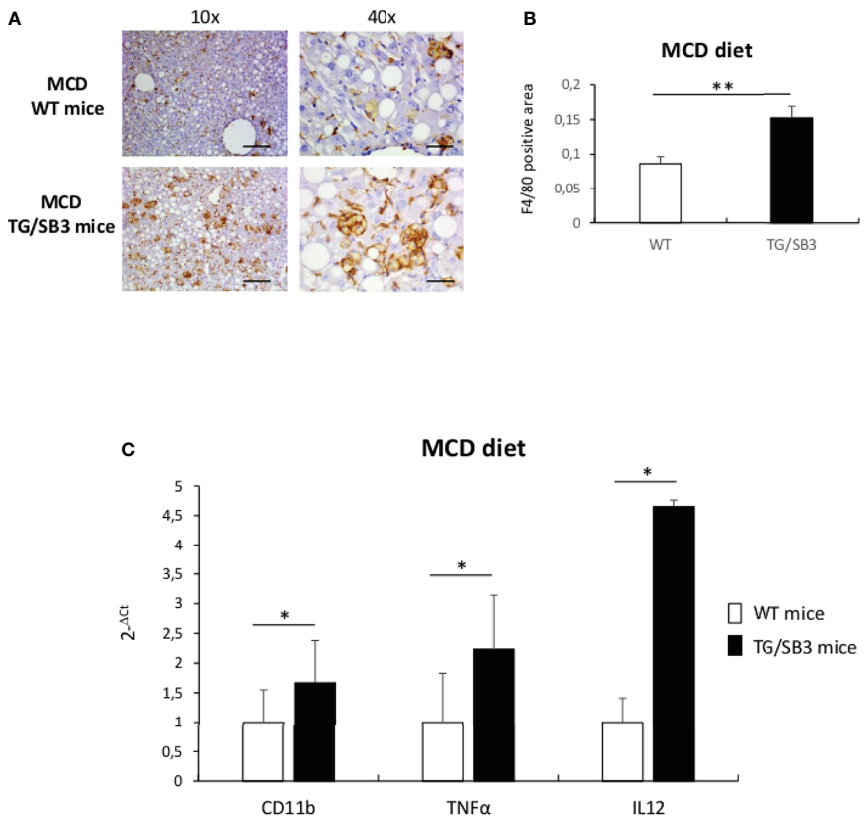

FIGURE 1 | **(A–C) (A)** Immunoistochemistry analysis for F4/80 on liver specimens obtained from C57Bl6J WT mice and C57Bl6J transgenic mice for SB3 (TG/SB3) fed on MCD diet for 8 weeks. Magnification 10x, scale bar 200μm, magnification 40x, scale bar 50μm. **(B)** ImageJ software analysis performed to evaluate the amount of F4/80 positive area in C57Bl6J WT mice and C57Bl6J transgenic mice for SB3 (TG/SB3) fed on MCD diet for 8 weeks. **p < 0.01 versus WT mice. **(C)** Quantitative real time PCR analysis of CD11b, TNFα and IL12 in C57Bl6J WT mice and transgenic mice for SB3 (TG/SB3) fed on MCD diet for 8 weeks. *p < 0.05 versus WT mice.

experiments performed on mice deficient of the reactive site loop of SerpinB3a gene (KO/SB3). In these animals, we observed that, following 12 weeks on the CDAA diet, the lack of SB3 anti-protease activity greatly lowered the formation of macrophage crown-like aggregates (**Figures 3A, B**) and dramatically reduced hepatic transcripts of TNFα, IL-1β and CCL2 (**Figures 3C–E**). Consistently, the severity of steatohepatitis as evaluated by transaminase release (**Figure 3F**) and by histopathological scores for steatosis (2.2 ± 0.7 vs 1.3 ± 0.7; p=0.03) and lobular inflammation (2.1 ± 0.7 vs 0.7 ± 0.8; p=0.007) was significantly improved in the absence of SB3 (**Figure 3G**). Interestingly, also the extension of liver fibrosis as evaluated by collagen staining with Sirius Red was appreciably reduced in KO/SB3 mice (**Supplementary Figure 1A**). A consistent decrease in steatosis, F4/80 positive cells and Sirius red staining was also evident in KO/SB3 mice receiving the MCD diet (**Supplementary Figures 1B–D**).

SB3 Can Directly Activate Macrophage Responses

From the above results we investigated by which mechanism SB3 may influence macrophage functions. In preliminary experiments we first tested *in vitro* the response of either human monocytes obtained from peripheral blood or undifferentiated human THP-1 cells to the addition of hrSB3 observing that, in both cell types, hrSB3 strongly up-regulated the expression of TNFα, IL-1β and IL-12 (**Supplementary Figures 2A–F**). We next tested the ability of hrSB3 to influence the response of human THP-1 cells differentiated into macrophages by 48 hours of incubation with 50 nM phorbol-12-myristate-13-acetate (PMA). Here again, differentiated THP-1 cells receiving hrSB3 underwent an appreciable and sustained up-regulation of TNFα and IL-1β transcripts (**Figures 4A, C**) and proteins (**Figures 4B, D**) along with an increase in the intracellular generation of ROS (**Figure 4E**). Interestingly, we found that hrSB3 stimulation of THP-1-derived macrophages led also to a significant increase at both mRNA (**Figures 5A, C**) and protein (**Figures 5B, D**) levels of pro-fibrogenic mediators VEGF-A and TGFβ1, indicating that these cells were acquiring the mixed pro-inflammatory and pro-fibrogenic phenotype characteristic of NASH-associated MoMFs (15–17). Since at present the receptor for SB3 on target cells has not yet been characterized, we next investigated whether hrSB3 may operate as pro-inflammatory mediator by up-regulating the

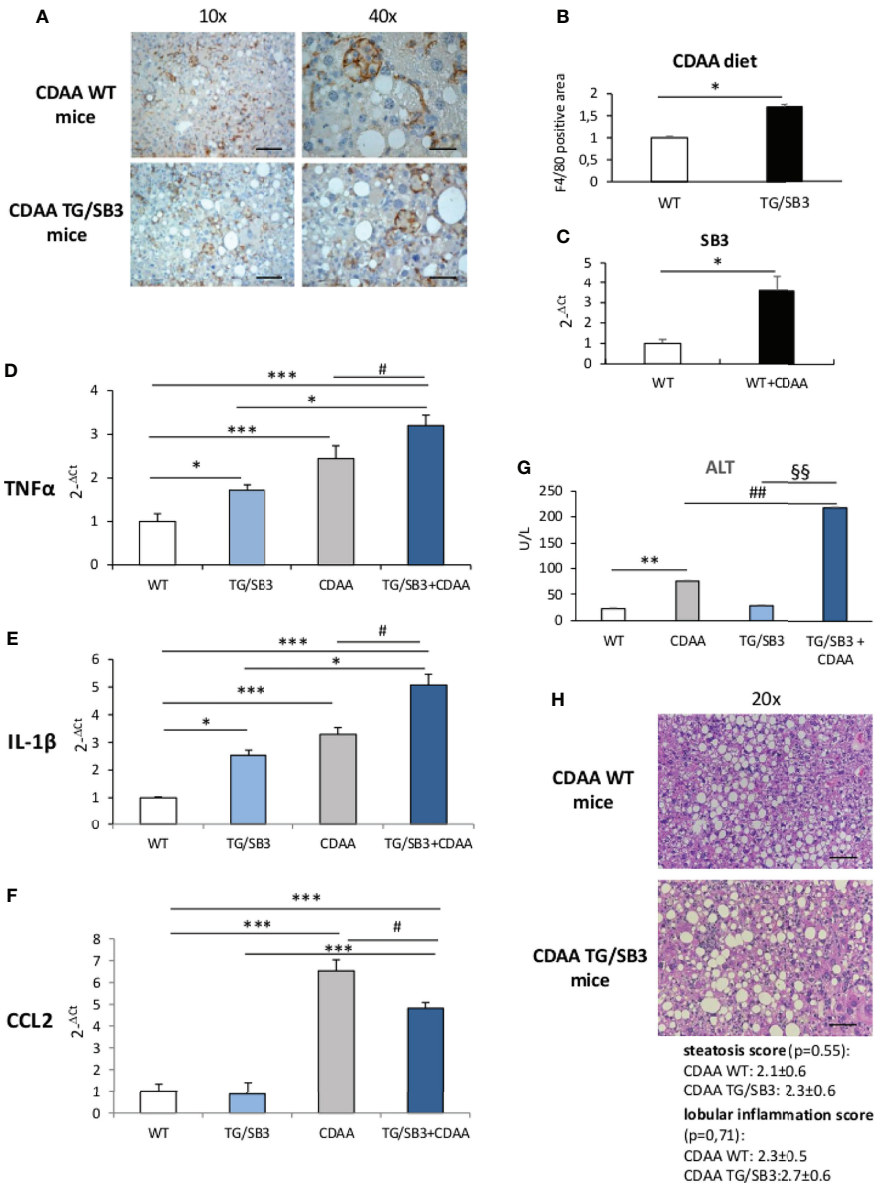

FIGURE 2 | **(A–H) (A)** Immunohistochemistry analysis for F4/80 on liver specimens obtained from C57Bl6J WT mice and transgenic mice for SB3 (TG/SB3) fed on CDAA for 12 weeks. Magnification 10x, scale bar 200μm, magnification 40x, scale bar 50μm. **(B)** ImageJ software analysis performed to evaluate the amount of F4/80 positive area in C57Bl6J WT mice and transgenic mice for SB3 (TG/SB3) fed on CDAA for 12 weeks. *p < 0.05 versus WT mice. **(C)** Quantitative real time PCR analysis of SB3 in C57Bl6J WT mice fed on control (WT) or CDAA diet (WT+CDAA). *p < 0.05 versus WT mice. Quantitative real time PCR analysis of TNFα **(D)**, IL-1β **(E)** and CCL2 **(F)** in C57Bl6J WT mice and transgenic mice for SB3 (TG/SB3) fed on control CSAA diet (WT and TG/SB3) or CDAA diet for 12 weeks (CDAA and TG/SB3+CDAA). ***p < 0.001 and *p < 0.05 versus WT mice fed on control CSAA diet (WT) or versus TG/SB3 mice fed on CSAA diet; $^{\#}$p < 0.05 versus C57Bl6J WT mice fed on CDAA diet (CDAA). **(G)** Serum levels of alanine amino transferase (ALT) analyzed as a parameter of parenchymal injury in C57Bl6J WT mice and transgenic mice for SB3 (TG/SB3) fed on control CSAA diet (WT and TG/SB3) or CDAA diet for 12 weeks (CDAA and TG/SB3+CDAA). **p < 0.01 versus WT mice fed on control CSAA diet (WT), $^{\#\#}$p < 0.01 versus WT mice fed on CDAA diet, §§p < 0.01 versus TG/SB3 mice fed on CSAA diet. **(H)** Hematoxylin eosin staining and score of steatosis and lobular inflammation in WT e TG/SB3 mice fed on CDAA diet for 12 weeks to evaluate steatosis and inflammation. Magnification 20x, scale bar 100μm.

NF-kB transcription factor. Results from these experiments showed that hrSB3 led to a rapid and progressive stimulation of NF-kB as well as of p-IKB, the NF-kB inhibitor that, when phosphorylated, is dissociated from the nuclear factor favoring NF-kB activation and then its nuclear translocation (**Figure 5E**); the NF-kB stimulation was blocked by cell pre-treatment with the IKK pharmacological inhibitor BAY 11-7082. The addition of the IKK inhibitor also reduced IL-1β production in the same cells (**Figure 5F**).

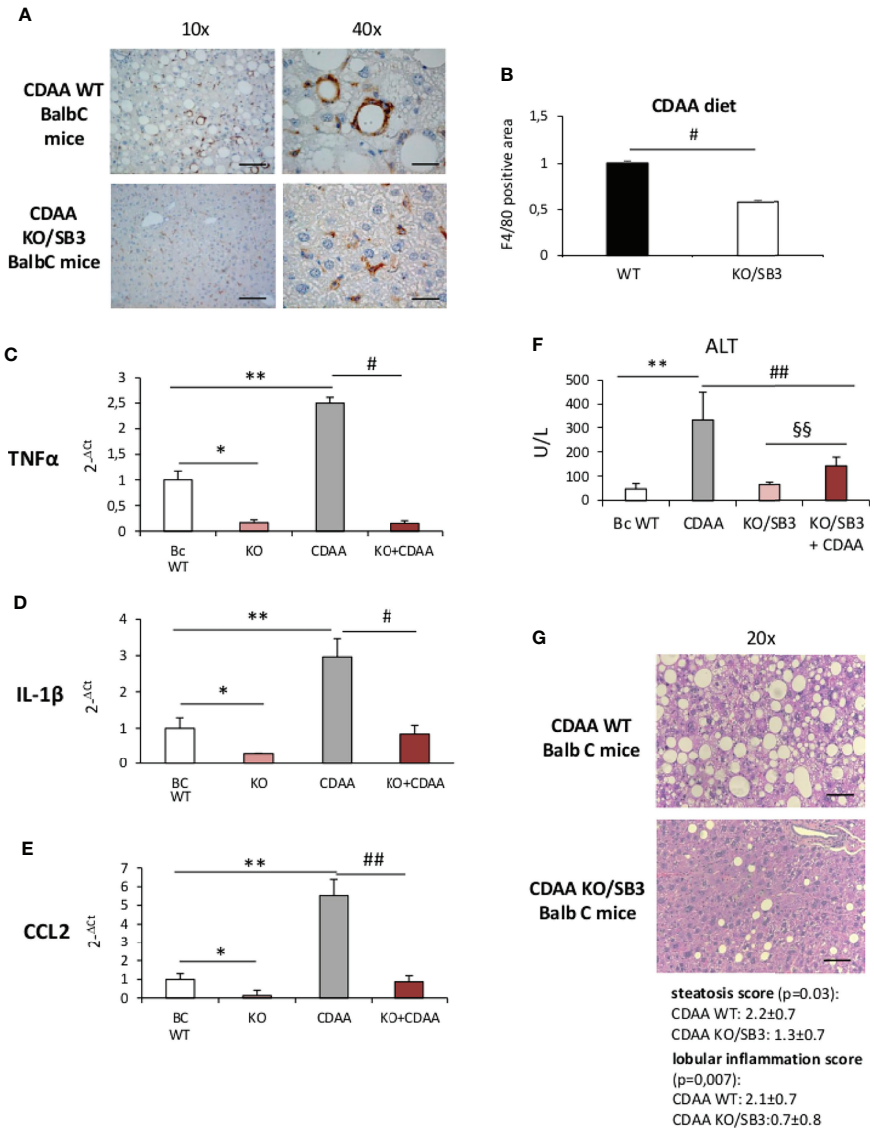

FIGURE 3 | **(A–G) (A)** Immunohistochemistry analysis for F4/80 on liver specimens obtained from BalbC WT mice and knock out mice for SB3 (KO/SB3) fed on CDAA diet for 12 weeks. Magnification 10x, scale bar 200μm, magnification 40x, scale bar 50μm. **(B)** ImageJ software analysis performed to evaluate the amount of F4/80 positive area. $^{\#}p < 0.05$ versus BalbC control mice. Quantitative real time PCR analysis of TNFα **(C)**, IL-1β **(D)** and CCL2 **(E)** in WT BalbC mice and knock out mice for SB3 (KO/SB3) fed on control CSAA diet (BC WT and KO) or CDAA diet for 12 weeks (CDAA and KO+CDAA). $^{*}p < 0.05$, $^{**}p < 0.01$ versus BalbC WT mice fed on control CSAA diet (BC WT); $^{\#}p < 0.05$ $^{\#\#}p < 0.01$ versus BalbC WT mice fed on CDAA (CDAA). **(F)** Serum levels of alanine amino transferase (ALT) analyzed as a parameter of parenchymal injury in BalbC WT mice and knock out mice for SB3 (KO/SB3) fed on control CSAA diet (BC WT and KO/SB3) or CDAA diet for 12 weeks (CDAA and KO/SB3+CDAA). $^{**}p < 0.01$ versus WT mice fed on control CSAA diet (BC WT), $^{\#\#}p < 0.01$ versus BalbC WT mice fed on CDAA diet (CDAA), §§ $p < 0.01$ versus KO/SB3 mice fed on CSAA diet. **(G)** Hematoxylin eosin staining and score of steatosis and lobular inflammation in WT e KO/SB3 mice fed on CDAA diet for 12 weeks to evaluate steatosis and inflammation. Magnification 20x, scale bar 100μm.

SB3 Influences NAM Markers in Mice With NASH

From these observations and the notion that NAMs are involved in forming crown-like structures in NASH livers (21), we went to investigate whether SB3 might influence the expression of NAM markers such as TREM2 and CD9 along with that of the fibrogenic Galectin-3 (Gal-3) (38–41) which is specifically associated with the macrophage phenotype (18–21). **Figure 6** shows that all these three markers were up-regulated in WT mice fed on CDAA diet and were further significantly enhanced in mice overexpressing SB3 in hepatocytes (**Figures 6A–C**). Furthermore, immunohistochemistry demonstrated that the increased expression of Gal-3 mainly involved macrophages aggregates (**Figures 6D, E**). Conversely, CD9 and TREM2 transcripts were significantly down-regulated in the livers of KO/SB3 mice fed on CDAA diet as compared to the respective

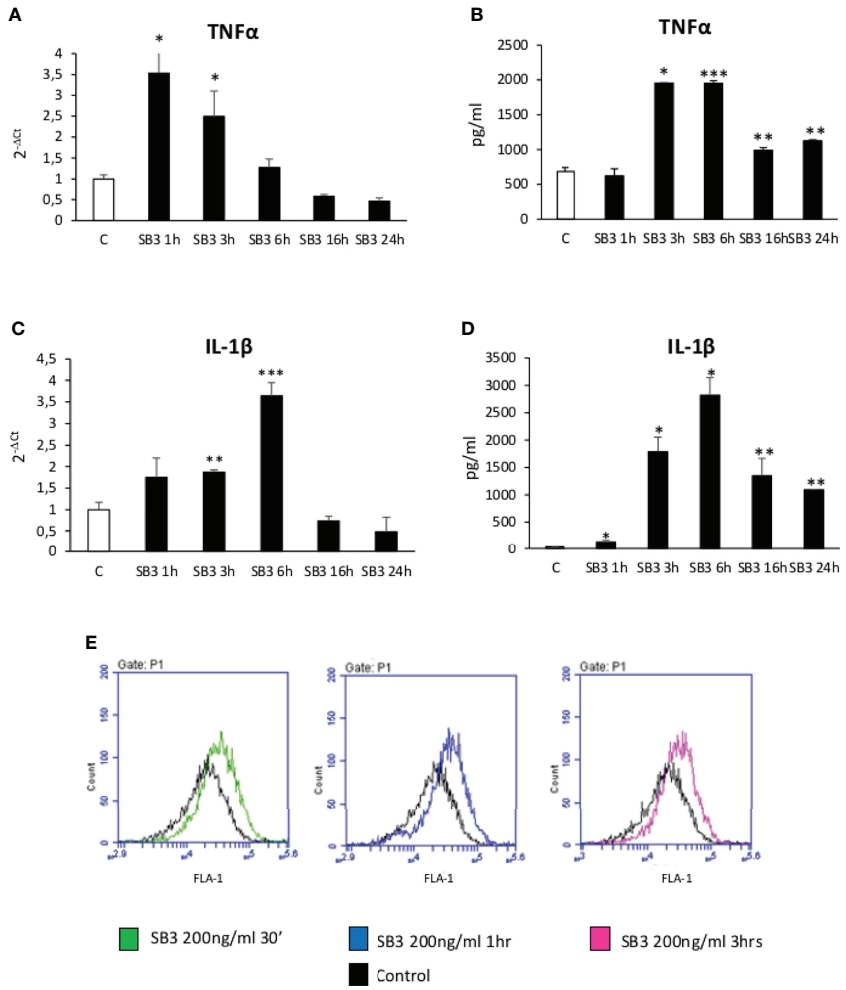

FIGURE 4 | **(A–E)** Time course analysis of transcript levels by quantitative real time PCR **(A, C)** as well as of protein levels by ELISA **(B, D)** of TNFα and IL-1β in human differentiated THP1 cells exposed or not to hrSB3 200ng/ml (SB3) up to 24 hours. *p < 0.05, **p < 0.01, ***p < 0.001 versus control cells. **(E)** DCFH-DA fluorescence in flow cytometry analysis to detect intracellular generation of reactive oxygen species induced by exposure of cells to hrSB3 200ng/ml for the indicated time points.

WT controls (**Figures 7A, B**). In the same animals the decrease Gal-3 mRNA did not reach statistical significance (**Figure 7C**), however immunohistochemistry demonstrated the disappearance of Gal-3 positive macrophage aggregates in KO/SB3 mice receiving the CDAA diet (**Figures 7D, E**). Altogether these data indicate that SB3 contributes to sustain macrophage pro-inflammatory responses during the progression of NASH.

DISCUSSION

It is now well established that hepatic macrophages play a key role in the progression of NAFLD by contributing to sustain both lobular inflammation and hepatic stellate cells (HSCs) activation to matrix producing myofibroblasts (15–17). In this setting great attention has been payed to the mechanisms that promote Kupffer cells activation at the onset of steatohepatitis as well as to the factors involved in favoring macrophage recruitment within the liver (15–17). What is less understood is the network of signals that contribute to maintain the pro-inflammatory and pro-fibrogenic activities of hepatic macrophages during the disease evolution. This is of particular interest on the light of recent findings showing that monocyte-derived macrophages recruited in NASH livers undergo to a specific phenotype reprogramming with increased expression of TREM2 and CD9 (19–21). Interestingly, the prevalence of these TREM2-positive macrophages also known as NAM is strongly associated with the severity of steatosis, inflammation, hepatocyte ballooning, and fibrosis (20).

Here we show that the protease inhibitor SB3 plays an important role among the signals that contributes to promote the pro-inflammatory phenotype of liver macrophage in NASH. The production of SB3 is strongly up-regulated in steatotic and hypoxic hepatocytes in relation to signaling mediated by HIF2α

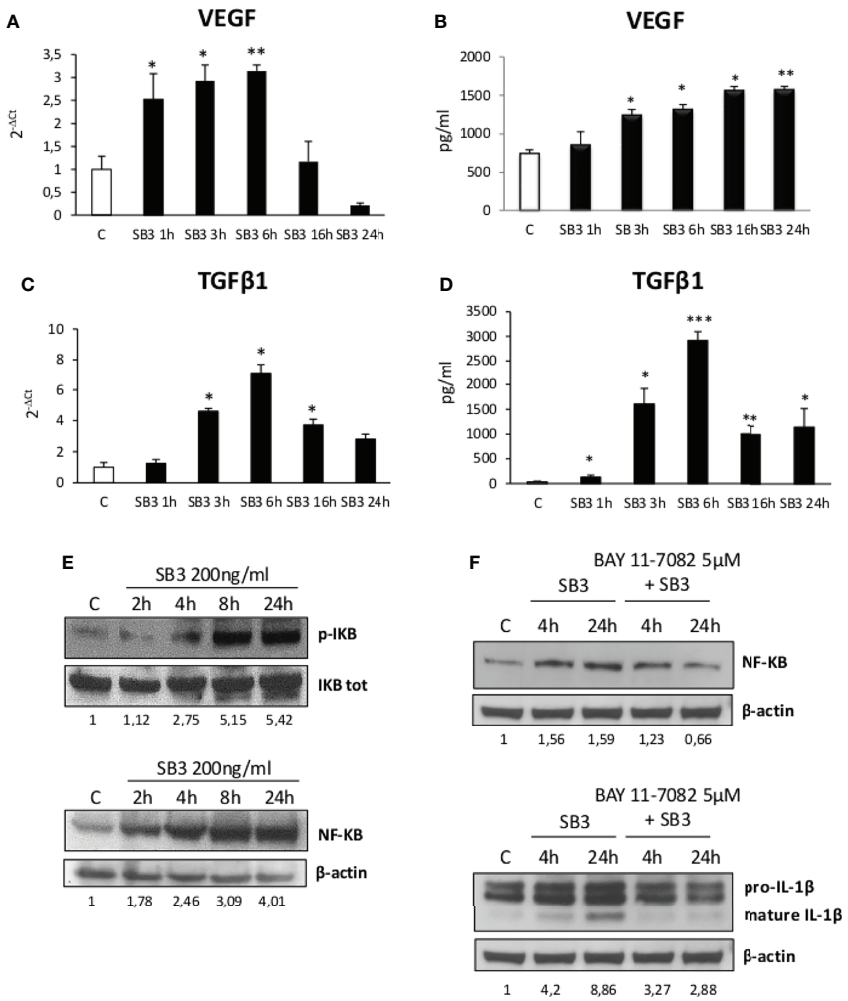

FIGURE 5 | **(A–F)** Time course analysis of transcript levels by quantitative real time PCR **(A, C)** as well as of protein levels by ELISA **(B, D)** of VEGF and TGFβ1 in human differentiated THP1 cells exposed or not to hrSB3 200ng/ml (SB3) up to 24 hours. *p < 0.05, **p < 0.01, ***p < 0.001 versus control cells. **(E)** Western blotting analysis of phosphorylated IKB and of protein levels of NF-kB in human differentiated THP-1 cells exposed or not to hrSB3 200ng/ml (starting from 2 hrs up to 24 hrs). Equal loading was confirmed by re-probing the same membrane with the un phosphorylated protein IKB or with β-actin. Values obtained from band densitometry analysis, using ImageJ software, are reported. **(F)** Western blot analysis of protein levels of NFkB and IL-1β in human THP-1 cells exposed to hrSB3 200ng/ml for 4 and 24 hrs or pre-treated with the inhibitor of IKK protein, BAY 11-7082 5μM and then exposed to hrSB3 200ng/ml for 4hrs and 24 hrs. Equal loading was confirmed by re-probing the same membrane with β-actin. Values obtained from band densitometry analysis, using ImageJ software, are reported.

(23, 25, 28–31). In a previous study we provided experimental evidence of the pro-fibrogenic action of SB3 by showing that mice overexpressing SB3 in hepatocytes and exposed to different protocols of chronic liver injury were characterized by an enhanced hepatic collagen deposition in relation to SB3 capability to directly up-regulate the transcription of fibrogenic genes in human activated, myofibroblast-like, hepatic stellate cells (HSC/MFs) or human stellate cell line (LX2 cells) (31). The evidence supporting the role of SB3 as a pro-inflammatory mediator comes from experiments in which mice genetically manipulated to carry hepatocyte specific SB3 overexpression (TG/SB3) or deficient in SB3 (KO/SB3) were fed with two different NASH-inducing dietary protocols. In particular, we have observed that SB3 overexpression not only leads to increased fibrosis, as previously reported (31), but also to an increase in transcript levels for TNFα and IL-1β and to recruitment of infiltrating monocyte-derived macrophages that accumulate mainly in crown-like aggregates, a feature which is characteristic of human advanced NAFLD (42, 43). Conversely, SB3 deletion greatly reduces lobular inflammation markers, macrophage aggregates and the severity of steatohepatitis.

Although the receptor for SB3 has not yet been identified, *in vitro* experiments support these observations by showing that hrSB3 can directly activate human monocytes from peripheral blood as well as undifferentiated or PMA-differentiated human THP1 macrophages. In these cells, SB3-mediated activation results in a NF-kB-dependent up-regulation of pro-inflammatory cytokines and ROS production. Such a pro-inflammatory action of SB3 on macrophages shows

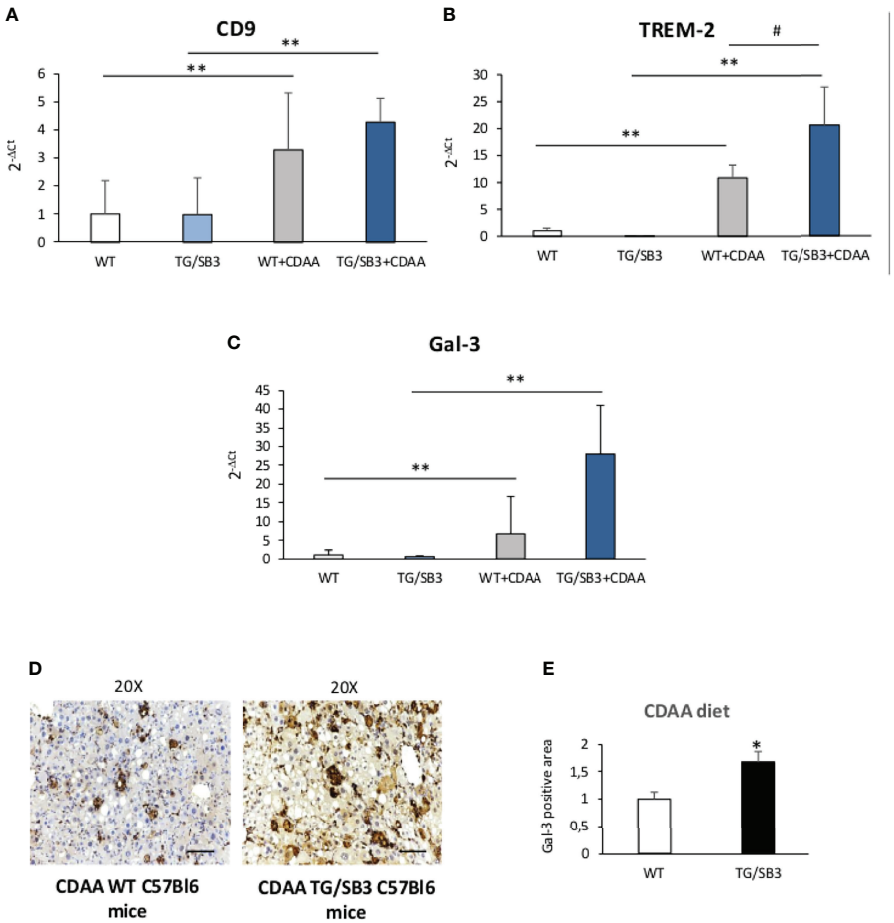

FIGURE 6 | **(A–E)** Quantitative real time PCR analysis of CD9, **(A)** TREM-2 **(B)** and Gal-3 **(C)** in control C57Bl6J mice and transgenic mice for SB3 fed on control diet (WT and TG/SB3) or CDAA diet for 12 weeks (WT+CDAA and TG/SB3+CDAA). **$p < 0.01$ versus C57Bl6J control mice fed with control diet (WT) #$p < 0.05$ versus C57Bl6J control mice fed with CDAA (WT+CDAA). **(D)** Immunohistochemistry analysis for Gal-3 on liver specimens obtained from C57Bl6J WT mice and transgenic mice for SB3 (TG/SB3) fed on CDAA for 12 weeks. Magnification 20x, scale bar 100μm. **(E)** ImageJ software analysis was performed to evaluate the amount of Gal-3 positive area in C57Bl6J WT mice and transgenic mice for SB3 (TG/SB3) fed on CDAA for 12 weeks. *$p < 0.05$ versus WT mice.

several analogies with that of the HRG which is similarly produced by hepatocytes in response to HIF2α-mediated signals (23, 26). Interestingly, SB3 addition to differentiated THP1 macrophages also induces a significant up-regulation of VEGF and TGFβ1, two cytokines that are related to macrophage pro-fibrogenic activity. This is consistent with previous observations concerning the role of SB3 in stimulating the progression of liver fibrosis (31). Thus, the data from the present study suggest that SB3 can operate in NASH as a peculiar hepatocyte-released mediator being able to induce a macrophage mixed pro-inflammatory/pro-fibrogenic phenotype that characterizes the evolution of CLD, including NAFLD/NASH (15–17, 44, 45). The latter phenotype has been reported to sustain the fibrogenic progression of chronic diseases by releasing several mediators, including TGFβ1, FGF, TGFα, Activin 1, PDGF, IGF-1, VEGF-A and Galectin 3 (45).

The action of SB3 in NASH is further emphasized by the fact that hepatocyte SB3 production influences the hepatic levels of NAM markers TREM2, CD9 and Galectin 3. These markers have been reported to identify a peculiar subset of hepatic macrophages emerging in conditions of either human of murine progressive NAFLD (19–21, 46, 47) showing similarities with TREM2 CD9 expressing scar-associated macrophages (SAMs). This suggests the possibility that, during NAFLD progression, SB3 might also contribute to the emergence of NAMs and/or SAMs. Such a SB3 action on liver macrophages is not in contrast with previous observations concerning the pro-fibrogenic role of SB3 (31) since the macrophage phenotype induced by SB3 involves the release pro-fibrogenic mediators such as Gal-3, VEGF and TGFβ1 that can sustain liver matrix production by HSC/MFs.

Although more research is needed to confirm this hypothesis, the data provided by the present study indicate that SB3 can be added to the list of peptide mediators contributing to NASH pathogenesis. Some of these mediators have been collectively termed "hepatokines", being defined as proteins synthetized and secreted by hepatocytes that can influence metabolic processes through autocrine, paracrine and endocrine signaling, playing a

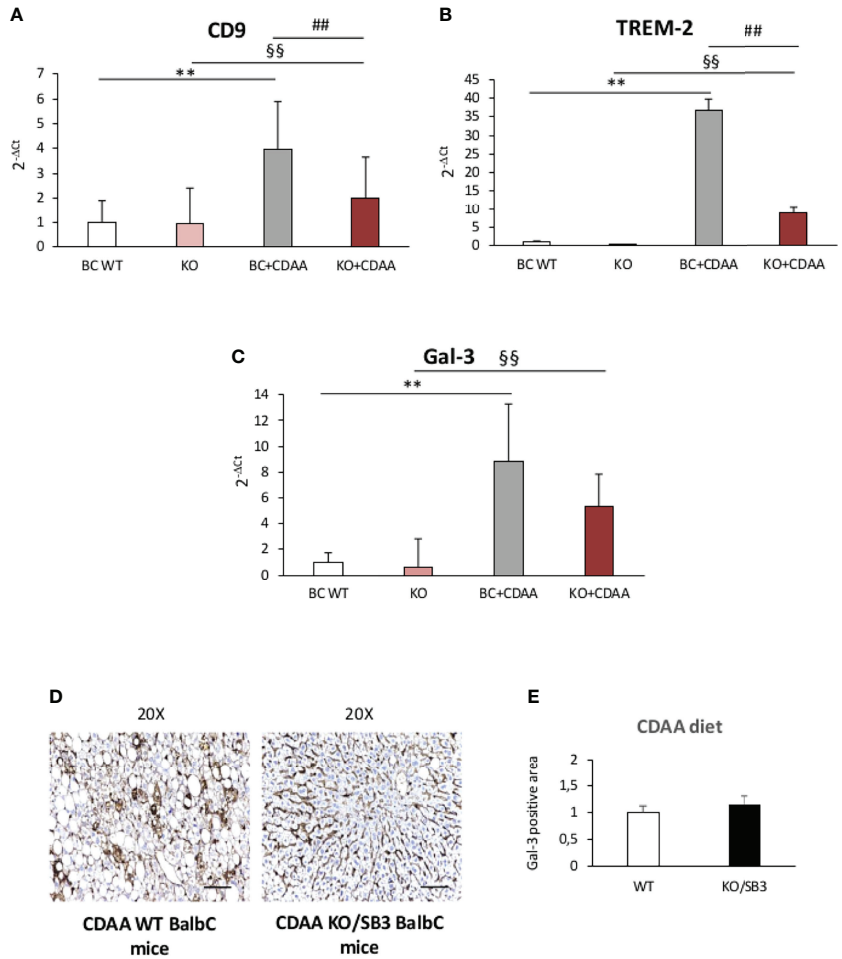

FIGURE 7 | **(A–E)** Quantitative real time PCR analysis of CD9, **(A)** TREM-2 **(B)** and Gal-3 **(C)** in control BalbC mice and knock out mice for SB3 fed on control diet (BC WT and KO) or CDAA diet for 12 weeks (BC+CDAA and KO+CDAA). **p < 0.01 versus BalbC control mice fed with control diet (BC WT); §§p < 0.01 versus BalbC control mice fed with control diet (KO), ##p < 0.01 versus BalbC control mice fed with CDAA diet (BC+CDAA). **(D)** Immunohistochemistry analysis for Gal-3 in liver specimens obtained from WT BalbC mice and KO/SB3 BalbC mice fed on CDAA diet for 12 weeks. Magnification 20x, scale bar 100μm. **(E)** ImageJ software analysis was performed to evaluate the amount of Gal-3 positive area in BalbC WT mice and knock out mice for SB3 (KO/SB3) fed on CDAA for 12 weeks.

central role in orchestrating whole-body energy metabolism (48–50). In particular, the development of fatty liver has been reported to promote the secretion of hepatokine such hepassocin, fetuins A and B and fibroblast growth factor 21 (FGF21) (49), that are also involved in causing liver inflammation (49, 50). Although SB3 has not been so far included in the list of hepatokines, the evidence emerging on their contribution to NAFLD progression suggest the possibility to consider SB3, which is selectively expressed by hepatocytes under CLD conditions, as a putative novel hepatokine.

CONCLUSIONS

Data reported in the present study provide novel evidence that SB3, produced and released by activated/injured hepatocytes, can operate as a pro-inflammatory mediator in NASH efficiently contributing to disease progression.

DATA AVAILABILITY STATEMENT

The original contributions presented in the study are included in the article/**Supplementary Material**. Further inquiries can be directed to the corresponding authors.

ETHICS STATEMENT

Human blood samples employed to purify monocytes were obtained under informed consent and the study protocol, which conformed to the ethical guidelines of the 1975 Declaration of Helsinki, was approved by the Ethics Committee of the Azienda Ospedaliera-Università, Padova, Italy. The patients/participants provided their written informed consent to participate in this study. The animal study was reviewed and approved by Animal Ethical Committee of

University of Padua and by the Animal Investigation Committee of the Italian Ministry of Health.

AUTHOR CONTRIBUTIONS

Conceptualization EN, AC, PP, EA, and MP; methodology, EN, AC, GV, MG, SQ, SC, CB, CT, MM, FP, SS, AP, MR, AB, and BF; software, EN, AC, SS, and EA; validation, EA, PP, and MP; formal analysis EN, AC, PP, EA, and MP; investigation, EN, AC, GV, CT, CB, MM, and FP; resources, EA, PP, and MP; data curation, EN, AC, GV, PP, and MP; writing—original draft preparation, PP and MP; writing—review and editing, EN, EA, and PP; visualization, EN, AC, PP, and MP; supervision, EA, PP, and MP; project administration, PP and MP; funding acquisition, EN, PP, and MP. All authors have read and agreed to the published version of the manuscript.

FUNDING

The research leading to these results has received funding from: (a) Associazione Italiana per la Ricerca sul Cancro (AIRC) under IG2017-ID 20361 – P.I. Maurizio Parola (MP); (b) the University of Torino (Fondo di Ateneo ex 60% - EN, MP); (c) University of Padova project No CPDA110795-P.P.

SUPPLEMENTARY MATERIAL

The Supplementary Material for this article can be found online at: https://www.frontiersin.org/articles/10.3389/fimmu.2022.910526/full#supplementary-material

REFERENCES

1. Kanwal F, Shubrook JH, Younossi Z, Natarajan Y, Bugianesi E, Rinella ME, et al. Preparing for the NASH Epidemic: A Call to Action. *Gastroenterology* (2021) 161:1030–42. doi: 10.1053/j.gastro.2021.04.074
2. Younossi Z, Tacke F, Arrese M, Chander Sharma B, Mostafa I, Bugianesi E, et al. Global Perspectives on Nonalcoholic Fatty Liver Disease and Nonalcoholic Steatohepatitis. *Hepatology* (2019) 69:2672–82. doi: 10.1002/hep.30251
3. Younossi Z, Anstee QM, Marietti M, Hardy T, Henry L, Eslam M, et al. Global Burden of NAFLD and NASH: Trends, Predictions, Risk Factors and Prevention. *Nat Rev Gastroenterol Hepatol* (2018) 15:11–20. doi: 10.1038/nrgastro.2017.109
4. McPherson S, Hardy T, Henderson E, Burt AD, Day CP, Anstee QM. Evidence of NAFLD Progression From Steatosis to Fibrosing-Steatohepatitis Using Paired Biopsies: Implications for Prognosis and Clinical Management. *J Hepatol* (2015) 62:1148–55. doi: 10.1016/j.jhep.2014.11.034
5. Younossi ZM, Golabi P, de Avila L, Minhui Paik J, Srishord M, Fukui N, et al. The Global Epidemiology of NAFLD and NASH in Patients With Type 2 Diabetes: A Systematic Review and Meta-Analysis. *J Hepatol* (2019) 71:793–801. doi: 10.1016/j.jhep.2019.06.021
6. Torres DM, Harrison SA. Nonalcoholic Steatohepatitis and Noncirrhotic Hepatocellular Carcinoma: Fertile Soil. *Semin Liver Dis* (2012) 32:30–8. doi: 10.1055/s-0032-1306424
7. Younes R, Bugianesi E. Should We Undertake Surveillance for HCC in Patients With NAFLD? *J Hepatol* (2018) 68:326–34. doi: 10.1016/j.jhep.2017.10.006
8. Younossi Z, Stepanova M, Ong JP, Jacobson IM, Bugianesi E, Duseja A, et al. Nonalcoholic Steatohepatitis Is the Fastest Growing Cause of Hepatocellular Carcinoma in Liver Transplant Candidates. Global Nonalcoholic Steatohepatitis Council. *Clin Gastroenterol Hepatol* (2019) 17:748–55. doi: 10.1016/j.cgh.2018.05.057
9. Asgharpour A, Dinani A, Friedman SL. Basic Science to Clinical Trials in non-Alcoholic Fatty Liver Disease and Alcohol-Related Liver Disease: Collaboration With Industry. *Transl Gastroenterol Hepatol* (2021) 6:5. doi: 10.21037/tgh.2020.01.04
10. Dufour JF, Caussy C, Loomba R. Combination Therapy for non-Alcoholic Steatohepatitis: Rationale, Opportunities and Challenges. *Gut* (2020) 69:1877–84. doi: 10.1136/gutjnl-2019-319104
11. Neuschwander-Tetri BA. Therapeutic Landscape for NAFLD in 2020. *Gastroenterology* (2020) 158:1984–98. doi: 10.1053/j.gastro.2020.01.051
12. Rinella ME, Tacke F, Sanyal AJ, Anstee QM. Participants of the AASLD/EASL Workshop. Report on the AASLD/EASL Joint Workshop on Clinical Trial Endpoints in NAFLD. *J Hepatol* (2019) 71:823–33. doi: 10.1016/j.jhep.2019.04.019
13. Friedman SL, Neuschwander-Tetri BA, Rinella M, Sanyal AJ. Mechanisms of NAFLD Development and Therapeutic Strategies. *Nat Med* (2018) 24:908–22. doi: 10.1038/s41591-018-0104-9
14. Trautwein C, Friedman SL, Schuppan D, Pinzani M. Hepatic Fibrosis: Concept to Treatment. *J Hepatol* (2015) 62(Suppl. l):S15–24. doi: 10.1016/j.jhep.2015.02.039
15. Krenkel O, Tacke F. Macrophages in Nonalcoholic Fatty Liver Disease: A Role Model of Pathogenic Immunometabolism. *Semin Liver Dis* (2017) 37:189–97. doi: 10.1055/s-0037-1604480
16. Parola M, Pinzani M. Liver Fibrosis: Pathophysiology, Pathogenetic Targets and Clinical Issues. *Mol Aspects Med* (2019) 65:37–55. doi: 10.1016/j.mam.2018.09.002
17. Wen Y, Lambrecht J, Ju C, Tacke F. Hepatic Macrophages in Liver Homeostasis and Diseases-Diversity, Plasticity and Therapeutic Opportunities. *Cell Mol Immunol* (2021) 18:45–56. doi: 10.1038/s41423-020-00558-8
18. Adhemar Jaitin DA, Adlung L, Thaiss CA, Weiner A, Li B, Descamps H, et al. Lipid-Associated Macrophages Control Metabolic Homeostasis in a Trem2-Dependent Manner. *Cell* (2019) 178:686–98. doi: 10.1016/j.cell.2019.05.054
19. Seidman JS, Troutman TD, Sakai M, Gola A, Spann NJ, Bennett H, et al. Niche-Specific Reprogramming of Epigenetic Landscapes Drives Myeloid Cell Diversity in Nonalcoholic Steatohepatitis. *Immunity* (2020) 52:1057–74. doi: 10.1016/j.immuni.2020.04.001
20. Xiong X, Kuang H, Ansari S, Liu T, Gong J, Wang S, et al. Landscape of Intercellular Crosstalk in Healthy and NASH Liver Revealed by Single-Cell Secretome Gene Analysis. *Mol Cell* (2019) 75:644–60. doi: 10.1016/j.molcel.2019.07.028
21. Ramachandran P, Dobie R, Wilson-Kanamori JR, Dora EF, Henderson BEP, Luu NT, et al. Resolving the Fibrotic Niche of Human Liver Cirrhosis at Single-Cell Level. *Nature* (2019) 575:512–18. doi: 10.1038/s41586-019-1631-3
22. Nath B, Szabo G. Hypoxia and Hypoxia Inducible Factors: Diverse Roles in Liver Diseases. *Hepatology* (2012) 55:622–33. doi: 10.1002/hep.25497
23. Foglia B, Novo E, Protopapa F, Maggiora M, Bocca C, Cannito S, et al. Hypoxia, Hypoxia-Inducible Factors and Liver Fibrosis. *Cells* (2021) 10:1764. doi: 10.3390/cells10071764
24. Morello E, Sutti S, Foglia B, Novo E, Cannito S, Bocca C, et al. Hypoxia-Inducible Factor 2α Drives Nonalcoholic Fatty Liver Progression by Triggering Hepatocyte Release of Histidine-Rich Glycoprotein. *Hepatology* (2018) 67:2196–214. doi: 10.1002/hep.29754
25. Cannito S, Turato C, Paternostro C, Biasiolo A, Colombatto S, Cambieri I, et al. Hypoxia Up-Regulates SERPINB3 Through HIF-2α in Human Liver Cancer Cells. *Oncotarget* (2015) 6:2206–21. doi: 10.18632/oncotarget.2943

26. Bartneck M, Fech V, Ehling J, Govaere O, Warzecha KT, Hittatiya K, et al. Histidine-Rich Glycoprotein Promotes Macrophage Activation and Inflammation in Chronic Liver Disease. *Hepatology* (2016) 63:1310–24. doi: 10.1002/hep.28418
27. Sun Y, Sheshadri N, Zong WX. SERPINB3 and B4: From Biochemistry to Biology. *Semin Cell Dev Biol* (2017) 62:170–77. doi: 10.1016/j.semcdb.2016.09.005
28. Turato C, Calabrese F, Biasiolo A, Quarta S, Ruvoletto M, Tono N, et al. SERPINB3 Modulates TGF-β Expression in Chronic Liver Disease. *Lab Invest* (2010) 90:1016–23. doi: 10.1038/labinvest.2010.55
29. Biasiolo A, Chemello L, Quarta S, Cavalletto L, Bortolotti F, Caberlotto C, et al. Monitoring SCCA-IgM Complexes in Serum Predicts Liver Disease Progression in Patients With Chronic Hepatitis. *J Viral Hep* (2008) 15:246–49. doi: 10.1111/j.1365-2893.2007.00935.x
30. Biasiolo A, Tono N, Ruvoletto M, Quarta S, Turato C, Villano G, et al. IgM-Linked SerpinB3 and SerpinB4 in Sera of Patients With Chronic Liver Disease. *PLoS One* (2012) 7:e40658. doi: 10.1371/journal.pone.0040658
31. Novo E, Villano G, Turato C, Cannito S, Paternostro C, Busletta C, et al. SerpinB3 Promotes Pro-Fibrogenic Responses in Activated Hepatic Stellate Cells. *Sci Rep* (2017) 7:3420. doi: 10.1038/s41598-017-03744-3
32. Cannito S, Foglia B, Villano G, Turato C, Delgado TC, Morello E, et al. SerpinB3 Differently Up-Regulates Hypoxia Inducible Factors -1α and -2α in Hepatocellular Carcinoma: Mechanisms Revealing Novel Potential Therapeutic Targets. *Cancers* (2019) 11:1933. doi: 10.3390/cancers11121933
33. Villano G, Quarta S, Ruvoletto M, Turato C, Vidalino L, Biasiolo A, et al. Role of Squamous Cell Carcinoma Antigen-1 on Liver Cells After Partial Hepatectomy. *Int J Mol Med* (2010) 25:137–43. doi: 10.3892/ijmm_00000323
34. Villano G, Lunardi F, Turato C, Schiff S, Tono N, Campagna F, et al. Increased Th1 Immune Response in SerpinB3 Transgenic Mice During Acute Liver Failure. *Exp Biol Med* (2012) 237:1474–82. doi: 10.1258/ebm.2012.012135
35. Villano G, Ruvoletto M, Ceolotto G, Quarta S, Calabrese F, Turato C, et al. SerpinB3 is Associated With Longer Survival in Transgenic Mice. *Sci Rep* (2013) 3:3056. doi: 10.1038/srep03056
36. Sivaprasad U, Askew DJ, Ericksen MB, Gibson AM, Stier MT, Brandt EB, et al. A Nonredundant Role for Mouse Serpinb3a in the Induction of Mucus Production in Asthma. *J Allergy Clin Immunol* (2011) 127:254–61. doi: 10.1016/j.jaci.2010.10.009
37. Sutti S, Jindal A, Locatelli I, Vacchiano M, Gigliotti L, Bozzola C, et al. Adaptive Immune Responses Triggered by Oxidative Stress Contribute to Hepatic Inflammation in NASH. *Hepatology* (2014) 59:886–97. doi: 10.1002/hep.26749
38. Foglia B, Sutti S, Cannito S, Rosso C, Maggiora M, Autelli R, et al. Hepatocyte-Specific Deletion of HIF2α Prevents NASH-Related Liver Carcinogenesis by Decreasing Cancer Cell Proliferation. *Cell Mol Gastroenterol Hepatol* (2021) 13:459–482. doi: 10.1016/j.jcmgh.2021.10.002
39. Iacobini C, Menini S, Ricci C, Blasetti Fantaluzzi C, Scipioni A, Salvi L, et al. Galectin-3 Ablation Protects Mice From Diet-Induced NASH: A Major Scavenging Role for Galectin-3 in Liver. *J Hepatol* (2011) 54:975–83. doi: 10.1016/j.jhep.2010.09.020
40. Jeftic I, Jovicic N, Pantic J, Arsenijevic N, Lukic ML, Pejnovic N. Galectin-3 Ablation Enhances Liver Steatosis, But Attenuates Inflammation and IL-33-Dependent Fibrosis in Obesogenic Mouse Model of Nonalcoholic Steatohepatitis. *Mol Med* (2015) 21:453–65. doi: 10.2119/molmed.2014.00178
41. Traber PG, Zomer E. Therapy of Experimental NASH and Fibrosis With Galectin Inhibitors. *PLoS One* (2013) 8(12):e83481. doi: 10.1371/journal.pone.0083481
42. Gadd VL, Skoien R, Powell EE, Fagan KJ, Winterford C, Horsfall L, et al. The Portal Inflammatory Infiltrate and Ductular Reaction in Human Nonalcoholic Fatty Liver Disease. *Hepatology* (2014) 59:1393–405. doi: 10.1002/hep.26937
43. Krenkel O, Puengel T, Govaere O, Abdallah AT, Mossanen JC, Kohlhepp M, et al. Therapeutic Inhibition of Inflammatory Monocyte Recruitment Reduces Steatohepatitis and Liver Fibrosis. *Hepatology* (2018) 67:1270–83. doi: 10.1002/hep.29544
44. Lefere S, Tacke F. Macrophages in Obesity and non-Alcoholic Fatty Liver Disease: Crosstalk With Metabolism. *J Hep Rep* (2019) 1:30–43. doi: 10.1016/j.jhepr.2019.02.004
45. Wynn TA, Vannella KM. Macrophages in Tissue Repair, Regeneration, and Fibrosis. *Immunity* (2016) 44:450–62. doi: 10.1016/j.immuni.2016.02.015
46. Remmerie A, Martens L, Thoné T, Castoldi A, Seurinck R, Pavie B, et al. Osteopontin Expression Identifies a Subset of Recruited Macrophages Distinct From Kupffer Cells in the Fatty Liver. *Immunity* (2020) 53:641–57. doi: 10.1016/j.immuni.2020.08.004
47. Remmerie A, Martens L, Scott CL. Macrophage Subsets in Obesity, Aligning the Liver and Adipose Tissue. *Front Endocrinol* (2020) 11:259. doi: 10.3389/fendo.2020.00259
48. Meex RCR, Watt MJ. Hepatokines: Linking Nonalcoholic Fatty Liver Disease and Insulin Resistance. *Nat Rev Endocrinol* (2017) 13:509–20. doi: 10.1038/nrendo.2017.56
49. Kucukoglu O, Sowa JP, Mazzolini GD, Syn WK, Canbay A. Hepatokines and Adipokines in NASH-Related Hepatocellular Carcinoma. *J Hepatol* (2021) 74:442–57. doi: 10.1016/j.jhep.2020.10.030
50. Meex RC, Hoy AJ, Morris A, Brown RD, Lo JC, Burke M, et al. Fetuin B Is a Secreted Hepatocyte Factor Linking Steatosis to Impaired Glucose Metabolism. *Cell Metab* (2015) 22:1078–89. doi: 10.1016/j.cmet.2015.09.023

Conflict of Interest: The authors declare that the research was conducted in the absence of any commercial or financial relationships that could be construed as a potential conflict of interest.

Publisher's Note: All claims expressed in this article are solely those of the authors and do not necessarily represent those of their affiliated organizations, or those of the publisher, the editors and the reviewers. Any product that may be evaluated in this article, or claim that may be made by its manufacturer, is not guaranteed or endorsed by the publisher.

4.2 PAPER N°2 (SUBMITTED TO MOLECULAR METABOLISM ON 27TH OCTOBER 2023)

The Protease Activated Receptor 2 - CCAAT/Enhancer-Binding Protein beta - SerpinB3 axis inhibition as a novel strategy for the treatment of Non-Alcoholic Steatohepatitis

This paper has been submitted to Molecular Metabolism on the 27th October 2023.

Authors: Villano Gianmarco[1*], Novo Erica[2*], Turato Cristian[3], Quarta Santina[4], Ruvoletto Mariagrazia[4], Biasiolo Alessandra[4], **Protopapa Francesca[2]**, Chinellato Monica[4], Martini Andrea[4], Trevellin Elisabetta[4], Granzotto Marnie[4], Cannito Stefania[2], Cendron Laura[5], De Siervi Silvia[3], Guido Maria[4], Parola Maurizio[2**], Roberto Vettor[4**], Pontisso Patrizia[4**§].

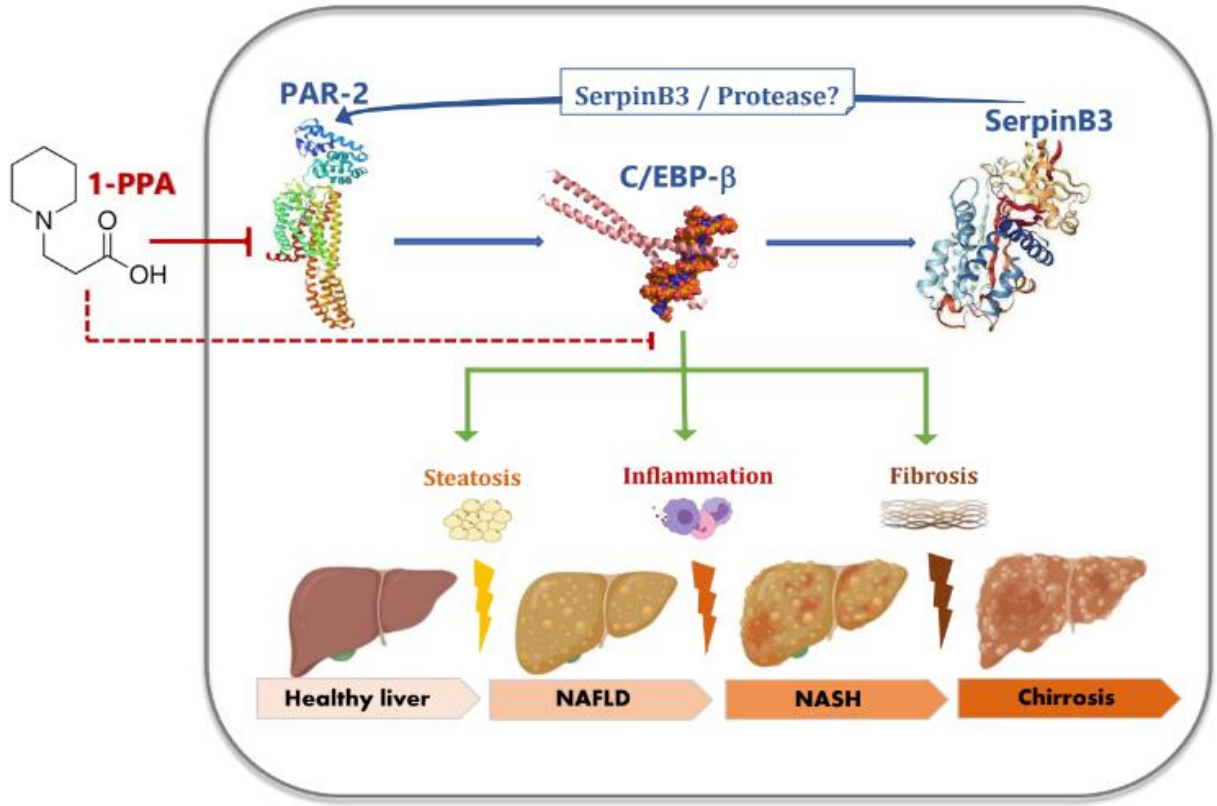

Molecular Metabolism

The Protease Activated Receptor 2 - CCAAT/Enhancer-Binding Protein beta - SerpinB3 axis inhibition as a novel strategy for the treatment of Non-Alcoholic Steatohepatitis

--Manuscript Draft--

Manuscript Number:	MOLMET-D-23-00899
Article Type:	Full Length Article
Keywords:	Serpins; genetically manipulated mice; experimental NASH; transcription factors; therapeutic drugs.
Corresponding Author:	PATRIZIA PONTISSO University of Padua Department of Medicine Padua, ITALY
First Author:	Gianmarco Villano
Order of Authors:	Gianmarco Villano
	Erica Novo
	Cristian Turato
	Santina Quarta
	Mariagrazia Ruvoletto
	Alessandra Biasiolo
	Francesca Protopapa
	Monica Chinellato
	Andrea Martini
	Elisabetta Trevellin
	Marnie Granzotto
	Stefania Cannito
	Laura Cendron
	Silvia De Siervi
	Maria Guido
	Maurizio Parola
	Roberto Vettor
	PATRIZIA PONTISSO
Abstract:	OBJECTIVE: The serine protease inhibitor SerpinB3 has been described as critical mediator of liver fibrosis and it has been recently proposed as an additional hepatokine involved in NASH development and insulin resistance. Protease Activated Receptor 2 has been identified as a novel regulator of hepatic metabolism. A targeted therapeutic strategy for NASH has been investigated, using 1-Piperidine Propionic Acid (1-PPA), since this compound has been recently proposed as both Protease Activated Receptor 2 and SerpinB3 inhibitor. METHODS: The effect of SerpinB3 on inflammation and fibrosis genes was assessed in human macrophage and stellate cell lines. Transgenic mice, either overexpressing SerpinB3 or carrying Serpinb3 deletion and their relative wild type strains, were used in experimental NASH models. Subgroups of SerpinB3 transgenic mice and their controls were also injected with 1-PPA to assess the efficacy of this compound in NASH inhibition. Results: 1-PPA did not present significant cell and organ toxicity and was able to inhibit SerpinB3 and PAR2 in a dose-dependent manner. This effect was associated to a parallel reduction of the synthesis of the molecules induced by endogenous SerpinB3

	or by its paracrine effects both in vitro and in vivo, leading to inhibition of lipid accumulation, inflammation and fibrosis in experimental NASH. At mechanistic level, the antiprotease activity of SerpinB3 was found essential for PAR2 activation, determining upregulation of the CCAAT Enhancer Binding Protein beta (C/EBP-β), another pivotal regulator of metabolism, inflammation and fibrosis, which in turn determined SerpinB3 synthesis. CONCLUSIONS: 1-PPA treatment was able to inhibit the PAR2 - C/EBP-β - SerpinB3 axis and to protect from NASH development and progression, supporting the potential use of a similar approach for a targeted therapy of NASH. [ct1] [ct1]Lo rivediamo alla fine
Suggested Reviewers:	Romero Gomez mromerogomez@us.es
	Sabina Janciauskiene Janciauskiene.Sabina@mh-hannover.de
	Annalisa Berzigotti annalisa.berzigotti@unibe.ch
Opposed Reviewers:	

DIPARTIMENTO DI MEDICINA
CLINICA MEDICA 5
Direttore: Prof. P.Angeli

Via Giustiniani, 2
35128 PADOVA

UNIVERSITÀ DEGLI STUDI DI PADOVA

Padua, October 23, 2023

To the Editor of Molecular Metabolism

Dear Editor,

Please find attached the manuscript entitled "The Protease Activated Receptor 2 - CCAAT/Enhancer-Binding Protein beta - SerpinB3 axis inhibition as a novel strategy for the treatment of Non-Alcoholic Steatohepatitis", by Villano et al. submitted for publication in your Journal.

In the present study we provide evidence that the Protease Activated Receptor 2 may represent a novel molecular target for NASH, a major cause of hepatic diseases where approved drugs are still not available. The manuscript describes that the Protease Activated Receptor 2 (PAR2) inhibitor 1-Piperidine Propionic Acid (1-PPA) is effective in the control of adipogenesis, inflammation and fibrosis in NASH models. At mechanistic level, the antiprotease activity of SerpinB3 was found essential for PAR2 activation, determining upregulation of the CCAAT Enhancer Binding Protein beta (C/EBP-β), another pivotal regulator of metabolism, inflammation and fibrosis, which in turn determined SerpinB3 synthesis. 1-PPA treatment was able to inhibit the PAR2 - C/EBP-β - SerpinB3 axis and to protect from NASH progression, supporting the use of this approach for a targeted therapy of NASH.
All authors have contributed significantly, and all authors agree with the contents of the manuscript.
The authors declare that P.P., B.A., M.A., Q.S., R.M., T.C. and V.G. are listed as inventors of patent N. IT 102017000026858 of the University of Padova. No conflict of interest exists for the other authors.

We do hope that the present manuscript will be found suitable for publication in your Journal.

Sincerely,
Patrizia Pontisso, MD

Tel: 049 8212285 – 2291
Fax 049 8218292
clmed5@unipd.it

CF 80006480281
P.IVA 00742430283

Declaration of interests

☐ The authors declare that they have no known competing financial interests or personal relationships that could have appeared to influence the work reported in this paper.

☒ The authors declare the following financial interests/personal relationships which may be considered as potential competing interests:

The authors declare that P.P., B.A., M.A., Q.S., R.M., T.C. and V.G. are listed as inventors of patent N. IT 102017000026858, European patent EP 392351 and P.P., B.A., L.C., M.C., Q.S., R.M., T.C. and V.G of the Italian Patent Application N. 102022000014593 filed by the University of Padova, PTC pending. No conflict of interest exists for the other authors.

The Protease Activated Receptor 2 - CCAAT/Enhancer-Binding Protein beta - SerpinB3 axis inhibition as a novel strategy for the treatment of Non-Alcoholic Steatohepatitis

Villano Gianmarco[1*], Novo Erica[2*], Turato Cristian[3], Quarta Santina[4], Ruvoletto Mariagrazia[4], Biasiolo Alessandra[4], Protopapa Francesca[2], Chinellato Monica[4], Martini Andrea[4], Trevellin Elisabetta[4], Granzotto Marnie[4], Cannito Stefania[2], Cendron Laura[5], De Siervi Silvia[3], Guido Maria[4], Parola Maurizio[2**], Roberto Vettor[4**], Pontisso Patrizia[4**§].

[1]Dept. of Surgical, Oncological and Gastroenterological Sciences, University of Padova, Italy; [2]Dept. of Clinical and Biological Sciences, University of Torino, Italy; [3]Dept. of Molecular Medicine, University of Pavia, Italy; [4]Dept. of Medicine, University of Padova, Italy; [5]Dept. of Biology, University of Padova, Italy.

HIGHTLIGHTS

- SerpinB3 is a mediator of liver inflammation, steatosis and fibrosis
- The Protease Activated Receptor 2 (PAR2) is activated by SerpinB3
- The CCAAT Enhancer Binding Protein-beta is essential for SerpinB3 synthesis
- 1-Piperidine Propionic Acid inhibits PAR2 and protects from non-alcoholic steatohepatitis

The Protease Activated Receptor 2 - CCAAT/Enhancer-Binding Protein beta - SerpinB3 axis inhibition as a novel strategy for the treatment of Non-Alcoholic Steatohepatitis

Villano Gianmarco[1*], Novo Erica[2*], Turato Cristian[3], Quarta Santina[4], Ruvoletto Mariagrazia[4], Biasiolo Alessandra[4], Protopapa Francesca[2], Chinellato Monica[4], Martini Andrea[4], Trevellin Elisabetta[4], Granzotto Marnie[4], Cannito Stefania[2], Cendron Laura[5], De Siervi Silvia[3], Guido Maria[4], Parola Maurizio[2**], Roberto Vettor[4**], Pontisso Patrizia[4**§].

[1]Dept. of Surgical, Oncological and Gastroenterological Sciences, University of Padova, Italy; [2]Dept. of Clinical and Biological Sciences, University of Torino, Italy; [3]Dept. of Molecular Medicine, University of Pavia, Italy; [4]Dept. of Medicine, University of Padova, Italy; [5]Dept. of Biology, University of Padova, Italy.

* These authors contributed equally to the study

** Shared senior authorship

[§]**Corresponding Author**: Prof. Patrizia Pontisso

Dept. of Medicine, University of Padova

Via Giustiniani 2 35128 Padova (Italy)

Tel: +39 049 8217872 e-mail: patrizia@unipd.it

Abbreviations: Serpins, serine-protease inhibitors; TIMP-1, tissue inhibitor of metalloproteases type 1; MCD, methionine- and choline-deficient; NAFLD, non-alcoholic fatty liver disease; MASLD, metabolic dysfunction-associated steatotic liver disease; NASH, non-alcoholic steatohepatitis; TGF, transforming growth factor; α-SMA, α-smooth muscle actin; HIF, hypoxia-inducible factor; 1-PPA, 1-Piperidine Propionic Acid; C/EBP-β, CCAAT Enhancer Binding Protein beta; KO, knock-out; WT, wild-type; CDAA, choline-deficient aminoacid-defined; SAT, subcutaneous adipose tissue; VAT, visceral adipose tissue; BAT, brown adipose tissue; WAT, white adipose tissue; LAP, Liver Activating Protein; LIP, Liver Inhibitory Protein; qRT-PCR, quantitative real-time PCR reaction.

ABSTRACT

OBJECTIVE: The serine protease inhibitor SerpinB3 has been described as critical mediator of liver fibrosis and it has been recently proposed as an additional hepatokine involved in NASH development and insulin resistance. Protease Activated Receptor 2 has been identified as a novel regulator of hepatic metabolism. A targeted therapeutic strategy for NASH has been investigated, using 1-Piperidine Propionic Acid (1-PPA), since this compound has been recently proposed as both Protease Activated Receptor 2 and SerpinB3 inhibitor.

METHODS: The effect of SerpinB3 on inflammation and fibrosis genes was assessed in human macrophage and stellate cell lines. Transgenic mice, either overexpressing SerpinB3 or carrying Serpinb3 deletion and their relative wild type strains, were used in experimental NASH models. Subgroups of SerpinB3 transgenic mice and their controls were also injected with 1-PPA to assess the efficacy of this compound in NASH inhibition.

RESULTS: 1-PPA did not present significant cell and organ toxicity and was able to inhibit SerpinB3 and PAR2 in a dose-dependent manner. This effect was associated to a parallel reduction of the synthesis of the molecules induced by endogenous SerpinB3 or by its paracrine effects both in vitro and in vivo, leading to inhibition of lipid accumulation, inflammation and fibrosis in experimental NASH. At mechanistic level, the antiprotease activity of SerpinB3 was found essential for PAR2 activation, determining upregulation of the CCAAT Enhancer Binding Protein beta (C/EBP-β), another pivotal regulator of metabolism, inflammation and fibrosis, which in turn determined SerpinB3 synthesis.

CONCLUSIONS: 1-PPA treatment was able to inhibit the PAR2 - C/EBP-β - SerpinB3 axis and to protect from NASH development and progression, supporting the potential use of a similar approach for a targeted therapy of NASH.

Keywords

Serpins, genetically manipulated mice, experimental NASH, transcription factors, therapeutic drugs.

1. INTRODUCTION

The liver has a key role in maintaining metabolic homeostasis, particularly in controlling and modulating lipid and glucose metabolism, as well as in drug detoxification. In addition, the liver has also unique immunological aspects that include fetal hematopoiesis, induction of immune tolerance but, at the same time, also a very efficient innate immunity, to mention just a few [1]. Chronic liver injury, irrespective of etiology, can lead to the induction of persistent inflammatory response and dysregulated activation of wound-healing repair, with hepatic macrophages and myofibroblasts cooperating in a finely regulated manner and playing a prominent role in sustaining fibrogenic progression of the disease [1-5]. Interactions among different hepatic cell populations and release of a large number of mediators (i.e., growth factors, chemokines, pro-inflammatory cytokines, plasma proteins, reactive oxygen species, hepatokines, adipokines and more) as well as the involvement of multiple molecular pathways and of genetic and environmental factors are believed to play a major role in chronic liver disease progression [2-5].

SerpinB3 is a peculiar member of the family of **ser**ine-**p**rotease **in**hibitor**s** (Serpins) which is almost undetectable in normal murine and human liver [6]. However, under conditions of chronic liver injury of different etiology, SerpinB3 expression is significantly upregulated in hepatocytes in human liver biopsies [7,8] and even in liver carcinogenesis [9-11]. More recently, SerpinB3 has been proposed as a critical mediator of liver inflammation and fibrosis. Regarding this aspect, SerpinB3 up-regulates the expression of transforming growth factor (TGF)-β1 in chronic liver disease [7] and exerts a direct pro-fibrogenic action on human liver myofibroblasts in culture by strongly up-regulating the expression of pro-fibrogenic genes (including collagen type 1A1, α-smooth muscle actin or α-SMA, TGF-β1, and tissue inhibitor of metalloproteases type 1 or TIMP-1) [12]. The pro-fibrogenic action of SerpinB3 was mechanistically confirmed using transgenic mice overexpressing SerpinB3 in hepatocytes that were submitted to two distinct experimental protocols of chronic liver injury, including the protocol of methionine- and choline-deficient (MCD) diet able to induce fatty liver and steatohepatitis [12]. In addition, studies on transgenic mice, either overexpressing SerpinB3 or carrying Serpinb3 deletion, and

in vitro studies on human macrophage cell lines have shown that SerpinB3 can operate as a pro-inflammatory mediator in two models of progressive non-alcoholic fatty liver disease (NAFLD) [13], a definition that has been recently replaced by the new definition of "*metabolic dysfunction-associated steatotic liver disease*" (MASLD) [14]. The involvement of SerpinB3 in NAFLD and in its progressive form non-alcoholic steatohepatitis (NASH) is relevant since NAFLD is emerging as the major cause of chronic liver disease worldwide, with epidemiological data indicating a 30% prevalence in the general population and an even higher prevalence (> 70%) in obese individuals and Type II diabetes patients, which represent the typical NAFLD/NASH patients [5,15]. Moreover, despite promising indications from preclinical studies, at present no pharmacological therapy has been approved for NASH treatment [16,17]. NAFLD and its progression towards NASH is a resultant of a complex scenario involving excess energy intake, insulin resistance and inflammation, resulting in an increased flux of fatty acids to the liver, dysregulation of hepatic lipid metabolism and de novo lipogenesis [18].

SerpinB3 expression is up-regulated by hypoxic conditions and its increased transcription is mediated by specific binding of hypoxia-inducible factor (HIF)-2α to the SerpinB3 promoter [19]. Moreover, SerpinB3 has been shown to act as a paracrine mediator able to affect the behavior of surrounding cells by differentially up-regulating, in normoxic conditions, HIF-1α and HIF-2α [20]. In particular, SerpinB3 through HIF-1α up-regulation can favor cell survival in a harsh (i.e., hypoxic) microenvironment by inducing early cellular metabolic switch to glycolytic phenotype [20]. By contrast, SerpinB3 can induce HIF-2α stabilization through direct NEDDylation and this has been suggested to promote proliferation of liver cancer and to favor hepatocellular carcinoma progression [20]. Considering a putative role in relation to NAFLD/NASH patients, which are mostly obese individuals and/or type II diabetes patients, by inducing HIF-2α stabilization SerpinB3 may represent a factor able to deeply affect lipid metabolism. Indeed, studies employing mouse models with Cre-lox mediated deletion of VHL, HIF1α and/or HIF2α have shown that HIF-2α, rather than HIF-1α, plays a major role in regulating hepatocellular lipid accumulation by various mechanisms, including up-regulation of lipid biosynthetic pathways and suppression of fatty acid oxidation [21,22]. Moreover, studies in transgenic

mice carrying hepatocyte-specific deletion of HIF-2α and analysis performed on NAFLD/NASH patients have shown that HIF-2α activation is a key feature of both experimental and human NASH [23] and is also involved in NASH-related carcinogenesis, where HIF-2α levels were found to be strictly associated with hepatocyte production of SerpinB3 [24]. Due to the interconnections between SerpinB3, HIF-2α-mediated regulation of lipid metabolism and NAFLD/NASH progression, we proposed in a recent study that SerpinB3, which is mainly expressed and released by stressed/injured hepatocytes, may represent an additional novel hepatokine [13]. Hepatokines are defined as proteins synthetized and secreted by hepatocytes, able to affect metabolic processes through autocrine, paracrine and endocrine signaling and know to play a key role in orchestrating whole-body energy metabolism and to be involved in NASH and insulin resistance [25-27].

To further investigate the role of SerpinB3 in NASH progression, in the present study we have investigated a novel therapeutic strategy for the treatment of NASH using 1-Piperidine Propionic Acid (1-PPA), a small molecule patented and proposed as SerpinB3 inhibitor [28,29]. More recently, 1-PPA was also found to sterically inhibit the protease activated receptor 2 (PAR2) [30], a cell surface sensor of extracellular inflammatory and coagulation proteases, that has been also recognized as a new regulator of hepatic metabolism [31-32]. PAR2 indeed not only controls cholesterol homeostasis and lipid metabolism [31], but also suppresses glucose internalization, glycogen storage, and insulin signaling [32]. In the present study we have assessed whether 1-PPA may be able to inhibit steatosis, inflammation and fibrosis, the hallmarks of progressive NASH, *in vitro* and after parenteral administration in transgenic and wild type mice with diet-induced NASH. The use of Serpinb3 knock-out mice and of 1-PPA allowed us to confirm the essential role of the antiprotease activity of this serpin in the pathogenesis of NASH. Moreover, by investigating the efficacy of 1-PPA in inhibiting NASH progression, we also found that 1-PPA, through the inactivation of PAR2, determines a down-regulation of the early transcription factor CCAAT Enhancer Binding Protein beta (C/EBP-β). This transcription factor is highly expressed not only in adipose tissue, but also in liver, kidney, intestine, pancreatic islets, and

innate immune cells. It regulates the expression of several genes involved in development, immune function, regeneration, differentiation, and metabolism [33].

Since both PAR2 and C/EBP-β are activated in proinflammatory conditions [34, 35] and recent data also support their possible relevance in the process of fibrogenesis [36,37], our results provide evidence for the pivotal role of SerpinB3 in the activation of the PAR2 - C/EBP-β axis and for its effective inhibition by the small molecule 1-PPA.

2. RESULTS

2.1 SerpinB3 and development of murine NASH

To mechanistically investigate the role of SerpinB3 in relation to the development of murine NASH, we took advantage of mice genetically manipulated to carry a deletion in the reactive site loop of Serpinb3a [38], the closest isoform to human SerpinB3, hereafter indicated as knock-out (KO) mice, as well as their related wild-type (WT) mice on the common genetic background BALB/c. These KO mice, recently used to characterize the pro-inflammatory role of Serpinb3 in murine NASH [13], were fed for this part of the study on choline-deficient aminoacid-defined (CDAA) dietary protocol to induce experimental NASH, very effective and reliable to induce steatosis, inflammatory response and fibrosis [12,13,23]. The lack of the antiprotease activity of Serpinb3a in KO vs WT mice, fed on CDAA diet, determined a number of critical results in which KO mice showed: i) a marked decrease in steatosis in KO mice vs WT mice, as evident from the macroscopic aspect of livers (Figure 1A), hematoxylin/eosin staining (Figure 1B) and histopathological score (Figure 1C); ii) a decrease of transcript levels of markers of inflammatory response like IL-1β, TNF-α and the chemokine CCL-2 (Figure 1D), fully confirming results of the recently published study in which KO mice fed on CDAA diet were showing significantly less inflammatory response and infiltrate [13]; iii) a decrease in extracellular matrix deposition (i.e., liver fibrosis) as shown by Sirius Red staining (Figure 1E) and by related image analysis of liver sections (Figure 1F) as well as by a significant decrease in transcript levels for fibrogenesis markers like TGF-β1, α-SMA and collagen 1A1 (Figure 1G).

These data overall indicate that KO mice are less prone to develop NASH than related WT mice, supporting the critical role of Serpinb3a in this experimental setting. Essentially similar results were obtained in the second experimental protocol of NASH used in this study, in which KO mice were fed on MCD diet. However, because this protocol is more aggressive and less translatable to human conditions of NASH, statistically significant differences were achieved only for some of the investigated parameters (Suppl. Figure 1 A-E), including the decrease in IL-1β and CCL-2 transcript levels (Suppl. Figure 1B), the decrease in collagen deposition (Suppl. Figure 1 C, D), TGF-β1 transcript levels (Suppl. Figure 1E). Moreover, at basal level, KO mice were characterized by a decreasing trend of adipose tissue deposition in subcutaneous -, visceral - and brown - adipose tissue (SAT, VAT and BAT, respectively) (Figure 2 A,B). It should be noted that an opposite profile was observed in untreated TG mice (i.e., mice overexpressing SerpinB3 in hepatocytes), with this time a significant increase in SAT compartment (Figure 2 C,D).

2.2 1-Piperidin Propionic acid protects from NASH development and progression

As a first step, we have checked the cytotoxicity of 1-PPA both *in vitro* and *in vivo*. For the first purpose, we employed the *in vitro* model of HepG2 cells stably transfected to overexpress SerpinB3, hereafter indicated as HepG2/SB3 cells, that we already used in previous studies [19,20]. Of interest, 1-PPA exerted significant cytotoxicity and then reduced viability of HepG2/SB3 cells only when used at much higher concentrations (>5 μg/ml) (Suppl. Figure 2A). Moreover, 1-PPA significantly affected cell proliferation (followed for 70 hrs) at similarly higher concentrations, with a calculated EC50 value of 139.9 uM (Suppl. Figure 2B). The compound 1-PPA was also injected *in vivo* in WT C57BL6/J mice (i.e. mice with the background of mice genetically manipulated to overexpress SerpinB3 in hepatocytes that we used to test 1-PPA *in vivo*) to test its cytotoxicity at doses of 70 and 700 ng/g b.w. The dose of 70 ng/g b.w, used as experimental treatment in the NASH animal model, did not affect significantly liver and kidney biochemical parameters and histological features, a part from a mild interstitial lymphocyte inflammation of the kidney, while the dose of 700 ng/g b.w. determined a

significant increase of bilirubin and a trend toward increased values of creatinine (Suppl. Fig.2C and Suppl. Table 1).

To test the effect of the small molecule 1-Piperidin Propionic acid (1-PPA), an inhibitor not only of SerpinB3 synthesis [28,29], but also of PAR2 [30], we have analyzed the real efficacy of the compound in inhibiting SerpinB3 and PAR2 transcription in the HA22T/VGH cell line which constitutively expresses SerpinB3. Very low concentrations of 1-PPA significantly down-regulated both PAR2 and SerpinB3 transcript levels, in a dose-dependent manner up to 1 ng/ml concentration (Suppl. Figure 3A, B).

The *in vivo* efficacy of 1-PPA was tested on WT and transgenic mice on the same C57BL6/J background, but genetically manipulated to overexpress SerpinB3, hereafter indicated as TG/SB3 mice. WT and TG/SB3 mice were fed on CDAA diet for 12 weeks, as previously described [12,13], and treated or not with 1-PPA (70 ng/g b.w., i.p.) to investigate the effects of 1-PPA on inflammatory and fibrogenic responses.

Concerning inflammatory response, we confirmed that liver specimens from TG/SB3 mice fed on CDAA diet were characterized, when compared to specimens from WT mice, by a significant increase in inflammatory infiltrate of F4/80 positive macrophages (Figure 3A,B), which were often aggregated to form the typical so-called *"crown-like structures"* (Figure 3A), and an increase in IL-1β and TNF-α transcript levels (Figure 3C), as recently reported [13]. Of interest, all these parameters were significantly reduced in TG/SB3 mice (some also in WT mice) following *in vivo* 1-PPA administration (Figure 3A, C). In particular, we noted not only a significant reduction of F4/80 positive macrophage infiltration and of IL-1β and TNF-α transcript levels, but also a very evident disappearance of *"crown-like"* aggregates of macrophages (Figure 3A). Along these lines, since literature reports that NASH-associated macrophages (NAMs) are involved in forming crown-like structures in NASH livers and that SerpinB3 influences the hepatic levels of NAMs markers CD9, TREM2 and Galectin 3 (13), we have investigated whether 1-PPA was able to modulate the expression of these markers. Interestingly, 1-PPA significantly reduced the transcript levels of Galectin 3, CD9, and TREM2 in TG/SB3 mice fed on

CDAA diet (Figure 3D). It is worth to note that SerpinB3 expression, that was detectable in WT mice, but more evident in TG/SB3 mice fed with CDAA, was markedly reduced in mice treated with 1-PPA of both strains (Figure 3E).

Data obtained in mice fed on CDAA were essentially confirmed also in TG/SB3 mice fed on MCD diet: in these mice 1-PPA administration reduced infiltration of F4/80 positive macrophages (Suppl. Figure 4A,B), "*crown-like*" aggregates of macrophages (Suppl. Figure 4A) and IL-1β, TNF-α transcript levels (Suppl. Figure 4C).

Similar results were obtained by analyzing parameters related to fibrogenesis. Histochemical Sirius Red staining (Figure 4A), by confirming the increased deposition of extracellular matrix in TG/SB3 mice vs WT mice, showed that administration of 1-PPA significantly reduced fibrosis in both TG/SB3 and WT mice (Figure 4A), as confirmed by image analysis of collagen positive areas (Figure 4B). Similarly, in TG/SB3 mice 1-PPA administration resulted in a significant down-regulation of the transcript levels for α-SMA, collagen 1A1 and TGF-β1 (Figure 4C). Once again, homologous results were obtained when parameters related to fibrogenesis were investigated in TG/SB3 mice fed on MCD diet: 1-PPA administration reduced also in these mice the steatosis score (Suppl. Figure 5A), Sirius Red staining and collagen positive area (Suppl. Figure 5B) and transcript levels of critical parameters (Suppl. Figure 5C) .

Data on the effect of 1-PPA on inflammatory response and fibrogenesis were essentially confirmed when the compound was directly employed on either LX2 cells (a human immortalized myofibroblast cell line) or THP-1 cells (a cell line of human macrophages) exposed to human recombinant SB3 (hrSB3). The results obtained for LX2 cells indicate that 1-PPA was able to down-regulate in these cells hrSB3 – induced transcription for critical genes like collagen 1A1, α-SMA, CCL-2 and VEGF-A (Figure 5A). Similarly, 1-PPA down-regulated transcript levels of TNF-α, IL-1β, CCL-2, CCL-15, IL-13 and TGF-β1 that were induced by hrSB3 in THP-1 cells (Figure 5B).

2.3 PAR2 inhibition by 1-Piperidin Propionic acid prevents the SerpinB3 induced promoter CEBP-β up-regulation

To better understand the mechanistic behaviour of 1-PPA, the possibility of a direct interaction of 1-PPA with SerpinB3, beside PAR2 steric inhibition [30], was explored. For this purpose, two different biophysical approaches were tested. The thermal shift assay was used to evaluate whether the possible interaction with 1-PPA could modify the thermic stability of this serpin. As reported in Suppl. Figure 6A, the denaturation curves showed irrelevant T melting differences, within the instrumental error (± 2°C), when SerpinB3 (5 μM) was mixed with different concentrations of 1-PPA, ranging from 5 to 500 μM.

To further confirm these data, the interaction was examined with isothermal titration calorimetry, widely used to assess biomolecular interactions, and also this approach provided negative results (Suppl. Figure 6B). The potential difference (μW) was indeed evaluated and no binding model was identified, confirming that the compound does not interact directly with SerpinB3.

On the basis of these results, and also considering the fact that 1-PPA determines transcriptional inhibition of SerpinB3 mRNA, we have assessed whether PAR2 activation could up-regulate possible promoters or enhancers for SerpinB3 gene, involved in metabolism and whether this effect could be abrogated following PAR2 inhibition by 1-PPA. Beside the already known up-regulator of SerpinB3 synthesis HIF-2α [19], previously found also to play a relevant role in lipid accumulation [21,22], in the human gene database GeneCards the CCAAT Enhancer Binding Protein Beta (CEPB-β) is listed. Since also this transcription factor is profoundly implicated in metabolic disturbances and in increased inflammatory response [33,35], we have assessed its expression in different cell lines with or without 1-PPA treatment and in mouse livers in relation to SerpinB3 expression. As expected, this transcription factor, that was found significantly up-regulated in HepG2 cells overexpressing SerpinB3, compared to control HepG2, was inhibited by 1-PPA in a dose dependent manner (Figure 6A). In the monocytic THP-1 cell line, the basal level the CEPB-β transcription factor was not detectable, but it was induced by exogenous hrSB3, suggesting a positive loop induction of both molecules. Also in this case, 1-PPA

efficiently switched down CEPB-β expression, even at low concentration (Figure 6B). In addition, using HepG2 cell lines stably transfected to overexpress the wild type SerpinB3 form or the isoform lacking its anti-protease activity, obtained from HepG2 cells transfected with a mutant plasmid deleted in the SerpinB3 reactive site loop [7], we could demonstrate that the anti-protease activity of this serpin is essential for the protein induction of both the isoforms Liver Activating Protein (LAP) and Liver Inhibitory Protein (LIP) of CEPB-β [39] (Figure 6C, D). These data are in line with the results obtained in untreated mouse livers, where CEPB-β was significantly up-regulated in SB3/TG mice, compared to the corresponding wild type mice, while it was barely lower than in controls in SB3/KO mice (Figure 6E).

Along these lines, we analyzed *in vitro* cellular models carrying different expression of SerpinB3, namely, the HepG2 cell lines stably transfected to overexpress the wild type SerpinB3 form or the isoform lacking its anti-protease activity and the HA22T cell line that constitutively expresses SerpinB3 (Suppl. 3A). Immunofluorescence results not only confirmed the requirement of the integrity of the anti-protease activity of SerpinB3 to up-regulate and to determine nuclear translocation of CEPB-β (Figure 7A), but also indicate that this is an essential requirement for the over-expression of PAR2. While HepG2/SB3 cells showed indeed a marked increase of this membrane receptor, compared to HepG2/WT, the lack of antiprotease activity carried by HepG2/Δ7 cells was associated to a reduced expression of PAR2 (Figure 7B). In addition, the HA22T/VGH cell line showed both up-regulation and nuclear translocation of CEPB-β and up-regulation of PAR2 (Figure 7A, B). In this cell line 1-PPA, beside the previously described ability to reduce SerpinB3 and of PAR2, determined also a significant reduction of CEPB-β transcription in a dose dependent manner (Suppl. Fig. 3C). On the other hand, silencing of CEPB-β led to a significant decrease not only of the target gene, but also of SerpinB3 (Figure 7 C, D). The inhibitory effect 1-PPA on PAR2 was also confirmed in the liver of mouse fed with CDAA, where PAR2 was significantly up-regulated in SB3/TG mice, compared to the corresponding wild type mice and strongly reduced after 1-PPA treatment (Figure 7 E, F).

3. DISCUSSION

While the successful treatments for hepatitis B and C have markedly reduced the burden of liver disease of viral etiology, non-alcoholic steatohepatitis (NASH) has emerged as a major cause of hepatic diseases in Western countries and it is expected to become the leading indication for liver transplantation and of liver-related mortality within a few years worldwide [40]. Despite the urgent need of effective therapies, approved drugs for NASH are still not available [41]. Several novel compounds, targeting different molecular events involved in the pathogenetic mechanism of NASH, including pathogenic metabolism, insulin resistance, inflammatory cell recruitment and pro-fibrogenic matrix profile, are currently in the pipeline, and while some of them failed in phase 2 or 3 clinical trials, others are providing promising results [5,42].

In the present study we provide evidence that SerpinB3-activated PAR2 can represent a novel molecular target for NASH. We have used the SerpinB3 and PAR2 inhibitor 1-PPA [28-30] to explore its ability to reduce the development of NASH in two different mouse models. PAR2 belongs to the protease-activated G-protein-coupled family of receptors and it has been recently described to play a pivotal role in metabolism control [31,32], beside to be a well-known driver of inflammatory responses [43]. The essential role of the anti-protease activity of SerpinB3 was supported by the results obtained in genetically modified mice, since mice lacking the anti-protease activity of SerpinB3 not only had lower fat accumulation in basal conditions, but were also less prone to develop NASH, compared to control littermates. These findings were supported by lower fibrogenic and inflammatory responses following both CDAA and MCD diets. Conversely, transgenic mice overexpressing SerpinB3 developed a more intense liver damage, compared to the corresponding wild-type strain, characterized by increased fat accumulation, higher features of fibrosis and higher inflammatory response. These results corroborate previous findings reporting a pivotal role of SerpinB3 in the activation of the fibrogenic and inflammatory responses in NASH experimental models [12, 13]. Further studies are required to identify the specific protease(s) involved in the interaction with SerpinB3, determining the activation of the PAR2 cellular receptor.

The small molecule 1-PPA, while did not induce significant cell and organ toxicity, was able to inhibit both PAR2 and SerpinB3 synthesis in a dose-dependent manner at very low concentrations. The inhibitory effect on SerpinB3 was associated to a parallel reduction in the synthesis of all the molecules induced by either the endogenous serpin or by its paracrine effect, as observed in the monocytic and stellate cell lines. The results obtained in experimental animals confirmed these findings and the weekly injection of 1-PPA was effective to markedly reduce the features of NASH not only in wild type mice but also in SerpinB3 overexpressing mice. In particular, as recently reported [13], SerpinB3 was able to influence the hepatic levels of Galectin 3, CD9 and TREM2, typical markers of NAMs, a population of hepatic macrophages emerging in progressive NAFLD-NASH and strictly associated with severity of steatosis, inflammation as well as fibrosis [44]. It is worth to note that 1-PPA was able to revert this effect by reducing hepatic levels of the typical markers of NAMs in mice transgenic for SerpinB3, suggesting a role of this compound in the shutdown of this class of macrophages induced by SerpinB3.

Concerning the mechanism of action of 1-PPA, it has been recently reported that it binds PAR2 in an allosteric pocket of the receptor inactive conformation, with antagonistic activity [30]. No information is available to date on its modality of SerpinB3 inhibition. To address this point, we have explored the possible direct interaction between 1-PPA and SerpinB3, but different biochemical approaches provided negative results. We have then explored the effect of this compound on C/EBP-β, a recently identified SerpinB3 transcription factors, documenting that it is upregulated in presence of SerpinB3, but only if carrying its active antiprotease activity. Several evidences indicate that C/EBP-β is profoundly involved in the processes related to metabolic syndrome [33] and these findings are in line with the fact that in our study mice lacking the active form of Serpinb3a presented at basal conditions a decreased fat mass and a trend toward lower levels of C/EBP-β. Like PAR2 [43] and SerpinB3[45], C/EBP-β is activated in pro-inflammatory and ER stress conditions [46], and also these data are in agreement with the fact that our KO-mice presented a lower inflammatory response after CDAA or MCD diet, while opposite results were observed in SerpinB3 transgenic mice which already at basal level showed C/EBP-β levels higher than those of control mice. Concerning the involvement of this transcription factor in fibrogenesis,

recent data indicate that alveolar accumulation of C/EBP-β in lung macrophages from patients and mice with pulmonary fibrosis causes upregulation of several profibrotic factors promoting pulmonary fibrosis, while its pharmacological degradation determines an effective therapeutic response against experimental fibrosis [37]. The compound 1-PPA was able not only to suppress PAR2 and SerpinB3, but also C/EBP-β transcription in hepatoma cells over-expressing SerpinB3.

On the basis of the results obtained, we propose that SerpinB3 is essential for PAR2 activation, which in turn up-regulates C/EBP-β, promoting SerpinB3 transcription. This cascade of events can be inhibited by 1-PPA that sterically determines PAR2 inhibition and blocks the described positive loop.

In conclusion, our study demonstrates that the PAR2 - C/EBP-β – SerpinB3 axis is relevant in the development of NASH. The small molecule 1-PPA is effective in the control of steatosis, inflammation and fibrosis in NASH experimental models through the inhibition of PAR2 activation and of its downstream molecules, like C/EBP-β and SerpinB3, implicated in metabolic alterations and NASH.

Further studies are warranted in order to confirm whether the PAR2 inhibitor 1-PPA could be considered a clinically relevant strategy for NASH treatment.

4. MATERIALS AND METHODS

4.1 Cell lines

Hepatoma cells (HepG2 cell line) (ATCC, Manassas, VA, USA), authenticated by BMR Genomics S.r.l. (Padova, Italy), according to PowerPlex® Fusion System protocol (Promega), have been engineered to stably overexpress SerpinB3, as previously described [47]. Briefly cells were transfected with a plasmid expression vector containing the whole human SerpinB3 gene, with a plasmid vector containing the SerpinB3 gene deleted of 7 aminoacids in the hinge region of the reactive site loop, lacking the antiprotease activity (Mutant B [7], kindly provided by Prof. Prof. TJ Harrison, University College, London) or with the plasmid vector alone (pcDNA3.1D/V5-His-TOPO™), as control, using Lipofectamine Reagent Plus (Invitrogen, Carlsbad, CA, USA). Transfected cells were selected using G418 (Geneticin) (Sigma-Aldrich, St. Louis, MO). Control HepG2 and HepG2 cells overexpressing

whole SerpinB3 (HepG2/SB3) were incubated for 24 hours with the SerpinB3 inhibitor 1-PPA (Sigma-Aldrich, St. Louis, Missouri, USA) at different concentrations (range 5-50 μg/ml) to assess cytotoxicity. For the assessment of 1-PPA cytotoxicity, real time cell proliferation was assessed using the xCELLigence instrument (ACEA Biosciences, Inc., San Diego, CA, USA), as previously described [48]. Dynamic cell proliferation was monitored at 15 min intervals and analyzed with RTCA software. The results were expressed as cell index value.

The human monocytic cell line THP-1 (kindly provided by Prof. Fabio Marra, University of Florence) and human LX2 cells (kindly provided by Prof. Scott L. Friedman, Icahn School of Medicine, Mount Sinai, New York) were cultured in Dulbecco's modified Eagle's medium (Sigma Aldrich Spa, Milan, Italy), supplemented with 10% fetal calf serum and 1% antibiotics. These cells, expressing trivial levels of SerpinB3, were incubated for 24 hours with the recombinant entire SerpinB3 protein (hrSB3), obtained in our laboratory as previously described [49], at 200 ng/ml (LX2 cells) or at 100 ng/ml (THP-1 cells). Cells were simultaneously treated with 1-PPA at a concentration of 1 ng/mL to 100 ng/ml, or with medium supplemented with 10% FCS alone and in the cellular extracts the transcriptional expression of different cytokines, including TGF-β, TNF-α, IL1-β, IL-13, CCL-2, CCL-15, VEGF, α–SMA, collagen 1A1, was analyzed.

The expression of PAR2 and of the transcription factor CEBP-β was assessed in the cell lines described above and also in the hepatoma cells HA22T/VGH (kind gift of Prof. Giuseppina De Petro, University of Brescia) that express constitutively SerpinB3, in presence of 1-PPA at a concentration of 1 ng/ml to 100 ng/ml, or in medium supplemented with 10% FBS, as control.

4.2 Molecular amplification techniques

In cell lines and in liver tissue samples total RNA was extracted using RNasy Trizol (Invitrogen, Carlsbad, CA, USA) according to the manufacturer's instructions. After determination of the purity and the integrity, total RNA, complementary DNA synthesis and quantitative real-time PCR reactions (qRT-PCR) were carried out as previously described [50] using the CFX96 real-time instrument (Bio-Rad

Laboratories Inc, Hercules, CA, USA). Relative gene expression was normalized to the housekeeping genes and was calculated using the $2^{-\Delta\Delta CT}$ method [51]. Specificity of the amplified PCR products was determined by melting curve analysis and confirmed by agarose gel electrophoresis. Human and mouse primer sequences used in the study are reported in Supplemental Table 2.

RNA interference experiments to knockdown C/EBP-β expression were carried out in HA22T/VGH cells by transient transfection. Cells ($0.5x10^6$ cells/well) were seeded in 6 well plates containing or not cover glasses for immunofluorescence or molecular amplification analysis the day before. The siRNA for C/EBP-β and a negative siRNA control (Qiagen, Hlden, Germany) were transfected using Lipofectamine 3000 (Invitrogen-Waltham, Massachusetts, USA), following manufacturer's instructions. Cells were harvested 48 h post-transfection and glasses were fixed using 4% PFA. The knockdown gene efficiency was confirmed by qRT-PCR and immunofluorescence analysis.

4.3 Animal models

4.3.1 *NASH experimental models*

The study was carried out on C57BL/6 mice (12 weeks old) transgenic for human SerpinB3, (kindly provided by Prof. Cassani, Tecnogen, Caserta, Italy) [52], and their corresponding wild type C57BL/6 mice of similar age. BALB/c mice, deficient of the reactive site loop of Serpinb3a (Serpinb3-KO, originally kindly provided by Dr. Gary Silverman and Dr. Cliff J. Luke, Dept of Pediatrics, Washington University School of Medicine, St. Louis, MO) [38] have been also used and compared with wild type BALB/c mice of similar age as control.

All animals were kept under specific pathogen-free conditions and maintained with free access to pellet food and water at the Animal Care Facility of the Experimental Surgery Division of the University of Padua.

In order to induce experimental NASH, SerpinB3-transgenic (TG) and Serpinb3-KO (Sb3-KO) mice and their control littermates were fed on (a) the choline-deficient, L-amino acid defined (CDAA) diet (Laboratorio Dottori Piccioni, Gessate, Italy) for 12 weeks or (b) the methionine-choline deficient

(MCD) diet (Laboratorio Dottori Piccioni, Gessate, Italy) for 8 weeks (7 animals/group). Parallel groups of TG and control mice, fed on CDAA diet (5 animals/group) or on MCD diet (5 animals/group), were injected weekly with PPA (70 ng/g) or with the vehicle alone, starting from the third and second month and were sacrificed at week 12 and week 8, respectively. Liver samples were obtained, and one part was formalin-fixed and paraffin-embedded, while one part was immediately frozen at -80°C for morphological or molecular analyses. Experiments and protocols were approved by the Animal Welfare Committee of University of Padua and by the Animal Investigation Committee of the Italian Ministry of Health (n° 442/2018-PR and n° 116/92), in accordance with European Union regulations.

4.3.2 *Fat assessment in different mice strains*

Fat distribution was assessed in untreated SerpinB3 transgenic or knockout mice and in their corresponding wild type strains (5 animals/group). For the adipose tissue sampling, the mice were weighed and euthanized at the end of the experiment. The adipose tissues were dissected and weighed after death. In detail, dorsal and ventral external surfaces of the mouse were sterilized with 70% ethanol to minimize contamination during dissection. The skin on the back was removed and a layer of white adipose tissue (WAT) was visible at the level of the shoulder blades. This layer covered the two lobes of interscapular brown adipose tissue (BAT). These two kinds of adipose tissue were dissected together and further separated outside the body, as the two tissue were clearly distinguishable based on their color. Similarly, after removal of the skin at the level of the flanks of the body, there was a layer of subcutaneous adipose tissue (SAT) positioned against the rib cage on both sides that was also removed. Lining the intestines and attached to each epididymis and testis were the large vessel-rich adipose depots, the visceral adipose tissue (VAT) that was collected after its separation from epididymis and vas deferens.

4.4 Histochemistry, immunohistochemistry and Sirius Red Staining

In paraffin-embedded murine liver sections, steatosis score was semi-quantified, after hematoxylin-eosin

staining, using a four-tier scoring scale based on the extent of fat content (0 = negative; 1+ = < 10%; 2+ = >10, ≥30%; 3+ = >30%). Immunohistochemistry for the monocytic marker F4/80, SerpinB3 and PAR2 was assessed as previously described [13]. Collagen deposition was analyzed by Picro-Sirius Red staining. Quantification of immunostaining and fibrosis were assessed by histomorphometric analysis and images were then analyzed using ImageJ software (National Institutes of Health,Bethesda, MD), as previously described [13].

4.5 Immunofluorescence

HepG2 and HAT22/VGH were seeded on slides (4×10^5 cells/slide) and cells were fixed with 4% paraformaldehyde, permeabilized with 0.4% Tryton X-100, and blocked with 5% goat serum (Invitrogen Life Technologies, Waltham, MA, USA) in PBS containing 1% BSA. Slides were incubated with rabbit monoclonal anti-C/EBP-β and anti-PAR2 (Abcam-Cambridge UK) antibodies for 1 h at room temperature, followed by incubation with the anti-rabbit Alexa Fluor 546 (Invitrogen Life Technologies, Waltham, MA, USA) secondary antibody. Cellular nuclei were counterstained with Dapi (Merck KGaA, Darmstadt, Germany). Slides were mounted with ELVANOL (Merck KGaA, Darmstadt, Germany) and observed under a fluorescence microscope (Axiovert 200M-Apotome.2, Carl Zeiss MicroImaging GmbH, Göttingen, Germany).

4.6 1-Piperidin Propionic acid animal toxicity

To assess 1-PPA toxicity, 6 weeks old C57BL/6 mice, kept with free access to pellet food and water, were injected weekly with the 1-PPA concentration used in the NASH models (70 ng/g) or with 10 times higher 1-PPA concentration (700 ng/g) for 26 weeks (3 mice/group), a time length that is two to three-fold higher than that of the NASH models. Blood samples were achieved by tail vein puncture before starting 1-PPA injections, while at the end of the study animals were sacrificed and blood samples were taken by cardiac puncture. Kidney and liver samples were removed, formalin fixed and paraffin embedded for histologic examination. In collected serum samples alanine amino transferase (ALT) and

bilirubin were analyzed to assess liver damage, while serum creatinine was analyzed to assess kidney function.

4.7 Biophysical analysis of 1-piperidin propionic acid-SerpinB3 interaction

To verify whether 1-PPA was physically interacting with SerpinB3, as possible mechanism of action, the following approaches were used:

*4.7.1 Differential Scanning Fluorimetry***.** Purified recombinant human SerpinB3, obtained in our laboratory, as previously described [49], was incubated at 5 µM concentration with increasing concentration of 1-PPA (0, 5, 50, 500 µM) and SYPRO® ORANGE (Thermofisher Scientific) 8x. The samples were prepared in triple technical replicates solubilized in PBS pH 7.4. The samples were then thermically denatured, with a linear gradient of +0.5 °C/min, and the fluorescence was measured with StepOne® Real-Time PCR System (Thermofisher Scientific).

4.7.2 Isothermal Titration Calorimetry. SerpinB3 was buffer exchanged in a 50 mM MES pH 5.5, 500 mM NaCl with final concentration of 57 µM and 1-PPA was solubilized in the same buffer at 10 mM concentration. Isothermal titration calorimetry (ITC) experiments were carried out in PEAQ-ITC Calorimeter (Malvern) at 25°C. The analysis was performed with recombinant SerpinB3 at 57 µM and 1-PPA was used as titrant at 2 mM in the injection syringe. The measure was carried for 40 injections and while the sample was stirred. Data were analyzed with Microcal PEAQ-ITC software.

4.8 Statistical analysis

Statistical significance was determined by non-parametric procedures using the Student's t test or ANOVA for analysis of variance. Normality of distribution for quantitative variables was assessed by Kolmogorov and Smirnov test. The calculations were carried out with Graph Pad InStat Software (San Diego, CA, USA). The null hypothesis was rejected at $P<0.05$. Data in bar graphs represent means $\pm$ SEM and were obtained from at least three independent experiments. Western-blot and morphological images are representative of at least three experiments with similar results.

Acknowledgments

The Authors are deeply grateful to Prof. Giuseppina De Petro, University of Brescia, for providing the HA22T/VGH cell line, to Prof. Fabio Marra, University of Florence, for providing the THP-1 cell line, to Prof. Scott L. Friedman, Icahn School of Medicine, Mount Sinai, New York, for providing the human LX2 cell line, to Prof. Prof. TJ Harrison, University College, London for providing the plasmid carrying the SerpinB3 deleted in the hinge region of the reactive site loop, to Prof. Cassani, Tecnogen, Caserta, Italy, for providing the initial colony of C57BL/6 mice transgenic for human SerpinB3, to Prof. Gary Silverman and Prof. Cliff J. Luke, Dept of Pediatrics, Washington University School of Medicine, St. Louis, MO, for providing the initial colony of Balb/C mice, deficient of the reactive site loop of Serpinb3a and to Dr. Luciano Adorini for his critical reading of the manuscript and for his valuable suggestions.

The study was supported in part by the University of Padova [Project No CPDA110795] (P.P.), National Ministry of Health (RF-2019-12369984) (P.P.), Associazione Italiana per la Ricerca sul Cancro (AIRC) under IG2017-ID 20361 (M.P.)

Author contributions

Conceptualization, V.G., N.E., P.M., V.R., P.P.; Methodology, T.C., S.Q., R.M., F.P., B.A., C.M., T.E., G.M., D.S.S., C.S., Formal analysis, V.G., N.E., P.M., V.R., P.F., G.M., C.L., D.S.S; Funding acquisition, P.M., V.R., P.P.; Investigation, V.M., N.E., T.C., M.A., P.F, G.M.; Project administration, P.P., P.M., R.V.; Resources, P.P., P.M., V.R.; Supervision P.P., P.M., R.V.; Validation, P.P., P.M.,V.R., A.M, C.L.; Visualization, V.G., T.C., P.P.; Writing original draft, V.G., T.C., M.A., N.E,; Writing review & editing, P.P., P.M., V.R.

Declaration of interests

The authors declare that P.P., B.A., M.A., Q.S., R.M., T.C. and V.G. are listed as inventors of patent N. IT 102017000026858, European patent EP 392351 and P.P., B.A., L.C., M.C., Q.S., R.M., T.C. and V.G of the Italian Patent Application N. 102022000014593 filed by the University of Padova, PTC pending. No conflict of interest exists for the other authors.

REFERENCES

1. Pellicoro, A., Ramachandran, P., Iredale, J.P., Fallowfield, J.A. (2014) Liver fibrosis and repair: immune regulation of wound healing in a solid organ. Nat Rev Immunol 14, 181-94. doi: 10.1038/nri3623.

2. Schuppan, D. (2015). Liver fibrosis: Common mechanisms and antifibrotic therapies. Clin Res Hepatol Gastroenterol 39 Suppl 1, S51-9. doi: 10.1016/j.clinre.2015.05.005.

3. Parola, M., Pinzani, M. (2019) Liver fibrosis: Pathophysiology, pathogenetic targets and clinical issues. Mol Aspects Med 65, 37-55. doi: 10.1016/j.mam.2018.09.002.

4. Wen, Y., Lambrecht, J., Ju, C., Tacke, F. (2021) Hepatic macrophages in liver homeostasis and diseases -diversity, plasticity and therapeutic opportunities. Cell Mol Immunol 18, 45-56. doi: 10.1038/s41423-020-00558-8.

5. Lee. Y.A., Friedman, S.L. (2022). Inflammatory and fibrotic mechanisms in NAFLD-Implications for new treatment strategies. J Intern Med 291,11-31. doi: 10.1111/joim.13380.

6. Sun, Y., Sheshadri, N., Zong, W.X. SERPINB3 and B4: From Biochemistry to Biology. Semin Cell Dev Biol (2017), 62,170–77. Doi: 10.1016/j.semcdb.2016.09.005

7. Turato, C., Calabrese, F., Biasiolo, A., Quarta, S., Ruvoletto, M., Tono, N., Paccagnella, D., Fassina, G., Merkel, C., Harrison, T.J., et al. (2010). SERPINB3 modulates TGF-β expression in chronic liver disease. Lab Invest 90, 1016–1023. doi: 10.1038/labinvest.2010.55.

8. Biasiolo, A., Chemello L, Quarta S, Cavalletto L, Bortolotti F, Caberlotto C, Beneduce L, Bernardinello E, Tono N, Fassina G, Gatta A, Pontisso P. (2008) Monitoring SCCA-IgM complexes in

serum predicts liver disease progression in patients with chronic hepatitis. J Viral Hep 15, 246–249. doi: 10.1111/j.1365-2893.2007.00935.x.

9. Pontisso, P., Calabrese, F., Benvegnù, L., Lise, M., Belluco, C., Ruvoletto, M., Marino, M., Valente, M., Nitti, D., Gatta, A. et al. (2004) Overexpression of squamous cell carcinoma antigen variants in hepatocellular carcinoma. Br J Cancer 90, 833–837. doi: 10.1038/sj.bjc.6601543.

10. Beneduce, L., Castaldi F, Marino M, Quarta S, Ruvoletto M, Benvegnù L, Calabrese F, Gatta A, Pontisso P, Fassina G. (2005) Squamous cell carcinoma antigen immunoglobulin M complexes as novel biomarkers for hepatocellular carcinoma. Cancer 103, 2558–2565. doi: 10.1002/cncr.21106

11. Guido, M., Roskams T, Pontisso P, Fassan M, Thung SN, Giacomelli L, Sergio A, Farinati F, Cillo U, Rugge M. (2008) Squamous cell carcinoma antigen in human liver carcinogenesis. J Clin Pathol 61, 445–447. doi: 10.1136/jcp.2007.051383.

12. Novo, E., Villano, G., Turato, C., Cannito, S., Paternostro, C., Busletta, C., Biasiolo, A., Quarta, S., Morello, E., Bocca, C. et al. (2017). SerpinB3 promotes pro-fibrogenic responses in activated hepatic stellate cells. Sci Rep 7, 3420-3423. doi: 10.1038/s41598-017-03744-3.

13. Novo, E., Cappon, A., Villano, G., Quarta, S., Cannito, S., Bocca, C., Turato, C., Guido, M., Maggiora, M., Protopapa, F., et al. (2022) SerpinB3 as a pro-inflammatory mediator in the progression of experimental non-alcoholic fatty liver disease. Front Immunol 13:910526. doi: 10.3389/fimmu.2022.910526

14. Rinella ME, Lazarus JV, Ratziu V, Francque SM, Sanyal AJ, Kanwal F, et al. A multi-society Delphi consensus statement on new fatty liver disease nomenclature. J. Hepatol. 2023; S0168-8278(23)00418-X. doi: 10.1016/j.jhep.2023.06.003.

15. Kanwal, F., Shubrook, J.H., Younossi, Z., Natarajan, Y., Bugianesi, E., Rinella, M.E., Harrison, S.A., Mantzoros, C., Pfotenhauer, K., Klein S. et al. (2021). Preparing for the NASH Epidemic: A Call to Action. Gastroenterology 161:1030–42. doi: 10.1053/j.gastro.2021.04.074

16. Younossi Z, Tacke F, Arrese M, Chander Sharma B, Mostafa I, Bugianesi E, Wong, V.W-S. Yilmaz, Y., George, J., Fan, J. et al. (2019). Global Perspectives on Nonalcoholic Fatty Liver Disease and

Nonalcoholic Steatohepatitis. Hepatology 69:2672–82. doi: 10.1002/hep.30251

17. Friedman, S.L., Neuschwander-Tetri, B.A., Rinella, M., Sanyal, A.J. (2018). Mechanisms of NAFLD development and therapeutic strategies. Nat Med 24:908-922. doi: 10.1038/s41591-018-0104-9.

18. Loomba, R., Friedman, S.L., Shulman, G.I. (2021). Mechanisms and disease consequences of nonalcoholic fatty liver disease. Cell 184:2537- 64. doi: 10.1016/j.cell.2021.04.015

19. Cannito, S., Turato, C., Paternostro, C., Biasiolo, A., Colombatto, S., Cambieri, I., Quarta, S., Novo, E., Morello, E., Villano, G., et al. (2015). Hypoxia up-regulates SERPINB3 through HIF-2α in human liver cancer cells. Oncotarget 6, 2206-21. doi: 0.18632/oncotarget.2943.

20. Cannito, S., Foglia, B., Villano, G., Turato, C., Delgado, C.T., Morello, E., Pin, F., Novo, E., Napione, L., Quarta, S. et al. (2019). SerpinB3 Differently Up-Regulates Hypoxia Inducible Factors -1α and -2α in Hepatocellular Carcinoma: Mechanisms Revealing Novel Potential Therapeutic Targets. Cancers 11,1933. doi: 10.3390/cancers11121933.

21. Rankin, E.B., Rha, J., Selak, M.A., Unger, T.L., Keith, B., Liu, Q., Haase, V.H. (2009). Hypoxia-inducible factor 2 regulates hepatic lipid metabolism. Mol Cell Biol 29, 4527–4538. doi: 10.1128/MCB.00200-09.

22. Qu, A., Taylor, M., Xue, X., Matsubara, T., Metzge,r D., Chambon, P., Gonzalez, F.J., Shah, Y.M. (2011). Hypoxia-inducible transcription factor 2a promotes steatohepatitis through augmenting lipid accumulation, inflammation, and fibrosis. Hepatology 54, 472–483. doi: 10.1002/hep.24400.

23. Morello, E., Sutti, S., Foglia, B., Novo, E., Cannito, S., Bocca, C., Rajsky, M., Bruzzì, S., Abate, M.L., Rosso, C., et al. (2018). Hypoxia inducible factor 2a drives nonalcoholic fatty liver progression by triggering hepatocyte release of histidine rich glycoprotein. Hepatology; 67, 2196–2214. doi: 10.1002/hep.29754.

24. Foglia, B., Sutti, S., Cannito, S., Rosso, C., Maggiora, M., Autelli, R., Novo, E., Bocca, C., Villano, G., Ramavath, N.N. et al. (2022). Hepatocyte-Specific Deletion of HIF2α Prevents NASH-Related Liver Carcinogenesis by Decreasing Cancer Cell Proliferation. Cell Mol Gastroenterol Hepatol 13:459-82.

doi: 10.1016/j.jcmgh.2021.10.002.

25. Meex, R.C.R., Watt, M.J. (2017). Hepatokines: Linking Nonalcoholic Fatty Liver Disease and Insulin Resistance. Nat Rev Endocrinol 13:509–20. doi: 10.1038/nrendo.2017.56

26. Kucukoglu, O., Sowa, J.P., Mazzolini, G.D., Syn, W.K., Canbay, A. (2021) Hepatokines and Adipokines in NASH-Related Hepatocellular Carcinoma. J Hepatol 74:442–57. doi: 10.1016/j.jhep.2020.10.030

27. Meex, R.C., Hoy, A.J., Morris, A., Brown, R.D., Lo, J.C., Burke, M., Goode, R.J., Kingwell, B.A., Kraakman, M.J., Febbraio, M.A. et al. (2015). Fetuin B Is a Secreted Hepatocyte Factor Linking Steatosis to Impaired Glucose Metabolism. Cell Metab 22:1078–89. doi: 10.1016/j.cmet.2015.09.023

28. Toshihiko H. (2009). An SCCA -1 production inhibitor comprising 1-piperidinepropionic acid and/or a salt thereof as an active ingredient. Patent JP2009242345.

29. Pontisso, P., Biasiolo, A., Cappon, A., Martini A., Quarta, S., Ruvoletto, M., Turato, C., Villano, G. (2018). SerpinB3 inhibitor for the control of fibrosis and steatohepatitis. Patent IT 102017000026858, PTC pending.

30. Chinellato M, Gasparotto M, Quarta S, Ruvoletto M, a Biasiolo A, Filippini F, et al. (2023). 1-Piperidine Propionic Acid as an allosteric inhibitor of Protease Activated Receptor-2. Pharmaceuticals 2023, 16, 1486.

31. Rana R, Shearer AM, Fletcher EK, Nguyen N, Guha S, Cox DH, et al. PAR2 controls cholesterol homeostasis and lipid metabolism in nonalcoholic fatty liver disease. Mol Metab. 2019; 29:99–113.

32. Shearer AM, Wang Y, Fletcher EK, Rana R, Michael ES, Nguyen N, et al. PAR2 promotes impaired glucose uptake and insulin resistance in NAFLD through GLUT2 and Akt interference. Hepatology 2022; 76:1778–1793.

33. van der Krieken, S.E., Popeijus, H.E., Mensink, R.P., Plat J. (2015). CCAAT/Enhancer Binding Protein β in relation to ER Stress, Inflammation, and Metabolic Disturbances. BioMed Res Int 324815. doi: 10.1155/2015/324815.

34. Chandrabalan A, Ramachandran R. (2021) Molecular mechanisms regulating Proteinase-Activated

Receptors (PARs). FEBS J. 288, 2697–2726. doi:10.1111/febs.15829

35. Ramji, D.P., Foka, P. (2002). CCAAT/enhancer-binding proteins: Structure, function and regulation. Biochem J 365, 561–575. doi: 10.1042/BJ20020508.

36. Hyunjae Chung H, Ramachandran R, Morley D. Hollenberg MD, and Muruve DA. (2013). Proteinase-activated Receptor-2 Transactivation of Epidermal Growth Factor Receptor and Transforming Growth Factor-β Receptor Signaling Pathways Contributes to Renal Fibrosis. J Biol Chem 288, 37319–37331. doi: 10.1074/jbc.M113.492793

37. Hui Ding, H., Chen, J., Qin. J., Chen, R.,Yi, Z.(2021). TGF‐β‐induced α‐SMA expression is mediated by C/EBPβ acetylation in human alveolar epithelial cells. Mol Med 27, 22. doi: 10.1186/s10020-021-00283-6.

38. Sivaprasad, U., Askew, D.J., Ericksen, M.B., Gibson, A.M., Stier, M.T., Brandt, E.B., Bass, S.A., Daines, M.O., Chakir, J., Stringer, K.F., et al. (2011). A nonredundant role for mouse Serpinb3a in the induction of mucus production in asthma. J Allergy Clin Immunol 127, 254-61, doi: 261.e1-6. 10.1016/j.jaci.2010.10.009.

39. Calkhoven, C. F., Müller, C., and Leutz, A. (2000). Translational Control of C/EBP alpha and C/EBP beta Isoform Expression. Genes Dev. 14, 1920–1932. doi:10.1101/gad.14.15.1920.

40. Estes, C., Anstee, Q.M., Arias-Loste, M.T., Bantel, H., Bellentani, S., Caballeria, J., Colombo, M., Craxi, A., Crespo, J., Day, C.P., et al. (2018). Modeling NAFLD disease burden in China, France, Germany, Italy, Japan, Spain, United Kingdom, and United States for the period 2016-2030. J Hepatol 69, 896- 904. doi: 10.1016/j.jhep.2018.05.036.

41. Rinella, M.E., Tacke, F., Sanyal, A.J, Anstee, Q.M.; participants of the AASLD/EASL Workshop. (2019). Report on the AASLD/EASL joint workshop on clinical trial endpoints in NAFLD. J Hepatol 71, 823- 33. doi: 10.1016/j.jhep.2019.04.019.

42. Huisman, T.M., Dieterich, D.T., Friedman, S.L. (2021). Experimental and investigational targeted therapies for the management of fibrosis in NASH: an update. J Exp Pharmacol. 13, 329-38. doi:10.2147/JEP.S265286.

43. Chandrabalan A, Ramachandranl R (2021). Molecular mechanisms regulating Proteinase-Activated Receptors (PARs). FEBS J, 288 :2697–2726. doi:10.1111/febs.15829

44. Ramachandran P, Dobie R, Wilson-Kanamori JR, Dora EF, Henderson BEP, Luu NT et al. (2019) Resolving the fibrotic niche of human liver cirrhosis at single-cell level. Nature, 2019 575: 512-18. doi: 10.1038/s41586-019-1631-3

45. Turato C, Pontisso P. (2015). SERPINB3 (serpin peptidase inhibitor, clade B (ovalbumin), member 3). Atlas Genet Cytogenet Oncol Haematol.19:202-209.

46. Sato, Y., Nishio, Y., Sekine, O., Kodama, K., Nagai, Y., Nakamura, T., Maegawa, H., Kashiwagi, A. (2007). Increased expression of CCAAT/enhancer binding protein-beta and -delta and monocyte chemoattractant protein-1 genes in aortas from hyperinsulinaemic rats. Diabetologia 50, 481–489. doi: 10.1007/s00125-006-0480-4.

47. Quarta, S., Vidalino, L., Turato, C., Ruvoletto, M., Calabrese, F., Valente, M., Cannito, S., Fassina, G., Parola, M., Gatta, A., et al. (2010). SERPINB3 induces epithelial-mesenchymal transition. J Pathol. 221,343-56. doi: 10.1002/path.2708.

48. Fasolato, S., Ruvoletto, M., Nardo, G., Rasola, A., Sciacovelli, M., Zanus, G., Turato, C., Quarta, S., Terrin, L, Fadini, G.P., et al. (2021). Low P66shc with High SerpinB3 Levels Favors Necroptosis and Better Survival in Hepatocellular Carcinoma. Biology 23, 363. doi: 10.3390/biology10050363.

49. Turato, C., Biasiolo, A., Pengo, P., Frecer, V., Quarta, S., Fasolato, S., Ruvoletto, M., Beneduce, L., Zuin, J., Fassina, G., et al. (2011). Increased antiprotease activity of the SERPINB3 polymorphic variant SCCA-PD. Exp Biol Med 236, 281-90. doi: 10.1258/ebm.2011.010229.

50. Turato, C., Cannito, S., Simonato, D., Villano, G., Morello, E., Terrin, L., Quarta, S., Biasiolo, A., Ruvoletto, M., Martini, A., et al. (2015). SerpinB3 and Yap Interplay Increases Myc Oncogenic Activity. Sci Rep 5,17701. doi:10.1038/srep17701.

51. Livak, K.J., Schmittgen, T.D. (2001). Analysis of relative gene expression data using real-time quantitative PCR and the 2(-Delta Delta C(T)) method. Methods 25,402–408. doi:10.1006/meth.2001.1262.

52. Villano, G., Ruvoletto, M., Ceolotto, G., Quarta, S., Calabrese, F., Turato, C., Tono, N., Crescenzi, M., Biasiolo, A., Cattelan, A., et al. (2013). SERPINB3 is associated with longer survival in transgenic mice. Sci Rep 3, 3056. doi:10.1038/srep03056.

FIGURE LEGENDS

Figure 1

SerpinB3, lipid accumulation and development of murine NASH. Representative examples of morphological findings at sacrifice of the liver of a BALB/c wild-type mouse (WT) and of a mouse deficient of the reactive site loop of Serpinb3a (KO), fed with CDAA diet. A) liver macroscopic features, B) liver histology after hematoxylin eosin staining, E) collagen deposition assessed by Sirius red staining. The pictures provide evidence of the lower extent of steatosis in KO mouse, confirmed by the lower levels of steatosis scores detected by liver histology in KO mice (7 animals) compared to WT mice (7 animals) (C). Similar findings are reported for the profile of inflammatory genes (D), including IL-1β, CCL2 and TNF-α, and of fibrosis genes (G), including TGF–β, α-SMA and collagen 1A1. Densitometric analysis of collagen deposition measured after Sirius red staining (F) shows the lower extent of collagen deposition detected in KO mice, compared to WT mice. The results are reported as mean ± SEM (Unpaired t test with Welch's correction). Levels of mRNA gene expression are reported as $2^{-\Delta\Delta CT}$.

Figure 2

Dysregulation of fat distribution in mice with different expression of SerpinB3. A) Representative examples of subcutaneous or visceral white fat and of brown fat distribution are shown after skin removal in BALB/c mice lacking the Serpinb3a reactive site loop (KO) and in the corresponding BALB/c control fed with normal diet. B) Values of relative adipose tissue in interscapular brown adipose tissue (BAT), subcutaneous adipose tissue (SAT) and in visceral adipose tissue (VAT), expressed as percentage of fat on total body weight (grams) in the WT and KO groups of mice. The results are reported as mean ± SEM (Unpaired t test with Welch's correction). C) Representative examples of subcutaneous or visceral white fat and of brown fat distribution in SerpinB3 transgenic (TG) mice and in the corresponding C57BL/6 controls fed with normal diet. D) Values of relative adipose tissue in interscapular brown adipose tissue

(BAT), subcutaneous adipose tissue (SAT) and in visceral adipose tissue (VAT), expressed as percentage of fat on total body weight (grams) in the WT and TG groups of mice. The results are reported as mean ± SEM (Unpaired t test with Welch's correction).

Figure 3

Inhibitory activity of 1-Piperidin Propionic acid on inflammatory response in mice fed with CDAA diet. A) Representative examples of macrophage infiltration, detected by F4/80 immunostaining, in the liver of control mice (WT) and of SerpinB3 transgenic mice (TG) injected or not with 1-PPA. B) Densitometric analysis of F4/80 immunostaining in the liver of the corresponding groups of mice (7 animals/group). C) mRNA levels of inflammatory genes in, including TNF-α and IL-1β in control mice (WT) or in SerpinB3 transgenic mice (TG), fed or not with CDAA diet and injected or not with 1-PPA. D) mRNA levels of markers of NAMs, Galectin 3 (GAL3), CD9 and TREM2, in control mice (WT) or in SerpinB3 transgenic mice (TG), fed or not with CDAA diet and injected or not with 1-PPA.
E) Representative results of SerpinB3 immunostaining in the liver of control mice (WT) and of SerpinB3 transgenic mice (TG) fed with CDAA and injected or not with 1-PPA.
The results are reported as mean ± SEM (Unpaired t test with Welch's correction). mRNA levels are expressed as $2^{-\Delta\Delta CT}$.

Figure 4

Inhibitory activity of 1-Piperidin Propionic acid on fibrosis in mice fed with CDAA diet. A) Representative examples of Sirius red staining in paraffin sections of mice livers in WT and in TG mice injected or not with 1-PPA. B) Densitometric analysis of collagen deposition measured after Sirius red staining in the liver of the corresponding groups of mice (7 animals/group). C) mRNA levels of fibrosis genes in the different groups of mice, including α-SMA, collagen 1A1 and TGF-β. The results are reported as mean ± SEM (Unpaired t test with Welch's correction). mRNA levels are expressed as $2^{-\Delta\Delta CT}$.

Figure 5

Inhibitory effect of 1-Piperidin Propionic acid on fibrogenesis and inflammatory response *in vitro*. A) Profile of fibrosis genes (collagen 1A1, α-SMA, CCL-2 and VEGF-A) in LX2 cells in presence of SerpinB3 (SB3, 200ng/ml) alone or mixed with 1-PPA at 100ng/ml concentration (SB3 + 1-PPA) after 24 hours incubation. B) Profile of inflammatory genes (TGF-β, CCL-15, TNF-α, IL-1β, IL-13, CCL-2) in THP1 cells exposed to human recombinant SerpinB3 (SB3, 100ng/ml) alone or mixed with 1-PPA at 100ng/ml concentration (SB3 + 1-PPA) after 24 hours incubation.

The results are reported as mean + SEM of at least three experiments (Unpaired t test with Welch's correction). mRNA levels are expressed as $2^{-\Delta\Delta CT}$.

Figure 6

1-Piperidin Propionic acid reduces CEBP-β transcription. A) CEBP-β expression in HepG2 cells transfected with the plasmid vector alone (HepG2/CTR) and in HepG2 cells transfected to overexpress SerpinB3 (HepG2/SB3) in presence of increasing concentrations of 1-PPA or of Medium alone. B) CEBP-β expression profile in the THP-1 cell line. This transcription factor, not detectable in THP-1 cells, is markedly induced by SerpinB3 and the effect is efficiently reverted by the addition of 1-PPA. C) Example of Western blot of the isoforms Liver Activating Protein (LAP) and Liver Inhibitory Protein (LIP) of CEPB-β in control HepG2 (empty vector), in HepG2 cells overexpressing SerpinB3 wild type (SB3/WT) and in HepG2 cells overexpressing SerpinB3 lacking the antiprotease activity (SB3/Δ7) . D) Densitometric analysis of protein expression of Liver Activating Protein (LAP) and of Liver Inhibitory Protein (LIP) of CEPB-β, normalized to GAPDH, in control HepG2 cells (Empty vector), in HepG2 cells overexpressing SerpinB3 wild type (SB3/WT) and in HepG2 cells lacking the antiprotease activity (SB3/Δ7). E) CEBP-β expression profile in C57BL6/J and BALB/c wild type mice (WT mice), SerpinB3 transgenic mice (SB3/TG) and mice deficient of the reactive site loop of Serpinb3a (SB3/KO).

Figure 7

C/EBP-β and PAR2 in relation to different extent of expression of SerpinB3. Immunofluorescence results for C/EBP-β (A) and for PAR2 (B) in HepG2 cells transfected with the plasmid vector alone (HepG2/CTR), in HepG2 cells transfected to overexpress SerpinB3 (HepG2/SB3), in HepG2 cells transfected with a plasmid vector carrying the SerpinB3 sequence deleted of 7aa in the reactive site loop (HepG2/SB3Δ7) and in the HA22T/VGH cells constitutively expressing SerpinB3. C) Effect of C/EBP-β silencing on the expression of C/EBP-β and of SerpinB3 (D) in the HA22T/HGV cell line. E) Representative results of immunostaining for PAR2 the liver in a wild type mouse (TG) and in SerpinB3 transgenic mice (TG/SB3) fed with CDAA and injected or not with 1-PPA. F) Densitometric analysis of PAR2 immunostaining in the liver of the corresponding groups of mice.

Graphical Abstract

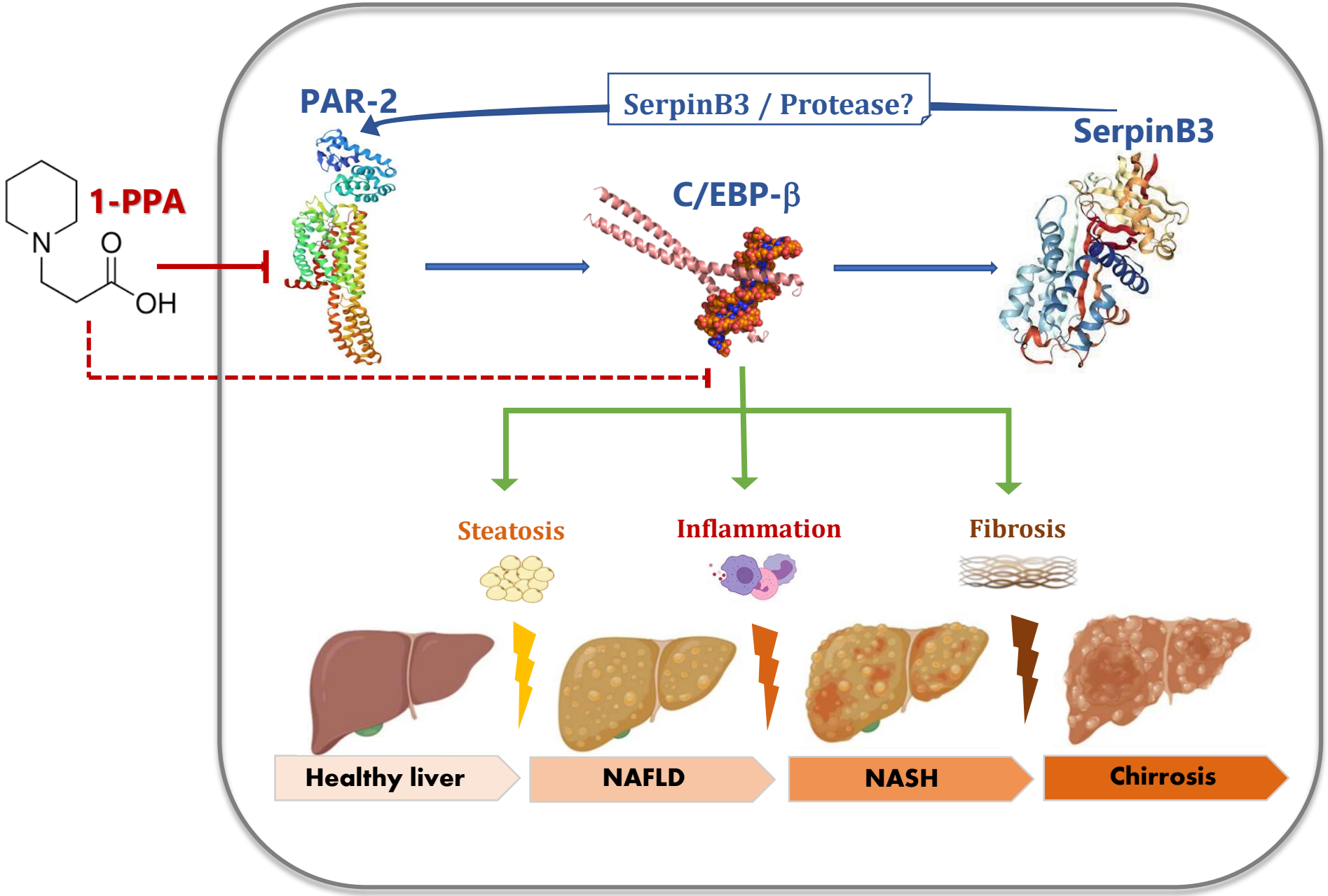

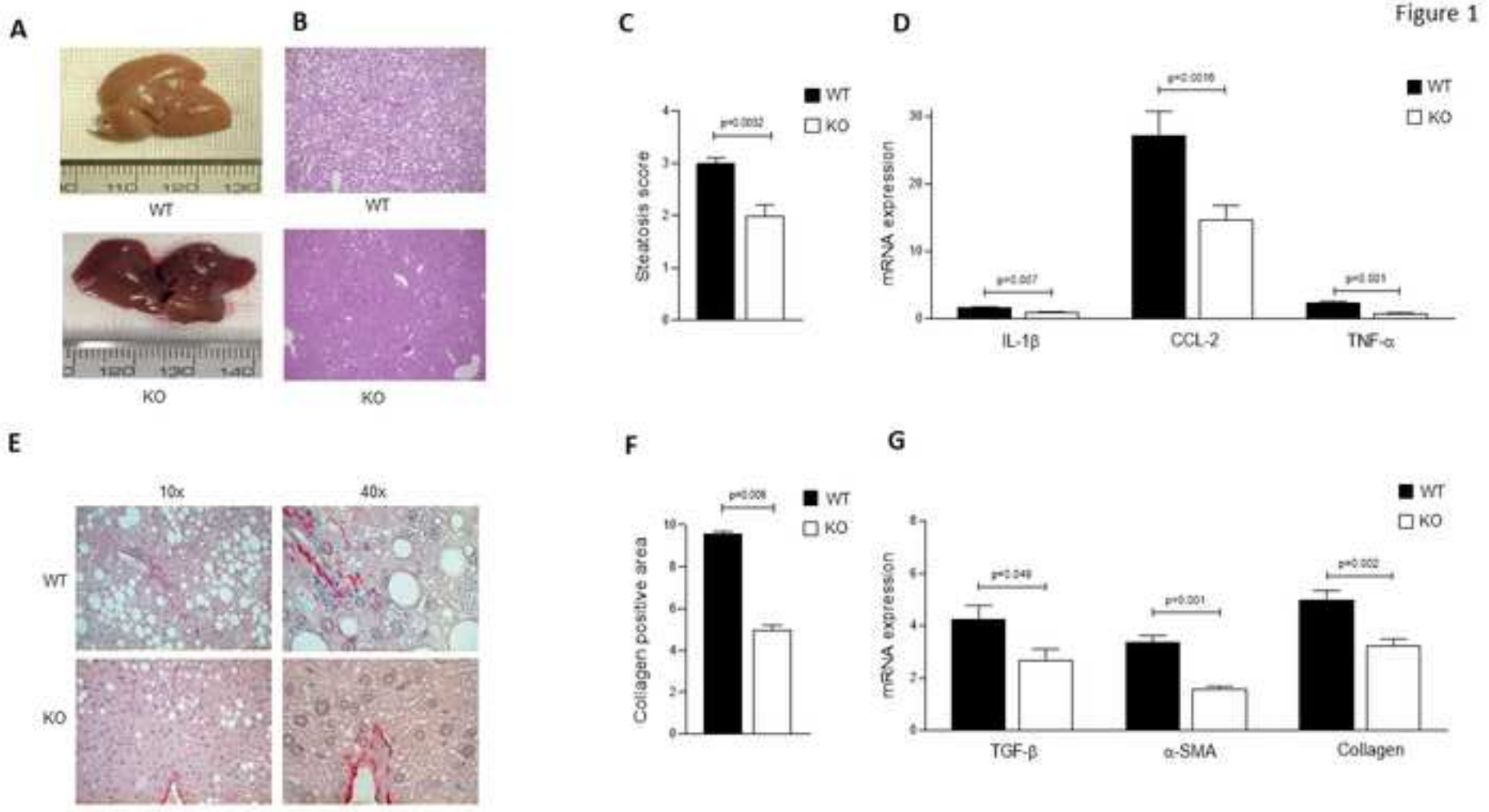

Figure 2

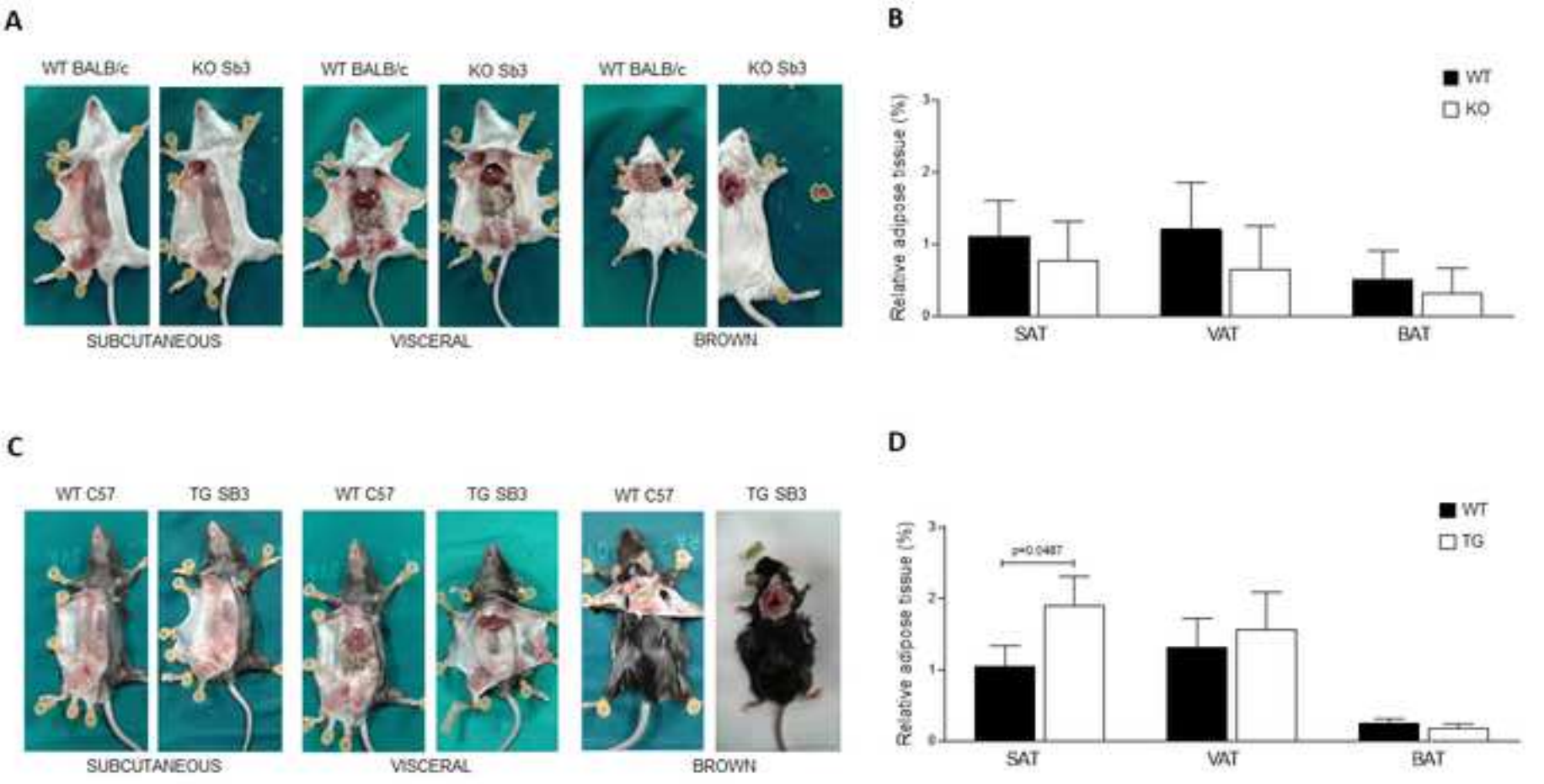

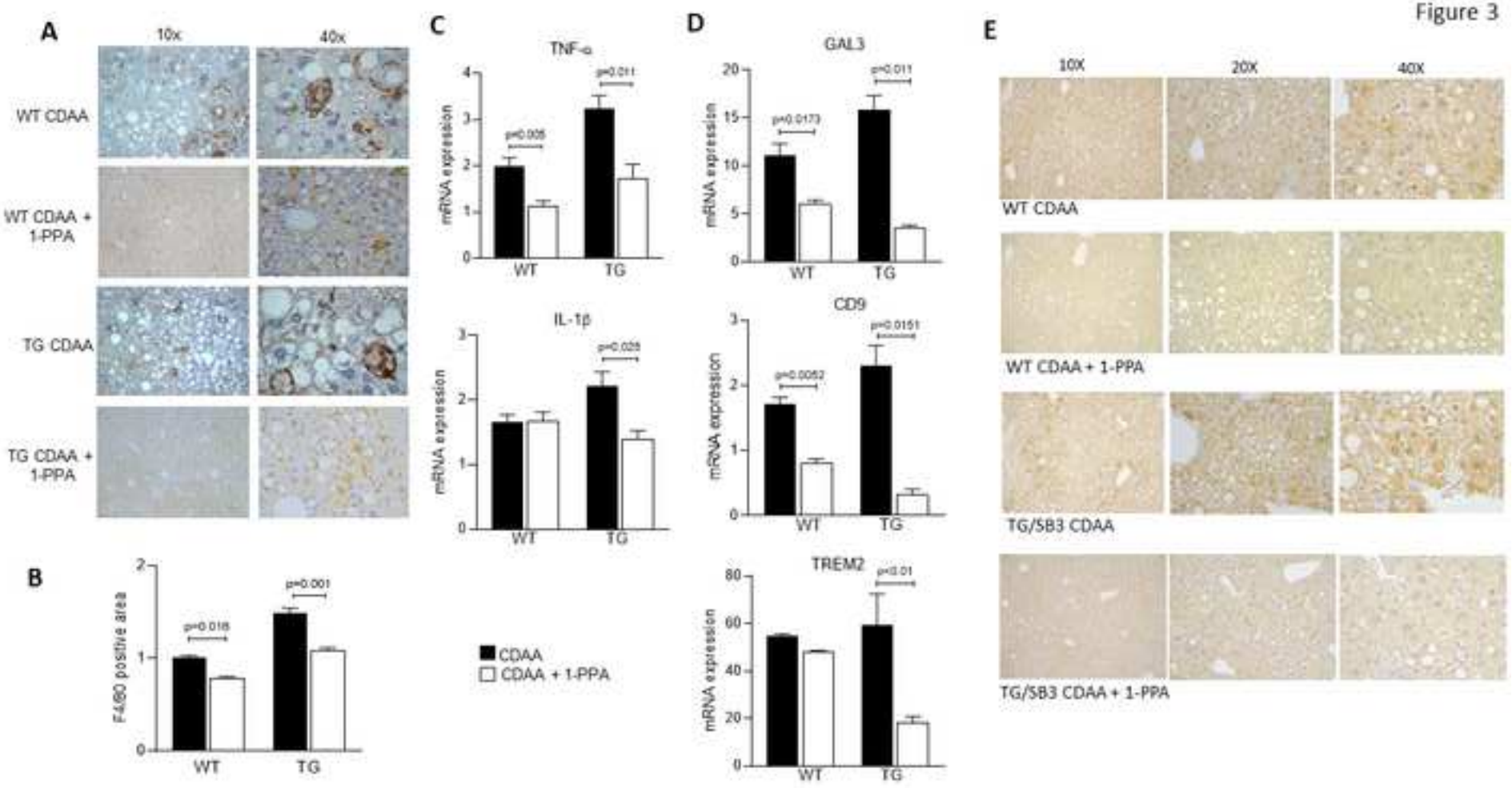

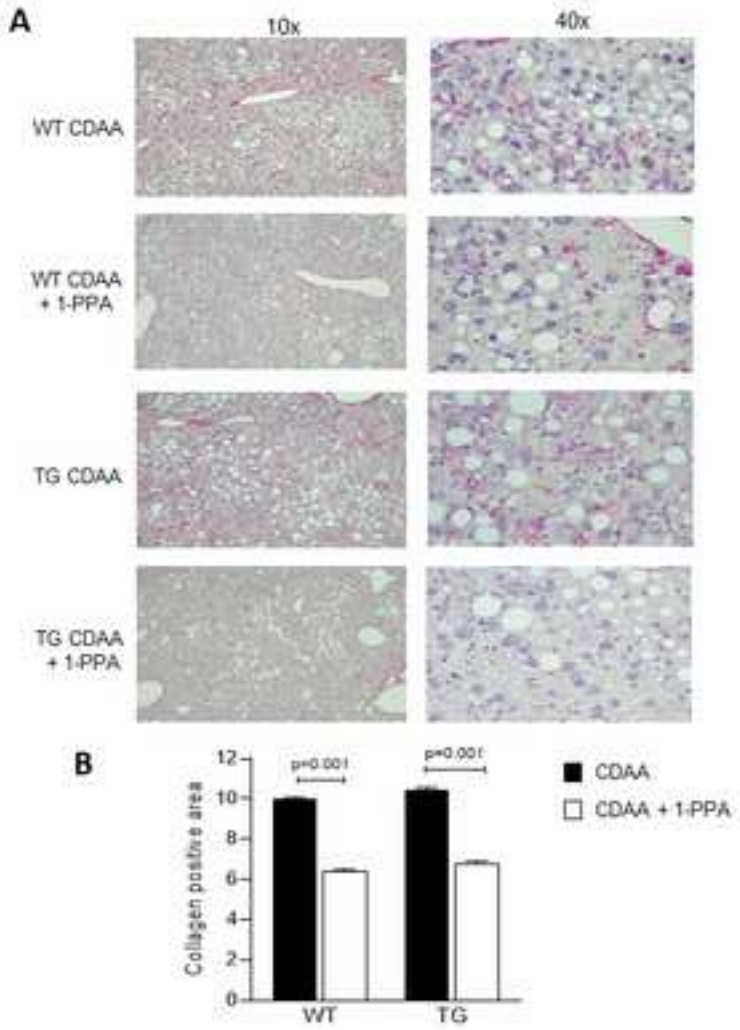

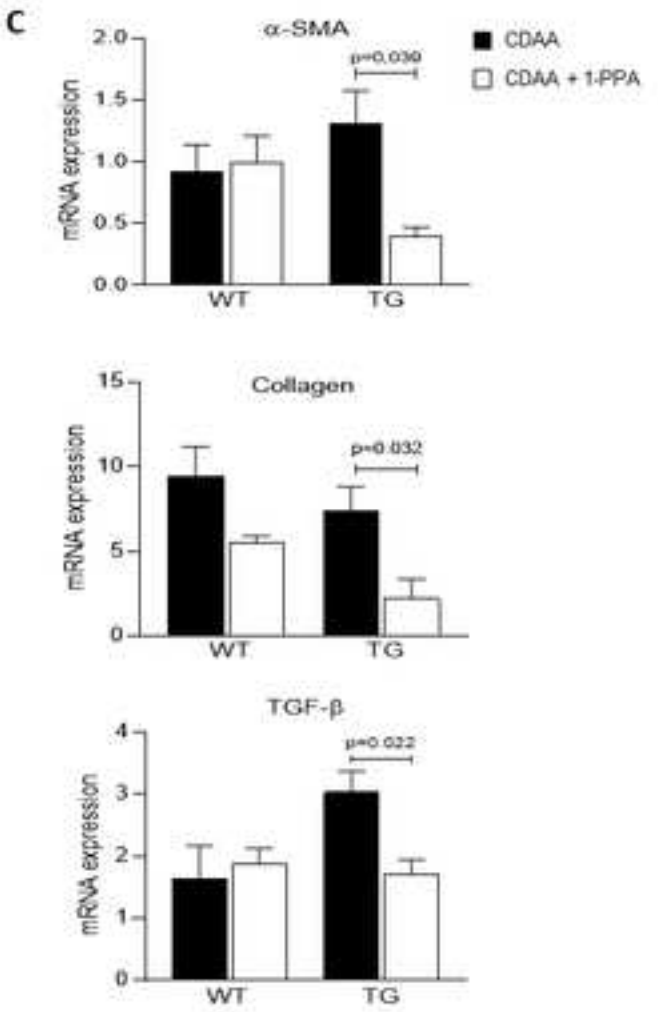

Figure 4

Diapositiva4.TIF

Figure 5

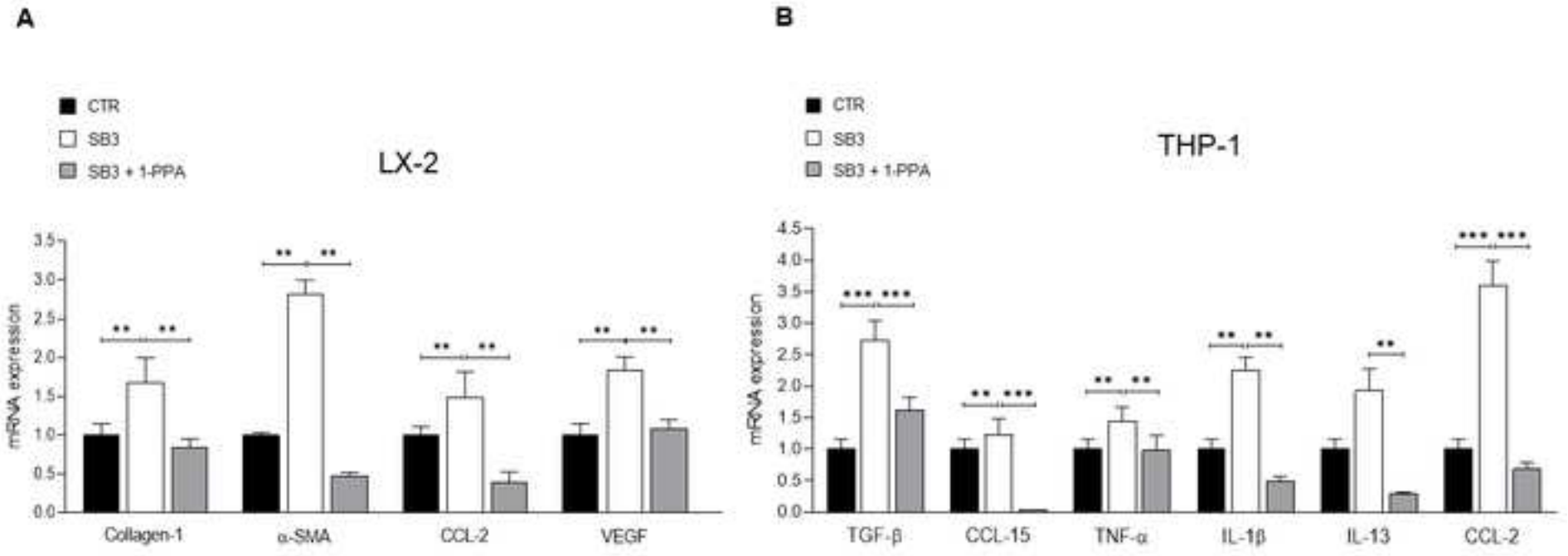

Figure 6

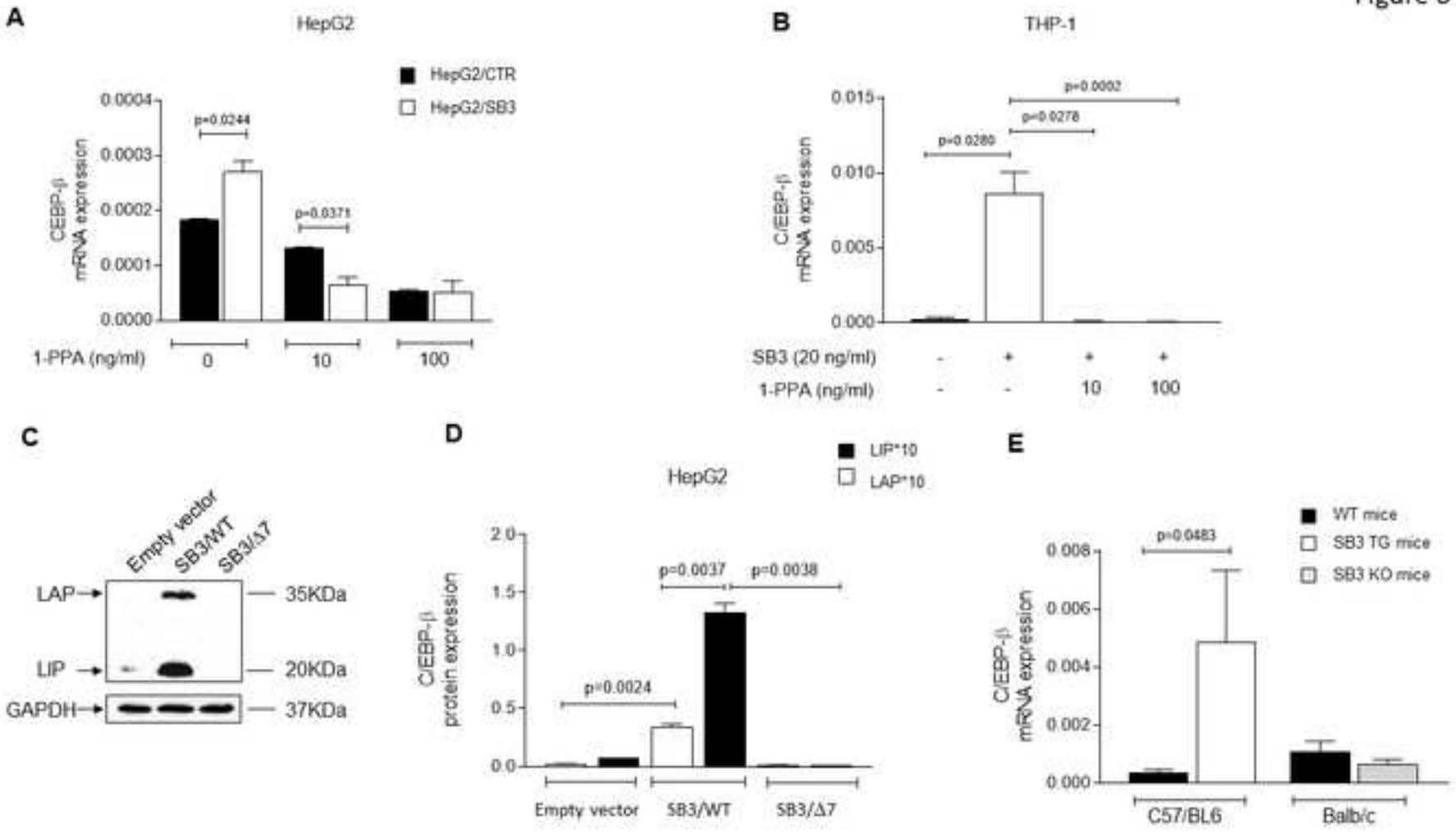

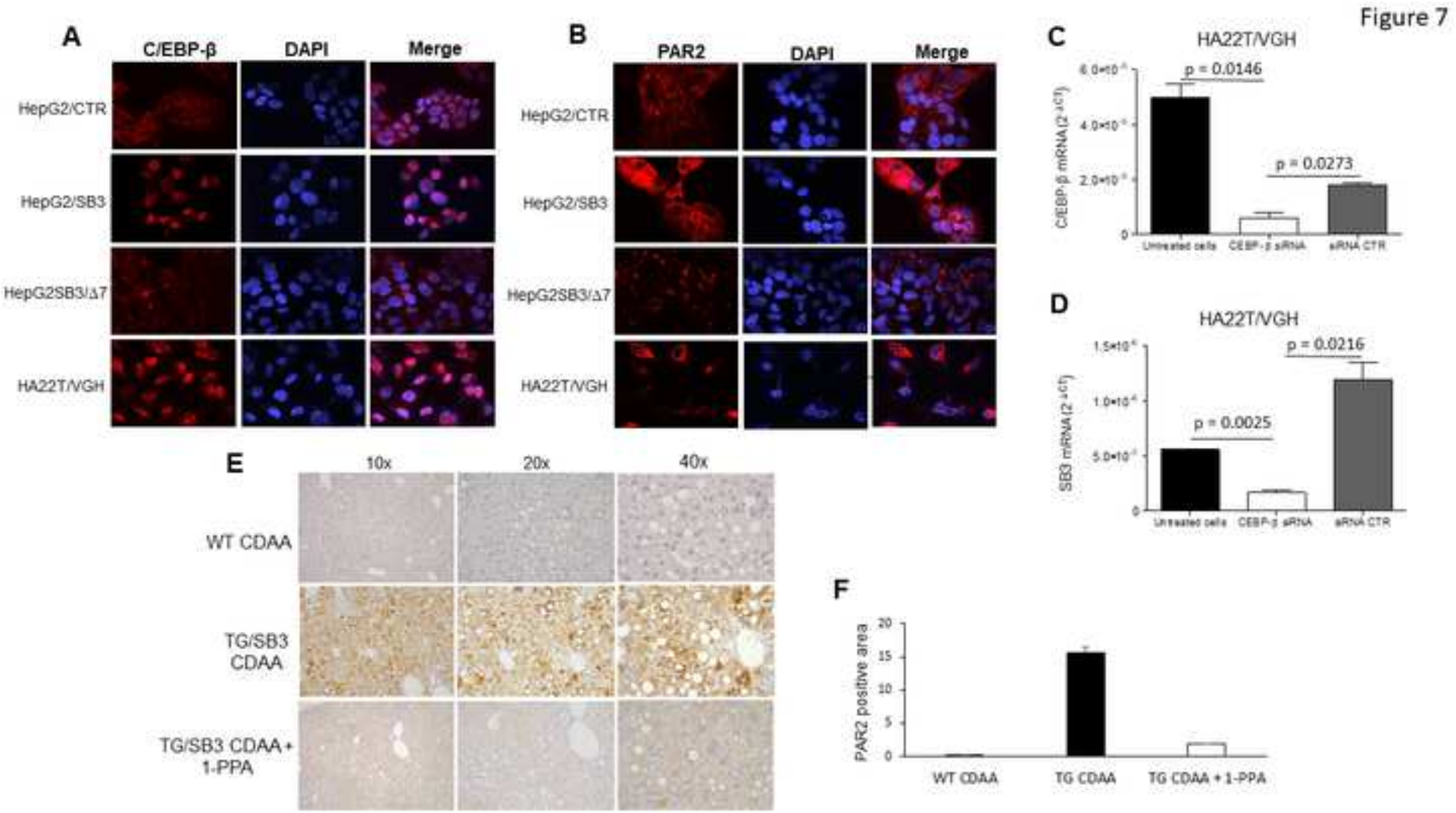

The Protease Activated Receptor 2 - CCAAT/Enhancer-Binding Protein beta - SerpinB3 axis inhibition as a novel strategy for the treatment of Non-Alcoholic Steatohepatitis

Villano Gianmarco[1*], Novo Erica[2*], Turato Cristian[3], Quarta Santina[4], Ruvoletto Mariagrazia[4], Biasiolo Alessandra[4], Protopapa Francesca[2], Chinellato Monica[4], Martini Andrea[4], Trevellin Elisabetta[4], Granzotto Marnie[4], Cannito Stefania[2], Cendron Laura[5], De Siervi Silvia[3], Guido Maria[4], Parola Maurizio[2**], Roberto Vettor[4**], Pontisso Patrizia[4**§].

[1]Dept. of Surgical, Oncological and Gastroenterological Sciences, University of Padova, Italy; [2]Dept. of Clinical and Biological Sciences, University of Torino, Italy; [3]Dept. of Molecular Medicine, University of Pavia, Italy; [4]Dept. of Medicine, University of Padova, Italy; [5]Dept. of Biology, University of Padova, Italy.

* Shared first authorship

** Shared senior authorship

SUPPLEMENTARY MATERIAL

SUPPLEMENTARY FIGURES

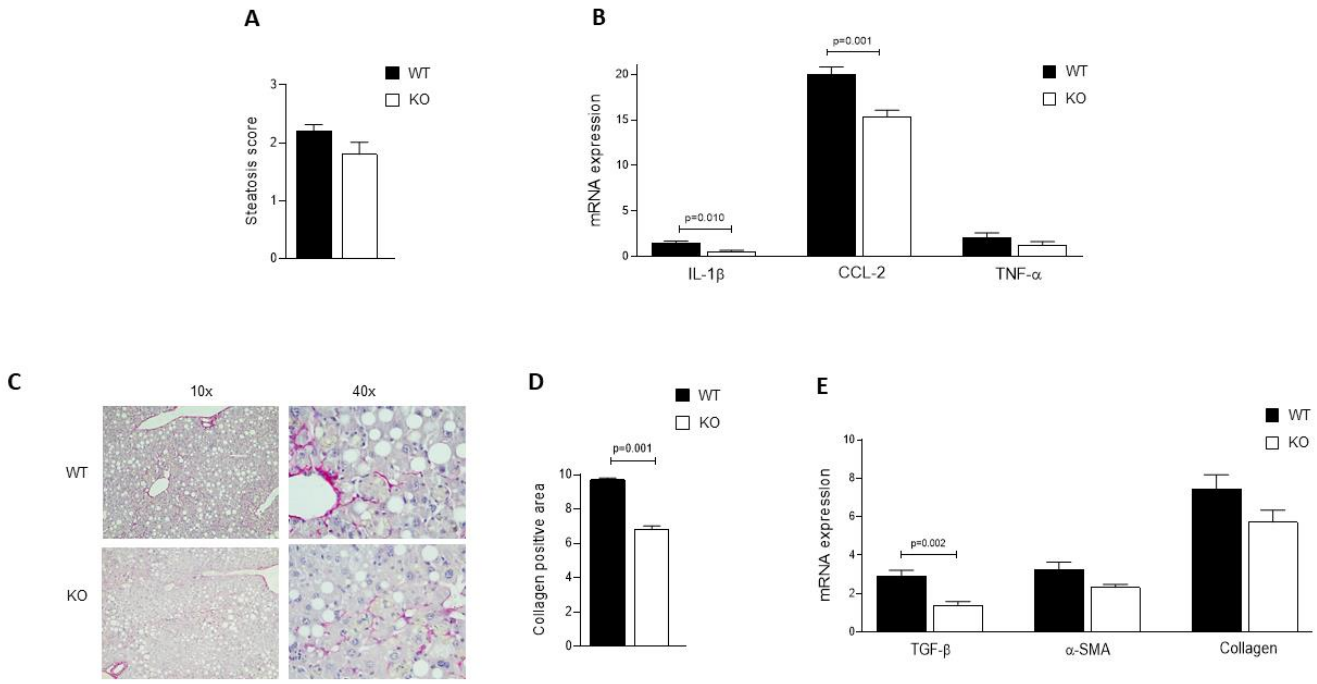

Supplementary Figure 1. Morphological and transcriptional findings in the liver after MCD diet in KO and control BALB/c mice. (A): Extent of steatosis score in KO mouse and in the BALB/c control mice. (B): Expression of genes involved in inflammation: IL-1β, CCL-2 and TNF-α. (C): Examples of Sirius red staining of the liver of a BALB/c wild type mouse (WT) and of a mouse deficient of the reactive site loop of Serpinb3a (KO), fed with MCD diet. (D): Densitometric analysis of collagen deposition measured after Sirius red staining in WT and KO mice. (E): Expression of genes involved in fibrosis: TGF−β, α-SMA and collagen 1A1. Columns represent mean values and bars refer to SEM. Levels of RNA gene expression are reported as $2^{-\Delta\Delta ct}$. N= 7 mice/group.

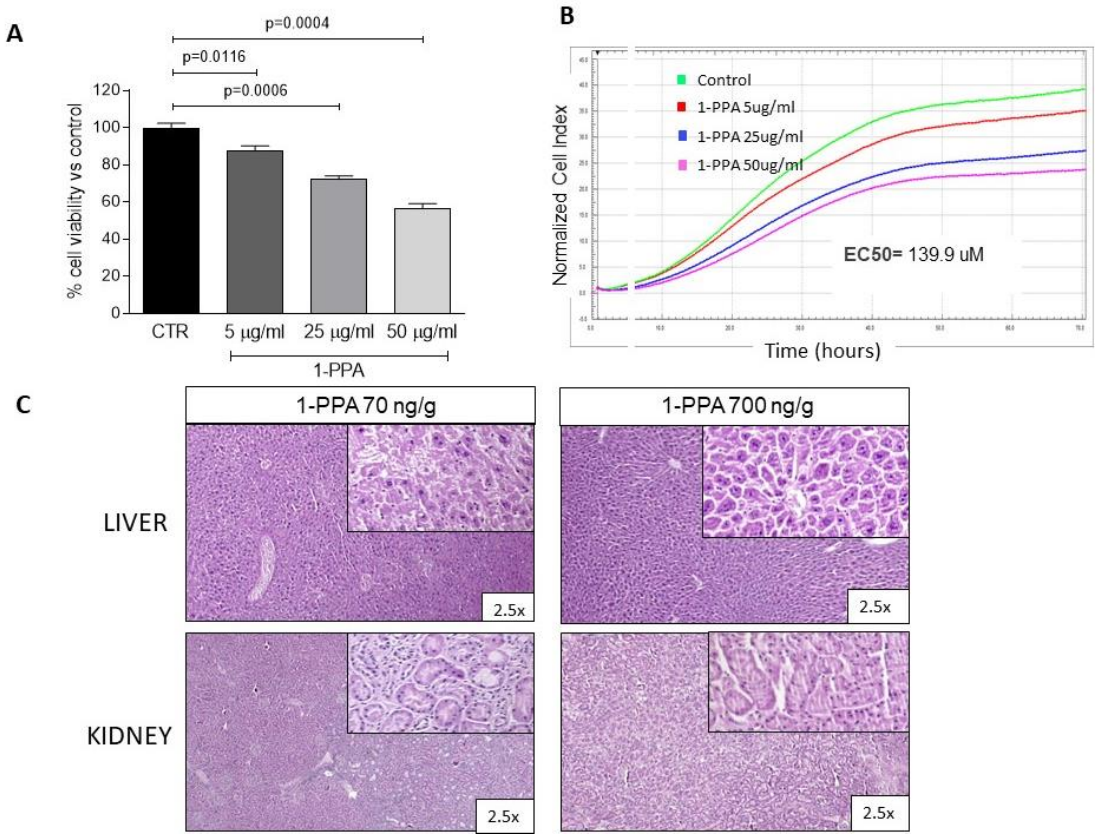

Supplementary Figure 2. Toxicity of 1-Piperidin Propionic acid. A) Cell viability calculated at 36 hours in the HepG2 cell line in control Medium or in presence of increasing concentrations of 1-PPA. Bars represent the mean values ± SEM of the results (Unpaired t test with Welch's correction) obtained in 6 wells for each experimental condition. B) Real time cell proliferation monitored over 70 hours in the HepG2 cell line in presence of increasing concentrations of 1-PPA. The results are expressed as normalized cell index. The EC50 has been calculated by the software of the XCelligence Instrument. C) Examples of histological features of the liver and of the kidney of mice intraperitoneally injected weekly with 1-PPA at the dose of 70 or of 700 ng/g for 26 weeks. Inserts magnification 10X.

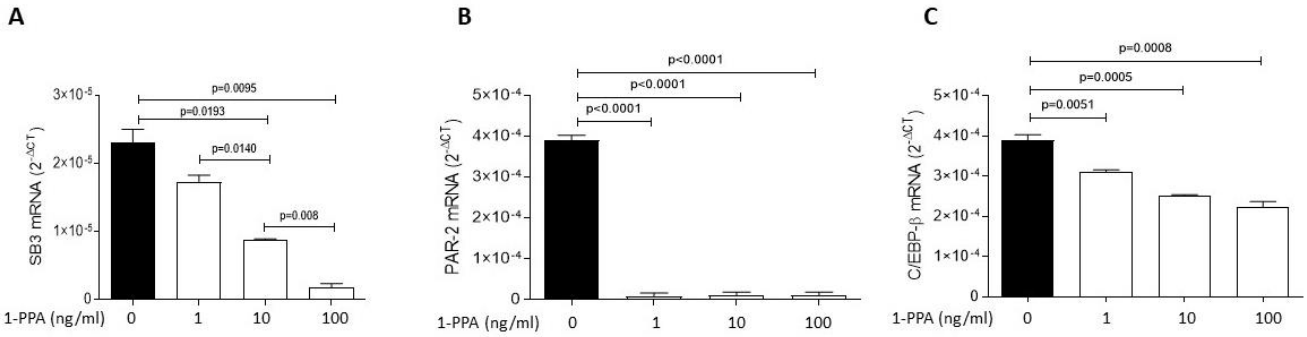

Supplementary Figure 3. Inhibitory activity of 1-Piperidin Propionic acid. Transcriptional levels of SerpinB3 mRNA (A), of PAR2 mRNA (B) and of C/EBP-β mRNA in HA22T/VGH cells obtained after 48 hours from seeding in medium, used as control (0) or in presence of different concentrations of 1-PPA. Levels of mRNA gene expression are reported as $2^{-\Delta\Delta CT}$**.**

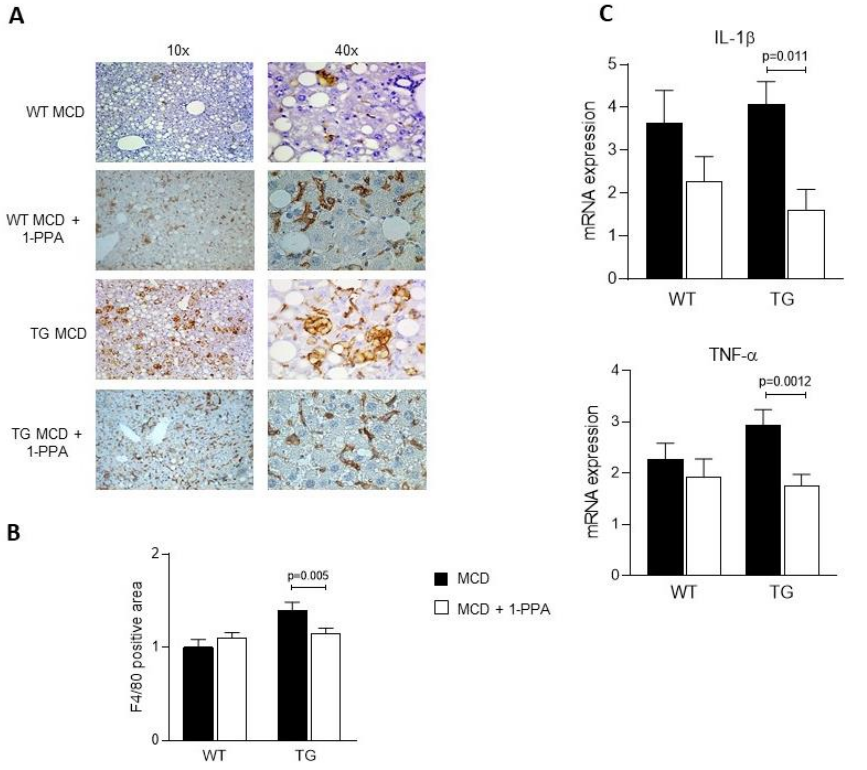

Supplementary Figure 4. Inhibitory activity of 1-Piperidin Propionic acid on inflammatory response in mice fed with MCD diet. A) Representative examples of macrophage infiltration, detected by F4/80 immunostaining, in the liver of control mice (WT) and of SerpinB3 transgenic mice (TG) injected or not with 1-PPA. B) Densitometric analysis of F4/80 immunostaining in the liver of the corresponding groups of mice (7 animals/group). C) RNA levels of inflammatory genes in the different groups of mice, including IL-1β and TNF-α. The results are reported as mean $\pm$ SEM (Unpaired t test with Welch's correction). RNA levels are expressed as $2^{-\Delta\Delta CT}$.

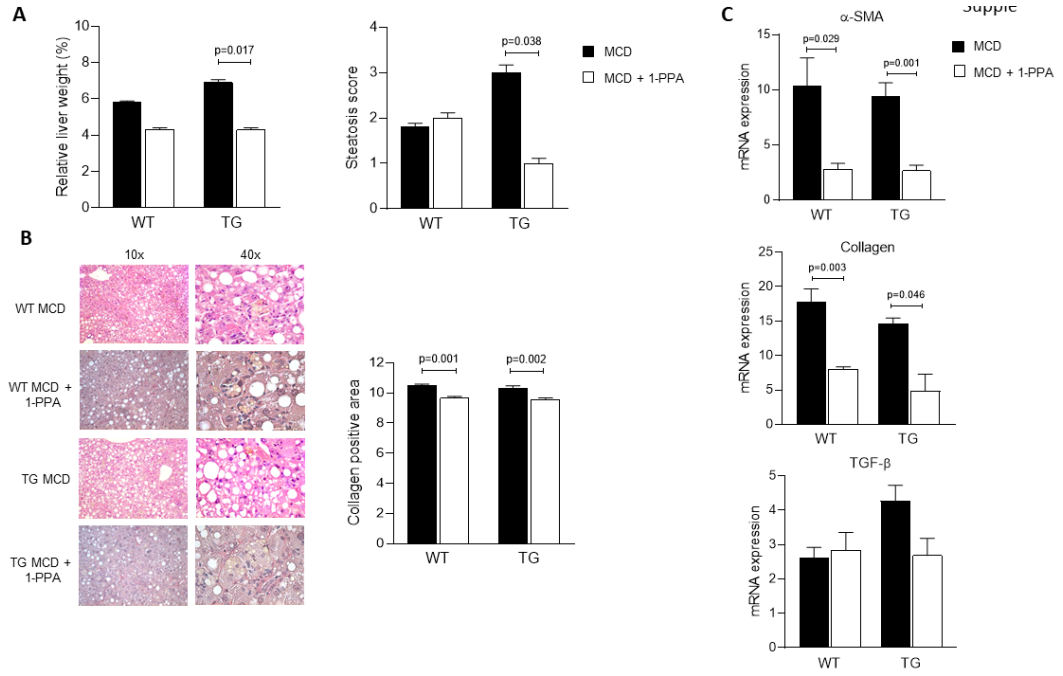

Supplementary Figure 5. Inhibitory activity of 1-Piperidin Propionic acid on steatosis and fibrosis in mice fed with MCD diet. A) Relative liver weight obtained at sacrifice after MCD diet and steatosis score in control mice (WT) and in SerpinB3 transgenic mice (TG) injected or not with 1-PPA (7 animals/group). B) Representative examples of Sirius red staining in paraffin sections of livers in WT and in TG mice fed with MCD and injected or not with 1-PPA. The right panel represents the densitometric analysis of collagen deposition measured after Sirius red staining in the corresponding groups of mice. C) RNA levels of fibrosis genes in the different groups of mice, including α-SMA, collagen 1A1 and TGF-β. The results are reported as mean ± SEM (Unpaired t test with Welch's correction). RNA levels are expressed as $2^{-\Delta\Delta CT}$.

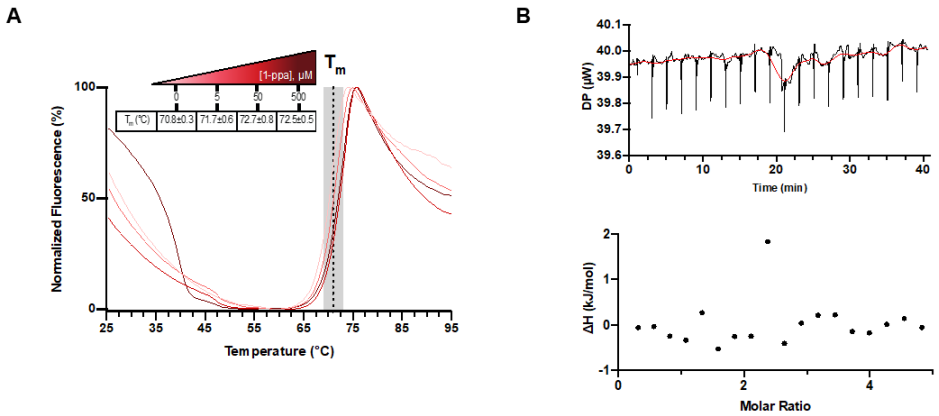

Supplementary Figure 6. Biophysical studies of interaction between SerpinB3 and 1-Piperidin Propionic acid. A) Differential Scanning Fluorimetry curves are reported as Relative fluorescence, normalized in percentage on the highest and lowest values of each dataset. The Melting Temperature (T_m) was calculated based on 3 technical replicates of each sample and it is shown with each Standard Deviation. B) Upper panel: Isothermal Titration Calorimetry assay, plot of heat changes in relation to molar ratio; Bottom panel represents the heat effects associated with 1-PPA injection. Both the techniques reveal that there is not interaction between SerpinB3 and 1-PPA.

SUPPLEMENTARY TABLES

Supplementary Table 1. Biochemical parameters of liver and kidney function in C57BL/6 mice injected weekly with the 1-PPA concentration of 70 ng/g or of 700 ng/g body weight (3 animals/group). All the parameters were assessed before 1-PPA injection (T_0) and after 26 weeks of weekly 1-PPA injection (T_{26}).

C57BL/6J mice	**1-PPA 70 ng/g**			**1-PPA 700 ng/g**		
	T_0	**T_{26}**	**p***	**T_0**	**T_{26}**	**p***
ALT (U/L)						
Median Range	38.3 30-45	46.5 30-57	ns	39 36-42	46.5 39-54	ns
Bilirubin (µmol/L)						
Median Range	0.53 0.1-0.9	0.75 ± 0.4 0-1.5	ns	0.45 0.1-0.9	1.65 1.2-2.1	0.0265
Creatinine (µmol/L)						
Median Range	19.5 12-33	22.5 9-36	ns	34.5 24-45	55.5 42-69	ns

ALT: Alanine Amino Transferase. *Mann-Whitney test

Supplementary Table 2. Mouse and human primer sequences used in the study.

GENE	Forward primer	Reverse primer
m-TGFβ	5’-TTGCTTCAGCTCCACAGAGA-3’	5’-TGGTTGTAGAGGGCAAGGAC-3’
m-α-SMA	5'-GACGTACAACTGGTATTGTG-3'	5'- TCAGGATCTTCATGAGGTAG -3'
m-Collagen 1	5’-AAATCTGCACACTGCCAT GA-3’	5’-GCATGTTCGAAATCCAGTGA-3’
m-IL1β	5’-GAAATGCCACCTTTTGACAGTGAT-3’	5’-TTGGAAGCAGCCCTTCATCTT-3’
m-CCL2	5’-GCCTGCTGTTCACAGTTGC-3’	5’GAGTGGGGCGTTAACTGCAT-3’
m-TNFα	5’-AGCCCCCAGTCTGTATCCTT-3’	5’- CTCCCTTTGCAG AACTCAGG-3’
m-CD9	5’- TTCGCCATTGAGATAGCCGC-3’	5’-GCTATGCCACAGCAGTCCAA-3’
m-TREM2	5’-CCTGCAGAAAGTACTGGTGGA-3’	5’-TCTCTTGATTCCTGGAGGTGC-3’
m-Gal3	5’-CCACTTTAACCCCCGCTTCA-3’	5’-CAAAGGGGAAGGCTGACTGT-3’
h-PAR2	5’- GCTAGCAGCCTCTCTCTCCT-3’	5’- GTGGGATGTGCCATCAACCT-3’
h-CEBP-β	5'-AAGCACAGCGACGAGTACAA-3'	5'-ACAGCTGCTCCACCTTCTTC-3'
h-Collagen 1	5'-GTGCTAAAGGTGCCAATGGT-3'	5'-ACCAGGTTCACCGCTGTTAC-3'
h-α-SMA	5'-ACCCACAATGTCCCCATCTA-3'	5'-GAAGGAATAGCCACGCTCAG-3'
h-CCL2	5'-CCCCAGTCACCTGCTGTTAT -3'	5'-AGATCTCCTTGGCCACAATG-3'
h-TGFβ	5′-AAGTGGACATCAACGGGTTC-3′	5′-GTCCTTGCGGAAGTCAATGT-3′
h-TNFα	5'-AACCTCCTCTCTGCCATCAA-3'	5'-GGAAGACCCCTCCCAGATAG-3'
h-IL1β	5'-TGAAAGCTCTCCACCTCCAG-3'	5'-CACGCAGGACAGGTACAGAT-3'
h-IL-13	5'-GTACTGTGCAGCCCTGGAAT-3'	5'-TTTACAAACTGGGCCACCTC-3'
h-VEGF	5’ CCCACTGAGGAGTCCAACAT 3’	5’ TTTCTTGCGCTTTCGTTTTT 3’
h-CCL 15	5’-TCATGCTTGTTGCTGTCCTT -3’	5’-CACGGGATGCTTTGTGAGAT-3’

m, mouse; h, human

4.3 PAPER N°3

SerpinB3 Upregulates Low-Density Lipoprotein Receptor-Related Protein (LRP) Family Members, Leading to Wnt Signaling Activation and Increased Cell Survival and Invasiveness

Published on Biology (Basel). 2023 May 26;12(6):771. doi: 10.3390/biology12060771.

Authors: Santina Quarta, Andrea Cappon, Cristian Turato, Mariagrazia Ruvoletto, Stefania Cannito, Gianmarco Villano, Alessandra Biasiolo, Maristella Maggi, **Francesca Protopapa**, Loris Bertazza, Silvano Fasolato, Maurizio Parola, Patrizia Pontisso.

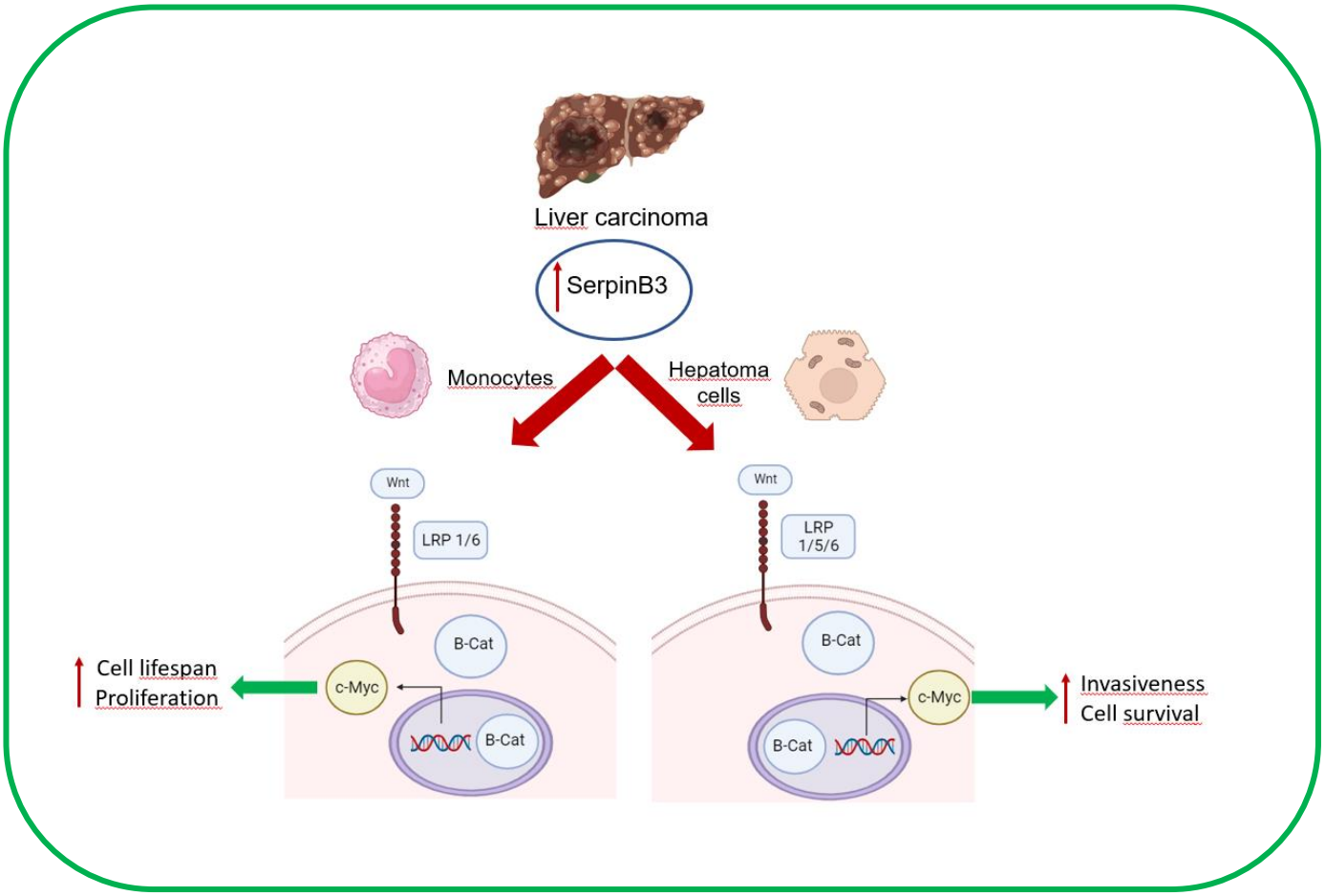

biology

MDPI

Article

SerpinB3 Upregulates Low-Density Lipoprotein Receptor-Related Protein (LRP) Family Members, Leading to Wnt Signaling Activation and Increased Cell Survival and Invasiveness

Santina Quarta [1], Andrea Cappon [1], Cristian Turato [2], Mariagrazia Ruvoletto [1], Stefania Cannito [3], Gianmarco Villano [4], Alessandra Biasiolo [1], Maristella Maggi [2], Francesca Protopapa [3], Loris Bertazza [1], Silvano Fasolato [1], Maurizio Parola [3] and Patrizia Pontisso [1,*]

[1] Department of Medicine, University of Padova, 35128 Padua, Italy
[2] Department of Molecular Medicine, University of Pavia, 27100 Pavia, Italy
[3] Department of Clinical and Biological Sciences, University of Torino, 10124 Turin, Italy
[4] Department of Surgical, Oncological and Gastroenterological Sciences, University of Padova, 35128 Padua, Italy
* Correspondence: patrizia@unipd.it

Simple Summary: The Wnt-β-catenin signaling regulates liver homeostasis and repair in adulthood, while its abnormal regulation is involved in the development of several chronic diseases and tumors. SerpinB3 has been shown to induce β-catenin, and both molecules are overexpressed in tumors, particularly in those with poor prognoses. The aim of our study was to evaluate the ability of SerpinB3 to modulate the Wnt pathway in liver cancer and monocytic cells, the main type of inflammatory cells in the tumor microenvironment. We have demonstrated that SerpinB3 modulates the Wnt cascade upregulating the Wnt co-receptors, low-density lipoprotein receptor-related protein 5 (LRP-5) and LRP-6, as well as LRP-1, implicated in cell survival and invasiveness. These data were confirmed in experimental carcinogenesis. In conclusion, the upregulation of LRP family members by SerpinB3 determines Wnt signaling activation and increased cell survival and invasiveness.

Abstract: Abnormal activation of the Wnt-β-catenin signaling cascade is involved in tumor growth and dissemination. SerpinB3 has been shown to induce β-catenin, and both molecules are overexpressed in tumors, particularly in those with poor prognoses. The aim of this study was to evaluate the ability of SerpinB3 to modulate the Wnt pathway in liver cancer and in monocytic cells, the main type of inflammatory cells in the tumor microenvironment. The Wnt cascade, Wnt co-receptors, and low-density lipoprotein receptor-related protein (LRP) members were analyzed in different cell lines and human monocytes in the presence or absence of SerpinB3. The Wnt-β-catenin axis was also evaluated in liver tumors induced in mice with different extents of SeprinB3 expression. In monocytic cells, SerpinB3 induced a significant upregulation of Wnt-1/7, nuclear β-catenin, and c-Myc, which are associated with increased cell lifespan and proliferation. In liver tumors in mice, the expression of β-catenin was significantly correlated with the presence of SerpinB3. In hepatoma cells, Wnt co-receptors LRP-5/6 and LRP-1, implicated in cell survival and invasiveness, were upregulated by SerpinB3. The LRP pan-inhibitor RAP not only induced a decrease in LRP expression, but also a dose–dependent reduction in SerpinB3-induced invasiveness. In conclusion, SerpinB3 determines the activation of the Wnt canonical pathway and cell invasiveness through the upregulation of LRP family members.

Keywords: β-catenin signaling; cell invasiveness; Wnt cell membrane co-receptors

Citation: Quarta, S.; Cappon, A.; Turato, C.; Ruvoletto, M.; Cannito, S.; Villano, G.; Biasiolo, A.; Maggi, M.; Protopapa, F.; Bertazza, L.; et al. SerpinB3 Upregulates Low-Density Lipoprotein Receptor-Related Protein (LRP) Family Members, Leading to Wnt Signaling Activation and Increased Cell Survival and Invasiveness. *Biology* **2023**, *12*, 771. https://doi.org/10.3390/biology12060771

Academic Editor: Soheil Tavakolpour

Received: 7 March 2023
Revised: 12 May 2023
Accepted: 22 May 2023
Published: 26 May 2023

1. Introduction

The Wnt-β-catenin signaling pathway is a highly conserved and tightly controlled signaling pathway that regulates not only hepatobiliary development and cell fate during embryogenesis, but also liver homeostasis and repair in adulthood [1]. During chronic liver injury, when massive extracellular matrix deposition parallels the impairment of hepatocytes and biliary cell proliferation, the stem cell niche, composed of quiescent progenitor cells, undergoes activation. Hepatic progenitor cells (HPCs) can differentiate into either hepatocytes or cholangiocytes, and the Notch-Wnt axis has a crucial role in HPC activation and fate [2]. In particular, in a mouse model of chronic biliary injury, it has been demonstrated that activated stellate cells and myofibroblast secrete Notch ligands in the hepatic progenitor niche milieu are used to promote biliary regeneration. On the other hand, during chronic hepatocellular injury, in the staminal niche, there is an increased recruitment of macrophages that secrete Wnt molecules in response to dead hepatocytes phagocytosis or other stimuli, such as lipid accumulation [3], with Wnt signaling driving HPCs toward differentiation into hepatocyte phenotypes. The core of the Wnt signaling cascade is β-catenin which, in addition to its role in embryogenesis, tissue homeostasis, and cell renewal, is also involved in tumor growth and dissemination [3,4]. In liver tumors, this molecule has been shown to be overexpressed in the presence of the serine protease inhibitor SerpinB3 [5], especially in tumors with poor prognosis [6,7]. This serpin is not detectable in normal adult hepatocytes; however, chronically damaged hepatocytes express SerpinB3, and the highest levels are achieved in the most aggressive forms of HCC, with a high risk of early recurrence [7]. It has been recently described that the subset of cholangiocarcinomas with stem-like features, associated with poor prognosis, expresses high levels of this serpin [8]. In vitro studies have shown that SerpinB3 protects neoplastic cells from apoptotic cell death through its interaction with Complex 1 of the mitochondrial respiratory chain [9] and also through the inhibition of lysoptosis, conferring resistance to chemoradiation in cervical cancer [10]. On the other hand, SerpinB3 has been reported to increase cell proliferation through the induction of not only β-catenin but also of Myc oncogene, a downstream gene of the Wnt pathway [11]. In line with these findings, it is not surprising that tumors overexpressing SerpinB3 and β-catenin are those characterized by poor prognosis not only in the liver but also in other types of cancer, including colon [5] and cervical cancer [10].

Low-density lipoprotein receptors (LRPs), especially LRP-5 and LRP-6, are fundamental co-receptors for the activation of canonical Wnt signaling. Their phosphorylation recruits axin to the cytoplasmic tail of LRP-6, preventing β-catenin phosphorylation and subsequent proteasomal degradation. As a consequence, β-catenin accumulates in the cytoplasm and translocates to the nucleus, where it regulates the expression of target genes [12]. It is interesting to note that another member of the LRP family, the low-density lipoprotein receptor-related protein-1 (LRP-1) is a ubiquitous membrane receptor with scavenger and regulatory functions [13], which can bind several proteins, including extracellular matrix proteins, growth factors, proteins involved in lipoprotein metabolism, and particularly, proteases alone or complexed to protease inhibitors, including alpha-1 antitrypsin (AAT), antithrombin III (ATIII), plasminogen activator inhibitor-1 (PAI-1), and nexin-1 (PN-1) [13]. The binding of the receptor to the serpin-enzyme complex (SEC) induces pro-survival and anti-inflammatory responses through the phosphorylation of protein kinase Akt [14].

On the basis of these considerations, we have investigated whether SerpinB3 may interact with LRP family members, modulating their cellular expression and functions in liver cancer.

2. Materials and Methods

2.1. Cell Cultures

2.1.1. Primary Human Monocytes

Human peripheral blood mononuclear cells (PBMCs) from healthy donors were isolated by density gradient centrifugation on a Ficoll–Paque (Merck KGaA, Darmstadt, Germany) solution at 500 rcf for 30 min. Mononuclear cells were harvested, resuspended

in a medium containing 10% FCS (Merck KGaA, Darmstadt, Germany), and separated from contaminating lymphocytes by adherence to plastic (1 h at 37 °C). Adherent monocytes were extensively washed with a medium to remove residual nonadherent cells. The percentage of CD14+ cells was greater than 98%. Primary human monocytes were routinely maintained in an RPMI 1640 medium supplemented with 10% *v/v* FCS, 2 mmol/L L-glutamine, and 1% *v/v* Penicillin/Streptomycin (Merck KGaA, Darmstadt, Germany) in 5% CO_2 in a humidified incubator at 37 °C.

2.1.2. THP-1 Cell Line

The monocytic THP-1 cell line (kindly provided by Prof. F. Marra, Florence University, Florence, Italy) was routinely maintained in an RPMI 1640 medium supplemented with 10% *v/v* FCS, 2 mmol/L L-glutamine, and 1% *v/v* Penicillin/Streptomycin (Merck KGaA, Darmstadt, Germany) in 5% CO_2 in air in a humidified incubator at 37 °C.

2.1.3. HepG2 Cell Line

Hepatoma cells (HepG2 cell line) (ATCC, Manassas, VA, USA), authenticated by BMR Genomics S.4.l. (Padova, Italy), were engineered to overexpress SerpinB3 (HepG2/SB3) by transfection with a plasmid expression vector containing the human SerpinB3 gene (pCDNA3/SB3), or with the plasmid vector alone (pcDNA3.1D/V5-His-TOPOTM) as a control (HepG2/control), using Lipofectamine Reagent Plus as the transfecting agent, according to the manufacturer's recommended indications (Invitrogen, Carlsbad, CA, USA), as previously reported [5]. Cells were maintained at 37 °C in a humidified chamber with 5% CO_2 and cultured in a minimum essential medium with the addition of G418 as a selective agent.

2.2. Cell Proliferation Assays

A real-time analysis of cell proliferation was performed on the xCELLigence DP instrument (ACEA BioSciences, St. Diego, CA, USA), as previously described [15]. The E-plate was engaged into xCELLigence and background measurements of the wells were recorded before adding 5×10^3 cells/well of primary human monocytes or THP1 cells supplemented with 100 ng/mL of recombinant SerpinB3 or with a medium alone as a control. Recombinant LPS-free SerpinB3 was obtained in our laboratory, as previously described [16].

Cells were allowed to settle for 30 min at room temperature before the E-plates were re-engaged onto the xCELLigence analyzer and incubated at 37 °C and 5% CO_2. The electrical impedance values were recorded every 15 min until 5 days and used for data analysis. The results were expressed as the cell index, a unitless readout that reflects the number of cells attached at the bottom of the cell culture plate wells via gold electrodes.

An MTT assay was also performed on monocytic cells. A total of 5×10^3 cells/well of primary human monocytes were seeded on 96 wells and treated with or without SerpinB3 in the presence or absence of the Wnt ICG-001 inhibitor (5 uM) for up to 8 days. Cell proliferation was measured by adding MTT (Merck KGaA, Darmstadt, Germany), and the absorbance of the resulting purple solution was spectrophotometrically measured at 570 nm.

2.3. Cell Invasion Assay

A real-time analysis of cell invasion was performed on the xCELLigence DP instrument (ACEA BioSciences, St. Diego, CA, USA), as previously described [17]. The surface of the upper chamber wells of a two-chamber device (CIM-plate 16) was coated with a monolayer of 1× collagen I solution (Merck KGaA, Darmstadt, Germany) in order to create a matrix suitable for the evaluation of invasive cellular activity. A medium with 10% serum was placed in the lower chamber as a chemoattractant. The two chambers are separated by a porous membrane and cells migrate through a solid matrix at the membrane where the electrodes reside. HepG2 cells were seeded (5×10^4 cells/well) in a serum-free medium

in the upper chamber, according to the manufacturer's instructions (ACEA, St. Diego, CA, USA). The following treatments were carried out: (a) pre-incubation with a mouse monoclonal antibody to LRP-1 515 kDa (Meridian Life Science, Inc., Memphis, USA) (0.5 and 5 g/mL) for 1 h, or with the same concentrations of a generic mouse antibody (Amersham, Bioscience, Arlington Height, IL, USA) as the control, followed by treatment with 100 ng/mL of recombinant SerpinB3 protein to induce invasiveness [5]; (b) incubation with the LRP inhibitor RAP (5 or 50 g/mL, Meridian Life Science, Inc., Memphis, TN, USA) in the presence of 100 ng/mL of recombinant SerpinB3 protein; and (c) HepG2/control cells with medium and vehicle-only (PBS) as a negative control. The cell index of each well was measured every 10 min for up to 23 h at 37 °C in a 5% CO_2 atmosphere using RTC software (version 2.0, ACEA BioSciences, San Diego, CA, USA).

2.4. SerpinB3 Quantification by ELISA

The protein concentration of cellular pellets was quantified by a bicinchoninic acid assay (BCA) protein kit (Pierce Merck, Darmstadt, Germany), following the manufacturer's instructions and using BSA as a standard on a Victor X3 microplate reader (Perkin Elmer, Waltham, MA, USA).

SerpinB3 concentration was measured by a sandwich ELISA (HEPA Lisa kit, Xeptagen, VEGA Park, Venice, Italy), as previously described [18]. Briefly, undiluted samples were incubated for 1 h at room temperature on plates coated with rabbit anti-human SerpinB3 capture Ab (10 µg/mL in PBS, pH 7.4). A standard curve, obtained by the dilution of the recombinant SerpinB3 from 16 to 0.25 ng/mL, was also included. All samples were tested in duplicate. After washing, SerpinB3 was revealed by incubation with HRP-conjugated streptavidin secondary anti-SerpinB3 Ab (0.5 µg/mL). The plate was developed with a ready-to-use 3,30,5,50-tetramethylbenzidine (TMB) substrate solution. The reaction was stopped with 1 mol/L HCl, and absorbance at 450 nm was measured on a microplate reader (Victor X3; Perkin Elmer, Waltham, MA, USA).

2.5. Immunofluorescence

2.5.1. Primary Human Monocytes and THP-1 Cells

Adherent primary human monocytes and THP-1 cells (3×10^5 cells/slide) were seeded on slides and cultured for 24 h. In some experiments, the Wnt inhibitor ICG-001 (5 uM for 24 h, kindly provided by Dr. M. Cadamuro, University of Padua, Padua, Italy), was used to confirm the activation of the Wnt pathway [19]. Cells were fixed in 4% paraformaldehyde and permeabilized with 0,4% Triton X-100 and blocked with 5% goat serum (Invitrogen Life Technologies, Waltham, MA, USA) in PBS containing 1% BSA. Slides were incubated with the primary antibodies (SerpinB3, LRP1, LRP6, Wnt1, Wnt7a, β-catenin, axin, cMyc) for one hour at room temperature and then incubated for 1 h at room temperature with a mouse or a rabbit secondary antibody, based on the origin of the primary antibody. The cellular nuclei were counterstained by DAPI (Merck KGaA, Darmstadt, Germany), mounted with ELVANOL Merck KGaA, Darmstadt, Germany), and observed under a fluorescence microscope (Axiovert 200M-Apotome.2, Carl Zeiss MicroImaging GmbH, Göttingen, Germany). The characteristics of the primary and secondary antibodies used in the study are reported in Supplementary Table S1.

2.5.2. HepG2 Cells

HepG2/control cells were seeded on slides (4×10^5 cells/slide) and cultured for 24 h. Cells were treated as follows: (a) overnight incubation with PBS as a negative control, (b) overnight incubation with 100 ng/mL of SerpinB3 recombinant protein as a positive control, (c) pre-treatment with 5 g/mL of the anti-LRP-1 85 kDa monoclonal antibody or with a generic mouse Ig for one hour followed by overnight incubation with 100 ng/mL of SerpinB3 recombinant protein, and (d) overnight incubation with 5 g/mL of RAP and 100 ng/mL of SerpinB3 recombinant protein. Cells were then fixed with 4% paraformaldehyde, permeabilized with 0.4% Tryton X-100, and blocked with

5% goat serum (Invitrogen Life Technologies, Waltham, MA, USA) in PBS containing 1% BSA. Slides were incubated with polyclonal anti-vimentin and anti-snail antibodies and with monoclonal anti-E-cadherin antibodies for 1 h at room temperature, followed by incubation with the Alexa-Goat 546 and 488 secondary antibodies, respectively. Cellular nuclei were counterstained with Dapi (Merck KGaA, Darmstadt, Germany). Slides were mounted with ELVANOL (Merck KGaA, Darmstadt, Germany) and observed under a fluorescence microscope (Axiovert 200M-Apotome.2, Carl Zeiss MicroImaging GmbH, Göttingen, Germany).

2.6. ImageStream Analysis

To assess the ImageStream analysis, which combines high-resolution microscopy and flow cytometry, 4×10^6 THP-1 cells, previously treated with SerpinB3 (100 ng/mL) in the presence of RAP (5 g/mL) or a medium alone for 24 h, were fixed and permeabilized with Fix and Perm (Invitrogen Life Technologies, Waltham, MA, USA), blocked with 5% goat serum (Invitrogen Life Technologies, Waltham, MA, USA) in PBS containing 1% BSA, and incubated with anti-LRP-1 for 1 h at room temperature. After washing, the cells were incubated for 30 min with secondary antibodies anti-mouse Alexa Fluor 488. Cellular nuclei were counterstained with Dapi by 3 min incubation (Merck KGaA, Darmstadt, Germany). For ImageStream analysis, 60 L of each sample was used, and the results were assessed by the IDEAS software (Luminex, Genk, Belgium).

2.7. RNA Isolation and Quantitative Real-Time PCR

Total RNA was extracted from cell lines and tissue samples using a Rnase Trizol reagent (Invitrogen, Carlsbad, CA, USA), according to the manufacturer's instructions. After the determination of the purity and the integrity, total RNA, complementary DNA synthesis, and quantitative real-time PCR reactions were carried out, as previously described [6], using the CFX96 real-time instrument (Bio-Rad Laboratories Inc., Hercules, CA, USA). The housekeeping gene glyceraldehyde-3-phosphate dehydrogenase (GAPDH) was analyzed in all amplification sets to assess the integrity of total RNA. Primer sequences used in the study are reported in Supplementary Table S2.

2.8. Western Blot Analysis

The total protein content (50 µg) from each cellular extract, prepared at 4 °C in a RIPA lysis buffer in the presence of phosphatase and protease inhibitors (Roche, Indianapolis, IN, USA), was loaded onto a 10% polyacrylamide gel. The blots were probed with the following primary antibodies: anti-LRP-1 extracellular domain (85 kDa), anti-Vimentin, and anti-E-cadherin; mouse monoclonal anti-β-actin was used as the housekeeping control. Anti-mouse and anti-rabbit horseradish peroxidase-conjugated antibodies were used as secondary antibodies. Antigenic detection was carried out by enhanced chemiluminescence (Amersham, Arlington Heights, IL, USA), and densitometric analysis was assessed using the VersaDoc Imaging System (Bio-Rad Laboratories, Hercules, CA, USA). Relative density units were obtained by assessing the ratio of the intensity of the antigen and the housekeeping reference band (β-Actin). Moreover, a Western blotting analysis for β-catenin and SerpinB3 was performed on liver samples derived from an experimental murine model of hepatic carcinogenesis.

2.9. Mouse Model of Liver Carcinogenesis

In order to assess the in vivo effect of SerpinB3 on the Wnt/β-catenin axis, we performed analyses on liver cancer samples with different extents of SerpinB3 expression using fully characterized animal experimentation [20]. NAFLD-related liver carcinogenesis was induced in mice carrying a specific hepatocyte deletion of Hypoxia-inducible factor-2α (hHIF-2α-/- KO mice, n = 5) and in the related control of wild type littermates without HIF-2α deletion (WT, n = 7). These mice were subjected to an established experimental protocol involving a single administration of DEN (25 mg/kg body weight, intraperitoneally) at

the age of 2 weeks, followed by feeding with a CDAA diet (Laboratorio Dottori Piccioni, Gessate, Italy) for 25 weeks starting from the age of 6 weeks [21]. Mice were kept under specific pathogen-free conditions and maintained with free access to pellet food and water. Liver samples were obtained and immediately frozen and thereafter maintained at −80 °C for further analysis. These experiments complied with EU and national ethical guidelines for animal experimentation, and experimental protocols were approved by the Animal Ethics Committee of the University of Oriental Piedmont, Novara, Italy, and the Italian Ministry of Health (authorization No. 1114/2016).

2.10. Immunohistochemistry

Immunostaining for Wnt-1 and the macrophage marker F4/80 was carried out as previously described [22]. Briefly, paraffin sections (2 μm thick), mounted on poly-L-lysine coated slides, were incubated with the following antibodies: a monoclonal antibody against Wnt-1 and a rabbit monoclonal antibody against F4/80. After blocking endogenous peroxidase activity with 3% hydrogen peroxide and performing microwave antigen retrieval, primary antibodies were labeled using EnVision, an HRP-labeled System (DAKO, Glostrup, Denmark), and visualized by a 3′-diaminobenzidine substrate. Conventional histological staining (Hematoxylin and Eosin, PAS stain for glycogen) was performed on paraffin sections (2 μm thick).

2.11. Patients

To confirm the effect of SerpinB3 on the Wnt/β-catenin axis, 38 surgically removed specimens of patients with hepatocellular carcinoma (HCC) were analyzed. Frozen liver tissue samples were maintained at −80 °C until use. The samples were obtained by the patients' written consent from all subjects involved in the study, following a procedure that was approved by the Ethical Committee of the Padua Teaching Hospital (11 December 2006). The demographic and clinical profiles of the patients included in the study are depicted in Supplementary Table S3.

2.12. Amino Acid and Structure Alignment

The amino acid sequences of 19 human serpins were aligned using the Clustal Omega multiple sequence alignment.

The structured image was performed in PyMol 2.5.1 (Schrödinger). The SerpinB3 (PDB ID: 2ZV6) structure in its metastable conformation was retrieved from the Protein Data Bank.

2.13. Statistical Analysis

Statistical analysis was performed by Student's *t*-test for analysis of variance when appropriate. Spearman's rank correlation was used to measure the statistical dependence between two variables. All *p*-values reported were two-tailed and considered significant if $p \leq 0.05$. Data in bar graphs are presented as mean ± SEM and were obtained from at least three independent experiments. Western blot and morphological images are representative of at least three experiments with similar results. Statistical tests were performed using GraphPad Prism and IDEAS software (Amnis-Imagestream Imaging Flow cytometer).

3. Results

3.1. Exogenous SerpinB3 Increases Monocyte Proliferation and Induces Its Endogenous Expression

Based on our previous studies on the increase in cellular proliferation promoted by SerpinB3 in hepatoma cells [15], we have evaluated whether this serpin is able to increase proliferation in monocytes, since monocytic cells are the main type of inflammatory cells in the tumor microenvironment and are profoundly involved in the pathogenesis and development of primary liver tumors, establishing a pro-inflammatory and pro-tumorigenic environment by the suppression of antitumor immune responses [23]. The results obtained in both primary human monocytes and in the THP-1 cell line demonstrate that the exoge-

nous addition of SerpinB3 significantly increases the lifespan and the proliferation of both cell types. In particular, the addition of recombinant SerpinB3 at 100 ng/mL resulted in a significant increase in the replication of primary monocytes, starting on the fifth day of culture (Figure 1A). The positive effect of this serpin was confirmed in THP-1 cells, in which increased proliferation was achieved starting on the second day of culture (Figure 1B). It is worth noting that increased monocyte proliferation promoted by exogenous SerpinB3 was associated with an increase in its endogenous expression, as documented by IF (Figure 1C) and ELISA assays (Figure 1D), leading to a paracrine positive loop induction.

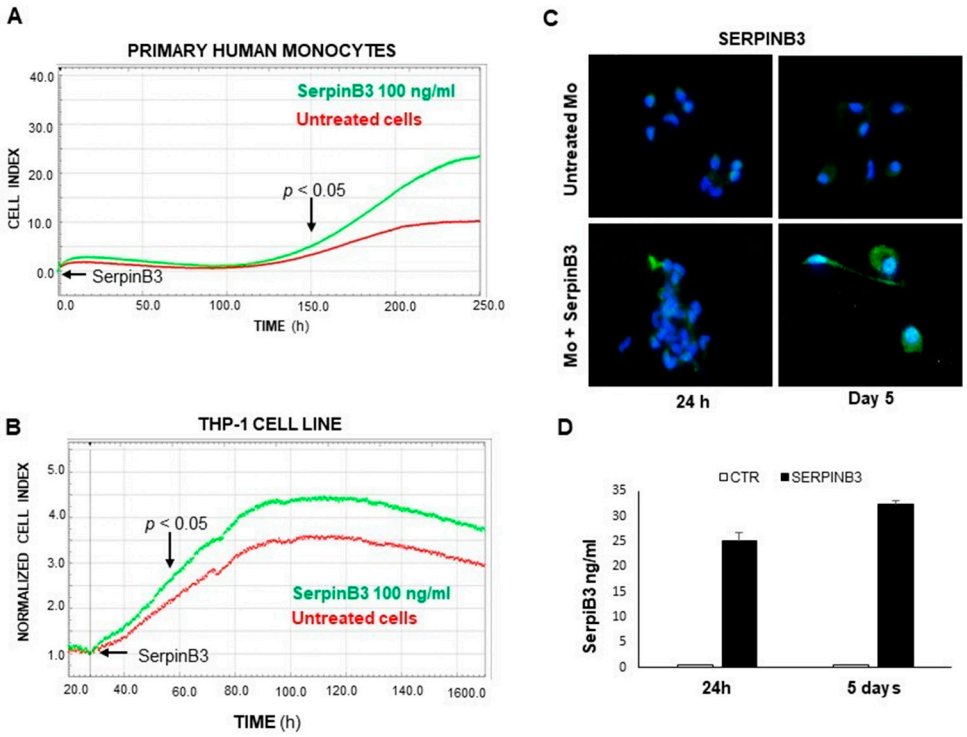

Figure 1. The Effect of SerpinB3 on the proliferation of monocytic cells. An example of a direct comparison of real-time growth curves, generated by the xCELLigence RTCA of primary human monocytes (**A**) and THP-1 cell lines (**B**) stimulated with 100 ng/mL of recombinant SerpinB3 vs. untreated cells. (**C**) An immunofluorescence analysis of the expression of SerpinB3 in primary human monocytes after 24 h and 5 days of treatment. Blue color: DAPI nuclear staining; green color: SerpinB3 staining. Original magnification 63×. (**D**) A time course quantification of SerpinB3 protein by ELISA in cellular extracts of primary monocytes after 24 h and 5 days of treatment. All graphs represent mean results from three independent experiments ± SD.

3.2. SerpinB3 Induces Wnt-1 and Wnt-7a

Based on the fact that SerpinB3 is able to increase β-catenin expression [11], we have evaluated whether this phenomenon can occur through the induction of members of the Wnt family, which are molecules responsible for activating catenin signaling. Primary human monocytes were stimulated with recombinant SerpinB3, and cells were harvested after 2 and 8 h to evaluate the mRNA expression of Wnt-1, Wnt-3a, Wnt-5a, Wnt-5b, and Wnt-7a genes. Interestingly, the cells treated with SerpinB3 showed a significant upregulation of Wnt-1, already detectable at 2 h (Figure 2A), and Wnt-7a, which was detectable at 8 h (Figure 2B). By contrast, no increase was observed for the expression of Wnt-3a, Wnt5a, and Wnt-5b (data not shown). An immunofluorescence analysis of Wnt-1 confirmed the ability of SerpinB3 to induce the expression of this protein that remained remarkably high for up to 72 h (Figure 2C).

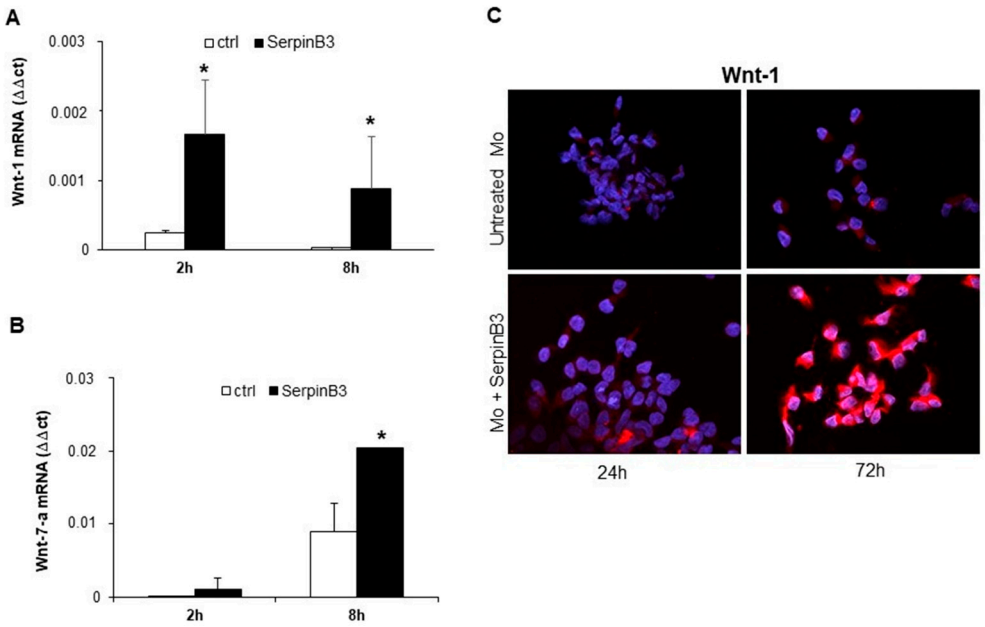

Figure 2. Wnt-1 and Wnt-7-a expression. Relative mRNA expression of Wnt-1 (**A**) and Wnt-7-a (**B**) in primary human monocytes (Mo) stimulated with 100 ng/mL of SerpinB3, calculated by the Ct method. Data were normalized to housekeeping gene glyceraldehyde-3-phosphate dehydrogenase (GAPDH). All graphs represent mean results from three independent experiments ± SD. * $p < 0.05$ vs. the control. (**C**) An immunofluorescence staining of Wnt-1 in primary human monocytes after 24 and 72 h of treatment with 100 ng/mL of human recombinant SerpinB3. Blue color: DAPI nuclear staining; red color: Wnt-1 staining. Original magnification 63×. * $p < 0.05$ vs. control.

3.3. SerpinB3 Activates the Wnt-Canonical Pathway

Since Wnt-1 and Wnt-7a are the key players in the activation of the Wnt-canonical pathway [24,25], the expression of β-catenin was evaluated by immunofluorescence staining in monocytes treated or not with SerpinB3. After 24 h of incubation with this serpin, a remarkable increase in β-catenin at the cytoplasmic level was observed only in cells treated with SerpinB3, while axin, the negative regulator of the Wnt signaling pathway, was reduced, confirming the positive modulation of this pathway by SerpinB3 (Figure 3A). Accordingly, SerpinB3-induced monocyte proliferation was abrogated by the Wnt inhibitor ICG-001 (Figure 3B).

To confirm the ability of SerpinB3 to activate the Wnt pathway and to induce monocyte proliferation, we evaluated c-Myc expression, a downstream gene of the same pathway. As observed in Figure 4A, treatment of THP-1 cells with human recombinant SerpinB3 led to the upregulation of c-Myc mRNA expression in a cyclic manner over time. Accordingly, the specific Wnt inhibitor ICG-001 was able to abrogate the upregulation of c-Myc protein expression induced by SerpinB3 in primary human monocytes (Figure 4B).

3.4. SerpinB3 and Wnt/β-Catenin Axis in an Experimental Model of Liver Carcinogenesis

In order to demonstrate the relation between SerpinB3 and the Wnt/β-catenin pathway at the mechanistic level in liver carcinogenesis, we used liver tumor samples with different extents of SerpinB3 expression, derived from mice carrying a specific hepatocyte deletion of HIF-2α (hHIF-2α-/- KO mice), a previously recognized transcriptor factor that upregulates SerpinB3 by binding to its promoter [26].

As shown in Figure 5A, HIF-2α-/- KO mice, which in the previous study presented a significant decrease in the volume and number of liver tumors compared with the controls [20], showed a remarkable reduction in SerpinB3 and of β-catenin protein levels, compared to wild type mice. Of relevance, β-catenin protein levels were significantly higher

in mice expressing high levels of SB3 (Figure 5B) and correlated with SerpinB3 (Figure 5C), confirming a positive relation between SerpinB3 and the Wnt/β-catenin pathway.

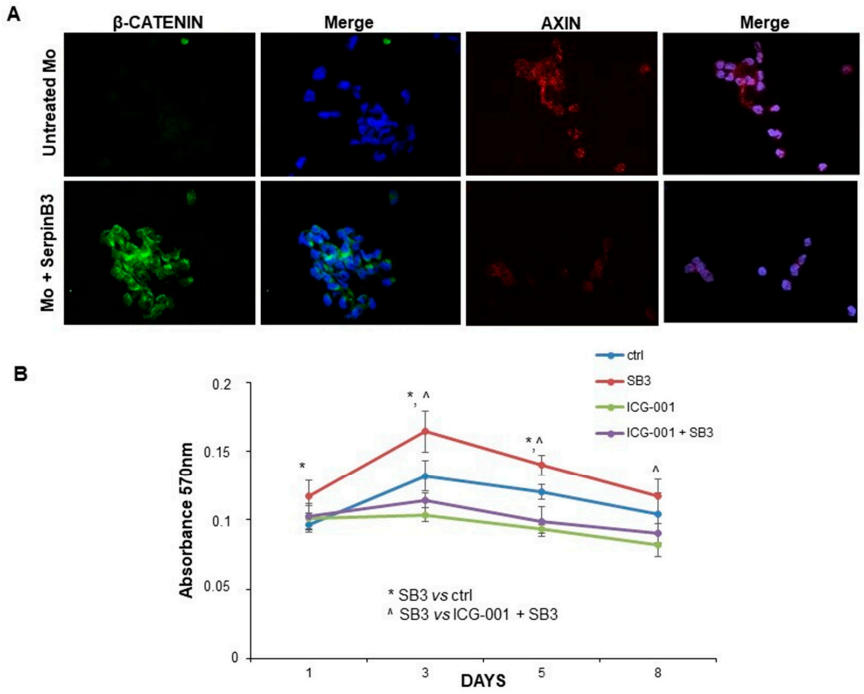

Figure 3. Expression of β-catenin and axin. (**A**) An immunofluorescence analysis of the expression of β-catenin and axin in monocytes treated with human recombinant SerpinB3. Cellular nuclei were counterstained with DAPI (blue). Original magnification 63×. (**B**) A time course analysis of the proliferation of monocytes treated with SerpinB3 +/−, the Wnt inhibitor ICG-001 by the MTT assay. * $p < 0.05$ vs. control, ^ $p < 0.05$ vs. ICG-001 + SB3.

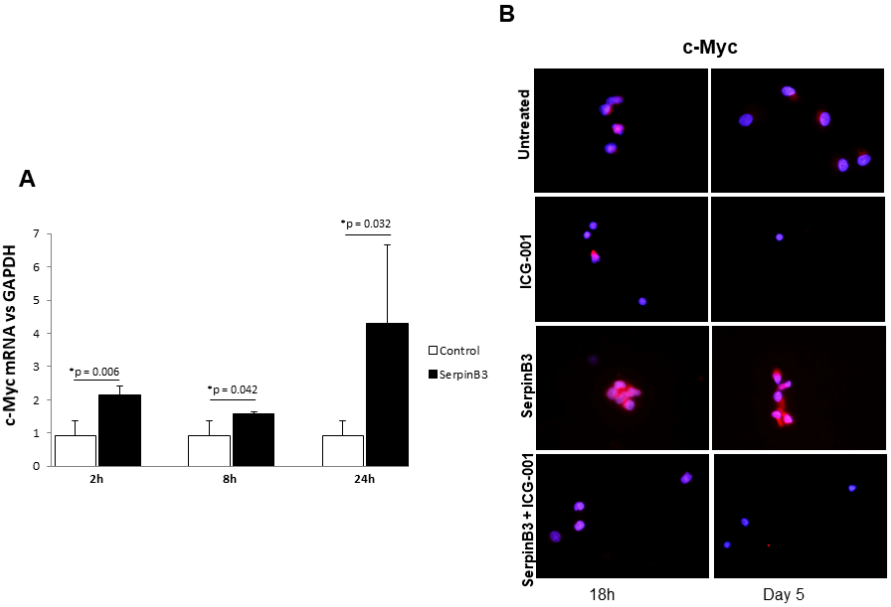

Figure 4. c-Myc expression in monocytic cells. (**A**) A time course analysis of c-Myc expression in THP-1 cells treated for 2, 8, and 24 h with 100 ng/mL of human recombinant SerpinB3. All graphs represent mean results from three independent experiments ± SD. *p*-values are indicated. (**B**) An immunofluorescence analysis of c-Myc +/− SerpinB3 or ICG-001 or SerpinB3 + ICG-001 in primary human monocytes after 18 h and 5 days of treatment. Blue color: DAPI nuclear staining; red color: c-Myc staining. Original magnification 63×.

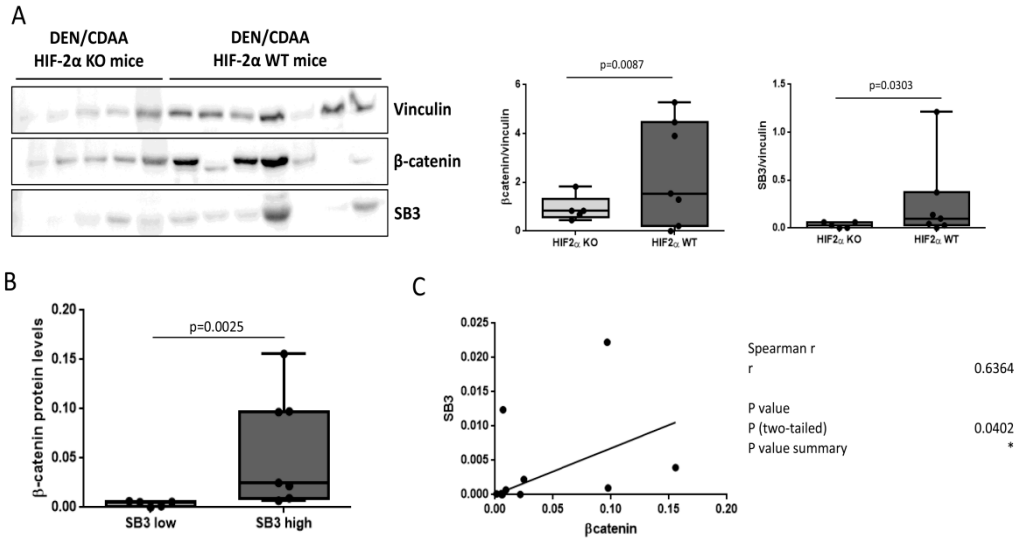

Figure 5. Correlation between SerpinB3 and β-catenin in DEN–CDAA liver carcinogenesis. (**A**) A Western blot analysis of SerpinB3 (SB3) and β-catenin protein levels in tumor masses obtained from HIF-2α wild type (WT, n = 7) or HIF-2α-/- KO (n = 5) mice treated with the DEN/CDAA protocol. For the Western blot analysis, Bio-Rad (Hercules, CA, USA) Quantity One software was used to perform the densitometric analysis. Equal loading was evaluated by reprobing membranes for Vinculin. Statistical differences were assessed by the Mann–Whitney test for nonparametric values. (**B**,**C**) The relationship between SerpinB3 and β-catenin protein levels in liver tumors, including all mice. Higher β-catenin protein levels were obtained in mice with high levels (>median values) of SerpinB3, compared to those with low (≤median values) SerpinB3 values. A correlation analysis between SerpinB3 and β-catenin was performed with the Spearman r test. In panel (**C**) *p* value is specified ($p = 0.0402$) and * indicates that it is < 0.05.

3.5. SerpinB3 and Wnt Family Members in Human Liver Tumors

Activation of the Wnt family members in relation to SerpinB3 expression was also assessed in the tumor tissue of 38 patients with HCC. When samples were divided according to the extent of SerpinB3 expression, tumors expressing a high level of SerpinB3 (>median value) showed a trend toward higher amounts of Wnt-1 and Wnt-7a compared to the corresponding figures observed in tumors with low SB3 level (<median value), although the difference did not reach statistical significance, probably due to the small sample size (Supplementary Figure S1). Again, no differences were observed for Wnt-5a and Wnt-3a mRNA between the two groups (data not shown). These data suggest that SerpinB3 is able to upregulate Wnt signaling not only in vitro but also in a more complex environment, such as liver cancer.

3.6. SerpinB3 Upregulates Low-Density Lipoprotein Receptors

Since members of low-density lipoprotein receptors (LRPs), particularly LRP-5/6, are key co-receptors for the activation of canonical Wnt signaling, we have evaluated the effect of SerpinB3 on LRP-6 expression in primary human monocytes. An immunofluorescence analysis showed a significant increase in LRP-6 in cells treated with SerpinB3, compared to untreated cells, for up to 7 days (Figure 6A). These results were also confirmed in the THP-1 cell line exposed to SerpinB3, where the upregulation of LRP-6 was inhibited by treatment with the receptor-associated protein (RAP), a known inhibitor of LRP family members [27].

Since LRP-1 has been involved in cellular internalization and subsequent degradation of serine proteinases [13], we have explored whether this member of the LRP family was upregulated by SerpinB3. In THP-1 cells, SerpinB3 induced an upregulation of LRP-1 similar to that observed for LRP-6, which also in this case was inhibited by RAP, both at transcription and protein levels (Figure 6C,D).

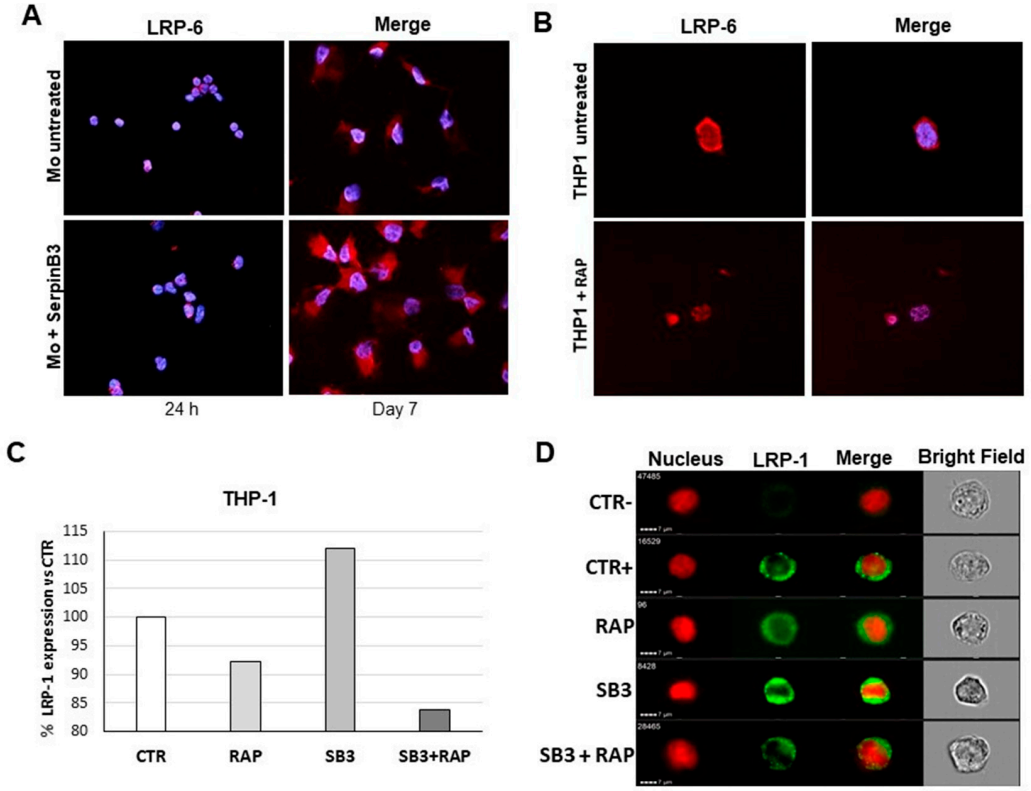

Figure 6. LRP-6 and LRP-1 expression in monocytic cells. (**A**) An immunofluorescence analysis of LRP-6 in human primary monocytes stimulated with 100 ng/mL of recombinant SerpinB3 for 24 h and 7 days. Blue color: DAPI nuclear staining; red color: LRP-6 staining. (**B**) An immunofluorescence analysis of LRP-6 in THP-1 cells, physiologically expressing SerpinB3, +/− RAP. Blue color: DAPI nuclear staining; red color: LRP-6 staining. Original magnification 63×. (**C**) The percentage of LRP-1 expression in THP-1 cells +/− SerpinB3 or SerpinB3 + RAP or RAP alone. Results are expressed as a percentage of LRP1 expression compared to the untreated cells. (**D**) Representative images of cellular expression of LRP1 in THP-1 cells +/− overnight incubation with SerpinB3 (100 ng/mL) or SerpinB3 + RAP or RAP (5 ug/mL) alone, generated by an ImageStream Flow Cytometer.

The effect of SerpinB3 on the expression of the LRP family members was also confirmed in HepG2 cells, where cells transfected to overexpress SerpinB3 showed upregulation of LRP family members, including LRP-1, LRP-5, and LRP-6 (Figure 7 and Supplementary Figure S2). In HCC specimens, in addition to the described trend toward a higher activation of the Wnt signaling in relation to SerpinB3 expression, statistically significant higher levels of LRP-1 transcription were found in tumors expressing high levels of SerpinB3 (Supplementary Figure S1).

3.7. Amino Acid and Structure Alignment of Serpins

In order to better assess the interaction of SerpinB3 with LRP-1, which is known to bind serine-proteinase complexes, we aligned the amino acid sequences of SerpinB3, alpha-1 antitrypsin (AAT), and several other human serpins in the region comprising the SEC binding pentapeptide described by Joslin et al. [28]. We found that the SerpinB3 369-FLFFI–373 pentapeptide, even if different from the one originally described in AAT, is highly conserved in Serpins, in particular in the SerpinB family, in nexin 1 (UniProt ID P07093, serpin E2) and in Alpha-2-antiplasmin (UniProt ID P08697, serpin F2) (Figure 8A). In relation to the aa sequence of SerpinB3, this region is located closely downstream of the reactive site loop (Figure 8B).

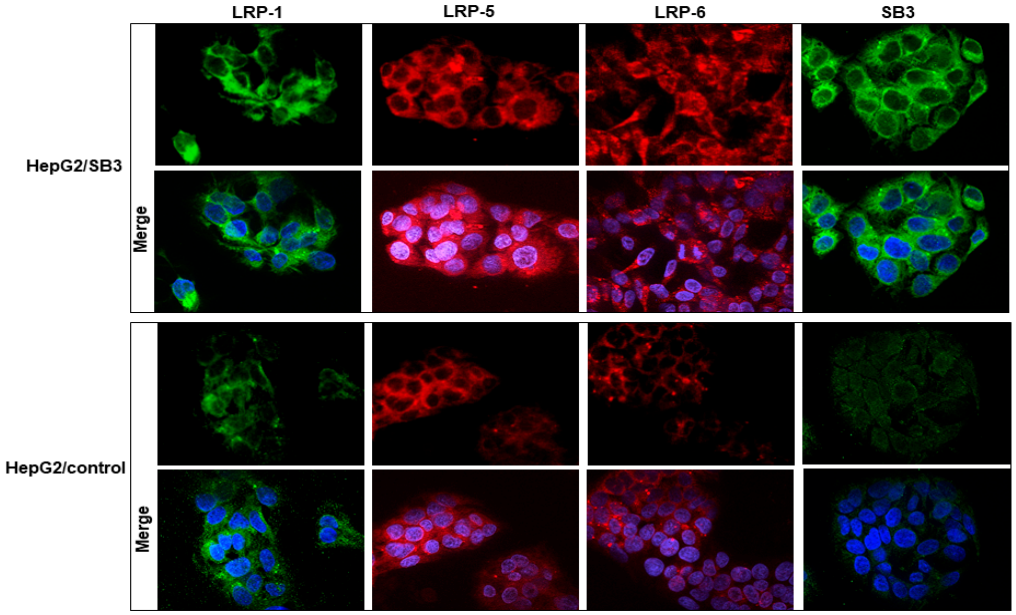

Figure 7. LRP expression in hepatoma cells. An example of an immunofluorescence analysis of LRP-1 (green), LRP-5 (red), LRP-6 (red), and SerpinB3 (green) in HepG2 overexpressing SerpinB3 (HepG2/SB3) compared with the HepG2/control cells tested 48 h from seeding. Cellular nuclei were counterstained with DAPI (blue). Original magnification 63×.

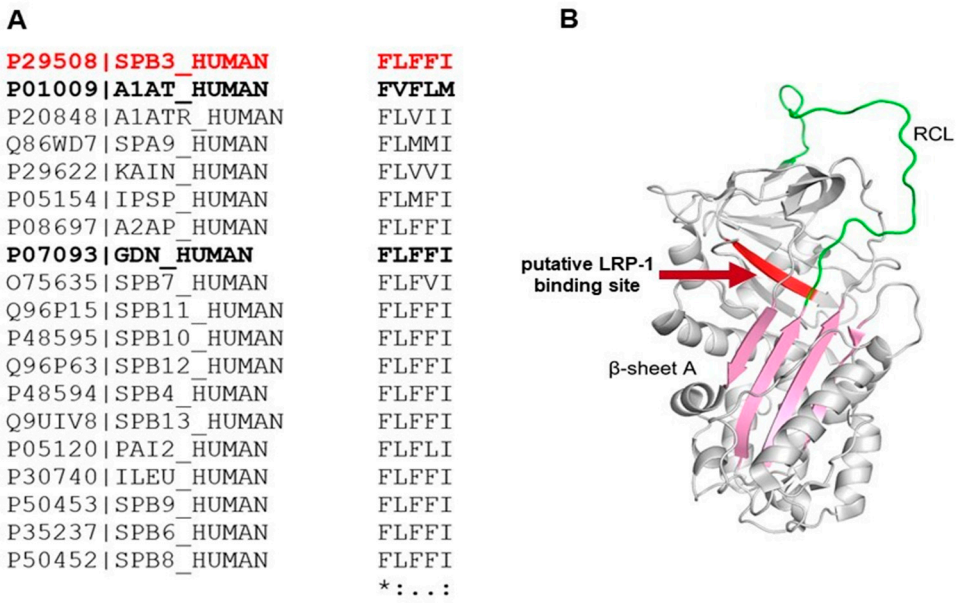

Figure 8. Alignment of the human serpin pentapeptide region and the structure of SerpinB3. (**A**) Amino acid sequence alignments of the human serpin pentapeptide region. In red, SerpinB3 sequence; in bold, α1-Antitrypsin (A1AT) and protease nexin-1 (GDN) sequences. * Positions with a single, fully conserved residue. : Positions with a conservation between amino acid groups of similar properties. (period) Positions with a conservation between amino acid groups of weakly similar properties. (**B**) The structure of native SerpinB3 (PDB ID: 2ZV6) represented as a cartoon. The β-strand containing the LRP-1 binding pentapeptide is in red. The reactive center loop (RCL) is in green. The functionally relevant β-sheet A is in pink.

Along the aligned human Serpins, F369 is fully conserved, and residues 370–373 correspond to amino acid groups of similar properties (i.e., hydrophobic). It is worth noting that structure alignment between SerpinB3 (PDB ID: 2ZV6) in the 336–379 region and the putative LRP-1 binding site of the AAT (29) (PDB ID: 1QLP) 364–380 region (peptides

FHCNHPFLFFIRQNKTN and VKFNKPFVFLMIEQNTK, respectively) shows an identical secondary structure organization, indicating a similar backbone organization in the selected regions of the two proteins (Figure 9A). As for the pentapeptide region, an overlap between the side chains of the first, highly conserved, and third phenylalanine can be observed, while SerpinB3 position 2 is occupied by an L instead of a V, and position 4 is occupied by a third F in place of an L, amino acids with similar properties in both cases (Figure 9B). Taken together, these observations suggest the possibility of a tridimensional organization in SerpinB3 pentapeptide compatible with the one described for AAT and relevant for binding to LPR-1, which is predicted to occur in the same binding site of LRP-1 by computational modeling (Figure 9B).

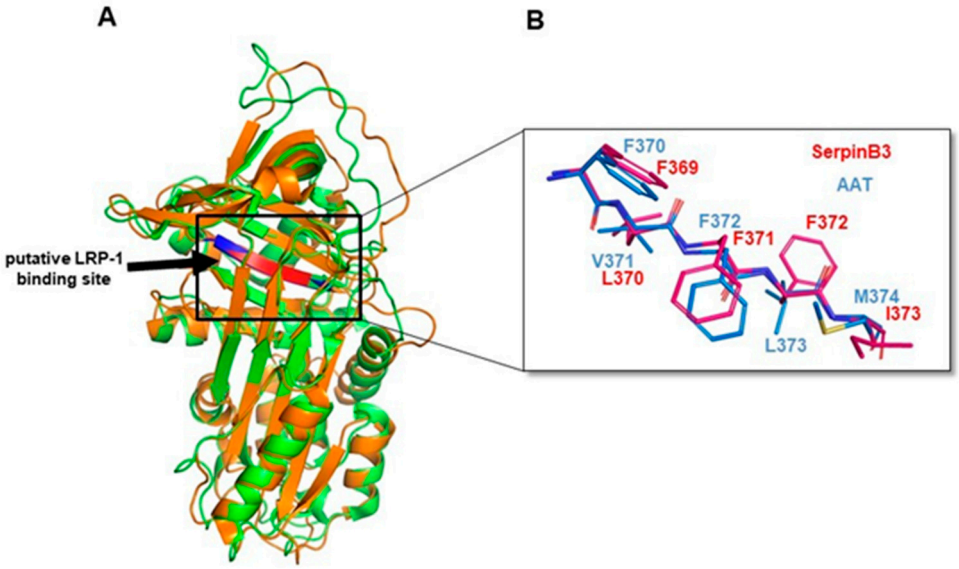

Figure 9. A Cartoon of SerpinB3-LRP-1 binding. (**A**) The structural alignment of native SerpinB3 (PDB ID: 2ZV6, green) and AAT (PDB ID: 1QLP, orange) represented as a cartoon. The β-strand containing the putative LRP-1 binding region is colored in red in SerpinB3 and blue in AAT. (**B**) Magnification of the structure alignment of native SerpinB3 (PDB ID: 2ZV6, red) and AAT (PDB ID: 1QLP, blue) in the putative LRP-1 binding pentapeptide region represented as sticks. Amino acids are labeled according to primary sequence numbering.

Moreover, in position 5 of the pentapeptide, SerpinB3 has a naturally occurring I, instead of M found in AAT, a replacement known to improve its stability and binding capability to LPR-1 [29]. Therefore, it is possible to speculate that the natural binding of SerpinB3 to LPR-1 would be favored if compared to the one described for AAT.

3.8. SerpinB3 Induces the Pro-Invasive Activity of LRP-1

A growing amount of evidence has strengthened the putative role of LRP-1 in crucial events during cancer progression by promoting cell migration and invasion [30], in addition to cell survival [14]. In order to evaluate whether SerpinB3 could induce these biological activities in hepatocytes, we have used stably transfected HepG2 cells overexpressing SerpinB3, which showed a remarkable increase in LRP-1 at the transcription and protein levels (Figure 7 and Supplementary Figure S2). It is worth noting that the already reported invasion capability induced by SerpinB3 in hepatocytes [5] and mouse fibroblasts [17] was significantly reduced in HepG2 cells treated with SerpinB3 by both an anti-LRP-1 antibody and RAP in a dose–dependent manner (Figure 10A). These results were associated with a parallel reduction not only of β-catenin but also of SNAIL and vimentin, together with the increased expression of E-cadherin (Figure 10B), as confirmed by a Western blot analysis (Supplementary Figure S3), supporting the hypothesis that the EMT profile induced by SerpinB3 can be reverted by the ligand inhibition of LRP family members.

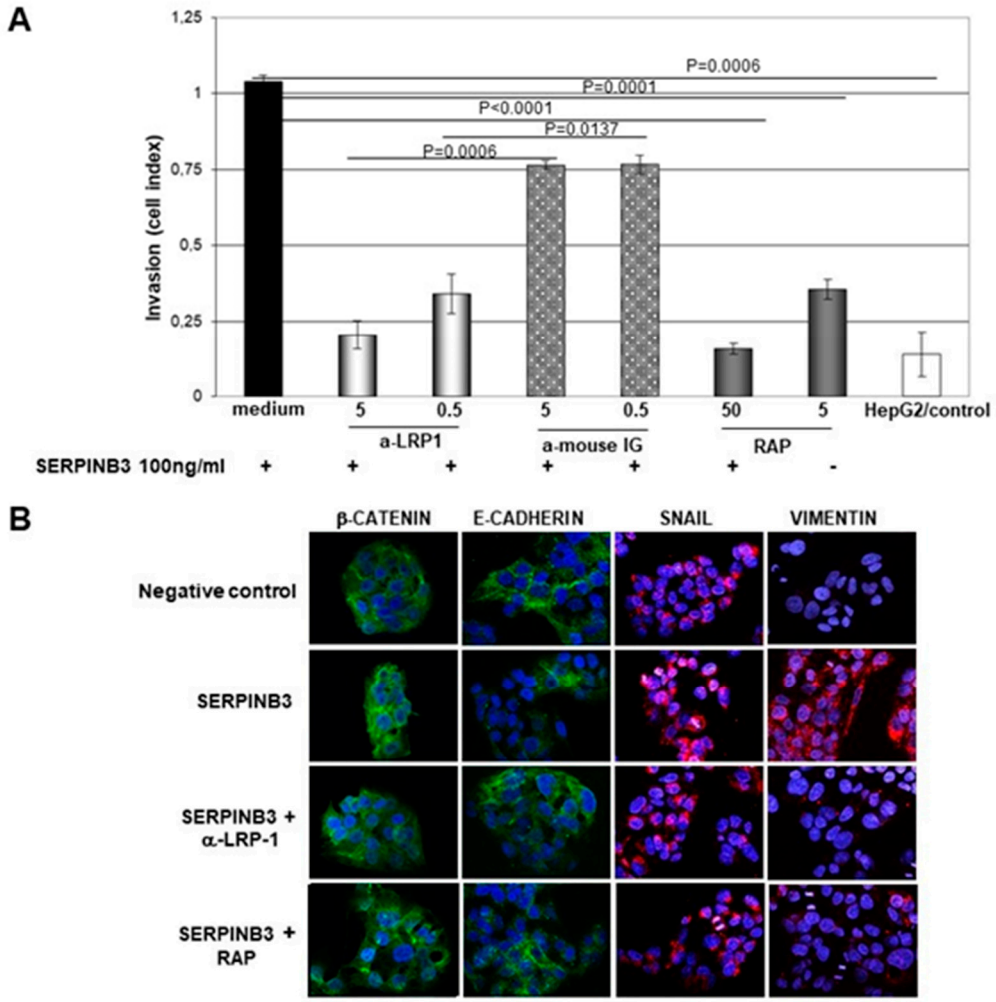

Figure 10. Real-time monitoring of cell invasion. (**A**) An invasion analysis of HepG2 cells treated with human recombinant SerpinB3 (100 ng/mL) with or without one-hour pre-treatment with 0.5 or 5 g/mL of anti-LRP-1, with 5 or 50 g/mL of RAP and PBS as the control. The invasion curves were monitored every 10 min for 23 h, using xCELLigence RTCA (ACEA, San Diego, CA, USA). Experiments were performed in quadruplicate. Invasion bars are depicted as mean ± SD cell index values of four wells/treatment processed in parallel at 10 h time points. (**B**) An immunofluorescence analysis of β-catenin (green), E-cadherin (green), snail (red), and vimentin (red) in HepG2/empty vector cells incubated overnight with PBS, as a negative control, with 100 ng/mL of recombinant SERPINB3 protein, as a positive control, pre-treated with 5 g/mL of anti-LRP-1 for 1 h, incubated overnight with 5 g/mL of RAP or with 100 ng/mL of recombinant SerpinB3. Blue color: DAPI nuclear staining. Original magnification 63×.

4. Discussion

Wnt-β-catenin signaling is known to regulate multiple cellular processes, including embryonic development and adult tissue homeostasis. However, the abnormal regulation of this signaling pathway is also involved in the development of several chronic diseases and tumors of different organs. Indeed, once activated, the Wnt pathway induces the increased stability of β-catenin and its nuclear translocation, which facilitates the expression of genes involved in cell proliferation, survival, differentiation, and migration [24].

In the present study, we have evaluated the ability of SerpinB3 to modulate the Wnt pathway in in vitro and in vivo models. In primary human monocytes and the monocytic cell line THP-1, the addition of SerpinB3 not only significantly increased cell lifespan and proliferation, but also resulted in a positive modulation of the Wnt pathway. SerpinB3 induced a significant upregulation of Wnt-1/7 and of β-catenin, mainly localized in the

nucleus, confirming its activation profile. These findings were also supported by the results obtained in experimental carcinogenesis, where liver tumors of hHIF-2 -/- KO mice presented not only a remarkable reduction in SerpinB3 expression, as a result of the lack of HIF-2a transcriptional activity for SerpinB3 [26], but also a parallel decrease in β-catenin expression, confirming the role of this serpin in the activation of Wnt pathway.

To further understand the mechanism of Wnt activation by SerpinB3, we focused our attention on LRP family members, initially on LRP-5 and LRP-6, which have been described as cellular receptors for Wnt pathway activation [25]. The results obtained have demonstrated that both receptors were upregulated by SerpinB3. We further expanded our study to another member of the LRPs family, namely LRP-1, since it was previously described that this receptor binds several protease complexed-serine protease inhibitors [13]. According to the hypothesis, this receptor was found to be upregulated by SerpinB3. In addition, computational analysis and 3D modeling revealed that the putative SerpinB3 binding site could determine an even more stable interaction with LRP-1 than initially described as responsible for the binding of the enzyme-complexed serpins with the cellular receptor [28], which was further expanded by Toldo et al. for AAT [29]. This hypothesis is supported by the fact that an AAT peptide, including a similar and structurally compatible aa sequence, is able to bind and activate LRP-1-mediated signaling [29]. It is interesting to note that the AAT pentapeptide neo-domain was identical in SerpinB3 and in Nexin-1, where it was involved in the invasion activity and metastasis formation induced by this serpin [31]. In addition, one should note that the LRP binding site of SerpinB3 is located downstream of the reactive site loop of the protein, and this fact supports our previous findings reporting that loop-deleted SerpinB3 had effects similar to those of wild type SerpinB3 on the expression of EMT markers and β-catenin expression [5]. The inhibition of LRP-1 by the corresponding antibody or by the use of the LRP pan-inhibitor RAP was able not only to determine a decrease in LRP cell surface expression but also a dose–dependent reduction in SerpinB3-induced invasiveness. These results were in line with the observed reversal of the expression of the SerpinB3-induced EMT profile markers by both the anti-LRP-1 antibody and RAP.

5. Conclusions

SerpinB3 upregulates LRP family members and determines not only the activation of the Wnt canonical pathway but also the activation of LRP-1, a cellular receptor profoundly implicated in cell survival and invasiveness. These findings could provide useful information for the development of targeted therapeutic strategies in an oncological setting.

Supplementary Materials: The following supporting information can be downloaded at https://www.mdpi.com/article/10.3390/biology12060771/s1, Figure S1: Relative mRNA expression of SerpinB3 compared with Wnt-1, Wnt-7a, and LRP-1 in human HCCs; Figure S2: LRP-1 expression in hepatoma cells; Figure S3: Western blot analysis of E-cadherin and vimentin. Table S1: List of the antibodies used in the study; Table S2: List of the primers used in the study; Table S3: Clinical and histological characteristics of the patients included in the study.

Author Contributions: Conceptualization, S.Q., A.C. and P.P.; methodology, C.T., M.R. and S.Q.; software, M.M.; validation, L.B., S.C., F.P. and S.F.; formal analysis, A.C., S.Q., A.B., G.V., C.T. and F.P.; investigation, S.Q.; writing—original draft preparation, S.Q. and A.C.; writing—review and editing, P.P., M.P. and S.C.; supervision, P.P.; funding acquisition, P.P. and M.P. All authors have read and agreed to the published version of the manuscript.

Funding: This research was funded in part by the University of Padova, grant number CPDA110795 (P.P.), the National Ministry of Health, grant number RF-2019-12369984 (P.P.), and the Associazione Italiana per la Ricerca sul Cancro (AIRC), grant number IG2017-ID 20361 (M.P).

Institutional Review Board Statement: The study was conducted in accordance with the Declaration of Helsinki and was approved by the Ethics Committee of Azienda Ospedale-Università of Padova (11 December 2006).

Informed Consent Statement: Informed consent was obtained from all subjects involved in the study.

Data Availability Statement: The data presented in this study are available upon request from the corresponding author. The data are not publicly available due to privacy reasons.

Acknowledgments: The Authors are grateful to F. Marra, Florence University, Italy, for providing the THP1 cell line, Massimiliano Cadamuro, University of Padua, Italy, for providing the Wnt inhibitor ICG-001, and Giorgio Fassina, Xeptagen SpA, VEGA Park, Venice), for providing the HEPA Lisa Kits.

Conflicts of Interest: The authors declare no conflict of interest.

References

1. Perugorria, M.J.; Olaizola, P.; Labiano, I.; Esparza-Baquer, A.; Marzioni, M.; Marin, J.J.G.; Bujanda, L.; Banales, J.M. Wnt-β-catenin signalling in liver development, health and disease. *Nat. Rev. Gastroenterol. Hepatol.* **2019**, *16*, 121–136. [CrossRef] [PubMed]
2. Boulter, L.; Govaere, O.; Bird, T.G.; Radulescu, S.; Ramachandran, P.; Pellicoro, A.; Ridgway, R.A.; Seo, S.S.; Spee, B.; Van Rooijen, N.; et al. Macrophage-derived Wnt opposes notch signaling to specify hepatic progenitor cell fate in chronic liver disease. *Nat. Med.* **2012**, *18*, 572–579. [CrossRef] [PubMed]
3. Debebe, A.; Medina, V.; Chen, C.-Y.; Mahajan, I.M.; Jia, C.; Fu, D.; He, L.; Zeng, N.; Stiles, B.W.; Chen, C.-L.; et al. Wnt/β-catenin activation and macrophage induction during liver cancer development following steatosis. *Oncogene* **2017**, *36*, 6020–6029. [CrossRef] [PubMed]
4. Valenta, T.; Hausmann, G.; Basler, K. The many faces and functions of β-catenin: β-catenin: A life by, beyond, and against the Wnt canon. *EMBO J.* **2012**, *31*, 2714–2736. [CrossRef] [PubMed]
5. Quarta, S.; Vidalino, L.; Turato, C.; Ruvoletto, M.; Calabrese, F.; Valente, M.; Cannito, S.; Fassina, G.; Parola, M.; Gatta, A.; et al. SERPINB3 induces Epithelial-Mesenchymal Transition. *J. Pathol.* **2010**, *221*, 343–356. [CrossRef]
6. Terrin, L.; Agostini, M.; Ruvoletto, M.; Martini, A.; Pucciarelli, S.; Bedin, C.; Nitti, D.; Pontisso, P. SerpinB3 Upregulates the cyclooxygenase-2/β-Catenin positive loop in colorectal cancer. *Oncotarget* **2017**, *8*, 15732–15743. [CrossRef]
7. Turato, C.; Vitale, A.; Fasolato, S.; Ruvoletto, M.; Terrin, L.; Quarta, S.; Ramirez Morales, R.; Biasiolo, A.; Zanus, G.; Zali, N.; et al. SERPINB3 is associated with TGF-B1 and cytoplasmic β-catenin expression in hepatocellular carcinomas with poor prognosis. *Br. J. Cancer* **2014**, *110*, 2708–2715. [CrossRef]
8. Correnti, M.; Cappon, A.; Pastore, M.; Piombanti, B.; Lori, G.; Oliveira, D.V.P.N.; Munoz-Garrido, P.; Lewinska, M.; Andersen, J.B.; Coulouarn, C.; et al. The protease-inhibitor SerpinB3 as a critical modulator of the stem-like subset in human cholangiocarcinoma. *Liver Int.* **2022**, *42*, 233–248. [CrossRef]
9. Ciscato, F.; Sciacovelli, M.; Villano, G.; Turato, C.; Bernardi, P.; Rasola, A.; Pontisso, P. SERPINB3 protects from oxidative damage by chemotherapeutics through inhibition of mitochondrial respiratory complex I. *Oncotarget* **2014**, *5*, 2418–2427. [CrossRef]
10. Wang, S.; Luke, C.J.; Pak, S.C.; Shi, V.; Chen, L.; Moore, J.; Andress, A.P.; Jayachandran, K.; Zhang, J.; Huang, Y.; et al. SERPINB3 (SCCA1) inhibits cathepsin L and lysoptosis, protecting cervical cancer cells from chemoradiation. *Commun. Biol.* **2022**, *5*, 46. [CrossRef]
11. Turato, C.; Buendia, M.A.; Fabre, M.; Redon, M.J.; Branchereau, S.; Quarta, S.; Ruvoletto, M.; Perilongo, G.; Grotzer, M.; Gatta, A. Over-expression of SERPINB3 in hepatoblastoma: A possible insight into the genesis of this tumour? *Eur. J. Cancer* **2012**, *48*, 1219–1226. [CrossRef] [PubMed]
12. Mao, J.; Wang, J.; Liu, B.; Pan, W.; Farr, G.H.; Flynn, C.; Yuan, H.; Takada, S.; Kimelman, D.; Li, L.; et al. Low-Density Lipoprotein Receptor-Related Protein-5 binds to axin and regulates the canonical Wnt signaling pathway. *Mol. Cell* **2001**, *7*, 801–809. [CrossRef] [PubMed]
13. Strickland, D.K.; Muratoglu, S.C.; Antalis, T.M. Serpin–Enzyme Receptors. *Meth. Enzymol* **2011**, *499*, 17–31. [CrossRef]
14. Tian, Y.; Wang, C.; Chen, S.; Liu, J.; Fu, Y.; Luo, Y. Extracellular Hsp90α and clusterin synergistically promote breast cancer epithelial-to-mesenchymal transition and metastasis via LRP1. *J. Cell Sci.* **2019**, *132*, jcs228213. [CrossRef] [PubMed]
15. Fasolato, S.; Ruvoletto, M.; Nardo, G.; Rasola, A.; Sciacovelli, M.; Zanus, G.; Turato, C.; Quarta, S.; Terrin, L.; Fadini, G.P.; et al. Low P66shc with high SerpinB3 levels favors necroptosis and better survival in hepatocellular carcinoma. *Biology* **2021**, *10*, 363. [CrossRef]
16. Turato, C.; Biasiolo, A.; Pengo, P.; Frecer, V.; Quarta, S.; Fasolato, S.; Ruvoletto, M.; Beneduce, L.; Zuin, J.; Fassina, G.; et al. Increased antiprotease activity of the SERPINB3 polymorphic variant SCCA-PD. *Exp. Biol. Med.* **2011**, *236*, 281–290. [CrossRef]
17. Albiero, M.; Fullin, A.; Villano, G.; Biasiolo, A.; Quarta, S.; Bernardotto, S.; Turato, C.; Ruvoletto, M.; Fadini, G.P.; Pontisso, P.; et al. Semisolid wet Sol–Gel Silica/Hydroxypropyl methyl cellulose formulation for slow release of Serpin B3 promotes wound healing in vivo. *Pharmaceutics* **2022**, *14*, 1944. [CrossRef]
18. Turato, C.; Scarpa, M.; Kotsafti, A.; Cappon, A.; Quarta, S.; Biasiolo, A.; Cavallin, F.; Trevellin, E.; Guzzardo, V.; Fassan, M.; et al. Squamous Cell Carcinoma Antigen 1 is associated to poor prognosis in esophageal cancer through immune surveillance impairment and reduced chemosensitivity. *Cancer Sci.* **2019**, *110*, 1552–1563. [CrossRef]
19. Emami, K.H.; Nguyen, C.; Ma, H.; Kim, D.H.; Jeong, K.W.; Eguchi, M.; Moon, R.T.; Teo, J.-L.; Oh, S.W.; Kim, H.Y.; et al. A small molecule inhibitor of β-catenin/cyclic AMP response element-binding protein transcription. *Proc. Natl. Acad. Sci. USA* **2004**, *101*, 12682–12687. [CrossRef]

20. Foglia, B.; Sutti, S.; Cannito, S.; Rosso, C.; Maggiora, M.; Autelli, R.; Novo, E.; Villano, M.; Ramavat, N.N.; Younes, R.; et al. Hepatocyte-specific deletion of HIF2α prevents NASH-related liver carcinogenesis by decreasing cancer cell proliferation. *Cell Mol. Gastgroenterol. Hepatol.* **2022**, *13*, 459–482. [CrossRef]
21. Morello, E.; Sutti, S.; Foglia, E.; Novo, E.; Cannito, S.; Bocca, C.; Rajsky, M.; Bruzzì, S.; Abate, M.L.; Rosso, C.; et al. Hypoxya-inducible factor 2α drives nonalcoholic fatty liver disease progression by triggering hepatocyte release of histidine-rich glycoprotein. *Hepatology* **2018**, *67*, 2196–2214. [CrossRef] [PubMed]
22. Novo, E.; Cappon, A.; Villano, G.; Quarta, S.; Cannito, S.; Bocca, C.; Turato, C.; Guido, M.; Maggi, M.; Protopapa, F.; et al. SerpinB3 as a pro-inflammatory mediator in the progression of experimental non-alcoholic fatty liver disease. *Front. Immunol.* **2022**, *13*, 910526. [CrossRef] [PubMed]
23. Juric, V.; Ruffell, B.; Evason, K.J.; Hu, J.; Che, L.; Wang, L.; Chen, X.; Bishop, M.J. Monocyte-dependent liver injury promotes carcinogenesis in an oncogene-specific manner. *J. Hepatol.* **2016**, *64*, 881–890. [CrossRef] [PubMed]
24. Liu, J.; Xiao, Q.; Xiao, J.; Niu, C.; Li, Y.; Zhang, X.; Zhou, Z.; Shu, G.; Yin, G. Wnt/β-catenin signalling: Function, biological mechanisms, and therapeutic opportunities. *Signal Transduct. Target. Ther.* **2022**, *7*, 3. [CrossRef] [PubMed]
25. Tamai, K.; Semenov, M.; Kato, Y.; Spokony, R.; Liu, C.; Katsuyama, Y.; Hess, F.; Saint-Jeannet, J.-P.; He, X. LDL-Receptor-Related Proteins in Wnt signal transduction. *Nature* **2000**, *407*, 530–535. [CrossRef]
26. Cannito, S.; Turato, C.; Paternostro, P.; Biasiolo, A.; Colombatto, S.; Cambieri, I.; Quarta, S.; Novo, E.; Morello, E.; Rovida, E.; et al. Hypoxya up-regulates SERPINB3 through HIF-2a in human liver cancer cells. *Oncotarget* **2015**, *6*, 2206–2221. [CrossRef]
27. Bu, G. The roles of Receptor-Associated Protein (RAP) as a molecular chaperone for members of the LDL receptor family. *Int. Rev. Cytol.* **2001**, *209*, 79–116. [CrossRef]
28. Joslin, G.; Fallon, R.J.; Bullock, J.; Adams, S.P.; Perlmutter, D.H. The SEC receptor recognizes a pentapeptide neodomain of alpha 1-antitrypsin-protease complexes. *J. Biol. Chem.* **1991**, *266*, 11282–11288. [CrossRef]
29. Toldo, S.; Austin, D.; Mauro, A.G.; Mezzaroma, E.; Van Tassell, B.W.; Marchetti, C.; Carbone, S.; Mogelsvang, S.; Gelber, C.; Abbate, A. Low-Density Lipoprotein Receptor–Related Protein-1 is a therapeutic target in acute myocardial infarction. *JACC Basic Transl. Sci.* **2017**, *2*, 561–574. [CrossRef]
30. Chiu, I.-J.; Hsu, Y.-H.; Chang, J.-S.; Yang, J.-C.; Chiu, H.-W.; Lin, Y.-F. Lactotransferrin Downregulation Drives the Metastatic Progression in Clear Cell Renal Cell Carcinoma. *Cancers* **2020**, *12*, 847. [CrossRef]
31. Fayard, B.; Bianchi, F.; Dey, J.; Moreno, E.; Djaffer, S.; Hynes, N.E.; Monard, D. The Serine Protease Inhibitor Protease Nexin-1 controls mammary cancer metastasis through LRP-1–mediated MMP-9 expression. *Cancer Res.* **2009**, *69*, 5690–5698. [CrossRef] [PubMed]

4.4 ONCOSTATIN M (OSM) CAN MODULATE NOTCH SIGNALING IN NAFLD PROGRESSION (PRELIMINARY STUDY - UNPUBLISHED)

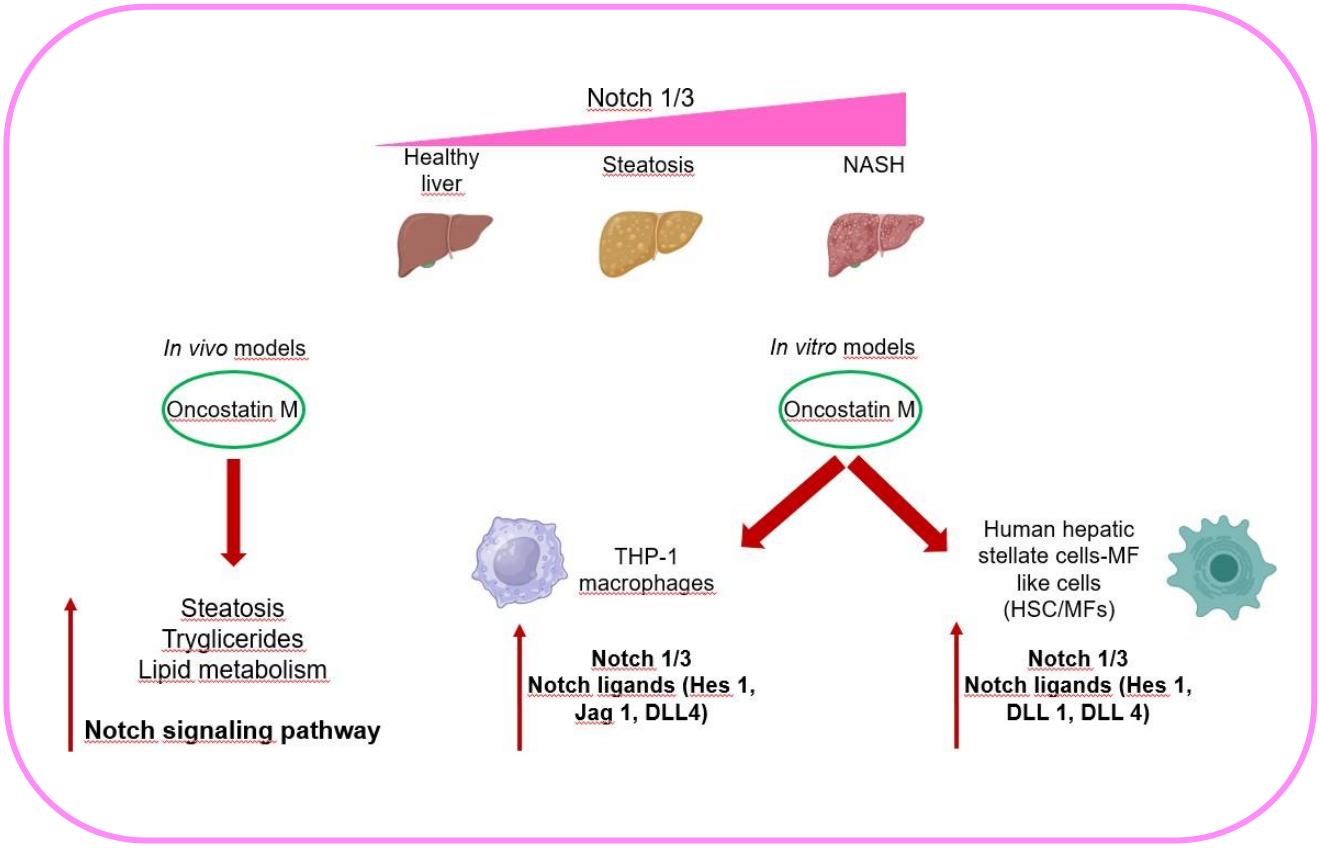

In the scenario of progressive NAFLD, OSM, a pleiotropic cytokine structurally and functionally related to the interleukin-6 (IL-6) cytokine family, orchestrate hypoxia-modulated hepatic processes involving the hypoxia-inducible factor 1 (HIF-1) (Foglia et al., 2019). This cytokine can signal through 2 different heterodimeric receptors that share gp130 (a common subunit receptor for ligands of IL-6 family) and involves either leukemia inhibitor factor receptor β (LIFRβ) or OSM receptor β (OSMRβ). OSM has been suggested to be involved also in the pathogenesis of steatosis and hepatic insulin resistance (Komori T et al., 2014). From literature data it is known that OSM can reduce cardiac injury by activating Notch signaling and in OSMRβ/KO mice myocardial injury has been reported to be exacerbated when Notch signalling is reduced (Zhang et al., 2015). Since recent data suggest the role of Notch in NASH progression (Xu and Wang, 2021), we decided to analyze whether Notch was involved in OSM action both *in vivo* and *in vitro*.

To this aim, we first assessed the extent of liver injury on liver specimens obtained from wild type mice (WT) and from mice genetically manipulated in order to delete the OSMRβ (KO/OSMRβ) fed or not with a lipogenic diet (choline-deficient aminoacid refined or CDAA) for 26 weeks. As expected, CDAA diet induced liver steatosis in WT mice, whereas in KO/OSMRβ mice a significant reduction of this parameter was observed, as showed by Hematoxylin-Eosin histological staining (Figure 1).

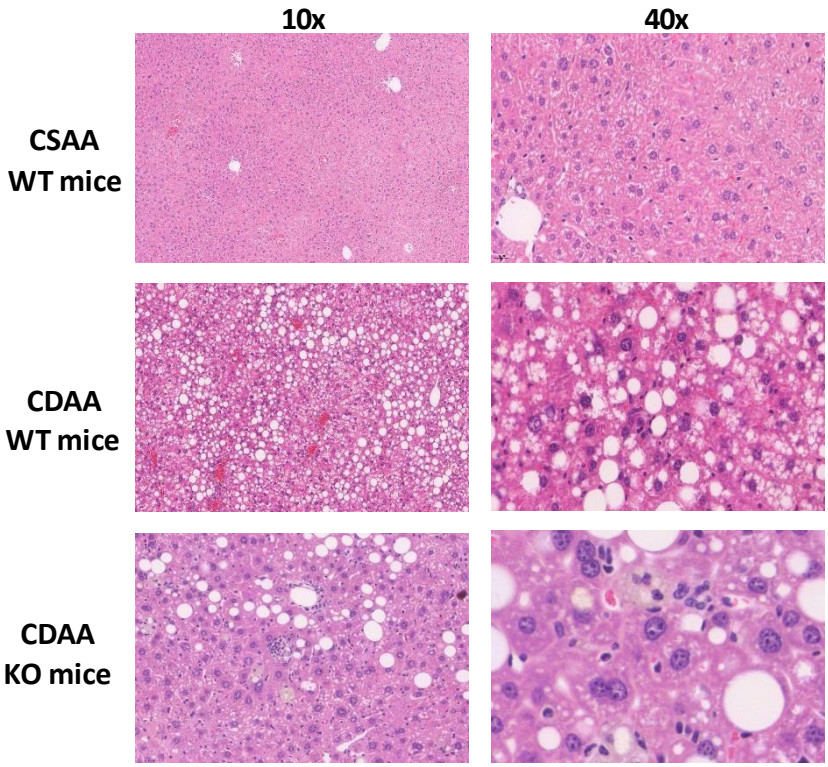

Figure 1. Evaluation of steatosis and inflammation by means of Hematoxilyn and Eosin staining in WT and KO/OSMRβ mice fed on CDAA diet (lipogenic diet) for 26 weeks.

Liver steatosis, which is typical of NAFLD, is due to triglycerides accumulation that could be seen as a form of surplus energy accumulation and as a result of deficient liver storage in white adipose tissue. Based on this knowledge, we performed triglycerides quantification on liver specimens obtained from our different mice models. This analysis showed that in KO/OSMRβ mice fed on control diet triglycerides accumulation is reduced as compared to WT mice fed on the same diet (p=0,0025) (Figure 2); in WT mice fed on lipogenic CDAA diet the accumulation of triglycerides significantly increases as compared to WT mice fed on control diet (p<0,001), while in KO/OSMRβ mice fed on CDAA triglycerides accumulation is reduced as compared to WT mice fed on the same diet (p=0,0031). (Figure 2). These data confirm the potential role of OSM in regulating the triglycerides accumulation and steatosis.

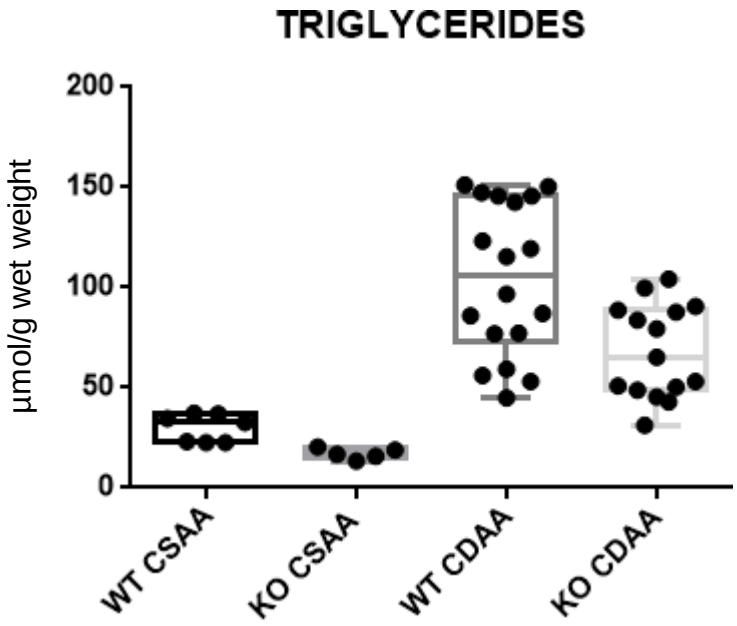

Figure 2. Triglycerides quantification from homogenized liver tissue (50mg) of WT and KO/OSMRβ mice fed on CDAA diet (lipogenic diet) or CSAA diet (control diet) for 26 weeks.

Along these lines, we focused our attention on lipid metabolism in order to confirm that OSM is directly involved in regulating this important feature of chronic liver disease. RT-PCR analysis was performed on liver specimens of mice models to evaluate the transcript levels of principal genes of lipid metabolism, CD36, involved in fatty acid up-take, carnitine palmytoil transferase 1 (Cpt1) and medium-chain acyl-CoA dehydrogenase (MCAD) important in fatty acid oxidation (Figure 3).

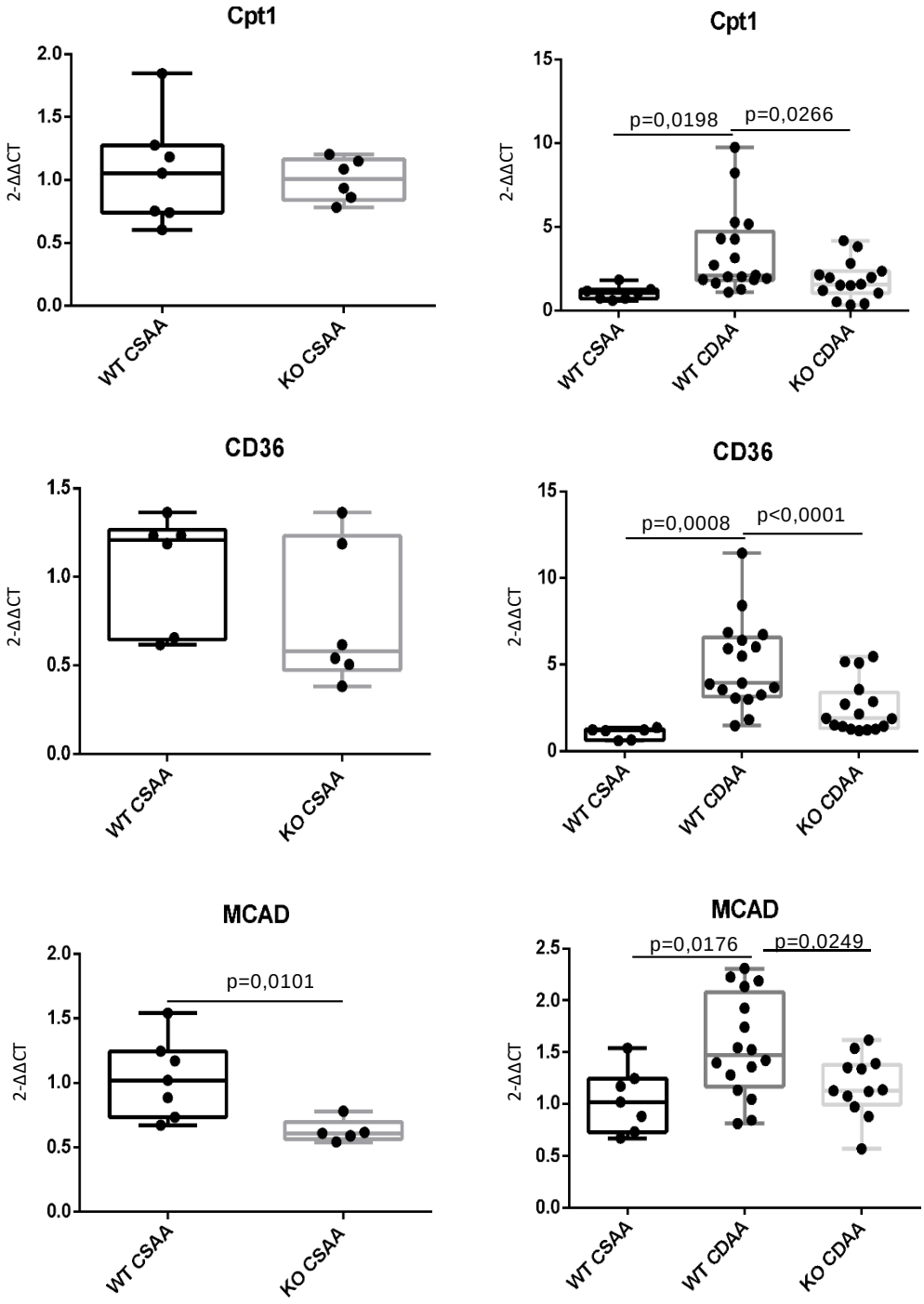

Figure 3. Analysis of transcript levels of lipid metabolism by means of quantitative real time PCR in WT and KO/OSMRβ mice fed on CDAA diet (lipogenic diet) or CSAA diet (control diet) for 26 weeks.

Our results indicate that in OSMRβ/KO mice fed on CDAA all the transcript levels of the investigated genes are reduced as compared to WT mice fed on the same diet, suggesting that OSM may have a key role also in regulating lipid metabolism in our experimental models.

Literature data suggest that the NOTCH signaling pathway is involved in different aspects of NAFLD (Xu and Wang 2022), like inflammation and fibrogenesis (Valenti et al, 2013; Zhu et al, 2018), insulin resistance (Bernsmeier et al, 2016) and lipid metabolism (Li et al, 2019; Ding et al 2020). Since OSM has been reported to activate Notch signaling pathway in cardiomyocytes (Zhang M et al., 2015), we decided to analyse whether OSM may modulate Notch signaling pathway in NASH settings.

As a first step, we performed RT-PCR analysis on liver samples obtained from WT mice and KO/ OSMRβ fed on CDAA diet or on the respective control diet (CSAA) to analyze gene expression of the different isoforms of Notch receptors and of the main ligands of Notch. We observed that in WT mice fed on CDAA there was an increase of Notch1, Notch3, Jag1, Hes1, Dll1 and Dll4, whereas all these genes were significantly down-regulated in KO/OSMRβ mice fed on CDAA diet (Figure 4 and Figure 5), indicating that Notch signaling pathway, increased in NASH, is reduced when OSMRβ is deleted. These results suggested that OSM may modulate Notch activity during NASH.

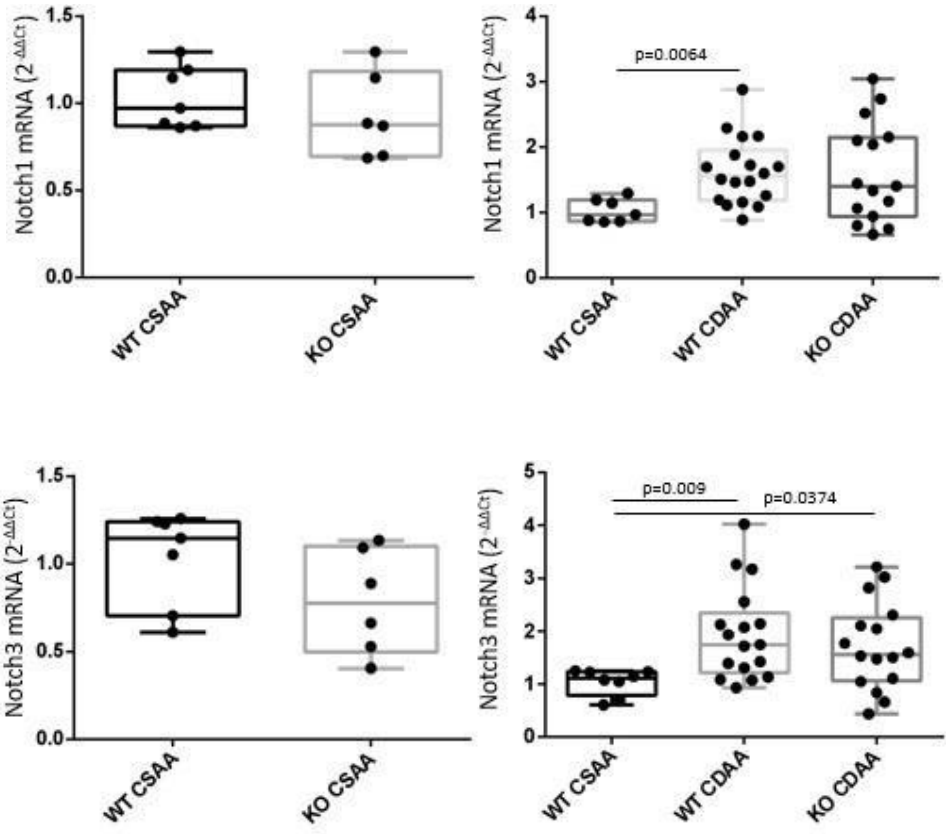

Figure 4. Analysis of transcript levels of Notch receptors (Notch1 and 3) by means of quantitative real time PCR in WT and KO/OSMRβ mice fed on CDAA diet (lipogenic diet) or CSAA diet (control diet) for 26 weeks.

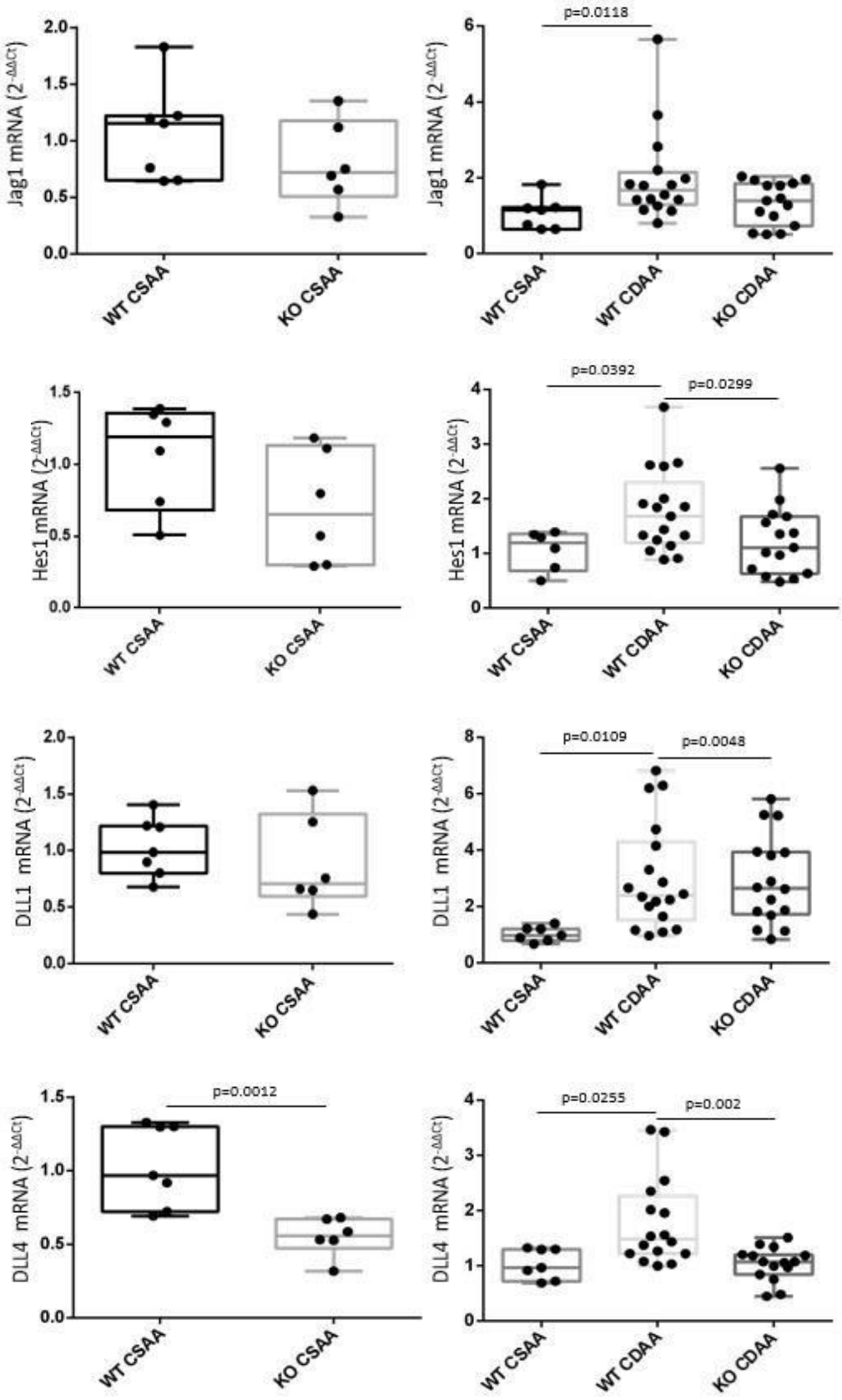

Figure 5. Analysis of transcript levels of Notch ligands (Jag1, Hes1, DLL1 and DLL4) by means of quantitative real time PCR in WT and KO/OSMRβ mice fed on CDAA diet (lipogenic diet) or CSAA diet (control diet) for 26 weeks.

In vivo we have also observed a significant positive correlation between the expression of OSM and of Notch receptor isoforms and ligands, especially for Notch1, Notch3, Hes1, Dll1 and Jag1 (Figure 6 and Figure 7).

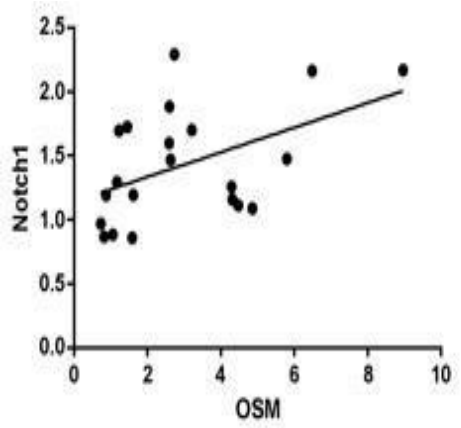

Spearman r	
r	0,4364
95% confidence interval	-0,008012 to 0,7368
P value	
P (two-tailed)	0,0480
P value summary	*
Exact or approximate P value?	Approximate
Significant? (alpha = 0.05)	Yes

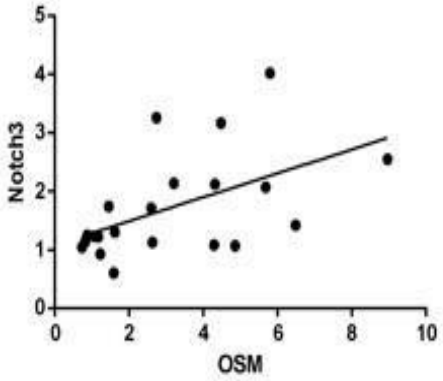

Spearman r	
r	0,5519
95% confidence interval	0,1444 to 0,7994
P value	
P (two-tailed)	0,0095
P value summary	**
Exact or approximate P value?	Approximate
Significant? (alpha = 0.05)	Yes

Figure 6. Correlation between the expression of OSM and Notch receptor isoforms.

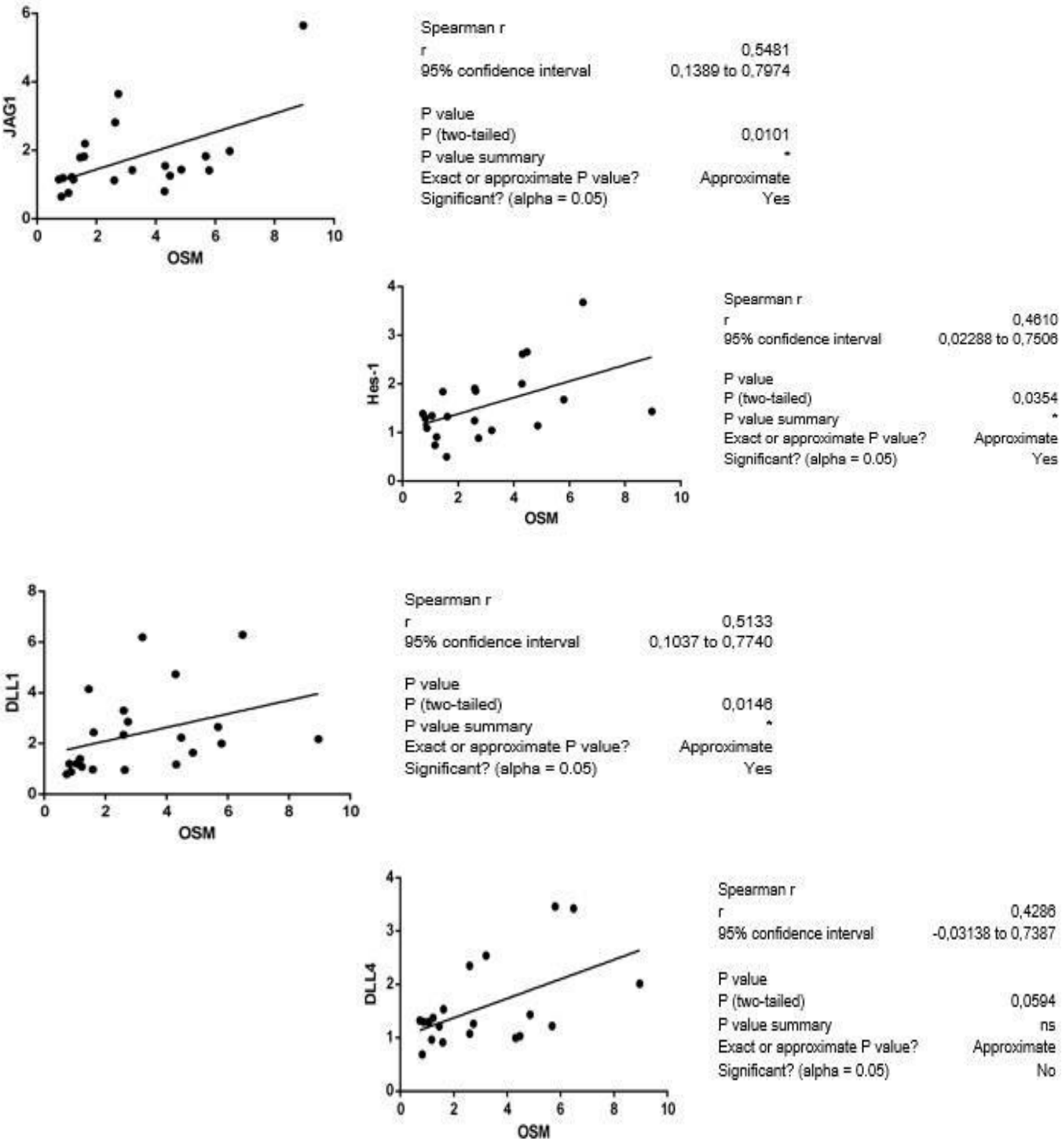

Figure 7. Correlation between the expression of OSM and Notch related ligands.

Since OSM has been shown to operate as a pro-inflammatory and a pro-fibrogenic mediator during the progression of NASH (Matsuda et al., 2018; Foglia et al., 2019), we further investigated whether OSM was also implicated in the modulation of Notch signaling in THP-1 differentiated macrophages and human hepatic stellate cells-MF like cells (HSC/MFs).

In particular, we exposed THP-1 differentiated macrophages and HSC/MFs to human recombinant OSM (10 ng/ml) at different time points (from 1hr up to 24 hrs) to evaluate, by means of quantitative RT-PCR, the transcript levels of different genes playing a role in Notch signaling. We observed an OSM-dependent up-regulation of Notch 1, Notch 3, Jag1 and Dll4 in THP1 differentiated macrophages (Figure 8) and of Notch 1, Notch 3, Dll1 and Dll4 in HSC/MFs (Figure 9).

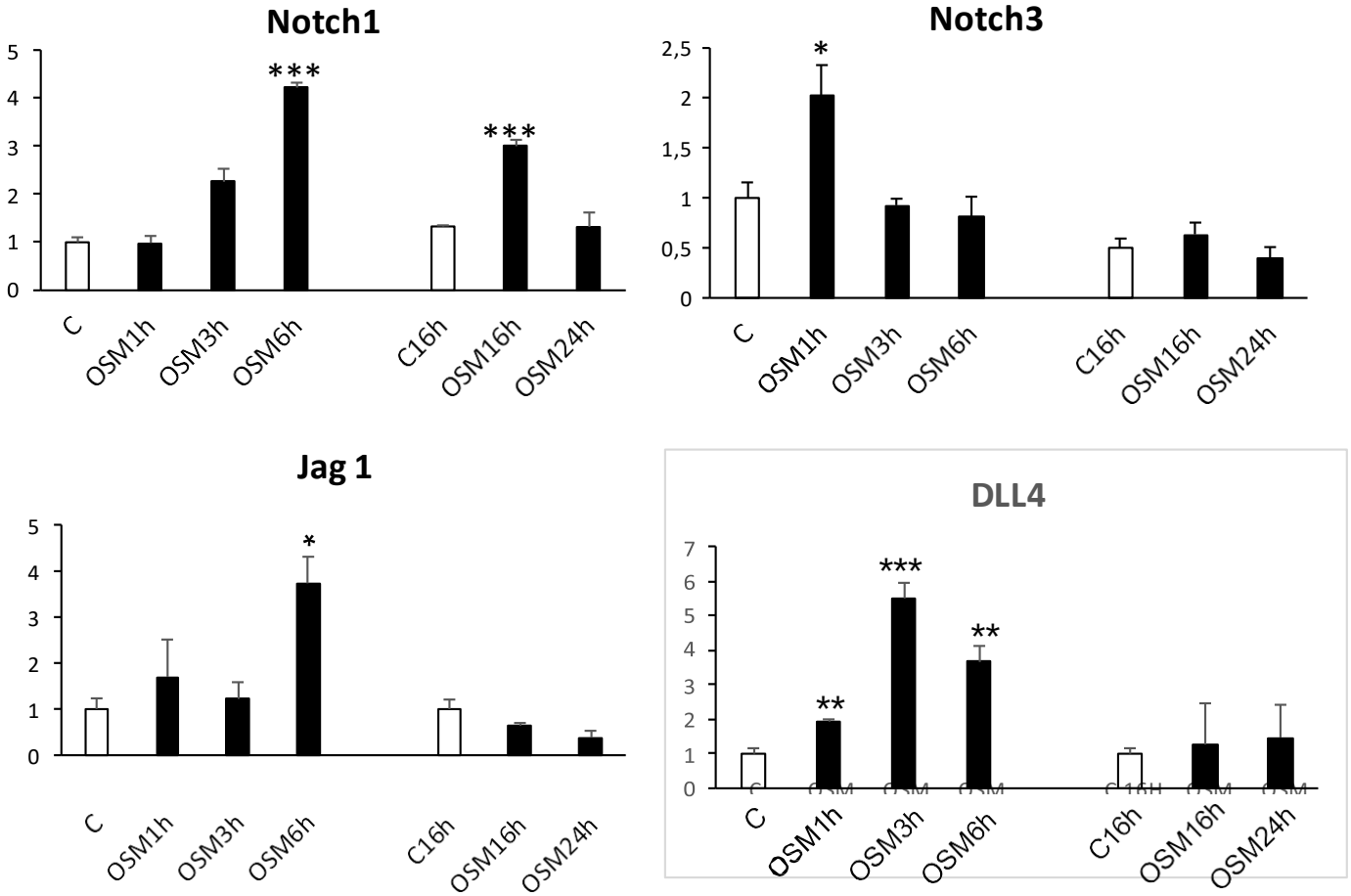

Figure 8. Analysis of transcript levels of Notch receptors and Notch ligands by means of quantitative real time PCR in THP-1 differentiated exposed to OSM 10 ng/ml at different time points or in un-treated cells (C). * $p < 0.05$ ** $p < 0.0$ and *** $p < 0.001$ versus C.

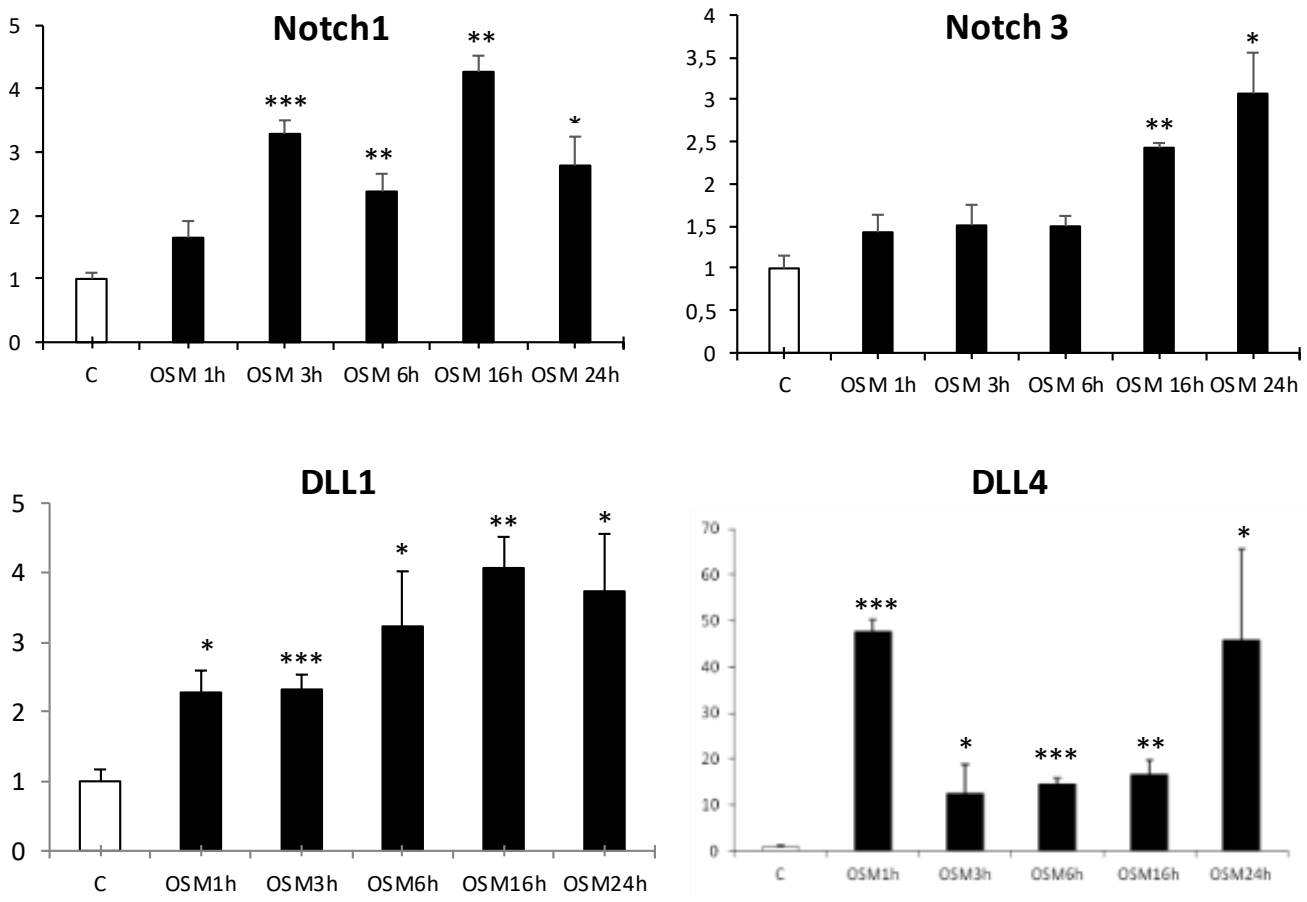

Figure 9. Analysis of transcript levels of Notch receptors and Notch ligands by means of quantitative real time PCR in HSC/MFs exposed to OSM 10 ng/ml at different time points or in un-treated cells (C). * p< 0.05, ** p< 0.01, *** p< 0.001 versus C.

Preliminary data obtained from western blot analysis showed also an increase of Notch1 in terms of protein levels in THP-1 differentiated macrophages exposed to OSM 10ng/ml starting from 3 hrs up to 24 hrs, whereas in HSC/MFs no significant change for Notch1 protein levels was appreciated (Figure 10).

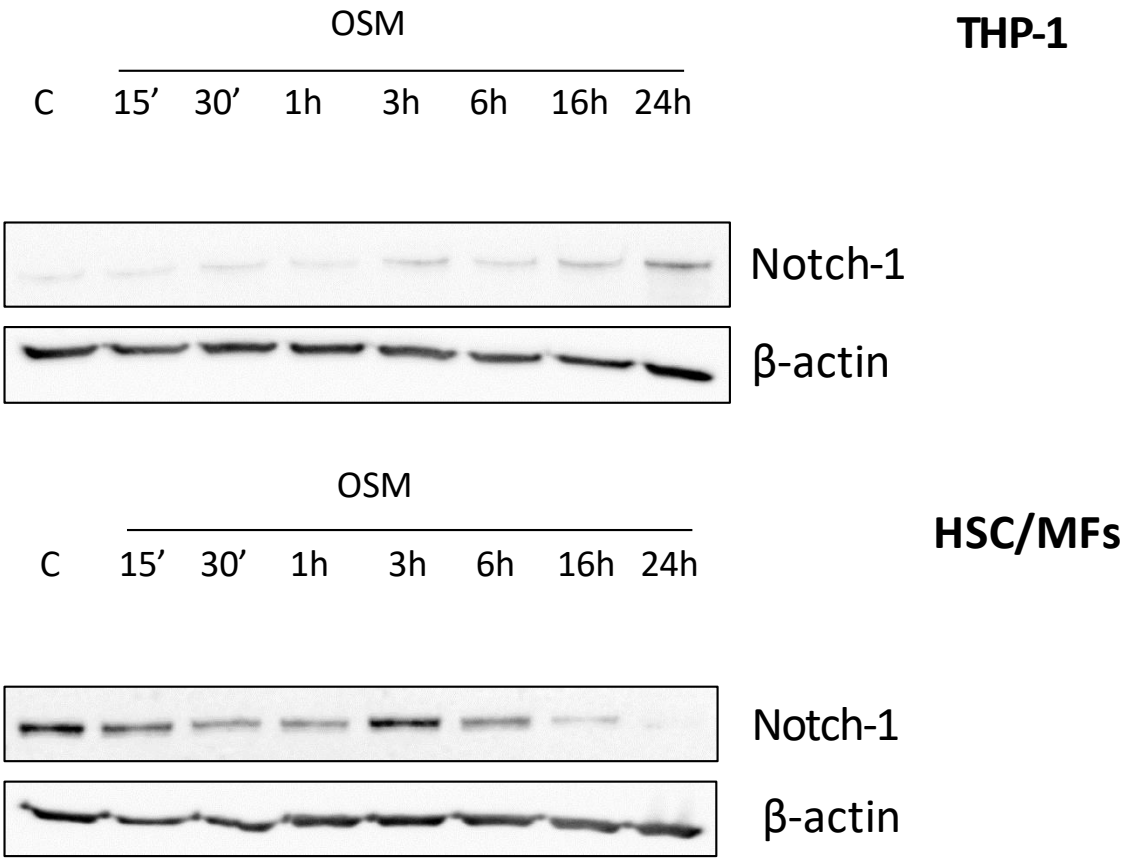

Figure 10. Analysis of protein levels of the receptor Notch-1 receptors by means of western blotting analysis in THP-1 differentiated macrophages and in HSC/MFs exposed to OSM 10 ng/ml at different time points or in un-treated cells (C). Equal loading was confirmed by re-probing the same membranes with β-actin

Data related to protein expression of the other different forms of Notch receptors as wells as of Notch ligands will be the object of future studies.

The preliminary data obtained *in vivo and in vitro* seem to suggest that OSM/Notch axis has a possible role in modulating NAFLD/NASH progression; of course, more experiments are needed to further support and detail this hypothesis.

DISCUSSION

SerpinB3 (SB3), a protein belonging to the serine-protease inhibitor family, is regulated by hypoxia through the hypoxia-inducible factor hypoxia -2α (HIF-2α) and is a mediator involved in the progression of CLDs and in the development of HCC (Cannito et al., 2015; Pontisso, 2014). In 2017 Novo and colleagues confirmed the production of this mediator by hepatic parenchymal cells and also its important role in modulating pro-fibrogenic responses of hepatic myofibroblasts and promoting hepatic fibrogenesis. In particular, mice genetically manipulated to over-express human SB3 (TG/SB3) in hepatocytes and fed on lipogenic diets showed an increase in collagen deposition as related to their controls. Moreover, this models presented significantly increased levels of pro-fibrogenic genes as compared to wild-type mice. *In vitro* studies carried out on human hepatic stellate cells (HSCs) or human stellate cell line (LX2) exposed to human recombinant SB3 confirmed that the addition of SB3 up-regulated the expression of genes involved in fibrogenesis and promoted oriented migration. Based on these literature data and considering that in the scenario of NAFLD/NASH progression an important role is played also by inflammatory process that involved hepatic macrophages, important to sustain lobular inflammation, we performed experiments both in *in vivo* and *in vitro* models in order to analyse whether SB3 could modulate also inflammatory process. As reported in paper n°1, mice were fed on two different diet protocols of murine NASH: methionine and choline deficient diet (MCD) for 8 weeks or choline deficient, L-amino acid defined diet (CDAA) for 12 weeks and the related control diets, methionine and choline supplemented (MCS) or choline-supplemented, L-amino acid defined (CSAA). TG/SB3 mice demonstrated an increase in macrophages infiltration, as crown-like aggregates and an up-regulation of trascript levels of pro-inflammatory genes, in particular TNF-α and IL-1β, as compared to wild-type mice fed on control diets. On the other hand, mice genetically manipulated in order to deplete SB3 expression (KO/SB3) presented a reduction in inflammatory infiltrate and a reduction in hepatic transcript levels of pro-inflammatory genes, like TNF-α, IL-1β and CCL-2. We also carried out experiments in *in vitro* models on human monocytes from peripheral blood and on undifferentiated human THP-1 cells. Both the models were exposed to human recombinant SB3 (hrSB3) at different time point in order to analyse the role of SB3 in modulating inflammatory pathway. We observed a significant up-regulation of TNF-α, IL-1β and IL-12, important markers of inflammation. Next, we evaluated the role of hr SB3 on THP-1 cells differentiated to macrophages after 48 hours of incubation with 50 nM phorbol-12-myristate-13-acetate (PMA). The exposition of cells to hrSB3 determined both the up-regulation of transcript levels and an increased protein levels of TNF-α and IL-1β, related to pro-inflammatory profile of macrophages. Interestingly, there

were also up-regulation of transcipt levels and increased protein levels of TGF- β and VEGF, related to pro-fibrogenic profile of macrophages. Then, we studied the involvement of hrSB3 in regulating NF-κB transcription factor; we observed that in differentiated THP-1 hrSB3 induced pro-inflammatory and ROS production by up-regulating NF-κB. Literature data suggest also the involvement of NASH-associated macrophages (NAM) in forming crown-like aggregated during NASH progression. Based on this knowledge, we investigated the action of SB3 in modulation of genes related to NAM: transcript levels of TREM2, CD9 and Galectin3 were up-regulated in TG/SB3 models.

In order to deeply investigate the involvement of SB3 in NAFLD/NASH progression, we studied a small molecule patented and proposed as SB3 inhibitor: 1-Piperidine Propionic Acid (1-PPA) (Toshihiko, 2009; Pontisso, 2018). During this year, Chinellato and colleagues (2023) found also that 1-PPA sterically inhibit the protease activated receptor 2 (PAR2), a cell surface sensor of extracellular inflammatory and coagulation proteases, recognized as a new regulator of hepatic metabolism (Rana et al., 2019; Shearer et al., 2022). In particular, PAR2 is important for cholesterol homeostasis and lipid metabolism, for suppressing glucose internalization, glycogen storage and insuline signaling (Shearer et al., 2022). As described in paper n°2, we analysed the role of 1-PPA on principal hallmarks (steatosis, inflammation and fibrosis) of progressive NASH, by using both *in vivo* and *in vitro* models. *In vivo* we used parallel groups of mice models: TG/SB3 and KO/SB3 mice and related controls fed on lipogenic diets CDAA or MCD for 12 weeks and 8 weeks respectively and TG/SB3 and related controls models fed on CDAA diet and injected weekly with 1-PPA (70 ng/g) or with vehicle alone. As expected, TG/SB3 mice fed on lipogenic diets showed an increase in inflammatory infiltrate and an up-regulation of TNF-α and IL-1β, confirming data obtained also in paper n°1. Based on this knowledge, we performed experiments on mice injected with 1-PPA and fed on CDAA diet and we observed a significant reduction in inflammatory infiltrate and a reduction of IL-1β and TNF-α transcript levels. Since in paper n°1 we observed an involvement of SB3 in modulating NASH-associated macrophages, we analyzed whether 1-PPA may be able to modulate the expression of NAMs markers (TREM-2, CD9, Gal-3). Interestingly, 1-PPA significantly reduced the transcript levels of TREM-2, CD9, Gal-3 in TG/SB3 mice fed on lipogenic diet. Moreover, data obtained in TG/SB3 mice fed on CDAA diet with the admistration of 1-PPA showed a reduction in infiltration of macrophages and IL-1β and TNF-α transcript levels. Then, we analyzed also the role of 1-PPA in fibrogenesis. The administration of 1-PPA in TG/SB3 mice fed on lipogenic diets resulted in both down-regulation α-SMA, Col1 A1 and TGF-β1 and of steatosis levels and

collagen deposition. *In vitro* experiments were carried out on LX2 cells and THP-1 cells exposed to human recombinant SB3 (hrSB3) after treating with 1-PPA inhibitor. Also these results indicated that 1-PPA down-regulated transcript levels of important genes, such as Col1 A1, α-SMA, CCL-2, VEGF, TNF-α, IL-1β and TGF-β. Concerning the mechanism of action of 1-PPA, Chinellato and colleagues (2023) have reported that 1-PPA binds PAR2 in an allosteric pocket of the receptor inactive conformation, with antagonistic activity. We performed experiments in order to understand whether the interaction between 1-PPA and SB3 is direct, but different biochemical approaches provided negative results. Based on this findings, we analysed the effect of 1-PPA on C/EBP-β, identified as SB3 transcription factor up-regulated in presence of SB3. Literature data suggest that C/EBP-β is involved in processes related to metabolic syndrome (van der Krieken et al., 2015). C/EBP-β, as PAR2 and SB3, is activated in pro-inflammatory conditions and ER stress, as confirmed with data obtained in KO/SB3 mice fed on lipogenic diets that presented a lower inflammatory response, while TG/SB3 mice showed opposite results that presented higher C/EBP-β levels related to controls. Of interest, we observed also that 1-PPA was able to suppress PAR2 and SB3 and also C/EBP- β transcription in hepatoma cells transfected in order to over-express SB3. Based on that it's possible to conclude that PAR2-C/EBP- β/SB3 axis is important to regulate the progression of NAFLD/NASH.

Concerning the paper n°3, we based our experiments starting from the knowledge that SB3 is not detectable in normal adult hepatocytes, wherease chronically damaged hepatocyte express SB3 and, in particular, in HCC the levels of SB3 are the highest (Turato et al., 2014). Data from literature suggest also that SB3 increases cell proliferation both through the induction of β-catenin and Myc oncogene a downstream gene of the Wnt pathway (Turato et al., 2012). In this study we evaluated the role of SB3 in modulating Wnt pathway through *in vitro* and *in vivo* models. In particular, in primary human monocytes and in monocytic cells THP-1, the addition of SB3 increased cell lifespan, proliferation and acted as positive modulator of the Wnt pathway. SB3 induced an up-regulation of Wnt-1/7 and of β-catenin. In experimental carcinogenesis, KO mice presented a reduction in SB3 expression and also a decrease in β-catenin expression, confirming the role of SB3 in regulating the activation of Wnt pathway. To analyse deeply, we studied also LRP family members, important for Wnt activation: both LRP-5 and LRP-6 were up-regulated by SB3. Knowning that LRP-1 is another receptor that binds several protease complexed- serine protease inhibitors, we found that also this receptor is up-regulated by SB3. Moreover, by using 3D modeling and

computational analysis we observed that the binding site for SB3 could determine a stable interaction with LRP-1.

In the background of progressive NAFLD is also involved a pleiotropic cytokine, known as Oncostatin M (OSM) belonging to the IL-6 family of cytokines. Komori and colleagues in 2014 observed that OSM is involved in the pathogenesis of steatosis and hepatic insuline resistance. Moreover, literature data suggest that OSM reduces cardiac injury by modulating Notch signaling and in OSMRβ/KO mice myocardial injury Notch signaling is reduced and cardiac injury is exacerbated. Furthermore, in 2021 Xu and Wang observed that Notch is involved in NASH progression. Based on this knowledge we analysed the possible involvement of Notch in OSM action. *In vivo* models for OSMRβ/KO mice fed on CDAA diet we observed a significant reduction of TGs accumulation, while in WT mice fed on control diet the accumulation significantly increased, explaining the possible role of OSM in regulating TGs accumulation. Moreover, in OSMRβ/KO mice fed on CDAA diet the transcript levels of principal genes involved in lipid metabolism were down-regulated as compared to WT mice fed on the same diet. Based on that we can hypothesize that OSM has a key role in regulating lipid metabolism, important feature of NAFLD/NASH progression. In addition, Xu and Wang in 2022 explained that Notch signaling pathway is involved in other important aspects of NAFLD, like inflammation and fibrogenesis, insulin resistance, lipid metabolism (Valenti et al., 2013; Zhu et al., 2018; Bernsmeier et al., 2016; Li et al., 2019; Ding et al., 2020). Literature data suggest also that Notch signaling pathway is activated by OSM in cardiomyocytes, so we decided to study whether OSM could modulate Notch signaling pathway even in NASH progression. In vivo studies performed on KO/OSMRβ mice fed on CDAA diet demonstrated a significant down-regulation of Notch receptors (Notch 1 and Notch3) and of Notch ligands (Jag1, Hes1, Dll1 and Dll4), related to their controls. These findings indicate that during NASH progression Notch signaling is up-regulated, while is reduced when the receptor β of OSM is deleted. Based on these data we can suggest that OSM can modulate Notch signaling pathway during NASH. Literature data also suggest the role of OSM as an important mediator inflammation and fibrogenesis during NASH progression (Matsuda et al., 2018; Foglia et al., 2019). *In vitro* studies performed on THP-1 differentiated macrophages and human hepatic stellate cells-MF like cells (HSC/MFs) exposed to human recombinant OSM showed an up-regulation of Notch receptors (Notch1 and Notch3) and of Notch ligands (Jag1 and Dll4 in THP-1 and Dll1 and Dll4 in HSC/MFs). We obtained also preliminary date demonstrating an increased of protein levels of Notch1 in THP-1 differentiated macrophages exposed to OSM, but not important changes in

HSC/MFs were observed. Preliminary data obtained both *in vivo* and *in vitro* may suggest that OSM/Notch axis could modulate NASH progression. At present additional *in vivo* and *in vitro* experiments are ongoing in order to further investigate in detail this hyphotesis.

In conclusion, data presented in this thesis fully support the concept that SB3 and OSM can act as mediators able to significantly modulate NAFLD/NASH progression.

REFERENCES

Abul-Husn, N.S., Cheng, X., Li, A.H., Xin, Y., Schurmann, C., Stevis, P., Liu, Y., Kozlitina, J., Stender, S., Wood, G.C., Stepanchick, A.N., Still, M.D., McCarthy, S., O'Dushlaine, C., Packer, J.S., Balasubramanian, S., Gosalia, N., Esopi, D., Kim, S.Y., Mukherjee, S., Lopez, A.E., Fuller, E.D., Penn, J., Chu, X., Luo, J.Z., Mirshahi, U.L., Carey, D.J., Still, C.D., Feldman, M.D., Small, A., Damrauer, S.M., Rader, D.J., Zambrowicz, B., Olson, W., Murphy, A.J., Borecki, I.B., Shuldiner, A.R., Reid, J.G., Overton, J.D., Yancopoulos, G.D., Hobbs, H.H., Cohen, J.C., Gottesman, O., Teslovich, T.M., Baras, A., Mirshahi, T., Gromada, J., Dewey, F.E., 2018. A Protein-Truncating HSD17B13 Variant and Protection from Chronic Liver Disease. N. Engl. J. Med. 378, 1096-1106. Doi: 10.1056/NEJMoa1712191.

Adams, L.A., Lymp, J.F., St Sauver, J., Sanderson, S.O., Lindor, K.D., Feldstein, A., and Angulo, P., 2005. The natural history of nonalcoholic fatty liver disease: a population-based cohort study. Gastroenterology 129, 113–121. Doi: 10.1053/j.gastro.2005.04.014.

Albano, E., Mottaran, E., Vidali, M., Reale, E., Saksena, S., Occhino, G., Burt, A.D., Day, C.P. 2005. Immune response toward lipid peroxidation products as a predictor of the progression of non- alcoholic fatty liver disease (NAFLD) to advanced fibrosis. Gut 54, 987-993. Doi: 10.1136/gut.2004.057968.

Alegre, F., Pelegrin, P., Feldstein, A.E., 2017. Inflammasomes in liver fibrosis. Semin. Liver Dis. 37, 119-127. Doi: 10.1055/s-0037-1601350.

American Association for the Study of the Liver, 2015. AASLD/IDSA HCV Guidance Panel. Hepatitis C guidance: AASLD/IDSA recommendations for testing, managing, and treating adults infected with hepatitis C virus. Hepatology 62, 932–954. Doi: 10.1002/hep.27950.

Amir, M., Czaja, M.J., 2011. Autophagy in nonalcoholic steatohepatitis. Expert Rev. Gastroenterol. Hepatol. 5, 159-166. Doi: 10.1586/egh.11.4.

Anstee, Q.M., Seth, D., Day, C.P., 2016. Genetic Factors That Affect Risk of Alcoholic and Nonalcoholic Fatty Liver Disease. Gastroenterology 150,1728-1744. Doi: 10.1053/j.gastro.2016.01.037.

Arndtz, K., Hirschfield, G.M., 2016. The Pathogenesis of Autoimmune Liver Disease. Dig Dis. 34, 327-333. Doi: 10.1159/000444471.

Arrese, M., Arab, J.P., Barrera, F., Kaufmann, B., Valenti, L., Feldstein, A.E., 2021. Insights into Nonalcoholic Fatty-Liver Disease Heterogeneity. Semin. Liver Dis. 41,421-434. Doi: 10.1055/s-0041-1730927.

Asahina, K., Tsai, S.Y., Li, P., Ishii, M., Maxson, R.E., Jr., Sucov, H.M., Tsukamoto, H., 2009. Mesenchymal origin of hepatic stellate cells, submesothelial cells, and perivascular mesenchymal cells during mouse liver development. Hepatology 49, 998-1011. Doi: 10.1002/hep.22721.

Asahina, K., Zhou, B., Pu, W.T., Tsukamoto, H., 2011. Septum transversum- derived mesothelium gives rise to hepatic stellate cells and perivascular mesenchymal cells in developing mouse liver. Hepatology 53, 983-995. Doi: 10.1002/hep.24119.

Asgharpour, A., Dinani, A., Friedman, S.L., 2021. Basic science to clinical trials in non-alcoholic fatty liver disease and alcohol-related liver disease: collaboration with industry. Transl. Gastroenterol. Hepatol. 6, 5. Doi:10.21037/tgh.2020.01.04.

Banales, J.M., Huebert, R.C., Karlsen, T., Strazzabosco, M., LaRusso, N.F., Gores, G.J., 2019. Cholangiocyte pathobiology, Nat. Rev. Gastroenterol. Hepatol. 16, 269-281. Doi: 10.1038/s41575-019-0125-y.

Barnes, R.C., Worrall, D.M., 1995. Identification of a novel human serpin gene; cloning sequencing and expression of leupin. FEBS Lett. 373:61-65. Doi: 10.1016/0014-5793(95)01015-7.

Barrow, F., Khan, S., Fredrickson, G., Wang, H., Dietsche, K., Parthiban, P., Robert, S., Kaiser, T., Winer, S., Herman, A., Adeyi, O., Mouzaki, M., Khoruts, A., Hogquist, K.A., Staley, C., Winer, D.A., Revelo, X.S., 2021. Microbiota-driven activation of intrahepatic B cells aggravates NASH through innate and adaptive signaling. Hepatology 74, 704-722. Doi: 10.1002/hep.31755.

Beneduce, L., Castaldi, F., Marino, M., Quarta, S., Ruvoletto, M., Benvegnù, L., Calabrese, F., Gatta, A., Pontisso, P., Fassina, G., 2005. Squamous cell carcinoma antigen-immunoglobulin M complexes as novel biomarkers for hepatocellular carcinoma. Cancer.;103: 2558-65. Doi: 10.1002/cncr.21106.

Bhattacharjee, J., Kirby, M., Softic, S., Miles, L., Salazar-Gonzalez, R.M., Shivakumar, P., Kohli, R., 2017. Hepatic natural killer T-cell and CD8+ T-cell signatures in mice with nonalcoholic steatohepatitis. Hepatol. Commun. 1, 299-310. Doi: 10.1002/hep4.1041.

Biasiolo, A., Chemello, L., Quarta, S., Cavalletto, L., Bortolotti, F., Caberlotto, C., Beneduce, L., Bernardinello, E., Tono, N., Fassina, G., Gatta, A., Pontisso, P., 2008. Monitoring SCCA-IgM Complexes in Serum Predicts Liver Disease Progression in Patients With Chronic Hepatitis. J Viral Hep.; 15:246-49. Doi: 10.1111/j.1365-2893.2007.00935.x.

Biasiolo, A., Tono, N., Ruvoletto, M., Quarta, S., Turato, C., Villano, G., Beneduce, L., Fassina, G., Merkel, C., Gatta, A., Pontisso, P., 2012. IgM-Linked SerpinB3 and SerpinB4 in Sera of Patients With Chronic Liver Disease. PLoS One.; 7:e40658. Doi: 10.1371/journal.pone.0040658.

Blériot, C., Barreby, E., Dunsmore, G., Ballaire, R., Chakarov, S., Ficht, X., De Simone, G., Andreata, F., Fumagalli, V., Guo, W., Wan, G., Gessain, G., Khalilnezhad, A., Zhang, X.M., Ang, N., Chen, P., Morgantini, C., Azzimato, V., Kong, W.T., Liu, Z., Pai, R., Lum, J., Shihui, F., Low, I., Xu, C., Malleret, B., Kairi, M.F.M., Balachander, A., Cexus, O., Larbi, A., Lee, B., Newell, E.W., Ng, L.G., Phoo, W.W., Sobota, R.M., Sharma, A., Howland, S.W., Chen, J., Bajenoff, M., Yvan-Charvet, L., Venteclef, N., Iannacone, M., Aouadi, M., Ginhoux, F., 2021. A subset of Kupffer cells regulates metabolism through the expression of CD36. Immunity 54, 2101-2116. Doi: 10.1016/j.immuni.2021.08.006.

Blomhoff, R., Wake, K., 1991. Perisinusoidal stellate cells of the liver: important roles in retinol metabolism and fibrosis. FASEB J. 5, 271-277. Doi: 10.1096/fasebj.5.3.2001786.

Bocca, C., Novo, E., Miglietta, A., Parola, M., 2015. Angiogenesis and Fibrogenesis in Chronic Liver Diseases. Cell. Mol. Gastroenterol. Hepatol. 1, 477-488. Doi: 10.1016/j.jcmgh.2015.06.011.

Bocca, C., Protopapa, F., Foglia, B., Maggiora, M., Cannito, S., Parola, M., Novo, E., 2022. Hepatic Myofibroblasts: A Heterogeneous and Redox-Modulated Cell Population in Liver Fibrogenesis. Antioxidants (Basel) 11, 1278. Doi: 10.3390/antiox11071278.

Boursier, J., Mueller, O., Barret, M., Machado, M., Fizanne, L., Araujo-Perez, F., Guy, C.D., Seed, P.C., Rawls, J.F., David, L.A., Hunault, G., Oberti, F., Calès, P., Diehl, A.M., 2016. The severity of nonalcoholic fatty liver disease is associated with gut dysbiosis and shift in the metabolic function of the gut microbiota. Hepatology 63, 764-775. Doi: 10.1002/hep.28356.

Brennan, M.A., Cookson, B.T., 2000. Salmonella induces macrophage death by caspase-1-dependent necrosis. Mol. Microbiol. 38, 31-40. Doi: 10.1046/j.1365-2958.2000.02103.x.

Brown, G.T., McIntyre, T.M., 2011. Lipopolysaccharide signaling without a nucleus: kinase cascades stimulate platelet shedding of proinflammatory IL-1β-rich microparticles. J. Immunol. 186, 5489-5496. Doi: 10.4049/jimmunol.1001623.

Broz, P., Pelegrin, P., Shao, F., 2020. The gasdermins, a protein family executing cell death and inflammation. Nature Rev. Immunol. 20, 143-157. Doi:10.1038/s41577-019-0228-2.

Bruzzì, S., Sutti, S., Giudici, G., Burlone, M.E., Ramavath, N.N., Toscani, A., Bozzola, C., Schneider, P., Morello, E., Parola, M., Pirisi, M., Albano, E., 2018. B2-Lymphocyte responses to oxidative stress-derived antigens contribute to the evolution of non-alcoholic fatty liver disease (NAFLD). Free Radic. Biol. Med. 124, 249-259. Doi: 10.1016/j.freeradbiomed.2018.06.015.

Byass, P., 2014. The global burden of liver disease: a challenge for methods and for public health. BMC Med. 12, 159. Doi:10.1186/s12916-014-0159-5.

Cadamuro, M., Lasagni, A., Sarcognato, S., Guido, M., Fabris, R., Strazzabosco, M., Strain, A.J., Simioni, P., Villa, E., Fabris, L., 2022. The Neglected Role of Bile Duct Epithelial Cells in NASH. Semin. Liver Dis. 42, 34-47. Doi: 10.1055/s-0041-1739455.

Calabrese, F., Lunardi, F., Giacometti, C., Marulli, G., Gnoato, M., Pontisso, P., Saetta, M., Valente, M., Rea, F., Perissinotto, E., Agostini, C., 2008. Overexpression of squamous cell carcinoma antigen in idiopathic pulmonary fibrosis: clinicopathological correlations. Thorax. 63:795-802. Doi: 10.1136/thx.2007.088583.

Canbay, A., Feldstein, A.E., Higuchi, H., Werneburg, N., Grambihler, A., Bronk, S.F., Gores, G.J., 2003a. Kupffer cell engulfment of apoptotic bodies stimulates death ligand and cytokine expression. Hepatology 38, 1188-1198. Doi: 10.1053/jhep.2003.50472.

Canbay, A., Taimr, P., Torok, N., Higuchi, H., Friedman, S., Gores, G.J., 2003b. Apoptotic body engulfment by a human stellate cell line is profibrogenic. Lab. Invest. 83, 655-663. Doi: 10.1097/01.lab.0000069036.63405.5c.

Cannito, S., Dianzani, U., Parola, M., Albano, E., Sutti, S., 2023. Inflammatory processes involved in NASH-related hepatocellular carcinoma. Biosci. Rep. 43, BSR20221271. Doi: 10.1042/BSR20221271.

Cannito, S., Milani, C., Cappon, A., Parola, M., Strazzabosco, M., Cadamuro, M., 2018. Fibroinflammatory liver injuries as preneoplastic condition in cholangiopathies. Int. J. Mol. Sci.19, 3875. Doi:10.3390/ijms19123875.

Cannito, S., Morello, E., Bocca, C., Foglia, B., Benetti, E., Novo, E., Chiazza, F., Rogazzo, M., Fantozzi, R., Povero, D., Sutti, S., Bugianesi, E., Feldstein, A.E., Albano, E., Collino, M., Parola, M., 2017b. Microvesicles released from fat-laden cells promote activation of hepatocellular NLRP3 inflammasome: A pro-inflammatory link between lipotoxicity and non-alcoholic steatohepatitis. PLoS One 12(3):e0172575. Doi: 10.1371/journal.pone.0172575.

Cannito, S., Novo, E., Parola, M., 2017a. Therapeutic pro-fibrogenic signaling pathways in fibroblasts. Adv Drug Deliv Rev.121, 57-84. Doi:10.1016/j.addr.2017.05.017.

Cannito, S., Paternostro, C., Busletta, C., Bocca, C., Colombatto, S., Miglietta, A., Novo, E., Parola, M., 2014. Hypoxia, hypoxia-inducible factors and fibrogenesis in chronic liver diseases. Histol. Histopathol. 29:33-44. Doi: 10.14670/HH-29.33.

Cannito, S., Turato, C, Paternostro, C., Biasiolo, A., Colombatto, S., Cambieri, I., Quarta, S., Novo, E., Morello, E., Villano, G.M., Fasolato, S., Musso, T., David, E., Tusa, I., Rovida, E., Autelli, R., Smedile, A., Cillo, U., Pontisso, P., Parola, M., 2015. Hypoxia up-regulates SERPINB3 through HIF-2α in human liver cancer cells. Oncotarget.;6:2206-21. Doi: 10.18632/oncotarget.2943.

Carlos, D., Costa, F.R., Pereira, C.A., Rocha, F.A., Yaochite, J.N., Oliveira, G.G., Carneiro, F.S., Tostes, R.C., Ramos, S.G., Zamboni, D.S., Camara, N.O., Ryffel, B., Silva, J.S., 2017. Mitochondrial DNA activates the NLRP3 inflammasome and predisposes to type 1 diabetes in murine model. Front. Immunol. 8, 164. Doi: 10.3389/fimmu.2017.00164.

Carter, J.K., Friedman, S.L., 2022. Hepatic Stellate Cell-Immune Interactions in NASH. Front Endocrinol (Lausanne) 13, 867940. Doi:10.3389/fendo.2022.867940.

Caussy, C., Tripathi, A., Humphrey, G., Bassirian, S., Singh, S., Faulkner, C., Bettencourt, R., Rizo, E., Richards, L., Xu, Z.Z., Downes, M.R., Evans, R.M., Brenner, D.A., Sirlin, C.B., Knight, R., Loomba, R., 2019. A gut microbiome signature for cirrhosis due to nonalcoholic fatty liver disease. Nat. Commun. 10, 1406. Doi: 10.1038/s41467-019-09455-9.

Chalasani, N., Younossi, Z., Lavine, J.E., Charlton, M., Cusi, K., Rinella, M., Harrison, S.A., Brunt, E.M., Sanyal, A.J., 2018. The diagnosis and management of nonalcoholic fatty liver disease: Practice guidance from the American Association for the Study of Liver Diseases. Hepatology 67, 328–357. Doi:10.1002/hep.29367.

Chen, R., Du, J., Zhu, H, Ling, Q., 2021. The role of cGAS-STING signalling in liver diseases. J. Hep. Rep. 3,100324. Doi: 10.1016/j.jhepr.2021.100324.

Chinellato, M., Gasparotto, M., Quarta, S., Ruvoletto, M., Biasiolo, A., Filippini, F., Spiezia, L., Cendron, L., Pontisso, P., 2023. 1-Piperidine Propionic Acid as an Allosteric Inhibitor of Protease Activated Receptor-2. Pharmaceuticals (Basel) 16, 1486. doi: 10.3390/ph16101486.

Crombach, G., Scharl, A., Vierbuchen, M., Wurz, H., Bolte, A., 1989. Detection of squamous cell carcinoma antigen in normal squamous epithelia and in squamous cellcarcinomas of the uterine cervix, Cancer. 63:1337-42. Doi: 10.1002/1097-0142(19890401)63:7<1337::aid-cncr2820630719>3.0.co;2-j.

Cui, J., Chen, C.H., Lo, M.T., Schork, N., Bettencourt, R., Gonzalez, M.P., Bhatt, A., Hooker, J., Shaffer, K., Nelson, K.E., Long, M.T., Brenner, D.A., Sirlin, C.B., Loomba, R., 2016. Shared genetic effects between hepatic steatosis and fibrosis: a prospective twin study. Hepatology 64, 1547–1558. Doi: 10.1002/hep.28674.

Czaja, M.J., 2016. Function of Autophagy in Nonalcoholic Fatty Liver Disease. Dig. Dis. Sci. 61, 1304-1313. Doi: 10.1007/s10620-015-4025-x.

Daemen, S., Gainullina, A., Kalugotla, G., He, L., Chan, M.M., Beals, J.W., Liss, K.H., Klein, S., Feldstein, A.E., Finck, B.N., Artyomov, M.N., Schilling, J.D., 2021. Dynamic shifts in the composition of resident and recruited macrophages influence tissue remodeling in NASH. Cell Rep. 34, 108626. Doi: 10.1016/j.celrep.2020.108626.

Day, C.P., James, O.F., 1998. Steatohepatitis: a tale of two “hit”? Gastroenterology 114, 842-845. Doi: 10.1016/s0016-5085(98)70599-2.

de Bruijn, H.W., Duk, J.M., van der Zee, A.G., Pras, E., Willemse, P.H., Boonstra, H., Hollema, H., Mourits, M.J., de Vries, E.G., Aalders, J.G., 1998. The clinical value of squamous cell carcinoma antigen in cancer of the uterine cervix, Tumour Biol. Doi: 10.1159/000030044.

Declerck, P.J., Gils, A., 2013. Three decades of research on plasminogen activator inhibitor-1: a multifaceted SERPIN. Semin Thromb Hemost. 39:356-64. Doi:10.1055/s-0033-1334487.

di Bonzo, L.V., Ferrero, I., Cravanzola, C., Mareschi, K., Rustichelli, D., Novo, E., Sanavio, F., Cannito, S., Zamara, E., Bertero, M., Davit, A., Francica, S., Novelli, F., Colombatto, S., Fagioli, F., Parola, M., 2008. Human mesenchymal stem cells as a two-edged sword in hepatic regenerative medicine: engraftment and hepatocyte differentiation versus profibrogenic potential. Gut 57, 223-231. Doi: 10.1136/gut.2006.111617.

Di Lillo, D.J., Horikawa, M., Tedder, T.F., 2011. B- lymphocyte effector functions in health and disease. Immunol. Res. 49, 281-292. Doi: 10.1007/s12026-010-8189-3.

Dixon, J.B., Bhathal, P.S., Hughes, N.R., O’Brien, P.E., 2004. Nonalcoholic fatty liver disease: improvement in liver histological analysis with weight loss. Hepatology 39, 1647-1654. Doi: 10.1002/hep.20251.

Donati, B., Dongiovanni, P., Romeo, S., Meroni, M., McCain, M., Miele, L., Petta, S., Maier, S., Rosso, C., De Luca, L., Vanni, E., Grimaudo, S., Romagnoli, R., Colli, F., Ferri, F., Mancina, R.M., Iruzubieta, P., Craxi, A., Fracanzani, A.L., Grieco, A., Corradini, S.G.,

Aghemo, A., Colombo, M., Soardo, G., Bugianesi, E., Reeves, H., Anstee, Q.M., Fargion, S., Valenti, L., 2017. MBOAT7 rs641738 variant and hepatocellular carcinoma in non-cirrhotic individuals. Sci. Rep. 7, 4492. Doi: 10.1038/s41598-017-04991-0.

Dranoff, J.A., Wells, R.G., 2010. Portal fibroblasts: Underappreciated mediators of biliary fibrosis. Hepatology 51, 1438-1444. Doi: 10.1002/hep.23405.

Dudek, M., Pfister, D., Donakonda, S., Filpe, P., Schneider, A., Laschinger, M., Hartmann, D., Hüser, N., Meiser, P., Bayerl, F., Inverso, D., Wigger, J., Sebode, M., Öllinger, R., Rad, R., Hegenbarth, S., Anton, M., Guillot, A., Bowman, A., Heide, D., Müller, F., Ramadori, P., Leone, V., Garcia-Caceres, C., Gruber, T., Seifert, G., Kabat, A.M., Mallm, J.P., Reider, S., Effenberger, M., Roth, S., Billeter, A.T., Müller-Stich, B., Pearce, E.J., Koch-Nolte, F., Käser, R., Tilg, H., Thimme, R., Boettler, T., Tacke, F., Dufour, J.F., Haller, D., Murray, P.J., Heeren, R., Zehn, D., Böttcher, J.P., Heikenwälder, M., Knolle, P.A., 2021. Auto-aggressive CXCR6(+) CD8 T cells cause liver immune pathology in NASH. Nature 592, 444-449. Doi: 10.1038/s41586-021-03233-8.

Dufour, J.F., Anstee, Q.M., Bugianesi, E., Harrison, S., Loomba, R., Paradis, V., Tilg, H., Wong, V.W., Zelber-Sagi, S., 2022. Current therapies and new developments in NASH. Gut 71, 2123-2134. Doi: 10.1136/gutjnl-2021-326874.

Dunstone, M.A., Whisstock, J.C., 2011. Chapter five – Crystallography of SERPINs and SERPIN complexes. In: JC Whisstock, PI Bird, eds. Methods in Enzymology. London: Academic Press. p. 63-87.

Eslam, M., George, J., 2020. Genetic contributions to NAFLD: leveraging shared genetics to uncover systems biology. Nat. Rev. Gastroenterol. Hepatol. 17, 40-52. Doi: 10.1038/s41575-019-0212-0.

Eslam, M., Valenti, L., Romeo, S., 2018. Genetics and epigenetics of NAFLD and NASH: Clinical impact. J. Hepatol. 68, 268-279. Doi: 10.1016/j.jhep.2017.09.003.

Estes, C., Anstee, Q.M., Arias-Loste, M.T., Bantel, H., Bellentani, S., Caballeria, J., Colombo, M., Craxi, A., Crespo, J., Day, C.P., Eguchi, Y., Geier, A., Kondili, L.A., Kroy, D.C., Lazarus, J.V., Loomba, R., Manns, M.P., Marchesini, G., Nakajima, A., Negro, F., Petta, S., Ratziu, V., Romero-Gomez, M., Sanyal, A., Schattenberg, J.M., Tacke, F., Tanaka, J., Trautwein, C., Wei, L., Zeuzem, S., Razavi, H., 2018. Modeling NAFLD disease burden in China, France, Germany, Italy, Japan, Spain, United Kingdom, and United States for the period 2016-2030. J. Hepatol. 69, 896–904. Doi: 10.1016/j.jhep.2018.05.036.

European Association for the Study of the Liver, 2018a. EASL recommendations on treatment of hepatitis C 2018. J. Hepatol. 69, 461–511. Doi: 10.1016/j.jhep.2018.03.026.

European Association for the Study of the Liver, 2018b. EASL Clinical Practice Guidelines: management of hepatocellular carcinoma. J Hepatol 69, 182-236. Doi:10.1016/j.jhep.2018.03.019.

Falade-Nwulia, O., Suarez-Cuervo, C., Nelson, D.R., Fried, M.W., Segal, J.B., Sulkowski, M.S., 2017. Oral direct-acting agent therapy for hepatitis C virus infection. Ann. Intern. Med. 166, 637–648. Doi:10.7326/M16-2575.

Feldstein, A.E., Werneburg, N.W., Canbay, A., Guicciardi, M.E., Bronk, S.F., Rydzewski, R., Burgart, L.J., Gores, G.J., 2004. Free fatty acids promote hepatic lipotoxicity by stimulating TNF-alpha expression via a lysosomal pathway. Hepatology 40, 185-194. Doi: 10.1002/hep.20283.

Ferreyra Solari, N.E., Inzaugarat, M.E., Baz, P., De Matteo, E., Lezama, C., Galoppo, M., Galoppo, C., Cherñavsky, A.C., 2012. The role of innate cells is coupled to a Th1-polarized immune response in pediatric nonalcoholic steatohepatitis. J. Clin. Immunol. 32, 611-621. Doi: 10.1007/s10875-011-9635-2.

Flannery, C., Dufour, S., Rabøl, R., Shulman, G.I., and Petersen, K.F., 2012. Skeletal muscle insulin resistance promotes increased hepatic de novo lipogenesis, hyperlipidemia, and hepatic steatosis in the elderly. Diabetes 61, 2711–2717. Doi: 10.2337/db12-0206.

Foglia, B., Novo, E., Protopapa, F., Maggiora, M., Bocca, C., Cannito, S., Parola, M., 2021. Hypoxia, hypoxia-inducible factors and liver fibrosis. Cells 10, 1764. Doi: 10.3390/cells10071764.

Foglia, B, Sutti, S, Pedicini, D, Cannito, S, Bocca, C, Maggiora, M, Bevacqua, MR, Rosso, C, Bugianesi, E, Albano, E, Novo, E, Parola, M. 2019. Oncostatin M, A Profibrogenic Mediator Overexpressed in Non-Alcoholic Fatty Liver Disease, Stimulates Migration of Hepatic Myofibroblasts. Cells 2019 Dec 20;9(1):28. doi: 10.3390/cells9010028.

Forbes, S.J., Russo, F.P., Rey, V., Burra, P., Rugge, M., Wright, N.A., Alison, M.R., 2004. A significant proportion of myofibroblasts are of bone marrow origin in human liver fibrosis. Gastroenterology 126, 955-963. Doi: 10.1053/j.gastro.2004.02.025.

Forbes, S.J., Parola M., 2011. Liver fibrogenic cells. Best. Pract. Res. Clin. Gastroenterol. 25, 207-217. Doi: 10.1016/j.bpg.2011.02.006.

Friedman, S.L., 2008. Hepatic stellate cells: protean, multifunctional, and enigmatic cells of the liver. Physiol. Rev. 88, 125-72. Doi: 10.1152/physrev.00013.2007.

Friedman, S.L., Pinzani, M., 2022 Hepatic fibrosis 2022: Unmet needs and a blueprint for the future. Hepatology 75, 473-488. Doi:10.1002/hep.32285.

Fukuo, Y., Yamashina, S., Sonoue, H., Arakawa, A., Nakadera, E., Aoyama, T., Uchiyama, A., Kon, K., Ikejima, K., Watanabe, S., 2014. Abnormality of autophagic function and cathepsin expression in the liver from patients with nonalcoholic fatty liver disease. Hepatol. Res. 44, 1026-1036. Doi: 10.1111/hepr.12282.

Gadd, V.L., Skoien, R., Powell, E.E., Fagan, K.J., Winterford, C., Horsfall, L., Irvine, K., Clouston, A.D., 2014. The portal inflammatory infiltrate and ductular reaction in human nonalcoholic fatty liver disease. Hepatology 59, 1393-405. Doi: 10.1002/hep.26937.

Gaggini, M., Morelli, M., Buzzigoli, E., DeFronzo, R.A., Bugianesi, E., Gastaldelli, A., 2013. Non-alcoholic fatty liver disease (NAFLD) and its connection with insulin resistance, dyslipidemia, atherosclerosis and coronary heart disease. Nutrients 5, 1544-1560. Doi: 10.3390/nu5051544.

Gaul, S., Leszczynska, A., Alegre, F., Kaufmann, B., Johnson, C.D., Adams, L.A., Wree, A., Damm, G., Seehofer, D., Calvente, C.J., Povero, D., Kisseleva, T., Eguchi, A., McGeough, M.D., Hoffman, H.M., Pelegrin, P., Laufs, U., Feldstein, A.E., 2021. Hepatocyte pyroptosis and release of inflammasome particles induce stellate cell activation and liver fibrosis. J. Hepatol. 74, 156-167. Doi: 10.1016/j.jhep.2020.07.041.

Gautheron, J., Vucur, M., Reisinger, F., Cardenas, D.V., Roderburg, C., Koppe, C., Kreggenwinkel, K., Schneider, A.T., Bartneck, M., Neumann, U.P., Canbay, A., Reeves, H.L., Luedde, M., Tacke, F., Trautwein, C., Heikenwalder, M., Luedde, T., 2014. A positive feedback loop between RIP3 and JNK controls non-alcoholic steatohepatitis. EMBO Mol. Med. 6, 1062-1074. Doi: 10.15252/emmm.201403856.

Gettins, P.G.W., 2002. Serpin structure, mechanism, and function. Chemical Reviews, 102(12),4751–4804. Doi: 10.1021/cr010170+.

Ghazarian, M., Revelo, X.S., Nøhr, M.K., Luck, H., Zeng, K., Lei, H., Tsai, S, Schroer, S.A., Park, Y.J., Chng, M.H.Y., Shen, L., D'Angelo, J.A., Horton, P., Chapman, W.C., Brockmeier, D., Woo, M., Engleman, E.G., Adeyi, O., Hirano, N., Jin, T., Gehring, A.J., Winer, S., Winer, D.A., 2017. Type I interferon responses drive intrahepatic T cells to promote metabolic syndrome. Sci Immunol 2, eaai7616. Doi: 10.1126/sciimmunol.aai7616.

Glass, O., Henao, R., Patel, K., Guy, C.D., Gruss, H.J., Syn, W.K., Moylan, C.A., Streilein, R., Hall, R., Diehl, A.M., Abdelmalek, M.F., 2018. Serum interleukin-8, osteopontin, and monocyte chemoattractant protein 1 are associated with hepatic fibrosis in patients with nonalcoholic fatty liver disease. Hepatol. Commun. 2, 1344-1355. Doi: 10.1002/hep4.1237.

Golabi, P., Isakov, V., Younossi, Z.M., 2023. Nonalcoholic Fatty Liver Disease: Disease Burden and Disease Awareness. Clin. Liver Dis. 27, 173-186. Doi: 10.1016/j.cld.2023.01.001.

Gong, T., Liu, L., Jiang, W., Zhou, R., 2020. DAMP-sensing receptors in sterile inflammation and inflammatory diseases. Nat. Rev. Immunol. 20, 95-112. Doi: 10.1038/s41577-019-0215-7.

Grohmann, M., Wiede, F., Dodd, G.T., Gurzov, E.N., Ooi, G.J., Butt, T., Rasmiena, A.A., Kaur, S., Gulati, T., Goh, P.K., Treloar, A.E., Archer, S., Brown, W.A., Muller, M., Watt, M.J., Ohara, O., McLean, C.A., Tiganis, T., 2018. Obesity drives STAT-1-dependent NASH and STAT-3-dependent HCC. Cell 175, 1289-1306. Doi: 10.1016/j.cell.2018.09.053.

Guido, M., Roskams, T., Pontisso, P., Fassan, M., Thung, S.N., Giacomelli, L., Sergio, A., Farinati, F., Cillo, U., Rugge, M., 2008. Squamous cell carcinoma antigen in human liver carcinogenesis. J. Clin. Pathol.; 61:445-47. Doi: 10.1136/jcp.2007.051383.

Guilliams, M., Bonnardel, J., Haest, B., Vanderborght, B., Wagner, C., Remmerie, A., Bujko, A., Martens, L., Thoné, T., Browaeys, R., De Ponti, F.F., Vanneste, B., Zwicker, C., Svedberg, F.R., Vanhalewyn, T., Gonçalves, A., Lippens, S., Devriendt, B., Cox, E., Ferrero, G., Wittamer, V., Willaert, A., Kaptein, S.J.F., Neyts, J., Dallmeier, K., Geldhof, P., Casaert, S., Deplancke, B., Ten Dijke, P., Hoorens, A., Vanlander, A., Berrevoet, F., Van Nieuwenhove, Y., Saeys, Y., Saelens, W., Van Vlierberghe, H., Devisscher, L., Scott, C.L., 2022. Spatial proteogenomics reveals distinct and evolutionarily conserved hepatic macrophage niches. Cell 185, 379-396. Doi: 10.1016/j.cell.2021.12.018.

Guillot, A., Tacke, F., 2019. Liver macrophages: old dogmas and new insights. Hepatol. Commun. 3, 730-743. Doi 10.1002/hep4.1356.

Ha, H., Han, D., Choi, Y., 2009. TRAF- mediated TNFR- family signaling. Curr. Protoc. Immunol. Doi: 10.1002/0471142735.im1109ds87.

Haas, J.T., Vonghia, L., Mogilenko, D.A., Verrijken, A., Molendi-Coste, O., Fleury, S., Deprince, A., Nikitin, A., Woitrain, E., Ducrocq-Geoffroy, L., Pic, S., Derudas, B., Dehondt, H., Gheeraert, C., Van Gaal, L., Driessen, A., Lefebvre, P., Staels, B., Francque, S., Dombrowicz, D., 2019. Transcriptional network analysis implicates altered hepatic immune function in NASH development and resolution. Nat. Metab. 1, 604-614. Doi: 10.1038/s42255-019-0076-1.

Hafeez, S., Ahmed, M.H., 2013. Bariatric surgery as potential treatment for nonalcoholic fatty liver disease: a future treatment by choice or by chance? J. Obes. 2013:839275. Doi: 10.1155/2013/839275.

Harrison, S.A., Loomba, R., Dubourg, J., Ratziu, V., Noureddin, M., 2023. Clinical Trial Landscape in NASH. Clin. Gastroenterol. Hepatol. S1542-3565(23)00265-3. Doi: 10.1016/j.cgh.2023.03.041.

Heijnen, H., van der Sluijs, P., 2015. Platelet secretory behaviour: as diverse as the granules . . . or not? J. Thromb. Haemost. 13, 2141-2151. Doi:10.1111/jth.13147.

Heit, C., Jackson, B.C., McAndrews, M., Wright, M.W., Thompson, D.C., Silverman, G.A., Nebert, D.W., Vasiliou, V., 2013. Update of the human and mouse SERPIN gene superfamily, Hum Genomics. 7:22. Doi: 10.1186/1479-7364-7-22.

Herman, M.A., Samuel, V.T., 2016. The Sweet Path to Metabolic Demise: Fructose and Lipid Synthesis. Trends Endocrinol. Metab. 27, 719–730. Doi: 10.1016/j.tem.2016.06.005.

Heymann, F., Tacke, F., 2016. Immunology in the liver–from homeostasis to disease. Nat. Rev. Gastroenterol. Hepatol. 13, 88-110. Doi: 10.1038/nrgastro.2015.200.

Higashi, T., Friedman, S.L., Hoshida, Y., 2017. Hepatic stellate cells as key target in liver fibrosis. Adv. Drug Deliv. Rev.121, 27-42. Doi:10.1016/j.addr.2017.05.007.

Hirsova, P., Gores, G.J., 2015. Death receptor-mediated cell death and proinflammatory signaling in nonalcoholic steatohepatitis. Cell. Mol. Gastroenterol. Hepatol. 1, 17–27. Doi: 10.1016/j.jcmgh.2014.11.005.

Hirsova, P., Ibrabim, S.H., Gores, G.J., Malhi, H., 2016. Lipotoxic lethal and sublethal stress signaling in hepatocytes: relevance to NASH pathogenesis. J. Lipid Res. 57, 1758-1770. Doi: 10.1194/jlr.R066357.

Hirsova, P., Weng, P., Salim, W., Bronk, S.F., Griffith, T.S., Ibrahim, S.H., Gores, G.J., 2017. TRAIL deletion prevents liver inflammation but not adipose tissue inflammation during murine diet- induced obesity. Hepatol. Commun. 1, 648-662. Doi: 10.1002/hep4.1069.

Holzner, L.M.W., Murray, A.J., 2021. Hypoxia-inducible factors as key players in the pathogenesis of non-alcoholic fatty liver disease and non-alcoholic steatohepatitis. Front. Med. (Lausanne). 8:753268. Doi: 10.3389/fmed.2021.753268.

Honda, M., Kimura, C., Uede, T., Kon, S., 2020. Neutralizing antibody against osteopontin attenuates non-alcoholic steatohepatitis in mice. J. Cell. Commun. Signal. 14, 223-232. Doi: 10.1007/s12079-020-00554-7.

Hou, J., Zhang, J., Cui, P., Zhou, Y., Liu, C., Wu, X., Ji, Y., Wang, S., Cheng, B., Ye, H., Shu, L., Zhang, K., Wang, D., Xu, J., Shu, Q., Colonna, M., Fang, X., 2021. TREM2 sustains macrophage-hepatocyte metabolic coordination in nonalcoholic fatty liver disease and sepsis. J. Clin. Invest. 131, e135197. Doi: 10.1172/JCI135197.

Hoyles, L., Fernández-Real, J.M., Federici, M., Serino, M., Abbott, J., Charpentier, J., Heymes, C., Luque, J.L., Anthony, E., Barton, R.H., Chilloux, J., Myridakis, A., Martinez-Gili, L., Moreno-Navarrete, J.M., Benhamed, F., Azalbert, V., Blasco-Baque, V., Puig, J., Xifra, G., Ricart, W., Tomlinson, C., Woodbridge, M., Cardellini, M., Davato, F., Cardolini, I., Porzio, O., Gentileschi, P., Lopez, F., Foufelle, F., Butcher, S.A., Holmes, E., Nicholson, J.K., Postic, C., Burcelin, R., Dumas, M.E., 2018. Molecular phenomics and metagenomics of hepatic steatosis in non-diabetic obese women. Nat. Med. 24, 1070-1080. Doi: 10.1038/s41591-018-0061-3.

Huang, D.Q., El-Serag, H.B., Loomba, R., 2021. Global epidemiology of NAFLD-related HCC: trends, predictions, risk factors and prevention. Nat. Rev. Gastroenterol. Hepatol. 18, 223–238. Doi: 10.1038/s41575-020-00381-6.

Huang, D.Q., Singal, A.G., Kono, Y., Tan, D.J.H., El-Serag, H.B., Loomba, R., 2022. Changing global epidemiology of liver cancer from 2010 to 2019: NASH is the fastest growing cause of liver cancer. Cell Metab. 34, 969-977. Doi:10.1016/j.cmet.2022.05.003.

Hughey, C.C., Puchalska, P., Crawford, P.A., 2022. Integrating the contributions of mitochondrial oxidative metabolism to lipotoxicity and inflammation in NAFLD pathogenesis. Biochim. Biophys. Acta Mol. Cell. Biol. Lipids 1867, 159209. Doi: 10.1016/j.bbalip.2022.159209.

Huisman, T.M., Dieterich, D.T., Friedman, S.L., 2021. Experimental and Investigational Targeted Therapies for the Management of Fibrosis in NASH: An Update. J. Exp. Pharmacol. 13, 329-338. Doi: 10.2147/JEP.S265286.

Ibrahim, S.H., Hirsova, P., Gores, G.J., 2018. Non-alcoholic steatohepatitis pathogenesis: sublethal hepatocyte injury as a driver of liver inflammation. Gut 67, 963-972. Doi: 10.1136/gutjnl-2017-315691.

Idrissova, L., Malhi, H., Werneburg, N.W., LeBrasseur, N.K., Bronk, S.F., Fingas, C., Tchkonia, T., Pirtskhalava, T., White, T.A., Stout, M.B., Hirsova, P., Krishnan, A., Liedtke, C., Trautwein, C., Finnberg, N., El-Deiry, W.S., Kirkland, J.L., Gores, G.J., 2015. TRAIL receptor deletion in mice suppresses the inflammation of nutrient excess. J. Hepatol. 62, 1156-1163. Doi: 10.1016/j.jhep.2014.11.033.

Inzaugarat, M.E., Ferreyra Solari, N.E., Billordo, L.A., Abecasis, R., Gadano, A.C., Cherñavsky, A.C., 2011. Altered phenotype and functionality of circulating immune cells

characterize adult patients with nonalcoholic steatohepatitis. J. Clin. Immunol. 31, 1120-1130. doi: 10.1007/s10875-011-9571-1.

Ioannou, G. N., Subramanian, S., Chait, A., Haigh, W.G., Yeh, M.M., Farrell, G.C., Lee, S.P., Savard, C., 2017. Cholesterol crystallization within hepatocyte lipid droplets and its role in murine NASH. J. Lipid Res. 58, 1067–1079. Doi: 10.1194/jlr.M072454.

Izuhara, K., Ohta, S., Kanaji, S., Shiraishi, H., Arima, K., 2008. Recent progress in understanding the diversity of the human ov-serpin/clade B serpin family. Cell Mol Life Sci. 65:2541-53. Doi: 10.1007/s00018-008-8049-7.

Jaitin, D.A., Adlung, L., Thaiss, C.A., Weiner, A., Li, B., Descamps, H., Lundgren, P., Bleriot, C., Liu, Z., Deczkowska, A., Keren-Shaul, H., David, E., Zmora, N., Eldar, S.M., Lubezky, N., Shibolet, O., Hill, D.A., Lazar, M.A., Colonna, M., Ginhoux, F., Shapiro, H., Elinav, E., Amit, I., 2019. Lipid associated macrophages control metabolic homeostasis in a trem2-dependent manner. Cell 178, 686-698. Doi 10.1016/j.cell.2019.05.054.

Janciauskiene, S.M., Bals, R., Koczulla, R., Vogelmeier, C., Köhnlein, T., Welte, T., 2011. The discovery of α1-antitrypsin and its role in health and disease. Respir Med. 105:1129-39. Doi:10.1016/j.rmed.2011.02.002.

Karlmark, K.R., Zimmermann, H.W., Roderburg, C., Gassler, N., Wasmuth, H.E., Luedde, T., Trautwein, C., Tacke, F., 2010. The fractalkine receptor CX_3CR1 protects against liver fibrosis by controlling differentiation and survival of infiltrating hepatic monocytes. Hepatology 52, 1769-1782. Doi: 10.1002/hep.23894.

Kato, H., Miyauchi, F., Morioka, H., Fujino, T., Torigoe, T., 1979. Tumor antigen of human cervical squamous cell carcinoma: correlation of circulating levels with disease progress. Cancer. 43:585-90. Doi: 10.1002/1097-0142(197902)43:2<585::aid-cncr2820430227>3.0.co;2-0.

Kato, H., Nagaya, T., Torigoe, T., 1984. Heterogeneity of a tumor antigen TA-4 of squamous cell carcinoma in relation to its appearance in the circulation, Gann. 75:433-35.

Kato, H., Torigoe, T., 1977. Radioimmunoassay for tumor antigen of human cervical squamous cell carcinoma. Cancer. 40:1621-28. Doi: 10.1002/1097-0142(197710)40:4<1621::aid-cncr2820400435>3.0.co;2-i.

Kayagaki, N., Stowe, I.B., Lee, B.L., O'Rourke, K., Anderson, K., Warming, S., Cuellar, T., Haley, B., Roose-Girma, M., Phung, Q.T., Liu, P.S., Lill, J.R., Li, H., Wu, J., Kummerfeld, S., Zhang, J., Lee, W.P., Snipas, S.J., Salvesen, G.S., Morris, L.X., Fitzgerald, L., Zhang, Y., Bertram, E.M., Goodnow, C.C., Dixit, V.M., 2015. Caspase-11 cleaves gasdermin D for non-canonical inflammasome signalling. Nature 526, 666-671. Doi: 10.1038/nature15541.

Kim, D., Kim, W.R., 2017. Non-obese Fatty Liver Disease. Clin. Gastroenterol. Hepatol. 15, 474-485. Doi: 10.1016/j.cgh.2016.08.028.

Kim, J.Y., Garcia-Carbonell, R., Yamachika, S., Zhao, P., Dhar, D., Loomba, R., Kaufman, R.J., Saltiel, A.R., Karin, M., 2018. ER Stress Drives Lipogenesis and Steatohepatitis via Caspase-2 Activation of S1P. Cell 175, 133-145. Doi: 10.1016/j.cell.2018.08.020.

Kisseleva, T., Cong, M., Paik, Y., Scholten, D., Jiang, C., Benner, C., Iwaisako, K., Moore-Morris, T., Scott, B., Tsukamoto, H., Evans, S.M., Dillmann, W., Glass, C.K., Brenner, D.A., 2012. Myofibroblasts revert to an inactive phenotype during regression of liver fibrosis. Proc. Natl. Acad. Sci. USA 109, 9448-9953. Doi: 10.1073/pnas.1201840109.

Kisseleva, T., Brenner, D., 2020. Molecular and cellular mechanisms of liver fibrosis and its regression. Nat. Rev. Gastroenterol. Hepatol. 18, 151-166. Doi: 10.1038/s41575-020-00372-7.

Knorr, J., Wree, A., Feldstein, A.E., 2022. Pyroptosis in Steatohepatitis and Liver Diseases. J. Mol Biol. 434, 167271. Doi: 10.1016/j.jmb.2021.167271.

Koyama, Y., Brenner, D.A., 2017. Liver inflammation and fibrosis. J. Clin. Invest. 27, 55-64. Doi:10.1172/JCI88881..

Komori T, Tanaka M, Senba E, Miyajima A, Morikawa Y. 2014. Deficiency of oncostatin M receptor β (OSMRβ) exacerbates high-fat diet-induced obesity and related metabolic disorders in mice J Biol Chem. 16;289(20):13821-37. doi: 10.1074/jbc.M113.542399.

Krenkel, O., Puengel, T., Govaere, O., Abdallah, A.T., Mossanen, J.C., Kohlhepp, M., Liepelt, A., Lefebvre, E., Luedde, T., Hellerbrand, C., Weiskirchen, R., Longerich, T., Costa, I.G., Anstee, Q.M., Trautwein, C., Tacke, F., 2018. Therapeutic inhibition of inflammatory monocyte recruitment reduces steatohepatitis and liver fibrosis. Hepatology 67, 1270-1283. Doi: 10.1002/hep.29544.

Kubala, M.H., DeClerck, Y.A., 2019. The plasminogen activator inhibitor-1 paradox in cancer: a mechanistic understanding. Cancer Metastasis Rev. 38:483-92. Doi:10.1007/s10555-019-09806-4.

Kwanten, W.J., Vandewynckel, Y.P., Martinet, W., De Winter, B.Y., Michielsen, P.P., Van Hoof, V.O., Driessen, A., Timmermans, J.P., Bedossa, P., Van Vlierberghe, H., Francque, S.M., 2016. Hepatocellular autophagy modulates the unfolded protein response and fasting-induced steatosis in mice. Am. J. Physiol. Gastrointest. Liver Physiol. 311, G599-G609. Doi: 10.1152/ajpgi.00418.2015.

Law, R.H., Zhang, Q., McGowan, S., Buckle, A.M., Silverman, G.A., Wong, W., Rosado, C.J., Langendorf, C.G., Pike, R.N., Bird, P.I., Whisstock, J.C., 2006. An overview of the SERPIN superfamily. Genome Biol. 7:216. Doi: 10.1186/gb-2006-7-5-216.

Lawlor, K.E., Khan, N., Mildenhall, A., Gerlic, M., Croker, B.A., D'Cruz, A.A., Hall, C., Kaur Spall, S., Anderton, H., Masters, S.L., Rashidi, M., Wicks, I.P., Alexander, W.S., Mitsuuchi, Y., Benetatos, C.A., Condon, S.M., Wong, W.W., Silke, J., Vaux, D.L., Vince, J.E., 2015. RIPK3 promotes cell death and NLRP3 inflammasome activation in the absence of MLKL. Nat. Commun. 6, 6282. Doi: 10.1038/ncomms7282.

Lazaridis, K.N., LaRusso, N.F., 2015. The cholangiopathies. Mayo Clin. Proc. 90, 791–800. Doi:10.1016/j.mayocp.2015.03.017.

Lee, Y.A., Friedman, S.L., 2022. Inflammatory and fibrotic mechanisms in NAFLD – Implications for new treatment strategies. J. Intern. Med. 291, 11-31. Doi: 10.1111/joim.13380.

Lee, Y.A., Wallace, M.C., Friedman, S.L., 2015. Pathobiology of liver fibrosis: a translational success story. Gut 64, 830-841. Doi:10.1136/gutjnl-2014-306842.

Lemasters, J.J., 2005. Selective mitochondrial autophagy, or mitophagy, as a targeted defense against oxidative stress, mitochondrial dysfunction, and aging. Rejuvenation Res. 8, 3-5. Doi: 10.1089/rej.2005.8.3.

Lemoinne, S., Thabut, D., Housset, C., 2016. Portal myofibroblasts connect angiogenesis and fibrosis in liver. Cell Tissue Res. 365, 583-589. Doi: 10.1007/s00441-016-2443-5.

Leung, T. M., Nieto, N., 2013. CYP2E1 and oxidant stress in alcoholic and non- alcoholic fatty liver disease. J. Hepatol. 58, 395–398. Doi: 10.1016/j.jhep.2012.08.018.

Li, J., Jia, H., Cai, X., Zhong, H., Feng, Q., Sunagawa, S., Arumugam, M., Kultima, J.R., Prifti, E., Nielsen, T., Juncker, A.S., Manichanh, C., Chen, B., Zhang, W., Levenez, F., Wang, J., Xu, X., Xiao, L., Liang, S., Zhang, D., Zhang, Z., Chen, W., Zhao, H., Al-Aama, J.Y., Edris, S., Yang, H., Wang, J., Hansen, T., Nielsen, H.B., Brunak, S., Kristiansen, K., Guarner, F., Pedersen, O., Doré, J., Ehrlich, S.D.; MetaHIT Consortium; Bork, P., Wang, J.; MetaHIT Consortium, 2014. An integrated catalog of reference genes in the human gut microbiome. Nat. Biotechnol. 32, 834-841. Doi: 10.1038/nbt.2942.

Li, Z., Soloski, M.J., Diehl, A.M., 2005. Dietary factors alter hepatic innate immune system in mice with nonalcoholic fatty liver disease. Hepatology 42, 880-885. Doi: 10.1002/hep.20826.

Liu, Y.L., Patman, G.L., Leathart, J.B., Piguet, A.C., Burt, A.D., Dufour, J.F., Day, C.P., Daly, A.K., Reeves, H.L., Anstee, Q.M., 2014a. Carriage of the PNPLA3 rs738409 C >G polymorphism confers an increased risk of non-alcoholic fatty liver disease associated hepatocellular carcinoma. J. Hepatol. 61, 75-81. Doi: 10.1016/j.jhep.2014.02.030.

Liu, Y.L., Reeves, H.L., Burt, A.D., Tiniakos, D., McPherson, S., Leathart, J.B., Allison, M.E., Alexander, G.J., Piguet, A.C., Anty, R., Donaldson, P., Aithal, G.P., Francque, S., Van Gaal, L., Clement, K., Ratziu, V., Dufour, J.F., Day, C.P., Daly, A.K., Anstee, Q.M., 2014b. TM6SF2 rs58542926 influences hepatic fibrosis progression in patients with non-alcoholic fatty liver disease. Nat. Commun. 5, 4309. Doi: 10.1038/ncomms5309.

Liu, X., Xu, J., Rosenthal, S., Zhang, L.J., McCubbin, R., Meshgin, N., Shang, L., Koyama, Y., Ma, H.Y., Sharma, S., Heinz, S., Glass, C.K., Benner, C., Brenner, D.A., Kisseleva, T., 2020. Identification of lineage specific transcription factors that prevent activation of hepatic stellate cells and promote fibrosis resolution. Gastroenterology 158, 1728-1744. Doi: 10.1053/j.gastro.2020.01.027.

Llovet, J.M., Kelley, R.K., Villanueva, A., Singal, A.G., Pikarsky, E., Roayaie, S., Lencioni, R., Koike, K., Zucman-Rossi, J., Finn, R.S., 2021. Hepatocellular carcinoma. Nat. Rev. Dis. Primers 7, 6. Doi:10.1038/s41572-020-00240-3.

Llovet, J.M., Willoughby, C.E., Singal, A.G., Greten, T.F., Heikenwälder, M., El-Serag, H.B., Finn, R.S., Friedman, S.L., 2023. Nonalcoholic steatohepatitis-related hepatocellular carcinoma: pathogenesis and treatment. Nat. Rev. Gastroenterol. Hepatol. Doi: 10.1038/s41575-023-00754-7.

Lodder, J., Denaes, T., Chobert, M.N., Wan, J., El-Benna, J., Pawlotsky, J.M., Lotersztajn, S., Teixeira-Clerc, F., 2015. Macrophage autophagy protects against liver fibrosis in mice. Autophagy 11, 1280-1292. Doi: 10.1080/15548627.2015.1058473.

Loomba, R., Adams, L.A., 2019. The 20% Rule of NASH Progression: The Natural History of Advanced Fibrosis and Cirrhosis due to NASH. Hepatology 70, 1885–1888. Doi: 10.1002/hep.30946.

Loomba, R., Lim, J.K., Patton, H., and El-Serag, H.B., 2020. AGA Clinical Practice Update on Screening and Surveillance for Hepatocellular Carcinoma in Patients With Nonalcoholic Fatty Liver Disease: Expert Review. Gastroenterology 158, 1822–1830. Doi: 10.1053/j.gastro.2019.12.053.

Loomba, R., Sanyal, A.J., 2013. The global NAFLD epidemic. Nat. Rev. Gastroenterol. Hepatol. 10, 686–690. Doi:10.1038/nrgastro.2013.171.

Loomba, R., Seguritan, V., Li, W., Long, T., Klitgord, N., Bhatt, A., Dulai, P.S., Caussy, C., Bettencourt, R., Highlander, S.K., Jones, M.B., Sirlin, C.B., Schnabl, B., Brinkac, L., Schork, N., Chen, C.H., Brenner, D.A., Biggs, W., Yooseph, S., Venter, J.C., Nelson, K.E., 2017. Gut Microbiome-Based Metagenomic Signature for Non-invasive Detection of Advanced Fibrosis in Human Nonalcoholic Fatty Liver Disease. Cell Metab. 25, 1054-1062. Doi: 10.1016/j.cmet.2017.04.001.

Luedde, T., Kaplowitz, N., Schwabe, R., 2014. Cell death and cell death responses in liver disease: mechanisms and clinical relevance. Gastroenterology 147, 765-783. Doi: 10.1053/j.gastro.2014.07.018.

Lund, F.E., 2008. Cytokine- producing B lymphocytes- key regulators of immunity. Curr. Opin. Immunol. 20, 332-338. Doi: 10.1016/j.coi.2008.03.003.

Luo, X., Li, H., Ma, L., Zhou, J., Guo, X., Woo, S.L., Pei, Y., Knight, L.R., Deveau, M., Chen, Y., Qian, X., Xiao, X., Li, Q., Chen, X., Huo, Y., McDaniel, K., Francis, H., Glaser, S., Meng, F., Alpini, G., Wu, C., 2018. Expression of STING is increased in liver tissues from patients with NAFLD and promotes macrophage-mediated hepatic inflammation and fibrosis in mice. Gastroenterology 155,1971-1984. Doi: 10.1053/j.gastro.2018.09.010.

Luo, X.Y., Takahara, T., Kawai, K., Fujino, M., Sugiyama, T., Tsuneyama, K., Tsukada, K., Nakae, S., Zhong, L., Li, X.K., 2013. IFN-γ deficiency attenuates hepatic inflammation and fibrosis in a steatohepatitis model induced by a methionine- and choline-deficient high fat diet. Am. J. Physiol. Gastroinstest. Liver Physiol. 305, G891-G899. Doi: 10.1152/ajpgi.00193.2013.

Luukkonen, P.K., Zhou, Y., Hyötyläinen, T., Leivonen, M., Arola, J., Orho-Melander, M., Orešič, M., Yki-Järvinen, H., 2016. The MBOAT7 variant rs641738 alters hepatic phosphatidylinositols and increases severity of non-alcoholic fatty liver disease in humans. J. Hepatol. 65, 1263-1265. Doi: 10.1016/j.jhep.2016.07.045.

Ma, Y., Wang, J., Gao, J., Yang, H., Wang, Y., Manithodyet, C., Li, J., Rezaie, A.R., 2015. Antithrombin up-regulates AMP-activated protein kinase signalling during myocardial ischaemia/reperfusion injury. Thromb Haemost., 113:338-49. Doi:10.1160/th14-04-0360.

Machado, M.V., Diehl, A.M., 2016. Pathogenesis of Nonalcoholic Steatohepatitis. Gastroenterology 150, 1769-1777. Doi: 10.1053/j.gastro.2016.02.066.

Machado, M.V., Michelotti, G.A., Pereira, Tde.A., Boursier, J., Kruger, L., Swiderska-Syn, M., Karaca, G., Xie, G., Guy, C.D., Bohinc, B., Lindblom, K.R., Johnson, E., Kornbluth, S., Diehl, A.M., 2015. Reduced lipoapoptosis, hedgehog pathway activation and fibrosis in caspase-2 deficient mice with non-alcoholic steatohepatitis. Gut 64, 1148-1157. Doi: 10.1136/gutjnl-2014-307362.

Malehmir, M., Pfister, D., Gallage, S., Szydlowska, M., Inverso, D., Kotsiliti, E., Leone, V., Peiseler, M., Surewaard, B.G.J., Rath, D., Ali, A., Wolf, M.J., Drescher, H., Healy, M.E., Dauch, D., Kroy, D., Krenkel, O., Kohlhepp, M., Engleitner, T., Olkus, A., Sijmonsma, T., Volz, J., Deppermann, C., Stegner, D., Helbling, P., Nombela-Arrieta, C., Rafiei, A., Hinterleitner, M., Rall, M., Baku, F., Borst, O., Wilson, C.L., Leslie, J., O'Connor, T., Weston, C.J., Chauhan, A., Adams, D.H., Sheriff, L., Teijeiro, A., Prinz, M., Bogeska, R., Anstee, N., Bongers, M.N., Notohamiprodjo, M., Geisler, T., Withers, D.J., Ware, J., Mann, D.A., Augustin, H.G., Vegiopoulos, A., Milsom, M.D., Rose, A.J., Lalor, P.F., Llovet, J.M., Pinyol, R., Tacke, F., Rad, R., Matter, M., Djouder, N., Kubes, P., Knolle, P.A., Unger, K., Zender, L., Nieswandt, B., Gawaz, M., Weber, A., Heikenwalder, M., 2019. Platelet GPIbα is a mediator and potential interventional target for NASH and subsequent liver cancer. Nat. Med. 25, 641-655. Doi: 10.1038/s41591-019-0379-5.

Mancina, R.M., Dongiovanni, P., Petta, S., Pingitore, P., Meroni, M., Rametta, R., Borén, J., Montalcini, T., Pujia, A., Wiklund, O., Hindy, G., Spagnuolo, R., Motta, B.M., Pipitone, R.M., Craxì, A., Fargion, S., Nobili, V., Käkelä, P., Kärjä, V., Männistö, V., Pihlajamäki, J., Reilly, D.F., Castro-Perez, J., Kozlitina, J., Valenti, L., Romeo, S., 2016. The MBOAT7-TMC4 Variant rs641738 Increases Risk of Nonalcoholic Fatty Liver Disease in Individuals of European Descent. Gastroenterology 150,1219-1230.e6. Doi: 10.1053/j.gastro.2016.01.032.

Marcellin, P., Kutala, B.K., 2018. Liver diseases: A major, neglected global public health problem requiring urgent actions and large-scale screening. Liver Int. 38, Suppl. 1, 2-6. Doi: 10.1111/liv.13682.

Marchesini, G., Brizi, M., Bianchi, G., Tomassetti, S., Bugianesi, E., Lenzi, M., McCullough, A.J., Natale, S., Forlani, G., Melchionda, N., 2001. Nonalcoholic fatty liver disease: a feature of the metabolic syndrome. Diabetes 50, 1844–1850. Doi: 10.2337/diabetes.50.8.1844.

Marra, F., Svegliati-Baroni, G., 2018. Lipotoxicity and the gut-liver axis in NASH pathogenesis. J. Hepatol. 68, 280-295. Doi: 10.1016/j.jhep.2017.11.014.

Marrero, J.A. Kulik, L.M., Sirlin, C.B., Zhu, A.X., Finn, R.S., Abecassis, M.M., Roberts, L.R., Heimbach, J.K., 2018. Diagnosis, staging, and management of hepatocellular carcinoma: 2018 practice guidance by the American Association for the Study of Liver Diseases. Hepatology 68, 723–750. Doi:10.1002/hep.29913.

Masjedi, A., Hajizadeh, F., Beigi Dargani, F., Beyzai, B., Aksoun, M., Hojjat-Farsangi, M., Zekiy, A., & Jadidi-Niaragh, F. 2021. Oncostatin M: A mysterious cytokine in cancers. In International Immunopharmacology (Vol. 90). Elsevier B.V. Doi: 10.1016/j.intimp.2020.107158.

Matsuda M, Tsurusaki S, Miyata N, Saijou E, Okochi H, Miyajima A, Tanaka M 2018.Oncostatin M causes liver fibrosis by regulating cooperation between hepatic stellate cells and macrophages in mice. Hepatology67(1):296-312. doi: 10.1002/hep.29421.

McPherson, S., Henderson, E., Burt, A.D., Day, C.P., Anstee, Q.M. 2014. Serum immunoglobulin levels predict fibrosis in patients with non- alcoholic fatty liver disease. J. Hepatol. 60, 1055-1062. Doi: 10.1016/j.jhep.2014.01.010.

McPherson, S., Hardy, T., Henderson, E., Burt, A.D., Day, C.P., Anstee, Q.M., 2015. Evidence of NAFLD progression from steatosis to fibrosing-steatohepatitis using paired biopsies: implications for prognosis and clinical management. J. Hepatol. 62, 1148–1155. Doi: 10.1016/j.jhep.2014.11.034.

Mederacke, I., Hsu, C.C., Troeger, J.S., Huebener, P., Mu, X., Dapito, D.H., Pradere, J.P., Schwabe, R.F., 2013. Fate tracing reveals hepatic stellate cells as dominant contributors to liver fibrosis independent of its aetiology. Nat. Commun. 4, 2823. Doi: 10.1038/ncomms3823.

Miyake, T., Abe, M., Tokumoto, Y., Hirooka, M., Furukawa, S., Kumagi, T., Hamada, M., Kawasaki, K., Tada, F., Ueda, T., Hiasa, Y., Matsuura, B., Onji, M., 2013. B cell- activating factor is associated with the histological severity of nonalcoholic fatty liver disease. Hepatol. Int. 7, 539-547. Doi: 10.1007/s12072-012-9345-8.

Molina, M.F., Abdelnabi, M.N., Fabre, T., Shoukry, N.H., 2019. Type 3 cytokines in liver fibrosis and liver cancer. Cytokine 124, 154497. Doi: 10.1016/j.cyto.2018.07.028.

Monetti, M., Levin, M.C., Watt, M.J., Sajan, M.P., Marmor, S., Hubbard, B.K., Stevens, R.D., Bain, J.R., Newgard, C.B., Farese, R.V. Sr., Hevener, A.L., Farese, R.V. Jr., 2007. Dissociation of hepatic steatosis and insulin resistance in mice overexpressing DGAT in the liver. Cell Metab. 6, 69–78. Doi: 10.1016/j.cmet.2007.05.005.

Morello, E., Sutti, S., Foglia, B., Novo, E., Cannito, S., Bocca, C., Rajsky, M., Bruzzì, S., Abate, M.L., Rosso, C., Bozzola, C., David, E., Bugianesi, E., Albano, E., Parola, M., 2018. Hypoxia-inducible factor 2α drives nonalcoholic fatty liver progression by triggering hepatocyte release of histidine-rich glycoprotein. Hepatology 67, 2196-2214. Doi: 10.1002/hep.29754.

Nath, B., Szabo, G., 2012. Hypoxia and hypoxia inducible factors: diverse roles in liver diseases. Hepatology.55:622-33. Doi: 10.1002/hep.25497.

Negro, F., 2020. Natural history of NASH and HCC. Liver Int. 40 (Suppl 1), 72–76. Doi: 10.1111/liv.14362.

Neuschwander-Tetri, B.A., Clark, J.M., Bass, N.M., Van Natta, M.L., Unalp- Arida, A., Tonascia, J., Zein, C.O., Brunt, E.M., Kleiner, D.E., McCullough, A.J., Sanyal, A.J., Diehl, A.M., Lavine, J.E., Chalasani, N., Kowdley, K.V.; NASH Clinical Research Network NASH Clinical Research Network, 2010. Clinical, laboratory and histological associations in adults with nonalcoholic fatty liver disease. Hepatology 52, 913–924. Doi:10.1002/hep.23784.

Novo, E., Bocca, C., Foglia, B., Protopapa, F., Maggiora, M., Parola, M., Cannito, S., 2020. Liver fibrogenesis: un update on established and emerging basic concepts. Arch. Biochem. Biophys. 689, 108445. Doi: 10.1016/j.abb.2020.108445.

Novo, E., Busletta, C., Bonzo, L.V., Povero, D., Paternostro, C., Mareschi, K., Ferrero, I., David, E., Bertolani, C., Caligiuri, A., Cannito, S., Tamagno, E., Compagnone, A., Colombatto, S., Marra, F., Fagioli, F., Pinzani, M., Parola, M., 2011. Intracellular reactive oxygen species are required for directional migration of resident and bone marrow-derived hepatic pro-fibrogenic cells. J. Hepatol. 54, 964-974. Doi: 10.1016/j.jhep.2010.09.022.

Novo, E., Parola, M., 2008. Redox mechanisms in hepatic chronic wound healing and fibrogenesis. Fibrogenesis Tissue Repair 1(1):5. Doi: 10.1186/1755-1536-1-5.

Novo, E., Busletta, C., Bonzo, L.V., Povero, D., Paternostro, C., Mareschi, K., Ferrero, I., David, E., Bertolani, C., Caligiuri, A., Cannito, S., Tamagno, E., Compagnone, A., Colombatto, S., Marra, F., Fagioli, F., Pinzani, M., Parola, M., 2011. Intracellular reactive oxygen species are required for directional migration of resident and bone marrow-derived hepatic pro-fibrogenic cells. J. Hepatol. 54, 964-974. Doi: 10.1016/j.jhep.2010.09.022.

Novo, E., Povero, D., Busletta, C., Paternostro, C., di Bonzo, L.V., Cannito, S., Compagnone, A., Bandino, A., Marra, F., Colombatto, S., David, E., Pinzani, M., Parola, M., 2012. The biphasic nature of hypoxia-induced directional migration of activated human hepatic stellate cells. J. Pathol. 226, 588-597. Doi: 10.1002/path.3005.

Novo, E., Villano, G., Turato, C., Cannito, S., Paternostro, C., Busletta, C., Biasiolo, A., Quarta, S., Morello, E., Bocca, C., Miglietta, A., David, E., Sutti, S., Plebani, M., Albano, E., Parola, M., Pontisso, P., 2017. SerpinB3 promotes pro-fibrogenic responses in activated hepatic stellate cells. Scientific Reports, 7(1), 1–10. Doi.org/10.1038/s41598-017-03744-3.

Novobrantseva, T.I., Majeau, G.R., Amatucci, A., Kogan, S., Brenner, I., Casola, S., Shlomchik, M.J., Koteliansky, V., Hochman, P.S., Ibraghimov, A., 2005. Attenuated liver fibrosis in the absence of B cells. J. Clin. Invest. 115, 3072-3082. Doi: 10.1172/JCI24798.

Paik, Y.H., Kim, J., Aoyama, T., De Minicis, S., Bataller, R., Brenner, D.A., 2014. Role of NADPH oxidases in liver fibrosis. Antioxid. Redox Signal. 20, 2854-2872. Doi: 10.1089/ars.2013.5619.

Parola, M., Marra, F., Pinzani, M., 2008. Myofibroblast - like cells and liver fibrogenesis: Emerging concepts in a rapidly moving scenario. Mol. Aspects Med. 29, 58-66. Doi: 10.1016/j.mam.2007.09.002.

Parola, M., Pinzani, M., 2019. Liver fibrosis: Pathophysiology, pathogenetic targets and clinical issues. Molecular Aspects of Medicine, 65(September), 37–55. Doi.org/10.1016/j.mam.2018.09.002.

Parola, M., Robino, G., 2001. Oxidative stress-related molecules and liver fibrosis. J. Hepatol. 35, 297-306. Doi: 10.1016/s0168-8278(01)00142-8.

Peiseler, M., Schwabe, R., Hampe, J., Kubes, P., Heikenwälder, M., Tacke, F., 2022. Immune mechanisms linking metabolic injury to inflammation and fibrosis in fatty liver disease - novel insights into cellular communication circuits. J. Hepatol. 77, 1136-1160. Doi:10.1016/j.jhep.2022.06.012.

Peiseler, M., Schwabe, R., Hampe, J., Kubes, P., Heikenwälder, M., Tacke, F., 2022. Immune mechanisms linking metabolic injury to inflammation and fibrosis in fatty liver disease - novel insights into cellular communication circuits. J. Hepatol. 77, 1136-1160. Doi:10.1016/j.jhep.2022.06.012.

Pellicoro, A., Ramachandran, P., Iredale, J.P., Fallowfield, J.A., 2014. Liver fibrosis and repair: immune regulation of wound healing in a solid organ. Nat. Rev. Immunol. 14, 181-94. Doi: 10.1038/nri3623.

Petersen, K.F., Dufour, S., Savage, D.B., Bilz, S., Solomon, G., Yonemitsu, S., Cline, G.W., Befroy, D., Zemany, L., Kahn, B.B., Papademetris, X., Rothman, D.L., Shulman, G.I., 2007. The role of skeletal muscle insulin resistance in the pathogenesis of the metabolic syndrome. Proc. Natl. Acad. Sci. USA 104, 12587–12594. Doi: 10.1073/pnas.0705408104.

Pinzani, M., Failli, P., Ruocco, C., Casini, A., Milani, S., Baldi, E., Giotti, A., Gentilini, P., 1992. Fat-storing cells as liver-specific pericytes. Spatial dynamics of agonist-stimulated intracellular calcium transients. J. Clin. Invest. 90, 642-646. Doi: 10.1172/JCI115905.

Pontisso, P., Calabrese, F., Benvegnu, L., Lise, M., Belluco, C., Ruvoletto, M.G., Marino, M., Valente, M., Nitti, D., Gatta, A., Fassina, G., 2004. Overexpression of squamous cell carcinoma antigen variants in hepatocellular carcinoma, Br J Cancer.;90:833-37. Doi: 10.1038/sj.bjc.6601543.

Portincasa, P., Bonfrate, L., Khalil, M., Angelis, M., Calabrese, F.M., D'Amato, M., Wang, D.Q., Di Ciaula, A., 2021. Intestinal barrier and permeability in health, obesity and NAFLD. Biomedicines 10, 83. Doi: 10.3390/biomedicines10010083.

Povero, D., Eguchi, A., Niesman, I.R., Andronikou, N., de Mollerat du Jeu, X., Mulya, A., Berk, M., Lazic, M., Thapaliya, S., Parola, M., Patel, H.H., Feldstein, A.E., 2013. Lipid-induced toxicity stimulates hepatocytes to release angiogenic microparticles that require Vanin-1 for uptake by endothelial cells. Sci. Signal. 6, (296):ra88. Doi: 10.1126/scisignal.2004512.

Povero, D., Panera, N., Eguchi, A., Johnson, C.D., Papouchado, B.G., de Araujo Horcel, L., Pinatel, E.M., Alisi, A., Nobili, V., Feldstein, A.E., 2015. Lipid-induced hepatocyte-derived extracellular vesicles regulate hepatic stellate cell via microRNAs targeting PPAR-γ. Cell. Mol. Gastroenterol. Hepatol. 1, 646-663. Doi: 10.1016/j.jcmgh.2015.07.007.

Powell, E.E., Wong, V.W., Rinella, M., 2021. Non-alcoholic fatty liver disease. Lancet 397, 2212–2224. Doi:10.1016/S0140-6736(20)32511-3.

Qiao, J.T., Cui, C., Qing, L., Wang, L.S., He, T.Y., Yan, F., Liu, F.Q., Shen, Y.H., Hou, X.G., Chen, L., 2018. Activation of the STING-IRF3 pathway promotes hepatocyte inflammation, apoptosis and induces metabolic disorders in nonalcoholic fatty liver disease. Metabolism 81, 13-24. Doi: 10.1016/j.metabol.2017.09.010.

Ramachandran, P., Dobie, R., Wilson-Kanamori, J.R., Dora, E.F., Henderson, B.E.P., Luu, N.T., Portman, J.R., Matchett, K.P., Brice, M., Marwick, J.A., Taylor, R.S., Efremova, M., Vento-Tormo, R., Carragher, N.O., Kendall, T.J., Fallowfield, J.A., Harrison, E.M., Mole, D.J., Wigmore, S.J., Newsome, P.N., Weston, C.J., Iredale, J.P., Tacke, F., Pollard, J.W., Ponting, C.P., Marioni, J.C., Teichmann, S.A., Henderson, N.C., 2019. Resolving the fibrotic niche of human liver cirrhosis at single-cell level. Nature 575, 512-518. Doi: 10.1038/s41586-019-1631-3.

Ramachandran, P., Pellicoro, A., Vernon, M.A., Boulter, L., Aucott, R.L., Ali, A., Hartland, S.N., Snowdon, V.K., Cappon, A., Gordon-Walker, T.T., Williams, M.J., Dunbar, D.R., Manning, J.R., van Rooijen, N., Fallowfield, J.A., Forbes, S.J., Iredale, J.P., 2012. Differential Ly-6C expression identifies the recruited macrophage phenotype, which orchestrates the regression of murine liver fibrosis. Proc. Natl. Acad. Sci. USA 109, E3186-E3195. Doi: 10.1073/pnas.1119964109.

Ramadori, P., Kam, S., Heikenwalder, M., 2022. T cells: friends and foes in NASH pathogenesis and hepatocarcinogenesis. Hepatology 75,1038-1049. Doi: 10.1002/hep.32336.

Ramadori, P., Klag, T., Malek, N.P., Heikenwalder, M., 2019. Platelets in chronic liver disease, from bench to bedside. JHEP Rep. 1, 448-459. Doi: 10.1016/j.jhepr.2019.10.001.

Ratziu, V., Francque, S., Sanyal, A., 2022. Breakthroughs in therapies for NASH and remaining challenges. J. Hepatol. 76, 1263-1278. Doi: 10.1016/j.jhep.2022.04.002.

Rau, M., Schilling, A.K., Meertens, J., Hering, I., Weiss, J., Jurowich, C., Kudlich, T., Hermanns, H.M., Bantel, H., Beyersdorf, N., Geier, A., 2016. Progression from nonalcoholic fatty liver to nonalcoholic steatohepatitis is marked by a higher frequency of Th17 cells in the liver and an increased Th17/resting regulatory T cell ratio in peripheral blood and in the liver. J. Immunol. 196, 97-105. Doi: 10.4049/jimmunol.1501175.

Remmerie, A., Martens, L., Thoné, T., Castoldi, A., Seurinck, R., Pavie, B., Roels, J., Vanneste, B., De Prijck, S., Vanhockerhout, M., Binte Abdul Latib, M., Devisscher, L., Hoorens, A., Bonnardel, J., Vandamme, N., Kremer, A., Borghgraef, P., Van Vlierberghe, H., Lippens, S., Pearce, E., Saeys, Y., Scott, C.L., 2020. Osteopontin expression identifies a subset of recruited macrophages distinct from Kupffer cells in the fatty liver. Immunity 53, 641-657. Doi: 10.1016/j.immuni.2020.08.004.

Rezaie, A.R., Giri, H., 2020. Anticoagulant and signaling functions of antithrombin. J Thromb Haemost. 18:3142-53. Doi:10.1111/jth.15052.

Richardson, M.M., Jonsson, J.R., Powell, E.E., Brunt, E.M., Neuschwander-Tetri, B.A., Bhathal, P.S., Dixon, J.B., Weltman, M.D., Tilg, H., Moschen, A.R., Purdie, D.M., Demetris,

A.J., Clouston, A.D., 2007. Progressive fibrosis in nonalcoholic steatohepatitis: association with altered regeneration and a ductular reaction. Gastroenterology 133, 80-90. Doi: 10.1053/j.gastro.2007.05.012.

Rinella, M.E., Lazarus, J.V., Ratziu, V., Francque, S.M., Sanyal, A.J., Kanwal, F., Romero, D., Abdelmalek, M.F., Anstee, Q.M., Arab, J.P., Arrese, M., Bataller, R., Beuers, U., Boursier, J., Bugianesi, E., Byrne, C., Castro Narro, G.E., Chowdhury, A., Cortez-Pinto, H., Cryer, D., Cusi, K., El-Kassas, M., Klein, S., Eskridge, W., Fan, J., Gawrieh, S., Guy, C.D., Harrison, S.A., Kim, S.U., Koot, B., Korenjak, M., Kowdley, K., Lacaille, F., Loomba, R., Mitchell-Thain, R., Morgan, T.R., Powell, E., Roden, M., Romero-Gómez, M., Silva, M., Singh, S.P., Sookoian, S.C., Spearman, C.W., Tiniakos, D., Valenti, L., Vos, M.B., Wai-Sun Wong, V., Xanthakos, S., Yilmaz, Y., Younossi, Z., Hobbs, A., Villota-Rivas, M., Newsome, P.N.; NAFLD Nomenclature consensus group, 2023. A multi-society Delphi consensus statement on new fatty liver disease nomenclature. J. Hepatol. Doi: 10.1016/j.jhep.2023.06.003.

Rockey, D.C., Friedman, S.L., 2021. Fibrosis Regression After Eradication of Hepatitis C Virus: From Bench to Bedside. Gastroenterology 160, 1502-1520.e1. Doi: 10.1053/j.gastro.2020.09.065.

Rockey, D.C., Friedman, S.L., 2021. Fibrosis Regression After Eradication of Hepatitis C Virus: From Bench to Bedside. Gastroenterology 160, 1502-1520.e1. Doi: 10.1053/j.gastro.2020.09.065.

Roden, M., 2006. Mechanisms of disease: hepatic steatosis in type 2 diabetes - pathogenesis and clinical relevance. Nat. Clin. Pract. Endocrinol. Metab. 2, 335–348. Doi: 10.1038/ncpendmet0190.

Rolla, S., Alchera, E., Imarisio, C., Bardina, V., Valente, G., Cappello, P., Mombello, C., Follenzi, A., Novelli, F., Carini, R., 2016. The balance between IL-17 and IL-22 produced by liver-infiltrating T-helper cells critically controls NASH development in mice. Clin. Sci. 130, 193-203. Doi: 10.1042/CS20150405.

Roth, K.J., Copple, B.L., 2015. Role of hypoxia-inducible factors in the development of liver fibrosis. Cell. Mol. Gastroenterol. Hepatol. 1:589-97. Doi: 10.1016/j.jcmgh.2015.09.005.

Russo, F.P., Alison, M.R., Bigger, B.W., Amofah, E., Florou, A., Amin, F., Bou-Gharios, G., Jeffery, R., Iredale, J.P., Forbes, S.J., 2006. The bone marrow functionally contributes to liver fibrosis. Gastroenterology 130, 1807-1821. Doi: 10.1053/j.gastro.2006.01.036.

Samuel, V.T., Shulman, G.I., 2018. Nonalcoholic Fatty Liver Disease as a Nexus of Metabolic and Hepatic Diseases. Cell Metab. 27, 22–41. Doi:10.1016/j.cmet.2017.08.002.

Satapathy, S.K., Sanyal, A.J., 2015. Epidemiology and natural history of nonalcoholic fatty liver disease. Semin. Liver Dis. 35, 221–235. Doi: 10.1055/s-0035-1562943.

Schneider, S.S., Schick, C., Fish, K.E., Miller, E., Pena, J.C., Treter, S.D., Hui, S.M., Silverman, G.A., 1995. A serine proteinase inhibitor locus at 18q21.3 contains a tandem duplication of the human squamous cell carcinoma antigen gene. Proc Natl Acad Sci USA. 92:3147-51. Doi: 10.1073/pnas.92.8.3147.

Schuster, S., Cabrera, D., Arrese, M., Feldstein, A.E., 2018. Triggering and resolution of inflammation in NASH. Nat. Rev. Gastroenterol. Hepatol. 15, 349–364. Doi: 10.1038/s41575-018-0009-6.

Schwabe, R.F., Tabas, I., Pajvani, U.B., 2020. Mechanisms of Fibrosis Development in Nonalcoholic Steatohepatitis. Gastroenterology 158, 1913-1928. Doi:10.1053/j.gastro.2019.11.311.

Schwimmer, J.B., Celedon, M.A., Lavine, J.E., Salem, R., Campbell, N., Schork, N.J., Shiehmorteza, M., Yokoo, T., Chavez, A., Middleton, M.S., Sirlin, C.B., 2009. Heritability of nonalcoholic fatty liver disease. Gastroenterology 136, 1585-1592. Doi: 10.1053/j.gastro.2009.01.050.

Schwimmer, J.B., Johnson, J.S., Angeles. J.E., Behling, C., Belt, P.H., Borecki, I., Bross, C., Durelle, J., Goyal, N.P., Hamilton, G., Holtz, M.L., Lavine, J.E., Mitreva, M., Newton, K.P., Pan, A., Simpson, P.M., Sirlin, C.B., Sodergren, E., Tyagi, R., Yates, K.P., Weinstock, G.M., Salzman, N.H., 2019. Microbiome signatures associated with steatohepatitis and moderate to severe fibrosis in children with nonalcoholic fatty liver disease. Gastroenterology 157, 1109-1122. Doi: 10.1053/j.gastro.2019.06.028.

Seki, E., Schwabe, R.F., 2015. Hepatic inflammation and fibrosis: functional links and key pathways. Hepatology 61, 1066-1079. Doi:10.1002/hep.27332.

Shalapour, S., Lin, X.J., Bastian, I.N., Brain, J., Burt, A.D., Aksenov, A.A., Lin, X.J., Bastian, I.N., Brain, J., Burt, A.D., Aksenov, A.A., Vrbanac, A.F., Li, W., Perkins, A., Matsutani, T., Zhong, Z., Dhar, D., Navas-Molina, J.A., Xu, J., Loomba, R., Downes, M., Yu, R.T., Evans, R.M., Dorrestein, P.C., Knight, R., Benner, C., Anstee, Q.M., Karin, M., 2017. Inflammation-induced IgA+ cells dismantle anti-liver cancer immunity. Nature 551, 340-345. Doi: 10.1038/nature24302.

Shi, J., Zhao, Y., Wang, K., Shi, X., Wang, Y., Huang, H., Zhuang, Y., Cai, T., Wang, F., Shao, F., 2015. Cleavage of GSDMD by inflammatory caspases determines pyroptotic cell death. Nature 526, 660-665. Doi: 10.1038/nature15514.

Shimada, K., Crother, T.R., Karlin, J., Dagvadorj, J., Chiba, N., Chen, S., Ramanujan, V.K., Wolf, A.J., Vergnes, L., Ojcius, D.M., Rentsendorj, A., Vargas, M., Guerrero, C., Wang, Y., Fitzgerald, K.A., Underhill, D.M., Town, T., Arditi, M., 2012. Oxidized mitochondrial DNA activates the NLRP3 inflammasome during apoptosis. Immunity 36, 401-414. Doi: 10.1016/j.immuni.2012.01.009.

Singh, R., Kaushik, S., Wang, Y., Xiang, Y., Novak, I., Komatsu, M., Tanaka, K., Cuervo, A.M., Czaja, M.J., 2009. Autophagy regulates lipid metabolism. Nature 458, 1131-1135. Doi: 10.1038/nature07976.

Singh, S., Venkatesh, S.K., Wang, Z., Miller, F.H., Motosugi, U., Low, R.N., Hassanein, T., Asbach, P., Godfrey, E.M., Yin, M., Chen, J., Keaveny, A.P., Bridges, M., Bohte, A., Murad, M.H., Lomas, D.J., Talwalkar, J.A., Ehman, R.L., 2015. Diagnostic performance of magnetic resonance elastography in staging liver fibrosis: a systematic review and meta-analysis of

individual participant data. Clin. Gastroenterol. Hepatol. 13, 440-451. e6. Doi: 10.1016/j.cgh.2014.09.046.

Smith, S.L., Watson, S.G., Ratschiller, D., Gugger, M., Betticher, D.C., Heighway, J., 2003 Maspin – the mostcommonly-expressed gene of the 18q21.3 serpin cluster in lung cancer – is strongly expressed in preneoplastic bronchial lesions. Oncogene, 22:8677-87. Doi: 10.1038/sj.onc.1207127.

Sookoian, S., Pirola, C.J., 2017. Genetic predisposition in nonalcoholic fatty liver disease. Clin. Mol. Hepatol. 23, 1–12. Doi: 10.3350/cmh.2016.0109.

Stephens, J. M., Elks, C. M., 2017. Oncostatin M: Potential Implications for Malignancy and Metabolism. *Current Pharmaceutical Design*, *23*(25). Doi: 10.2174/1381612823666170704122559.

Suminami, Y., Kishi, F., Sekiguchi, K., Kato, H., 1991. Squamous cell carcinoma antigen is a new member of the serine protease inhibitors, Biochem Biophys Res Commun. 181:51-58. Doi: 10.1016/s0006-291x(05)81380-4.

Sun, Y., Sheshadri, N., Zong, W.X., 2017. SERPINB3 and B4: from biochemistry to biology. Sem Cell Dev Biol., 62:170-77. Doi: 10.1016/j.semcdb.2016.09.005.

Sutti, S., Albano, E., 2020. Adaptive immunity: an emerging player in the progression of NAFLD. Nat. Rev. Gastroenterol. Hepatol. 17, 81–92. Doi: 10.1038/s41575-019-0210-2.

Sutti, S., Jindal, A., Locatelli, I., Vacchiano, M., Gigliotti, L., Bozzola, C., Albano, E., 2014. Adaptive immune responses triggered by oxidative stress contribute to hepatic inflammation in NASH. Hepatology 59, 886-897. Doi: 10.1002/hep.26749.

Tacke, F., 2017. Targeting hepatic macrophages to treat liver diseases. J. Hepatol. 66. 1300-1312. Doi:10.1016/j.jhep.2017.02.026.

Tacke, F., Puengel, T., Loomba, R., Friedman, S.L., 2023. An integrated view of anti-inflammatory and antifibrotic targets for the treatment of NASH. J. Hepatol. 79, 552-566. Doi: 10.1016/j.jhep.2023.03.038.

Tang, Y., Bian, Z., Zhao, L., Liu, Y., Liang, S., Wang, Q., Han, X., Peng, Y., Chen, X., Shen, L., Qiu, D., Li, Z., Ma, X., 2011. Interleukin-17 exacerbates hepatic steatosis and inflammation in non-alcoholic fatty liver disease. Clin. Exp. Immunol. 166, 281-290. Doi: 10.1111/j.1365-2249.2011.04471.x.

Taus, F., Meneguzzi, A., Castelli, M., Minuz, P., 2019. Platelet-derived extracellular vesicles as target of antiplatelet agents. what is the evidence? Front. Pharmacol. 10, 1256. Doi: 10.3389/fphar.2019.01256.

Thapa, M., Chinnadurai, R., Velazquez, V.M., Tedesco, D., Elrod, E., Han, J.H., Sharma, P., Ibegbu, C., Gewirtz, A., Anania, F., Pulendran, B., Suthar, M.S., Grakoui, A., 2015. Liver fibrosis occurs through dysregulation of MyD88-dependent innate B- cell activity. Hepatology 61, 2067-2079. Doi: 10.1002/hep.27761.

Thrift, A.P., El-Serag, H.B., Kanwal, F., 2017. Global epidemiology and burden of HCV infection and HCV-related disease. Nat. Rev. Gastroenterol. Hepatol. 14, 122-132. Doi:10.1038/nrgastro.2016.176.

Tilg. H., Moschen, A.R., Roden, M., 2017. NAFLD and diabetes mellitus. Nat. Rev. Gastroenterol. Hepatol. 14, 32-42. Doi: 10.1038/nrgastro.2016.147.

Trautwein, C., Friedman, S.L., Schuppan, D., Pinzani, M., 2015. Hepatic fibrosis: concepts to treatment. J. Hepatol. 62(1 Suppl), S15-24. Doi:10.1016/j.jhep.2015.02.039.

Trépo, E., Valenti, L., 2020. Update on NAFLD genetics: from new variants to the clinic. J. Hepatol. 72, 1196-1209. Doi: 10.1016/j.jhep.2020.02.020.

Trivedi, P., Wang, S., Friedman, S.L., 2021. The Power of Plasticity-Metabolic Regulation of Hepatic Stellate Cells. Cell Metab. 33, 242-257. Doi: 10.1016/j.cmet.2020.10.026.

Troeger, J.S., Mederacke, I., Gwak, G.Y., Dapito, D.H., Mu, X., Hsu, C.C., Pradere, J.P., Friedman, R.A., Schwabe, R.F., 2012. Deactivation of hepatic stellate cells during liver fibrosis resolution in mice. Gastroenterology 143, 1073-1083. Doi: 10.1053/j.gastro.2012.06.036.

Tsiantoulas, D., Sage, A.P., Mallat, Z., Binder, C.J., 2015. Targeting B cells in atherosclerosis: closing the gap from bench to bedside. Arterioscler. Thromb. Vasc. Biol. 35, 296-302. Doi: 10.1161/ATVBAHA.114.303569.

Tsuchida, T., Friedman, S.L., 2017. Mechanisms of hepatic stellate cell activation. Nat. Rev. Gastroenterol. Hepatol. 14, 397-411. Doi: 10.1038/nrgastro.2017.38.

Turato, C., Calabrese, F., Biasiolo, A., Quarta, S., Ruvoletto, M., Tono, N., Paccagnella, D., Fassina, G., Merkel, C., Harrison, T.J., Gatta, A., Pontisso, P., 2010. SERPINB3 Modulates TGF-β Expression in Chronic Liver Disease. Lab Invest. 90:1016-23. Doi: 10.1038/labinvest.2010.55.

Valenti, L., Alisi, A., Galmozzi, E., Bartuli, A., Del Menico, B., Alterio, A., Dongiovanni, P., Fargion, S., Nobili, V., 2010. I148M patatin-like phospholipase domain-containing 3 gene variant and severity of pediatric nonalcoholic fatty liver disease. Hepatology 52,1274-1280. Doi: 10.1002/hep.23823.

Valenti, L., Alisi, A., Nobili, V., 2012. Unraveling the genetics of fatty liver in obese children: additive effect of P446L GCKR and I148M PNPLA3 polymorphisms. Hepatology 55, 661–663. Doi: 10.1002/hep.25617.

Vallianou, N., Christodoulatos, G.S., Karampela, I., Tsilingiris, D., Magkos, F., Stratigou, T. Kounatidis, D., Dalamaga, M., 2021. Understanding the role of the gut microbiome and microbial metabolites in non-alcoholic fatty liver disease: current evidence and perspectives. Biomolecules 12, 56. Doi: 10.3390/biom12010056.

Vidalino, L., Doria, A., Quarta, S., Zen, M., Gatta, A., Pontisso, P., 2009. SERPINB3, apoptosis and autoimmunity. Autoimmunity Reviews, 9(2), 108–112. Doi: 10.1016/j.autrev.2009.03.011.

Wallace, S.J., Tacke, F., Schwabe, R.F., Henderson, N.C., 2022. Understanding the cellular interactome of non-alcoholic fatty liver disease. JHEP Rep. 4,100524. Doi: 10.1016/j.jhepr.2022.100524.

Wang J, Hu W, Shen Z, Liu T, Dai W, Shen B, Li, X., Wu, J., Lu, L., Li, S., Cai, X., 2021. Dissecting the single cell transcriptome underlying chronic liver injury. Mol. Ther. Nucleic Acids 26, 1364-1373. Doi: 10.1016/j.omtn.2021.11.008.

Wang, X., Rao, H., Zhao, J., Wee, A., Li, X., Fei, R., Huang, R., Wu, C., Liu, F., Wei, L., 2020. STING expression in monocyte-derived macrophages is associated with the progression of liver inflammation and fibrosis in patients with nonalcoholic fatty liver disease. Lab. Invest. 100, 542-552. Doi: 10.1038/s41374-019-0342-6.

Watanabe, A., Hashmi, A., Gomes, D.A., Town, T., Badou, A., Flavell, R.A., Mehal, W.Z., 2007. Apoptotic hepatocyte DNA inhibits hepatic stellate cell chemotaxis via toll- like receptor 9. Hepatology 46, 1509-1518. Doi: 10.1002/hep.21867.

Wells, R.G., Schwabe, R.F., 2015. Origin and function of myofibroblasts in the liver. Semin. Liver Dis. 35, 97-106. Doi: 10.1055/s-0035-1550061.

Weston, C.J., Shepherd, E.L., Claridge, L.C., Rantakari, P., Curbishley, S.M., Tomlinson, J.W., Hubscher, S.G., Reynolds, G.M., Aalto, K., Anstee, Q.M., Jalkanen, S., Salmi, M., Smith, D.J., Day, C.P., Adams, D.H., 2015. Vascular adhesion protein-1 promotes liver inflammation and drives hepatic fibrosis. J. Clin. Invest. 125, 501-520. Doi: 10.1172/JCI73722.

Wiering, L., Tacke, F., 2022. Treating inflammation to combat non-alcoholic fatty liver disease. J. Endocrinol. 256, e220194. Doi: 10.1530/JOE-22-0194.

Wolf, M.J., Adili, A., Piotrowitz, K., Abdullah, Z., Boege, Y., Stemmer, K., Ringelhan, M., Simonavicius, N., Egger, M., Wohlleber, D., Lorentzen, A., Einer, C., Schulz, S., Clavel, T., Protzer, U., Thiele, C., Zischka, H., Moch, H., Tschöp, M., Tumanov, A.V., Haller, D., Unger, K., Karin, M., Kopf, M., Knolle, P., Weber, A., Heikenwalder, M., 2014. Metabolic activation of intrahepatic CD8+ T cells and NKT cells causes nonalcoholic steatohepatitis and liver cancer via cross- talk with hepatocytes. Cancer Cell 26, 549-564. Doi: 10.1016/j.ccell.2014.09.003.

Xiang, M., Wang, P.X., Wang, A.B., Zhang, X.J., Zhang, Y., Zhang, P., Mei, F.H., Chen, M.H., Li, H., 2016. Targeting hepatic TRAF1-ASK1 signaling to improve inflammation, insulin resistance, and hepatic steatosis. J. Hepatol. 64, 1365–1377. Doi: 10.1016/j.jhep.2016.02.002.

Xu, B., Jiang, M., Chu, Y., Wang, W., Chen, D., Li, X., Zhang, Z., Zhang, D., Fan, D., Nie, Y., Shao, F., Wu, K., Liang, J., 2018. Gasdermin D plays a key role as a pyroptosis executor of non-alcoholic steatohepatitis in humans and mice. J. Hepatol. 68, 773-782. Doi: 10.1016/j.jhep.2017.11.040.

Xu H, Wang L. 2021. The Role of Notch Signaling Pathway in Non-Alcoholic Fatty Liver Disease. Front Mol Biosci. 8:792667. doi: 10.3389/fmolb.2021.792667. eCollection 2021.

Yamaguchi, K., Yang, L., McCall, S., Huang, J., Yu, X.X., Pandey, S.K., Bhanot, S., Monia, B.P., Li, Y.X., Diehl, A.M., 2007. Inhibiting triglyceride synthesis improves hepatic steatosis but exacerbates liver damage and fibrosis in obese mice with nonalcoholic steatohepatitis Hepatology 45, 1366-1374. Doi: 10.1002/hep.21655.

Yang, L., Li, P., Fu, S., Calay, E.S., Hotamisligil, G.S., 2010. Defective hepatic autophagy in obesity promotes ER stress and causes insulin resistance. Cell Metab. 11, 467-478. Doi: 10.1016/j.cmet.2010.04.005.

Yeh, M.M., Brunt, E.M., 2014. Pathological features of fatty liver disease. Gastroenterology 147, 754-764. Doi: 10.1053/j.gastro.2014.07.056.

Yoshitaka, H., Hamaguchi, M., Kojima, T., Fukuda, T., Ohbora, A., and Fukui, M., 2017. Nonoverweight nonalcoholic fatty liver disease and incident cardiovascular disease: A post hoc analysis of a cohort study. Medicine (Baltimore) 96, e6712. Doi: 10.1097/MD.0000000000006712.

Younossi, Z., Anstee, Q.M., Marietti, M., Hardy, T., Henry, L., Eslam, M., George, J., Bugianesi, E., 2018. Global burden of NAFLD and NASH: trends, predictions, risk factors and prevention. Nat. Rev. Gastroenterol. Hepatol. 15, 11-20. Doi: 10.1038/nrgastro.2017.109.

Younossi, Z., Stepanova, M., Ong, J.P., Jacobson, I.M., Bugianesi, E., Duseja, A., Eguchi, Y., Wong, V.W., Negro, F., Yilmaz, Y., Romero-Gomez, M., George, J., Ahmed, A., Wong, R., Younossi, I., Ziayee, M., Afendy, A., 2019b. Global Nonalcoholic Steatohepatitis Council. Nonalcoholic Steatohepatitis Is the Fastest Growing Cause of Hepatocellular Carcinoma in Liver Transplant Candidates. Clin. Gastroenterol. Hepatol. 17, 748–755. Doi: 10.106/j.cgh.2018.05.057.

Younossi, Z., Tacke, F., Arrese, M., Chander Sharma, B., Mostafa, I., Bugianesi, E., Wai-Sun Wong, V., Yilmaz, Y., George, J., Fan, J., and Vos, M.B. 2019a. Global Perspectives on Nonalcoholic Fatty Liver Disease and Nonalcoholic Steatohepatitis. Hepatology 69, 2672–2682. Doi: 10.1002/hep.30251.

Younossi, Z.M., Koenig, A.B., Abdelatif, D., Fazel, Y., Henry, L., Wymer, M., 2016. Global epidemiology of nonalcoholic fatty liver disease-Meta-analytic assessment of prevalence, incidence, and outcomes. Hepatology 64, 73–84. Doi:10.1002/hep.28431.

Yu, X.X., Murray, S.F., Pandey, S.K., Booten, S.L., Bao, D., Song, X.Z., Kelly, S., Chen, S., McKay, R., Monia, B.P., Bhanot, S., 2005. Antisense oligonucleotide reduction of DGAT2 expression improves hepatic steatosis and hyperlipidemia in obese mice. Hepatology 42, 362-371. Doi:10.1002/hep.20783.

Zeerleder, S., 2011. C1-inhibitor: more than a serine protease inhibitor. Semin Thromb Hemost. 37:362-74. Doi:10.1055/s-0031-1276585.

Zhang M, Wang C, Hu J, Lin J, Zhao Z, Shen M, Gao H, Li N, Liu M, Zheng P, Qiu C, Gao E, Wang H, Sun D. 2015. Notch3/Akt signaling contributes to OSM-induced protection against cardiac ischemia/reperfusion injury. Apoptosis 20(9):1150-63. doi: 10.1007/s10495-015-1148-7.

Zhang, P., Wang, P.X., Zhao, L.P., Zhang, X., Ji, Y.X., Zhang, X.J., Fang, C., Lu, Y.X., Yang, X., Gao, M.M., Zhang, Y., Tian, S., Zhu, X.Y., Gong, J., Ma, X.L., Li, F., Wang, Z., Huang, Z., She, Z.G., Li, H., 2018. The deubiquitinating enzyme TNFAIP3 mediates inactivation of hepatic ASK1 and ameliorates nonalcoholic steatohepatitis. Nat. Med. 24, 84–94. Doi: 10.1038/nm.4453.

Zhao, G.N., Zhang, P., Gong, J., Zhang, X.J., Wang, P.X., Yin, M., Jiang, Z., Shen, L.J., Ji, Y.X., Tong, J., Wang, Y., Wei, Q.F., Wang, Y., Zhu, X.Y., Zhang, X., Fang, J., Xie, Q., She, Z.G., Wang, Z., Huang, Z., Li, H., 2017. Tmbim1 is a multivesicular body regulator that protects against non-alcoholic fatty liver disease in mice and monkeys by targeting the lysosomal degradation of Tlr4. Nat. Med. 23, 742-752. Doi: 10.1038/nm.4334.

Zhou, T., Kundu, D., Robles-Linares, J., Meadows, V., Sato, K., Baiocchi, L., Ekser, B., Glaser, S., Alpini, G., Francis, H., Kennedy, L., 2021. Feedback signaling between cholangiopathies, ductular reaction, and non-alcoholic fatty liver disease. Cells 10, 2072. Doi: 10.3390/cells10082072.

Zychlinsky, A., Prevost, M.C., Sansonetti, P.J., 1992. Shigella flexneri induces apoptosis in infected macrophages. Nature 358 (6382), 167-169. Doi: 10.1038/358167a0.